

# Triangle crosstalk: Gut microbiota, immune reaction and metabolism

**Edited by**

Yubin Luo, Yuan-Ping Han, Cong-Qiu Chu and Haitao Niu

**Published in**

Frontiers in Microbiology

Frontiers in Cellular and Infection Microbiology



## FRONTIERS EBOOK COPYRIGHT STATEMENT

The copyright in the text of individual articles in this ebook is the property of their respective authors or their respective institutions or funders. The copyright in graphics and images within each article may be subject to copyright of other parties. In both cases this is subject to a license granted to Frontiers.

The compilation of articles constituting this ebook is the property of Frontiers.

Each article within this ebook, and the ebook itself, are published under the most recent version of the Creative Commons CC-BY licence. The version current at the date of publication of this ebook is CC-BY 4.0. If the CC-BY licence is updated, the licence granted by Frontiers is automatically updated to the new version.

When exercising any right under the CC-BY licence, Frontiers must be attributed as the original publisher of the article or ebook, as applicable.

Authors have the responsibility of ensuring that any graphics or other materials which are the property of others may be included in the CC-BY licence, but this should be checked before relying on the CC-BY licence to reproduce those materials. Any copyright notices relating to those materials must be complied with.

Copyright and source acknowledgement notices may not be removed and must be displayed in any copy, derivative work or partial copy which includes the elements in question.

All copyright, and all rights therein, are protected by national and international copyright laws. The above represents a summary only. For further information please read Frontiers' Conditions for Website Use and Copyright Statement, and the applicable CC-BY licence.

ISSN 1664-8714  
ISBN 978-2-83251-756-7  
DOI 10.3389/978-2-83251-756-7

## About Frontiers

Frontiers is more than just an open access publisher of scholarly articles: it is a pioneering approach to the world of academia, radically improving the way scholarly research is managed. The grand vision of Frontiers is a world where all people have an equal opportunity to seek, share and generate knowledge. Frontiers provides immediate and permanent online open access to all its publications, but this alone is not enough to realize our grand goals.

## Frontiers journal series

The Frontiers journal series is a multi-tier and interdisciplinary set of open-access, online journals, promising a paradigm shift from the current review, selection and dissemination processes in academic publishing. All Frontiers journals are driven by researchers for researchers; therefore, they constitute a service to the scholarly community. At the same time, the *Frontiers journal series* operates on a revolutionary invention, the tiered publishing system, initially addressing specific communities of scholars, and gradually climbing up to broader public understanding, thus serving the interests of the lay society, too.

## Dedication to quality

Each Frontiers article is a landmark of the highest quality, thanks to genuinely collaborative interactions between authors and review editors, who include some of the world's best academicians. Research must be certified by peers before entering a stream of knowledge that may eventually reach the public - and shape society; therefore, Frontiers only applies the most rigorous and unbiased reviews. Frontiers revolutionizes research publishing by freely delivering the most outstanding research, evaluated with no bias from both the academic and social point of view. By applying the most advanced information technologies, Frontiers is catapulting scholarly publishing into a new generation.

## What are Frontiers Research Topics?

Frontiers Research Topics are very popular trademarks of the *Frontiers journals series*: they are collections of at least ten articles, all centered on a particular subject. With their unique mix of varied contributions from Original Research to Review Articles, Frontiers Research Topics unify the most influential researchers, the latest key findings and historical advances in a hot research area.

Find out more on how to host your own Frontiers Research Topic or contribute to one as an author by contacting the Frontiers editorial office: [frontiersin.org/about/contact](https://frontiersin.org/about/contact)

# Triangle crosstalk: Gut microbiota, immune reaction and metabolism

## Topic editors

Yubin Luo — Sichuan University, China

Yuan-Ping Han — Sichuan University, China

Cong-Qiu Chu — Oregon Health and Science University, United States

Haitao Niu — Jinan University, China

## Citation

Luo, Y., Han, Y.-P., Chu, C.-Q., Niu, H., eds. (2023). *Triangle crosstalk: Gut microbiota, immune reaction and metabolism*. Lausanne: Frontiers Media SA.  
doi: 10.3389/978-2-83251-756-7

# Table of contents

04	<b>Editorial: Triangle crosstalk: Gut microbiota, immune reaction and metabolism</b> Cong-Qiu Chu, Yubin Luo, Yuan-Ping Han and Haitao Niu
06	<b>Comparison of Intestinal Microbes in Noninfectious Anterior Scleritis Patients With and Without Rheumatoid Arthritis</b> Mengyao Li, Li Yang, Liangliang Zhao, Feng Bai and Xiaoli Liu
16	<b>Intestinal Microbiota Participates in the Protective Effect of HO-1/BMMSCs on Liver Transplantation With Steatotic Liver Grafts in Rats</b> Mengshu Yuan, Ling Lin, Huan Cao, Weiping Zheng, Longlong Wu, Huaiwen Zuo, Xiaorong Tian and Hongli Song
34	<b>Fermented Soy and Fish Protein Dietary Sources Shape Ileal and Colonic Microbiota, Improving Nutrient Digestibility and Host Health in a Piglet Model</b> Ying Li, Yunsheng Han, Qingyu Zhao, Chaohua Tang, Junmin Zhang and Yuchang Qin
49	<b>Gut microbiome is associated with metabolic syndrome accompanied by elevated gamma-glutamyl transpeptidase in men</b> Shifeng Sheng, Su Yan, Jingfeng Chen, Yuheng Zhang, Youxiang Wang, Qian Qin, Weikang Li, Tiantian Li, Meng Huang, Suying Ding and Lin Tang
63	<b>Orlistat and ezetimibe could differently alleviate the high-fat diet-induced obesity phenotype by modulating the gut microbiota</b> Jin Jin, Jiani Wang, Ruyue Cheng, Yan Ren, Zhonghua Miao, Yating Luo, Qingqing Zhou, Yigui Xue, Xi Shen, Fang He and Haoming Tian
82	<b>Metabolomic analysis in spondyloarthritis: A systematic review</b> Tianwen Huang, Yaoyu Pu, Xiangpeng Wang, Yanhong Li, Hang Yang, Yubin Luo and Yi Liu
100	<b>Corrigendum: Metabolomic analysis in spondyloarthritis: A systematic review</b> Tianwen Huang, Yaoyu Pu, Xiangpeng Wang, Yanhong Li, Hang Yang, Yubin Luo and Yi Liu
102	<b>Gut microbiome and metabolites: The potential key roles in pulmonary fibrosis</b> Yinlan Wu, Yanhong Li, Yubin Luo, Yu Zhou, Ji Wen, Lu Chen, Xiuping Liang, Tong Wu, Chunyu Tan and Yi Liu
113	<b>The change of plasma metabolic profile and gut microbiome dysbiosis in patients with rheumatoid arthritis</b> Jing Zhu, Tingting Wang, Yifei Lin, Minghao Xiong, Jianghua Chen, Congcong Jian, Jie Zhang, Huanhuan Xie, Fanwei Zeng, Qian Huang, Jiang Su, Yi Zhao, Shilin Li and Fanxin Zeng





## OPEN ACCESS

EDITED AND REVIEWED BY  
Takema Fukatsu,  
National Institute of Advanced Industrial  
Science and Technology (AIST), Japan

\*CORRESPONDENCE  
Cong-Qiu Chu  
✉ chuc@ohsu.edu

SPECIALTY SECTION  
This article was submitted to  
Microbial Symbioses,  
a section of the journal  
Frontiers in Microbiology

RECEIVED 09 January 2023  
ACCEPTED 16 January 2023  
PUBLISHED 31 January 2023

CITATION  
Chu C-Q, Luo Y, Han Y-P and Niu H (2023)  
Editorial: Triangle crosstalk: Gut microbiota,  
immune reaction and metabolism.  
*Front. Microbiol.* 14:1141016.  
doi: 10.3389/fmicb.2023.1141016

COPYRIGHT  
© 2023 Chu, Luo, Han and Niu. This is an  
open-access article distributed under the terms  
of the [Creative Commons Attribution License  
\(CC BY\)](https://creativecommons.org/licenses/by/4.0/). The use, distribution or reproduction  
in other forums is permitted, provided the  
original author(s) and the copyright owner(s)  
are credited and that the original publication in  
this journal is cited, in accordance with  
accepted academic practice. No use,  
distribution or reproduction is permitted which  
does not comply with these terms.

# Editorial: Triangle crosstalk: Gut microbiota, immune reaction and metabolism

Cong-Qiu Chu<sup>1,2\*</sup>, Yubin Luo<sup>3</sup>, Yuan-Ping Han<sup>4</sup> and Haitao Niu<sup>5</sup>

<sup>1</sup>Division of Arthritis and Rheumatic Diseases, Oregon Health and Science University, Portland, OR, United States, <sup>2</sup>Innovent Biologics (USA), Rockville, MD, United States, <sup>3</sup>Department of Rheumatology and Immunology, Rare Disease Center, Institute of Immunology and Inflammation, West China Hospital, Sichuan University, Chengdu, Sichuan, China, <sup>4</sup>The College of Life Sciences, Sichuan University, Chengdu, Sichuan, China, <sup>5</sup>Institute of Laboratory Animal Sciences, School of Medicine, Jinan University, Guangzhou, Guangdong, China

## KEYWORDS

microbiome, metabolites, immune response, crosstalk, dysbiosis

## Editorial on the Research Topic

### Triangle crosstalk: Gut microbiota, immune reaction and metabolism

Gut microbiota exerts pleiotropic roles in human health and wellbeing, ranging from digestive function and absorption of nutrients, defense against infection, to the regulation of immune system development and immune homeostasis. Apart from the direct contact with the mucosal barrier of the host tissue, gut microbes are beneficial to the host through production of a variety of metabolites which may act on distant sites of the body. The concept of gut-other organ system axis, such as the “gut-lung axis” and “gut-joint axis” has been introduced to depict the relation of gut microbiota on the distant organ systems (Budden et al., 2017). Although there were many studies indicating the correlation between the gut microbiome, metabolites, and immune reaction, there is a huge knowledge gap as to how they interact and what are the outcomes.

The question is how to identify the key intestinal bacteria or metabolites, how to illustrate the crosstalk between microbiome, metabolites, and host immune reaction in disease, and how to take advantage of this triangle crosstalk in the future studies for clinical diagnosis and/or intervention. Four articles in this collection are concerning gut dysbiosis and metabolites in rheumatic diseases. Using untargeted metabolomics survey, Zhu et al. analyzed plasma metabolites of 244 patients with active disease (DAS28  $5.5 \pm 1.5$ ) of rheumatoid arthritis (RA) and demonstrated that 63 metabolites are differently expressed compared with healthy controls. In particular, L-arginine and phosphorylcholine are substantially increased in RA patients. Not surprisingly, the changes in metabolites in RA patients were associated with dysbiosis of gut microbiota. Of particular interest is that increased L-arginine level was positively correlated with enriched fecal *Rhodotorula* of fungi. Several previous studies have shown alteration of fecal bacterial composition in RA patients but only few analyzed fungal composition (Lee et al., 2022; Sun et al., 2022). Another study analyzed fecal metabolites in RA patients and found depletion of L-arginine (Yu et al., 2021). These studies apparently have some common limitations: whether RA patients in the studies were treated with disease modifying anti-rheumatic drugs (DMARDs) was not clearly stated. Ideally, future studies should include the newly onset, DMARDs-naïve patients and focus on fungal composition concomitantly with analysis of fecal and blood metabolites to further delineate the changes of metabolites in correlation with fungal composition. In a systematic review of 31 studies investigating metabolites in spondyloarthritis (SpA) patients, Huang et al. (see also Huang et al., corrigendum) found that the profile of metabolites in SpA patients is distinctly different from that of healthy controls. In general, higher levels of metabolites of glucose, succinic acid, malic acid and lactate in carbohydrate metabolism, but lower levels of

fatty acid in lipid metabolism; tryptophan and glutamine in amino acid metabolism were found in SpA patients. However, inconsistent results were also evident among studies which are likely due to the heterogeneous patient populations and various sources of samples ranging from plasma, synovial fluids, feces and urine. Interestingly, conventional DMARDS nor biological DMARDS treatment were able to normalize the changes of metabolites although they could control the clinical disease activity. In the narrative review, Wu et al. discussed the “gut-lung axis” focusing on interstitial lung fibrosis in the setting of a variety of lung conditions including idiopathic pulmonary fibrosis, fibrosis associated with systemic sclerosis, radiation induced lung fibrosis and silicosis-related pulmonary fibrosis. Changes of gut microbiota are seen in each of the conditions or their animal models. Discussion extended to mechanism how these metabolites affect immune cell function and fibroblasts and myofibroblasts. In a preliminary study, Li M. et al. reported the distinctive profile of gut microbiota in patients with non-infective anterior scleritis than that of patients associated with RA. Further experiments are required to investigate how different groups of microbes might affect the inflammation of eyes.

Metabolic syndrome affects about 25% of the population worldwide and the prevalence is increasing (Saklayen, 2018). Gamma glutamyl transpeptidase (GGT) is a biomarker for hepatocyte necrosis and surrogate marker for subclinical inflammation and independent risk factor for atherosclerosis. Individuals with metabolic syndrome having elevated GGT levels may render an increased risk for cardiovascular disease. Sheng et al. found that men with metabolic syndrome accompanied with elevated GGT harbor more “harmful gut microbes” compared those without elevated levels of GGT. Importantly, individuals with elevated GGT levels can be recognized through routine health checkout and intervention to reduce the “harmful gut microbes” may be implemented early for a better prognosis.

In the three original research articles, investigators focused on manipulations to affect gut microbiome to change the clinical outcomes in animal models. In a rat liver transplant model, Yuan et al. transferred heme oxygenase-1 (HO-1) gene transfected bone marrow mesenchymal stem cells (HO-1/BMMSCs) into steatotic liver recipient rats. Surprisingly, HO-1/BMMSCs enhanced levels of gut *Desulfovibrionaceae* which promote energy metabolism, especially lipid metabolism, and increased the levels of butyrate-producing bacteria, such as *Lachnospiraceae*. The changes of these gut bacterial composition contribute to the improved steatosis and improved the survival of the recipients. These results exemplified the “gut-liver axis.” Jin et al. investigated the mechanism of action of two weight loss drugs, orlistat and ezetimibe by analyzing the effect of them on

gut microbiome in animal models of high fat diet induced obesity. Orlistat significantly reduced the number of gut *Firmicutes*, *Alistipes*, and *Desulfovibrio* and simultaneously increased *Verrucomicrobia* and *Akkermansia*. In comparison, ezetimibe decreased *Proteobacteria* and *Desulfovibrio*, but increased *Bacteroides*. Apparently, orlistat and ezetimibe influenced different populations of gut bacteria although both can alleviate fat-diet induced obesity. Another group of investigators (Li Y. et al.) fed weaned piglets with different protein diets in their early life to observe the influence on growth of the animals. Three groups of animals were fed with 16% of proteins from fermented soybean (FSB) meal, fish meal (FM) or mixture of fish and soybean meal (MFSM), respectively. MFSM diet significantly improved growth performance of the animals. The effect was attributed to gut microbiome shaped by MFSM diet. Findings of these animal models have implications for human health and intervention of disease by manipulation of gut microbiome.

“抛砖引玉 (Casting a stone to attract jades)”—this Chinese saying reflects the intent of the topic editors. Research in some articles of this collection is preliminary and descriptive but has raised more questions to be answered. We hope investigators will be inspired for a deep dive into the insight of interaction between microbiome and host.

## Author contributions

All authors contributed to the manuscript drafting and revision. All authors contributed to the article and approved the submitted version.

## Conflict of interest

C-QC is employed by Innovent Biologics (USA).

The remaining authors declare that the research was conducted in the absence of any commercial or financial relationships that could be construed as a potential conflict of interest.

## Publisher's note

All claims expressed in this article are solely those of the authors and do not necessarily represent those of their affiliated organizations, or those of the publisher, the editors and the reviewers. Any product that may be evaluated in this article, or claim that may be made by its manufacturer, is not guaranteed or endorsed by the publisher.

## References

- Budden, K. F., Gellatly, S. L., Wood, D. L., Cooper, M. A., Morrison, M., Hugenholtz, P., et al. (2017). Emerging pathogenic links between microbiota and the gut-lung axis. *Nat. Rev. Microbiol.* 15, 55–63. doi: 10.1038/nrmicro.2016.142
- Lee, E. H., Kim, H., Koh, J. H., Cha, K. H., Lee, K. K., Kim, W. U., et al. (2022). Dysbiotic but nonpathogenic shift in the fecal mycobiota of patients with rheumatoid arthritis. *Gut Microbes* 14, 2149020. doi: 10.1080/19490976.2022.2149020
- Saklayen, M. G. (2018). The Global Epidemic of the Metabolic Syndrome. *Curr. Hypertens. Rep.* 20, 12. doi: 10.1007/s11906-018-0812-z
- Sun, X., Wang, Y., Li, X., Wang, M., Dong, J., Tang, W., et al. (2022). Alterations of gut fungal microbiota in patients with rheumatoid arthritis. *PeerJ* 10, e13037. doi: 10.7717/peerj.13037
- Yu, D., Du, J., Pu, X., Zheng, L., Chen, S., Wang, N., et al. (2021). The Gut Microbiome and Metabolites Are Altered and Interrelated in Patients With Rheumatoid Arthritis. *Front. Cell. Infect. Microbiol.* 11, 763507. doi: 10.3389/fcimb.2021.763507



# Comparison of Intestinal Microbes in Noninfectious Anterior Scleritis Patients With and Without Rheumatoid Arthritis

Mengyao Li, Li Yang, Liangliang Zhao, Feng Bai and Xiaoli Liu\*

Ophthalmologic Center of the Second Hospital, Jilin University, Changchun, China

## OPEN ACCESS

### Edited by:

Cong-Qiu Chu,  
Oregon Health and Science  
University, United States

### Reviewed by:

Chrysa Voidarou,  
University of Ioannina, Greece  
Lingshu Zhang,  
Sichuan University, China

### \*Correspondence:

Xiaoli Liu  
lpw\_lxl@126.com

### Specialty section:

This article was submitted to  
Microbial Symbioses,  
a section of the journal  
Frontiers in Microbiology

Received: 22 April 2022

Accepted: 23 May 2022

Published: 09 June 2022

### Citation:

Li M, Yang L, Zhao L, Bai F and  
Liu X (2022) Comparison of Intestinal  
Microbes in Noninfectious Anterior  
Scleritis Patients With and Without  
Rheumatoid Arthritis.  
Front. Microbiol. 13:925929.  
doi: 10.3389/fmicb.2022.925929

We compared intestinal microbes in anterior noninfectious scleritis patients with and without rheumatoid arthritis. Active noninfectious anterior scleritis patients without other immune diseases (G group, 16 patients) or with active rheumatoid arthritis (GY group, seven patients) were included in this study. Eight age- and sex-matched healthy subjects served as controls (N group). DNA was extracted from fecal samples. The V3-V4 16S rDNA region was amplified and sequenced by high-throughput 16S rDNA analysis, and microbial contents were determined. A significant decrease in species richness in the GY group was revealed by  $\alpha$ - and  $\beta$ -diversity analyses ( $p=0.02$  and  $p=0.004$ , respectively). At the genus level, 14 enriched and 10 decreased microbes in the G group and 13 enriched and 18 decreased microbes in the GY group were identified. Among them, four microbes were enriched in both the G and GY groups, including *Turicibacter*, *Romboutsia*, *Atopobium*, and *Coprobacillus*. Although two microbes (*Lachnospiraceae\_ND3007\_group* and *Eggerthella*) exhibited similar tendencies in the G and GY groups, changes in these microbes were more significant in the GY group ( $p<0.05$ ). Interaction analysis showed that *Intestinibacter*, *Romboutsia*, and *Turicibacter*, which were enriched in both the G and GY groups, correlated positively with each other. In addition, nine microbes were decreased in the GY group, which demonstrates a potential protective role for these microbes in the pathogenesis of scleritis via interactions with each other.

**Keywords:** intestinal microbes, scleritis, rheumatoid arthritis, noninfectious anterior scleritis, *Turicibacter*, *Romboutsia*, *Atopobium*, *Coprobacillus*

## INTRODUCTION

Scleritis is an immune-mediated disease with initial symptoms of red eyes and pain. Scleritis can be divided into anterior scleritis and posterior scleritis according to anatomical location. Furthermore, anterior scleritis can be divided based on clinical manifestations into nodular anterior scleritis, diffuse anterior scleritis and necrotizing anterior scleritis. Overall, the pathogenesis of scleritis has not been completely elucidated. Although the immune response and infection are considered the main two causes of anterior scleritis, scleritis caused by direct infection of the sclera by pathogenic microorganisms such as bacteria is relatively rare. More than 50% of scleritis cases are associated with immune-mediated diseases, including rheumatoid arthritis and antineutrophil

cytoplasmic antibody (ANCA)-associated granulomatosis (GPA; Vergouwen et al., 2020). Among them, rheumatoid arthritis is the most common immune-mediated disease associated with scleritis, and 8%–15% of patients with scleritis have rheumatoid arthritis (RA; Promelle et al., 2021). It has been reported that the level of anti-cyclic citrullinated peptide antibody in RA patients correlates strongly with the severity of ocular manifestations, including scleritis (Vignesh and Srinivasan, 2015). The mechanism of rheumatoid arthritis-associated scleritis is unclear and may be related to the similar structure between the synovium and sclera. Indeed, cells infiltrating the synovium of patients with RA and the sclera of patients with scleritis are similar (Wakefield et al., 2013). Furthermore, HLA-DR4, HLA-DR1, HLA-DR13, and HLA-DR15 are significantly associated with scleritis complicated with RA (Karami et al., 2019).

Intestinal microbes are closely related to the occurrence of RA. However, the role of intestinal microbiota in the pathogenesis of scleritis has not been reported, and whether the intestinal microbiota involved in RA is also related to scleritis is still unknown. Therefore, we investigated the relationship between intestinal microbes and scleritis by comparing intestinal microbes between noninfectious scleritis patients with and without RA. Our results showed four bacterial genera to be enriched in noninfectious anterior scleritis patients both with and without RA, including *Coprobacillus*, *Romboutsia*, *Atopobium*, and *Turicibacter*. In addition, the abundances of three microbes (*Candidatus\_Stoquefichus*, *Anaeroplasma*, and *Lactococcus*) were altered in noninfectious anterior scleritis patients without other immune-mediated diseases, and the abundances of nine microbes (*Eubacterium\_eligens\_group*, *Odoribacter*, *Family\_XIII\_UCG-001*, *Ruminiclostridium\_9*, *Ruminococcaceae\_UCG-003*, *Ruminococcaceae\_UCG-009*, *Eubacterium\_rectale\_group*, *Roseburia*, and *Catabacter*) were changed in noninfectious anterior scleritis patients with RA. All these results suggest that intestinal microbes have coexisting identical and distinct roles in the development of scleritis in patients with and without RA.

## MATERIALS AND METHODS

### Participants

Thirty-one individuals were enrolled in the study, including 16 patients with active noninfectious anterior scleritis (G group, average age:  $56.1 \pm 7.8$  years, male/female: 0.14:1), seven patients with active noninfectious anterior scleritis combined with active RA (GY group, average age:  $59.7 \pm 10.1$  years, male/female: 0.16:1),

and eight healthy controls without immune-mediated diseases (N group, average age:  $56.1 \pm 10.5$  years, male/female: 0.14:1). Healthy controls consisted of family members from scleritis patients and age-related cataract patients without immune-mediated diseases. There was no significant difference in age or sex among the three groups in this study. The inclusion criteria for individuals enrolled in the study were as follows: (1) without other immune system diseases, such as ulcerative colitis, systemic lupus erythematosus, or Crohn's disease; (2) without infectious disease; and (3) patients in the active stage of disease and not taking any medications. The diagnosis of noninfectious anterior scleritis was based on characteristic clinical manifestations, including ocular tenderness to touch, painful inflammation radiating to the forehead, edema affecting episcleral and scleral tissues, and injections of both the superficial and deep episcleral vessels (Dutta Majumder et al., 2020). The diagnosis of active RA was based on the American College of Rheumatology/European League Against Rheumatism 2010 criteria for RA, including confirmed presence of synovitis in at least one joint, absence of an alternative diagnosis better explaining the synovitis, and a total score of 6 or greater (of a possible 10) from the individual scores in the following four domains: number and site of involved joints (range 0–5), serological abnormality (range 0–3), elevated acute-phase response (range 0–1), and symptom duration (two levels; range 0–1; Aletaha et al., 2010). Informed consent was obtained from all subjects. This study met the requirements of the Declaration of Helsinki and was approved by the Clinical Ethics Committee.

### Fecal Sample Collection and DNA Extraction

Feces were collected from patients with anterior scleritis and healthy controls admitted to the Ophthalmologic Center of the Second Hospital between July 2018 and December 2019 and stored at  $-80^{\circ}\text{C}$  for analysis. DNA extraction from feces was performed according to E.Z.N.A. Stool DNA Kit (Omega Bio-Tek, Norcross, GA, United States) following the manufacturer's instructions. The quality of the extracted DNA was assessed by 1% agarose gel electrophoresis and spectrophotometry (260/280 nm optical density ratio). The target sequence that needed to be amplified was introduced in the sequencing of the 16S ribosomal RNA (rRNA) gene amplicon.

### Sequencing of 16S rRNA Gene Amplicons

The extracted DNA was sent to Beijing Aowei Gene Technology Co., Ltd. (Beijing, China). We referred to previously reported experimental methods to amplify the target gene (Li et al., 2022), as follows. We detected the DNA using the Illumina MiSeq PE300 platform (Santiago, CA, United States) and used the universal primers 338F (5'-ACTCCTACGGGAGGCAGCAG-3') and 806R (5'-GGACTACNNGGG TATCTAAT-3') to amplify the V3 to V4 16S ribosomal DNA (rDNA) region. Next, we amplified the target sequence by polymerase chain reaction.

### Sequence Analysis

We used previously reported experimental methods to analyze the sequence (Li et al., 2022) as follows. Paired-end sequencing

**Abbreviations:** ANCA, Antineutrophil cytoplasmic antibody; HLA-DR, Human leukocyte antigen DR; RA, Rheumatoid arthritis; DNA, Deoxyribonucleic acid; RNA, Ribonucleic acid; 16S rRNA, 16S Ribosomal RNA; OTU, Operational taxonomic unit; ACE, Abundance-based coverage estimator; LDA, Linear discriminant analysis; LEfSe, LDA effect Size; AMOVA, Analysis of Molecular Variance; VKH, Vogt-Koyanagi-Harada Syndrome; MMPs, Matrix metalloproteinases; TIMPs, Tissue inhibitor of matrix metalloproteinases; H<sub>2</sub>S, Hydrogen sulfide; SCFA, Short-chain fatty acid; CD, Crohn's disease; UC, Ulcerative colitis; MS, Multiple sclerosis; G, Patients with active noninfectious anterior scleritis; GY, Patients with active noninfectious anterior scleritis combined with active rheumatoid arthritis; N, Healthy controls without immune-mediated diseases.



of the target sequence was performed using the Illumina MiSeq platform, and QIIME (Professor Gregory Caporaso, Flagstaff, United States; version 1.8.0) was used to filter, split, and remove chimeras. Sequences with scores less than 20 or that had base ambiguity, primer mismatch, or a length less than 150bp were excluded. The sequences were clustered and grouped as operational taxonomic units (OTUs) based on barcodes. We set the OTU similarity to 97%, and we matched every OTU to corresponding species classification information by comparison with the Silva database. Then, we calculated the microbial  $\alpha$ -diversity, including the Shannon, abundance-based coverage estimator (ACE), and Chao1 indices, in Mothur (version 1.31.2, Professor Patrick Schloss; MI, United States). The species communities of each sample were compared, and  $\beta$ -diversity was calculated by UniFrac. Clustering was performed using ph heatmap in TBtools (version 1.098652, Chengjie, Chen; Guangzhou, China) based on the weighted UniFrac distance. The data are presented based on the row scale. Raw reads were uploaded to the Sequence Read Archive (SRA) database on the National Center for Biotechnology Information website. The BioProject ID is PRJNA836534.

## Statistical Analysis

To explore differences between groups, Mothur software (version 1.31.2) was used to perform Metastats analysis, and a  $p < 0.05$  indicated significance. Linear discriminant analysis (LDA) coupled with effect size (LEfSe) was performed using Galaxy (The Huck Institutes of the Life Sciences, The Institute for CyberScience at Penn State, and Johns Hopkins University, United States). Only data with a  $p < 0.05$  and a log LDA score  $> 2$  are reported. Spearman correlation analysis was used as the mapping parameter of the correlation diagram. We visualized and analyzed the network using the personalbio platform (Zikui Sun, Shanghai, China), and the correlation was  $|R| > 0.6$ ,  $p < 0.05$ .

## RESULTS

### Microbiome Species Diversity and Number of Samples Sequenced

The  $\alpha$ -diversity (Chao1, observed\_species, PD\_whole\_tree, and Shannon) and  $\beta$ -diversity [analysis of molecular variance (AMOVA)] of the intestinal microbes in each group were analyzed (Figures 1A,B). According to  $\alpha$ -diversity analysis, the species in the N group were most abundant, followed by the G and GY groups, and there were significant differences in species richness between the N and GY ( $p = 0.02$ ) groups. Differences in species richness between the N and GY ( $p = 0.004$ ) groups were detected by  $\beta$ -diversity analysis, and differences between the G and GY ( $p = 0.04$ ) groups were significant.

We examined the number of reads sampled and found that the number of OTUs did not further increase with an increase in the number of samples sequenced. Thus, the sequencing depth and coverage were sufficient to cover the total diversity of the microbiomes examined (Figure 1C).

### Changes in Intestinal Microbes in Noninfectious Anterior Scleritis Patients Without Other Immune-Related Diseases

To investigate microbes involved in the pathogenesis of noninfectious anterior scleritis, we screened microorganisms with significantly different abundances between healthy people (Group N) and patients with noninfectious anterior scleritis without RA (Group G; Figure 2A).

At the genus level, 14 enriched and 10 decreased microbes were detected in the G group. Among these enriched microbes, six were only detected in Group G, including *Rikenellaceae\_RC9\_gut\_group*, *Candidatus\_Stoquefichus*, *Anaeroplasmataceae*, *Enterorhabdus*, *Howardella*, and *Coprobaecillus*. Eight microbes were detected in both Group G and Group N, but the contents in the former were higher, including *Prevotella*, *Megasphaera*, *Romboutsia*, *Intestinibacter*, *Lactobacillus*, *Atopobium*, *Turicibacter*, and *Eggerthella*. Among the 10 microbes with decreased abundance, 4 were only detected in Group N: *Senegalimassilia*, *Dielma*, *Gelria*, and *Prevotellaceae\_Ga6A1\_group*. Six microbes were detected in both Group G and Group N, but the content in Group G was lower, including *Ruminococcaceae\_UCG-007*, *Lactococcus*, *Holdemanella*, *Cellulosilyticum*, *Lachnospiraceae\_ND3007\_group*, and *Lactonifactor*.

To identify possible biomarkers, LEfSe analysis was performed to examine different microbial features between active noninfectious anterior scleritis patients and healthy controls. The results were similar to those above, with enrichment of *Romboutsia*, *Turicibacter*, and *Eggerthella* and a decrease in *Lachnospiraceae\_ND3007\_group*, *Holdemanella*, and *Dielma* in the G group (Figure 2B).

At the family level, *Anaeroplasmataceae*, *Family\_XI*, *Peptostreptococcaceae*, and *Lactobacillaceae* were increased and *Thermoanaerobacteraceae* and *Flavobacteriaceae* decreased. At the order level, *Anaeroplasmatales* and *Selenomonadales* were enriched, whereas *Thermoanaerobacterales* and *Flavobacteriales* were reduced. At the class level, *Negativicutes* was increased and *Flavobacteriia* decreased. At the phylum level, *Saccharibacteria* showed enrichment.

### Changes in Intestinal Microbes in Noninfectious Anterior Scleritis Patients With RA

Next, we screened microbes with significantly different abundances in noninfectious anterior scleritis patients with RA (GY group; Figure 2C).

At the genus level, 13 enriched and 18 decreased microbes were detected in the GY group. Among the enriched microbes, four were only detected in the GY group, including *Peptoniphilus*, *Anaerofustis*, *Catabacter*, and *Coprobaecillus*. Nine microbes were detected in Group GY and Group N, but the content in Group GY was higher than that in Group N, including *Clostridium\_innocuum\_group*, *Leuconostoc*, *Atopobium*, *Turicibacter*, *Peptoclostridium*, *Eggerthella*, *Enterococcus*, *Subdoligranulum*, and *Romboutsia*. The 18 microbes with decreased abundance in the GY group included *Bilophila*, *Eubacterium\_eligens\_group*, *Odoribacter*, *Eubacterium*—

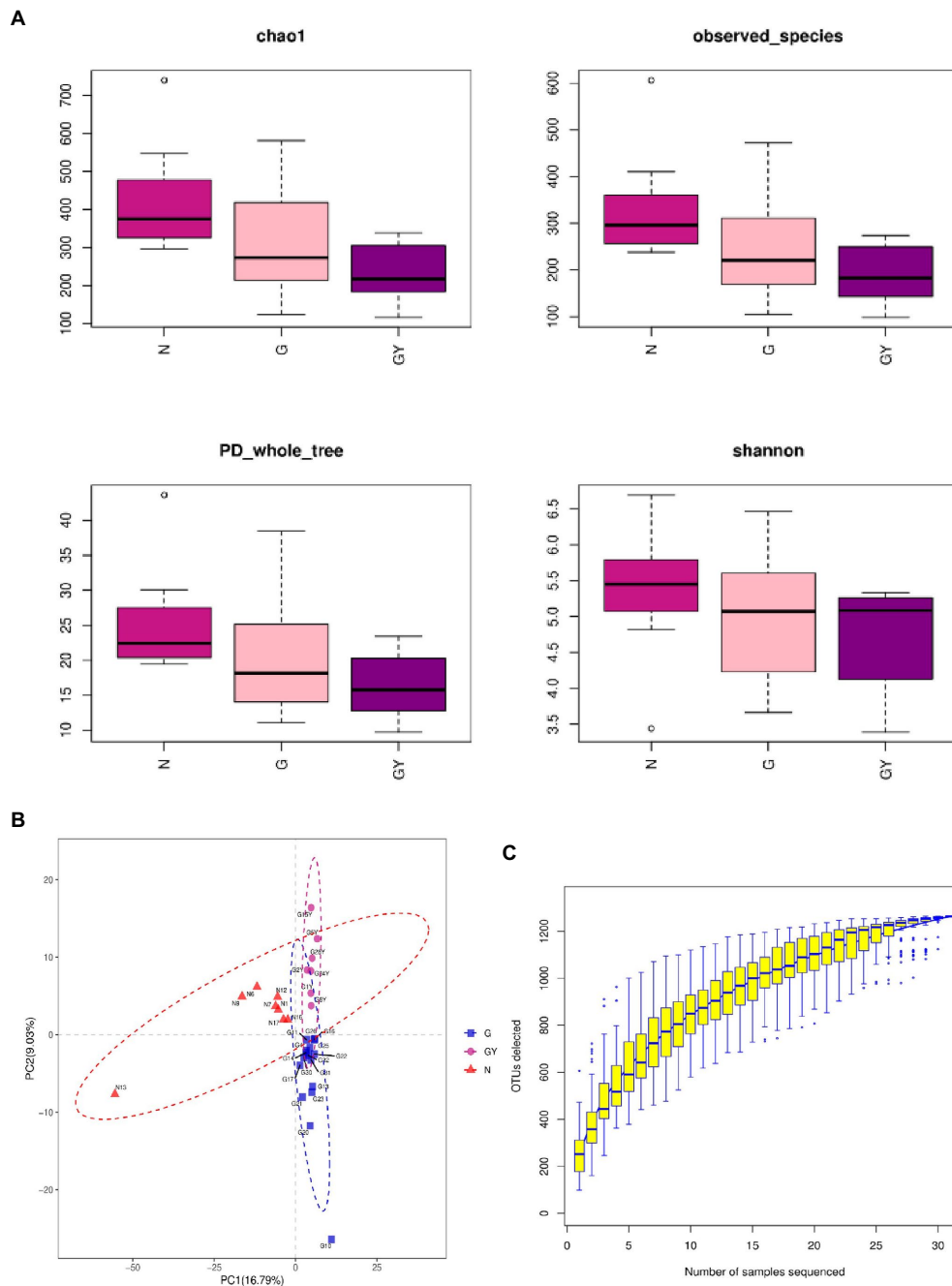


**FIGURE 1 | (A)**  $\alpha$ -Diversity using the Chao1, observed OTUs, PD\_whole\_tree, and Shannon measures for patients with active noninfectious anterior scleritis, patients with active noninfectious anterior scleritis combined with active rheumatoid arthritis, and healthy controls. **(B)**  $\beta$ -Diversity was assessed by analysis of molecular variance (ANOVA) in patients with active noninfectious anterior scleritis, patients with active noninfectious anterior scleritis combined with active rheumatoid arthritis, and healthy controls. **(C)** Rarefaction curves of the gut microbes from 16 patients with active noninfectious anterior scleritis, seven patients with active noninfectious anterior scleritis combined with active rheumatoid arthritis, and 11 healthy controls.

*ruminantium\_group*, *Family\_XIII\_UCG-001*, *Ruminococcaceae\_UCG-005*, *Ruminoclostridium\_9*, *Ruminococcaceae\_UCG-003*, *Lachnospiraceae\_NK4A136\_group*, *Parabacteroides*, *Ruminococcaceae\_UCG-009*, *Paraprevotella*, *Eubacterium\_rectale\_group*, *Butyrivibrio*, *Roseburia*, *Ruminococcaceae\_UCG-002*, *Lachnospira*, and *Lachnospiraceae\_ND3007\_group*. The

*Intestinibacter* content in the GY group was higher than that in the N group, but the difference was not significant.

In LefSe analysis of was performed to examine microbial features between noninfectious anterior scleritis patients with RA and healthy controls. Similar findings were found, including *Subdoligranulum*, *Peptoclostridium*, and *Eggerthella* enrichment

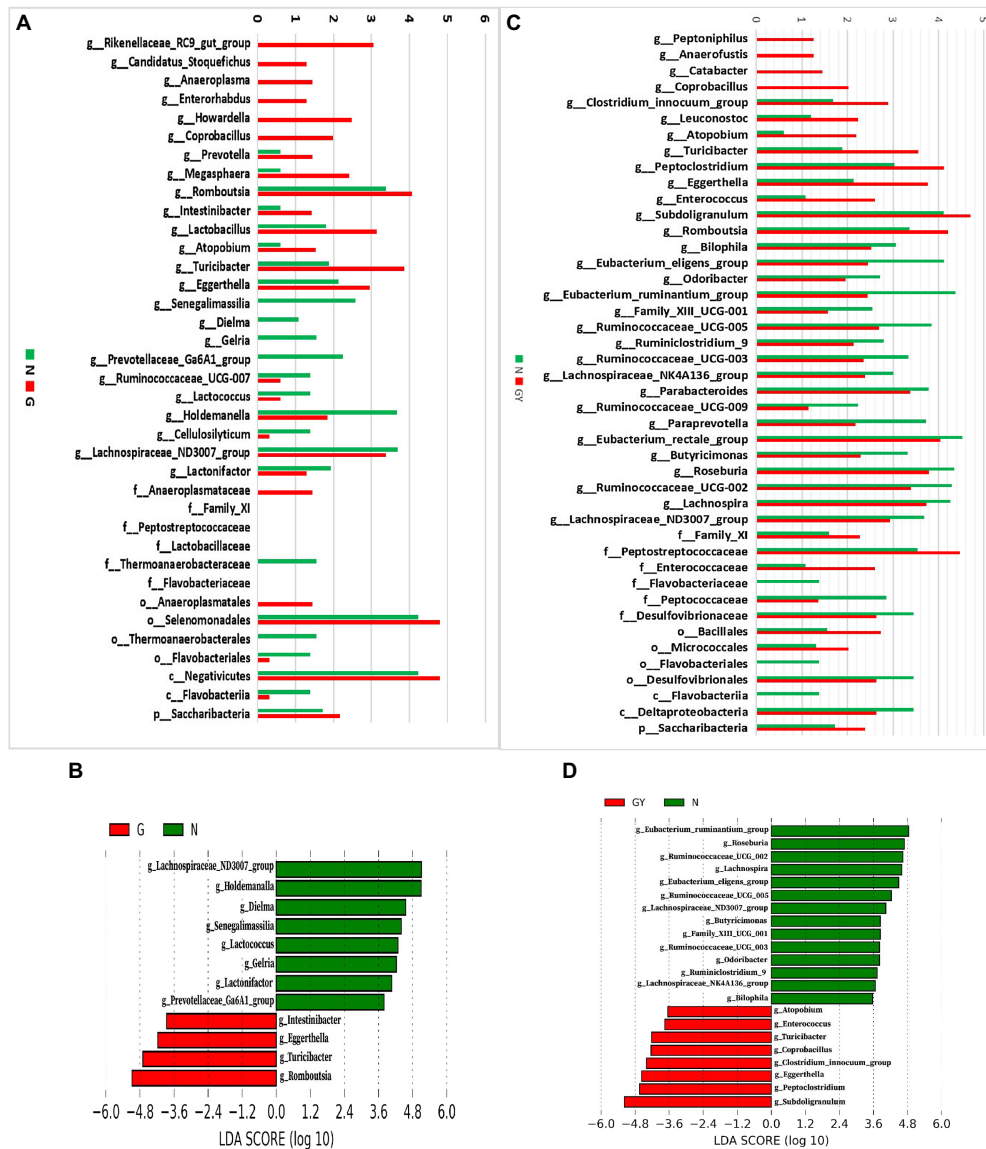


**FIGURE 2 | (A)** Relative abundance of microbes in 16 patients with active noninfectious anterior scleritis (G) and 11 healthy controls (N); **(B)** Linear discrimination analysis (LDA) effect size (LEfSe) analysis results comparing active noninfectious anterior scleritis patients (G) and 11 healthy controls (N); **(C)** Relative abundance of microbes in seven patients with active noninfectious anterior scleritis combined with active rheumatoid arthritis (GY) and 11 healthy controls (N); **(D)** LDA LEfSe analysis results comparing patients with active noninfectious anterior scleritis combined with active rheumatoid arthritis (GY) and 11 healthy controls (N). The content of microbes **(A,C)** was increased by  $10^6$ -fold; the logarithm was taken, and the base number was 10. LDA scores **(B,D)** ( $\log_{10}$ )  $> 2$  are listed.

and decreases in *Eubacterium\_ruminantium\_group*, *Roseburia*, and *Ruminococcaceae\_UCG-002* in the GY group (Figure 2D).

At the family level, *Family\_XI*, *Peptostreptococcaceae*, and *Enterococcaceae* were enriched in the GY group, but *Flavobacteriaceae*, *Peptococcaceae*, and *Desulfovibrionaceae* were decreased. *Bacillales* and *Micrococcales* were enriched at the order level, whereas *Flavobacteriales* and *Desulfovibrionales* were decreased. *Flavobacteriia* and *Deltaproteobacteria* were decreased at the class level, and *Saccharibacteria* was enriched at the phylum level (Figure 2C).

## Comparison of Intestinal Microbes Between the Two Groups of Patients

To identify microbes related to noninfectious scleritis, we compared the three groups and divided microorganisms into four types (Figure 3).

### Type A

Four microbes were enriched in both Groups G and GY, including *Coprobacillus* (both  $p < 0.05$ ), *Romboutsia* (both



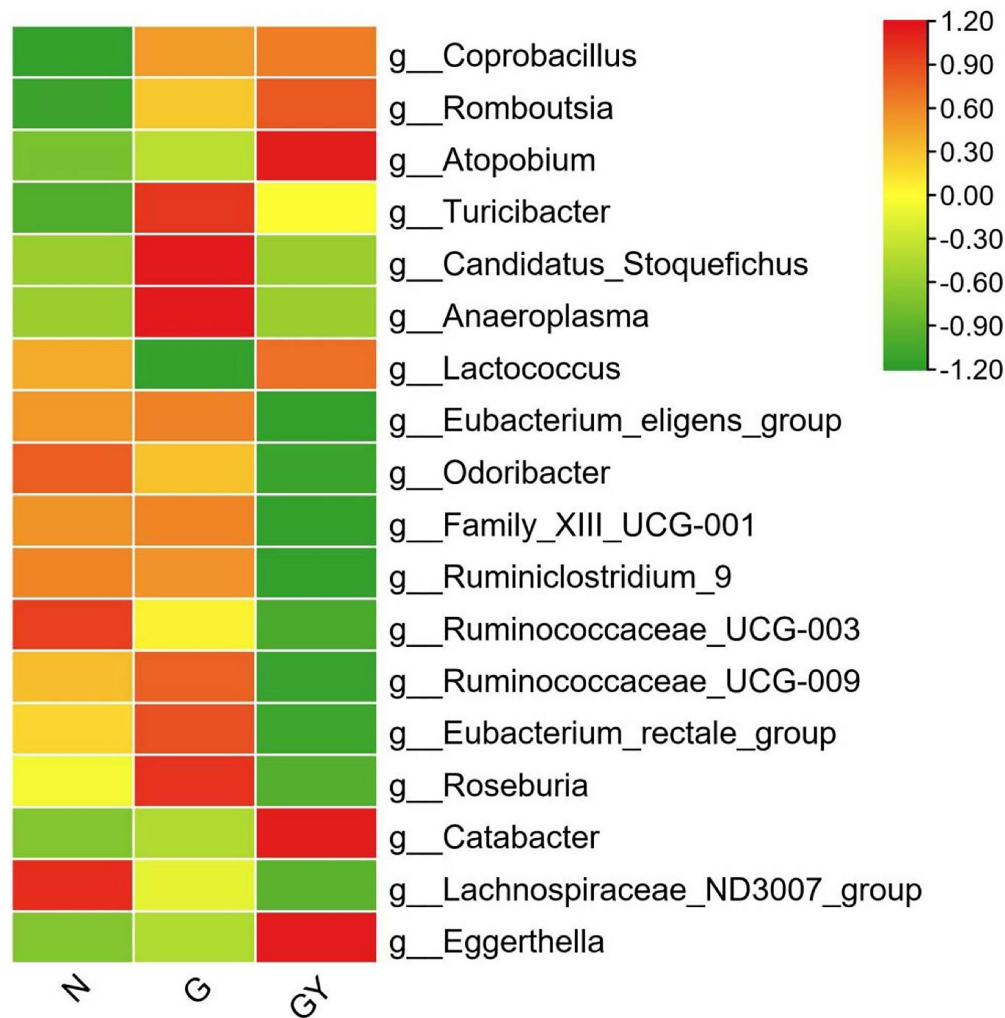


**FIGURE 3 |** Relative abundance of microbes from 16 patients with active noninfectious anterior scleritis (G), seven patients with active noninfectious anterior scleritis combined with active rheumatoid arthritis (GY), and 11 healthy controls (N). The content of microbes is presented based on the row scale.

$p < 0.01$ ), *Atopobium* (both  $p < 0.05$ ), and *Turicibacter* (both  $p < 0.01$ ). The abundances of these microbes were significantly different between Groups N and G or GY, but there was no significant difference between Groups G and GY. We consider these microbes to be related to the pathogenesis of scleritis.

### Type B

Microbes were enriched or decreased only in the G group, and not in the GY group, including *Candidatus\_Stoquefichus*, *Anaeroplasm*, and *Lactococcus*. We consider that these microbes may be specifically related to scleritis pathogenesis.

### Type C

Microbes were enriched or decreased only in the GY group, and not in Group G, including *Eubacterium\_eligens\_group*, *Odoribacter*, *Family\_XIII\_UCG-001*, *Ruminiclostridium\_9*, *Ruminococcaceae\_UCG-003*, *Ruminococcaceae\_UCG-009*, *Eubacterium\_rectale\_group*, *Roseburia*, and *Catabacter*.

We consider these microbes to be related to the pathogenesis of RA or the shared pathogenesis pathway of scleritis and RA.

### Type D

Two microbes (*Lachnospiraceae\_ND3007\_group*, *Eggerthella*) that exhibited similar abundances in both the G and GY groups. The abundance of *Lachnospiraceae\_ND3007\_group* was decreased and that of *Eggerthella* enriched. The changes in both the G and GY groups were significant compared with those in the N group, but the *Eggerthella* content was higher and the *Lachnospiraceae\_ND3007\_group* content lower in the GY group than in the G group. Interestingly, these two microbes also exhibited similar changes between patients with active VKH and patients with scleritis (Li et al., 2022). This result suggests that these two microbes may be nonspecifically involved in various immune-related eye diseases. Whether the content of these two microbes in each disease correlates with the severity of eye disease needs to be further studied.

## Interactions Between Microbes

To better understand the role of these microbes, we analyzed the interaction of these significantly changed microbes using the personalbio platform and identified three modules. The first is the module associated with active anterior scleritis, which included *Intestinibacter*, *Romboutsia*, and *Turicibacter*; all were enriched in both the G and GY groups and correlated positively with each other. This suggests that these microbes participate in the pathogenesis of noninfectious scleritis by promoting each other (**Figure 4A**).

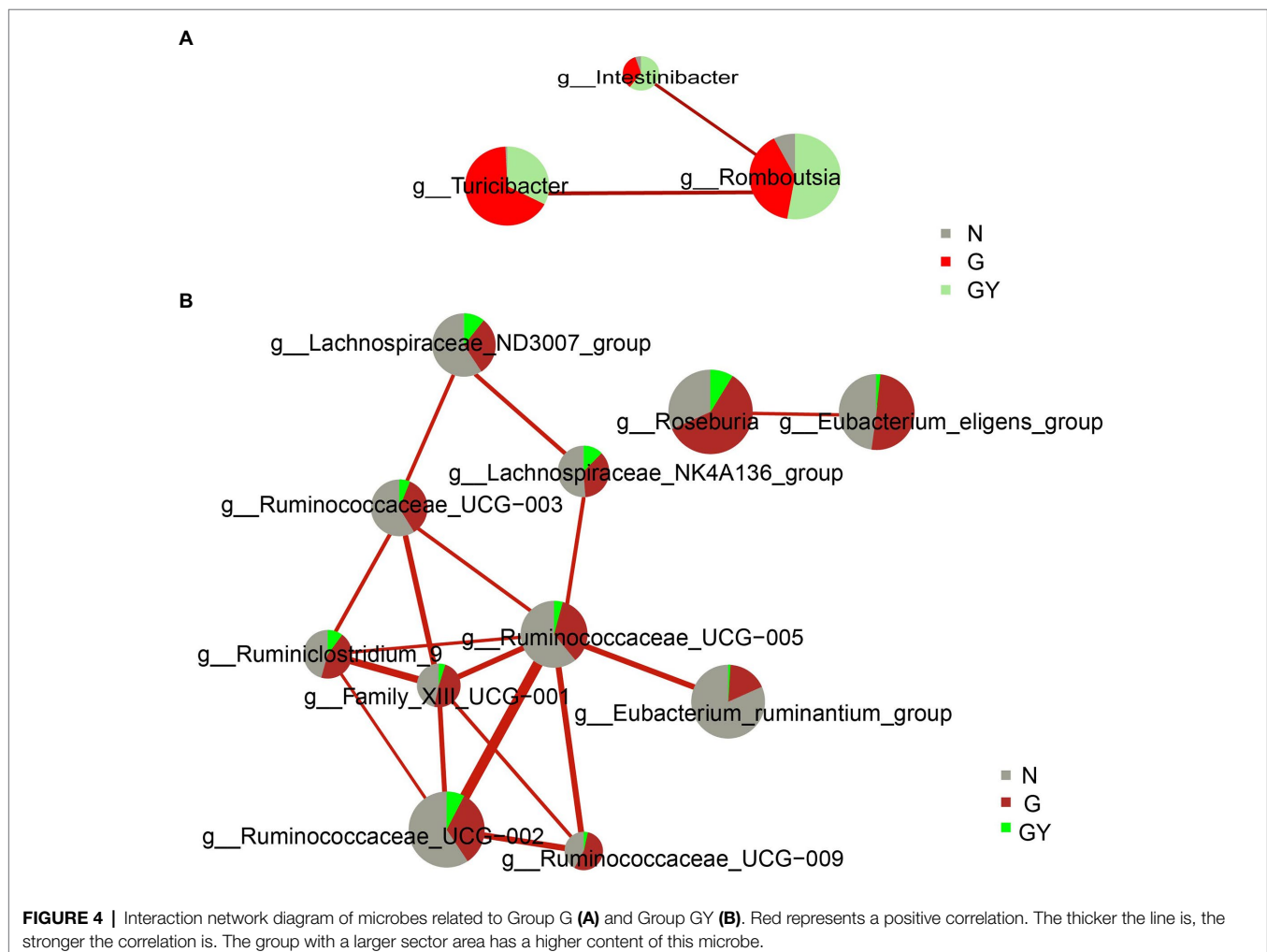
The second module is associated with RA or the shared pathogenesis pathway of scleritis and RA, including the following nine microbes with decreased contents: *Family\_XIII\_UCG-001*, *Eubacterium\_ruminantium\_group*, *Ruminococcus\_UCG-002*, *Ruminococcus\_UCG-003*, *Ruminococcus\_UCG-005*, *Ruminococcus\_UCG-009*, *Lachnospiraceae\_NK4A136\_group*, *Lachnospiraceae\_ND3007\_group*, and *Ruminiclostridium\_9*. These microbes were decreased in both the GY and G groups; however, the difference was significant only in the former. Hence, these microbes may play a protective role in the pathogenesis of RA or the shared pathogenesis pathway of scleritis and RA. In addition, *Ruminococcaceae\_UCG-005* and *Family\_XIII\_UCG-001* were at the

center of the association network and closely associated with other microbes. Therefore, we consider that these two microbes may play a key role in the whole mechanism of action (**Figure 4B**).

The third module included two microbes (*Eubacterium\_eligens\_group*, *Roseburia*), which only exhibited significantly decreased contents in the GY group and were negatively related to each other. The final consequence of the mutual negative regulation between the two microbes appears to be related to the pathogenesis of RA or the shared pathogenesis pathway of scleritis and RA (**Figure 4B**).

## DISCUSSION

At the genus level, compared with healthy controls, noninfectious anterior scleritis patients without rheumatoid arthritis showed 14 enriched and 10 decreased microbes, whereas noninfectious anterior scleritis patients with rheumatoid arthritis showed 13 enriched microbes and 18 decreased microbes. Among them, four bacterial genera exhibited the same changes between the G and GY groups. This result suggests that these four genera may be related to noninfectious anterior scleritis.



*Lachnospiraceae\_ND3007\_group* and *Eggerthella* are detected in both anterior scleritis and active-onset VKH patients, indicating that they may be nonspecifically involved in various immune-related eye diseases. The biomarkers of each group were analyzed by LEFse, and the interaction between these microbes was explored by a correlation diagram.

By analyzing  $\alpha$ - and  $\beta$ -diversity, we found a significant decrease in species richness in the GY group compared with the G and N groups, indicating more severe intestinal dysbiosis in the GY group. This finding suggests that such changes in intestinal microbes may be closely related to the pathogenesis of active anterior scleritis with RA. However, whether the change in intestinal microbes is associated with the severity of scleritis needs to be further evaluated.

To explore microbes related to scleritis, we referred to a series of studies on changes in intestinal microbes in patients with RA (Figure 5; de Oliveira et al., 2017; Maeda and Takeda, 2017, 2019; Forbes et al., 2018; Xu et al., 2020; Chu et al., 2021; Reyes-Castillo et al., 2021). Comparing these reported microbes with our results, *Turicibacter* and *Eggerthella* enrichment and *Lachnospiraceae* reduction were found in Groups G and GY and patients with RA. Therefore, these microbes may be involved in the pathogenesis of both scleritis and RA. Increases in *Romboutsia*, *Atopobium* and *Coprobaecillus* were found in both Groups G and GY but not in patients with RA, indicating that these microbes may be closely related to the pathogenesis of scleritis. As decreased abundances of *Eubacterium*, *Odoribacter*, *Roseburia*, and *Ruminococcaceae* were observed in GY group

and RA patients, these microbes may be closely related to the pathogenesis of RA.

The mechanisms of these microbes involved in the occurrence of scleritis are not completely clear. It has been proven that increases in IL-1 $\beta$ , TNF- $\alpha$  and IL-6 play a key role in the pathogenesis of scleritis and that biological agents such as antitumor necrosis factor agents and interleukin-1 and interleukin-6 inhibitors control scleral inflammation either in an idiopathic manner or in a background of immune-mediated systemic disorders (Sota et al., 2021). *Romboutsia* and *Turicibacter* are positively related to IL-6, IL-1 $\beta$ , TNF- $\alpha$ , IL-23 and IFN- $\gamma$  (Bosshard et al., 2002; Munyaka et al., 2016; Li et al., 2020). These cytokines can lead to an increase in macrophages and B cells, which are important in the pathogenesis of scleritis (Nishio et al., 2021). In addition, TNF- $\alpha$  elevates the level of MMPs, which may disrupt the balance between MMPs (MMP3 and MMP9) and TIMPs and induce scleritis (Wakefield et al., 2013; Vergouwen et al., 2020). Our results show *Romboutsia* and *Turicibacter* to be enriched and promote each other in active anterior scleritis patients with and without RA. Hence, these two microbes may participate in the pathogenesis of scleritis by increasing inflammatory cytokines, which in turn induce a subsequent immune response. *Lactococcus lactis* is also related to inflammatory cytokines. Simčić et al. found that *L. lactis* effectively downregulates the TNF- $\alpha$  response (Simčić et al., 2019). In patients with active anterior scleritis, decreased *Lactococcus* indicates reduced ability to downregulate TNF- $\alpha$ , which in turn causes disease via relatively elevated TNF- $\alpha$

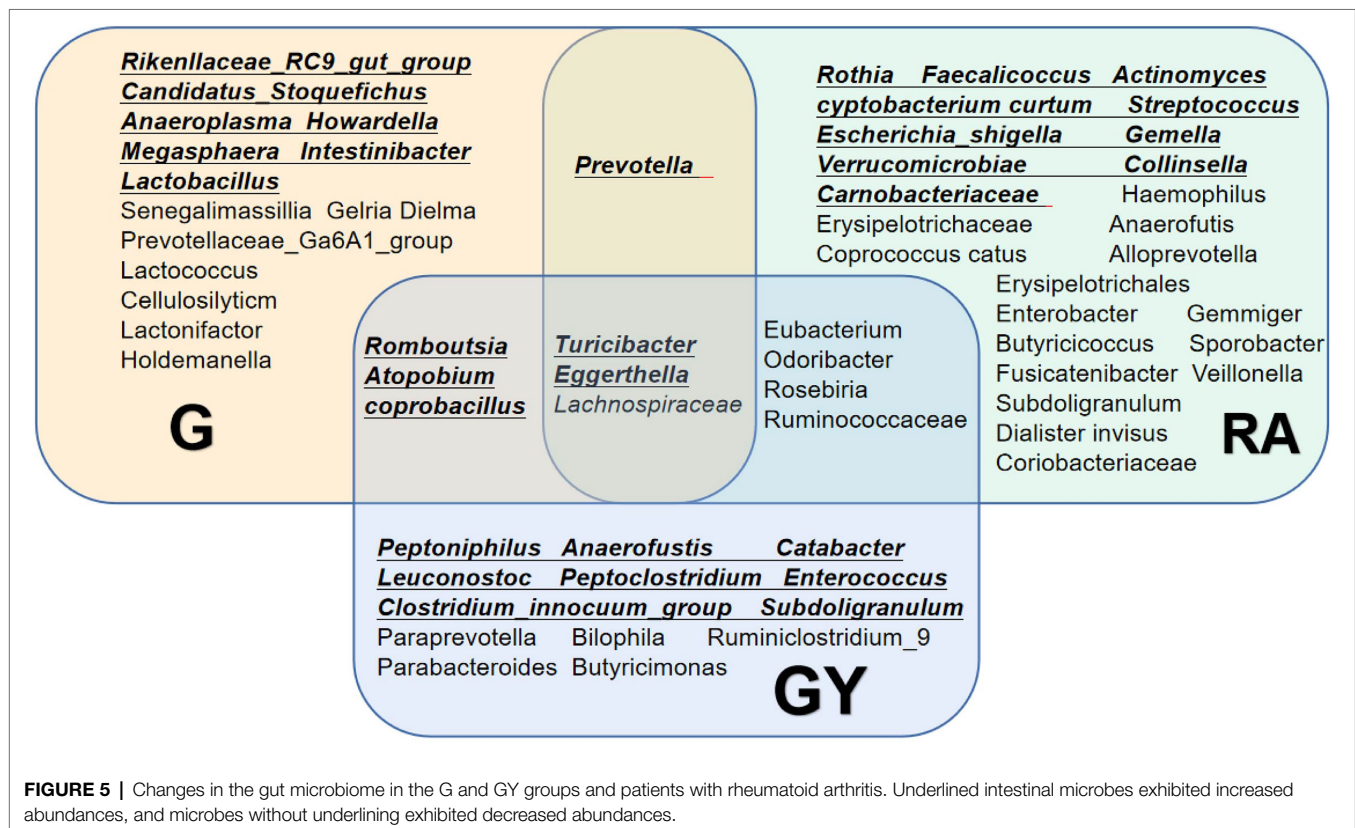


**FIGURE 5 |** Changes in the gut microbiome in the G and GY groups and patients with rheumatoid arthritis. Underlined intestinal microbes exhibited increased abundances, and microbes without underlining exhibited decreased abundances.

levels. Enriched *Atopobium* was found in both the G and GY groups. It has been reported that *Atopobium* is an H<sub>2</sub>S-producing bacterium (Yang and Jobin, 2017), and an increase in H<sub>2</sub>S can exacerbate intestinal epithelial barrier damage (Ye et al., 2018). In our patients, enriched *Atopobium* may be involved in the pathogenesis of scleritis through this mechanism.

The mechanism by which these microbes became decreased only in Group GY, and not in Group G (Type C), is related to SCFAs. Previous studies have shown that a decrease in SCFA levels is closely related to the pathogenesis of RA (Yang and Cong, 2021). *Odoribacter* (Turna et al., 2020), *Roseburia* (Tamanai-Shacoori et al., 2017), and *Ruminiclostridium\_9* (Hsiao et al., 2021) are butyrate producers (butyrate is a type of SCFA); *Ruminococcaceae* (Kang et al., 2017) and *Eubacterium* (Li et al., 2022) are short-chain fatty acid (SCFA) producers. In our patients, the abundances of all these microbes were decreased, as was SCFA production. However, whether the decrease in SCFA also promotes the occurrence of scleritis needs to be further explored.

An increase in *Eggerthella* and a decrease in *Lachnospiraceae* were found in both the G and GY groups, with the changes in the latter being more severe. *Lachnospiraceae* is an SCFA producer, and the decreased abundance of *Lachnospiraceae\_ND3007\_group* may have decreased SCFA production (Kang et al., 2017). *Eggerthella* enrichment might induce inflammatory cytokines, including TNF- $\alpha$ , IL-1 $\beta$ , and IL-6 (Li et al., 2022). An increase in *Eggerthella* and a decrease in *Lachnospiraceae* have also been found in other immune-mediated diseases, including Vogt–Koyanagi–Harada (VKH; Li et al., 2022) Crohn's disease (CD), ulcerative colitis (UC) and multiple sclerosis (MS; Forbes et al., 2018). This result suggests that the roles of *Eggerthella* and *Lachnospiraceae* are not specific. The content of *Lachnospiraceae\_ND3007\_group* was lower and that of *Eggerthella* higher in the GY group. Whether the levels of these two microbes are related to the severity of eye disease needs to be further studied.

Our study suggests the existence of a gut-eye axis. Intestinal dysbiosis may be a crucial factor influencing ocular diseases. Dysbiosis of the intestinal microbiota causes upregulated expression of inflammatory cytokines in peripheral blood, which in turn causes ocular inflammation. In addition, the gut microbiota may cause extraintestinal diseases, including RA, through antigenic mimicry (Pianta et al., 2017). These are potential pathways or mechanisms by which dysbiosis induces autoimmunity and the link with scleritis or RA-associated physiopathology.

In conclusion, our study indicates that intestinal microbes are involved in the pathogenesis of noninfectious anterior scleritis in patients with and without rheumatoid arthritis. The roles of these microbes are both pathogenic and protective.

They may participate in the pathogenesis of anterior scleritis by interacting with each other and altering immunity.

## LIMITATION

This is a descriptive study about changes in intestinal microbes in noninfectious anterior scleritis patients with and without RA, and there is a lack of research on the mechanisms by which these altered intestinal microbes cause scleritis. As there is currently no accepted animal model of anterior scleritis, it is not feasible to validate the mechanisms of these intestinal microbes. *In vitro* studies of the effects of these intestinal microbes on patient's immune cells might provide some clues. Additionally, whether the extent of these changed microbes correlates with the severity of scleritis requires further investigation.

## DATA AVAILABILITY STATEMENT

The original contributions presented in the study are included in the article/supplementary material, further inquiries can be directed to the corresponding author.

## ETHICS STATEMENT

This study was approved by the Ethics Committee of the Second Hospital of Jilin University. The number is 2021120. The patients/participants provided their written informed consent to participate in this study.

## AUTHOR CONTRIBUTIONS

ML: data collection and analysis and writing the manuscript. LY, FB, and LZ: collection of samples, data analysis, and editing the manuscript. XL: acquisition of funding, supervision and planning of experiments, data analysis, and writing the manuscript. All authors contributed to the article and approved the submitted version.

## FUNDING

This work was supported by the National Natural Science Foundation of China, grant no. 81300752, the Jilin Province Science and Technology Development Plan Project, grant no. 20200201333JC, and the Jilin Province Health Special Project, grant no. 2020SCZT058.

## REFERENCES

- Aletaha, D., Neogi, T., Silman, A. J., Funovits, J., Felson, D. T., Bingham, C. O. 3rd, et al. (2010). 2010 rheumatoid arthritis classification criteria: an American College of Rheumatology/European League Against Rheumatism collaborative initiative. *Ann. Rheum. Dis.* 69, 1580–1588. doi: 10.1136/ard.2010.138461
- Bosshard, P. P., Zbinden, R., and Altwegg, M. (2002). *Turicibacter sanguinis* gen. nov., sp. nov., a novel anaerobic, Gram-positive bacterium. *Int. J. Syst. Evol. Microbiol.* 52, 1263–1266. doi: 10.1099/00207713-52-4-1263
- Chu, X. J., Cao, N. W., Zhou, H. Y., Meng, X., Guo, B., Zhang, H. Y., et al. (2021). The oral and gut microbiome in rheumatoid arthritis patients: a systematic review. *Rheumatology* 60, 1054–1066. doi: 10.1093/rheumatology/keaa835



- de Oliveira, G. L. V., Leite, A. Z., Higuchi, B. S., Gonzaga, M. I., and Mariano, V. S. (2017). Intestinal dysbiosis and probiotic applications in autoimmune diseases. *Immunology* 152, 1–12. doi: 10.1111/imm.12765
- Dutta Majumder, P., Agrawal, R., McCluskey, P., and Biswas, J. (2020). Current approach for the diagnosis and management of noninfective scleritis. *Asia Pac. J. Ophthalmol.* 10, 212–223. doi: 10.1097/APO.0000000000000341
- Forbes, J. D., Chen, C. Y., Knox, N. C., Marrie, R. A., El-Gabalawy, H., de Kievit, T., et al. (2018). A comparative study of the gut microbiota in immune-mediated inflammatory diseases—does a common dysbiosis exist? *Microbiome* 6:221. doi: 10.1186/s40168-018-0603-4
- Hsiao, Y. P., Chen, H. L., Tsai, J. N., Lin, M. Y., Liao, J. W., Wei, M. S., et al. (2021). Administration of *Lactobacillus reuteri* combined with *Clostridium butyricum* attenuates Cisplatin-induced renal damage by gut microbiota reconstitution, increasing butyric acid production, and suppressing renal inflammation. *Nutrients* 13:28. doi: 10.3390/nu13082792
- Kang, C., Wang, B., Kaliannan, K., Wang, X., Lang, H., Hui, S., et al. (2017). Gut microbiota mediates the protective effects of dietary capsaicin against chronic low-grade inflammation and associated obesity induced by high-fat diet. *MBio* 8:9. doi: 10.1128/mBio.00900-17
- Karami, J., Aslani, S., Jamshidi, A., Garshasbi, M., and Mahmoudi, M. (2019). Genetic implications in the pathogenesis of rheumatoid arthritis; an updated review. *Gene* 702, 8–16. doi: 10.1016/j.gene.2019.03.033
- Li, M., Yang, L., Cao, J., Liu, T., and Liu, X. (2022). Enriched and decreased intestinal microbes in active VKH patients. *Invest. Ophthalmol. Vis. Sci.* 63:21. doi: 10.1167/iov.63.2.21
- Li, R., Yao, Y., Gao, P., and Bu, S. (2020). The therapeutic efficacy of Curcumin vs. metformin in modulating the gut microbiota in NAFLD rats: A comparative study. *Front. Microbiol.* 11:555293. doi: 10.3389/fmicb.2020.555293
- Maeda, Y., and Takeda, K. (2017). Role of gut microbiota in rheumatoid arthritis. *J. Clin. Med.* 6:3. doi: 10.3390/jcm6060060
- Maeda, Y., and Takeda, K. (2019). Host-microbiota interactions in rheumatoid arthritis. *Exp. Mol. Med.* 51, 1–6. doi: 10.1038/s12276-019-0283-6
- Munyaka, P. M., Rabbi, M. F., Khafipour, E., and Ghia, J. E. (2016). Acute dextran sulfate sodium (DSS)-induced colitis promotes gut microbial dysbiosis in mice. *J. Basic Microbiol.* 56, 986–998. doi: 10.1002/jobm.201500726
- Nishio, Y., Taniguchi, H., Takeda, A., and Hori, J. (2021). Immunopathological analysis of a mouse model of arthritis-associated scleritis and implications for molecular targeted therapy for severe scleritis. *Int. J. Mol. Sci.* 23, 12–13. doi: 10.3390/ijms23010341
- Pianta, A., Arvikar, S. L., Strle, K., Drouin, E. E., Wang, Q., Costello, C. E., et al. (2017). Two rheumatoid arthritis-specific autoantigens correlate microbial immunity with autoimmune responses in joints. *J. Clin. Invest.* 127, 2946–2956. doi: 10.1172/JCI93450
- Promelle, V., Goeb, V., and Gueudry, J. (2021). Rheumatoid arthritis associated Episcleritis and Scleritis: An update on treatment perspectives. *J. Clin. Med.* 10:1. doi: 10.3390/jcm10102118
- Reyes-Castillo, Z., Valdes-Miramontes, E., Llamas-Covarrubias, M., and Munoz-Valle, J. F. (2021). Troublesome friends within us: the role of gut microbiota on rheumatoid arthritis etiopathogenesis and its clinical and therapeutic relevance. *Clin. Exp. Med.* 21, 1–13. doi: 10.1007/s10238-020-00647-y
- Simic, S., Berlec, A., Stopinsek, S., Strukelj, B., and Orel, R. (2019). Engineered and wild-type *L. lactis* promote anti-inflammatory cytokine signalling in inflammatory bowel disease patient's mucosa. *World J. Microbiol. Biotechnol.* 35:45. doi: 10.1007/s11274-019-2615-z
- Sota, J., Girolamo, M. M., Frediani, B., Tosi, G. M., Cantarini, L., and Fabiani, C. (2021). Biologic therapies and small molecules for the management of non-infectious scleritis: a narrative review. *Ophthalmol. Ther.* 10, 777–813. doi: 10.1007/s40123-021-00393-8
- Tamanai-Shacoori, Z., Smida, I., Bousarghin, L., Loreal, O., Meuric, V., Fong, S. B., et al. (2017). Roseburia spp.: a marker of health? *Future Microbiol.* 12, 157–170. doi: 10.2217/fmb-2016-0130
- Turna, J., Grosman Kaplan, K., Anglin, R., Patterson, B., Soreni, N., Bercik, P., et al. (2020). The gut microbiome and inflammation in obsessive-compulsive disorder patients compared to age- and sex-matched controls: a pilot study. *Acta Psychiatr. Scand.* 142, 337–347. doi: 10.1111/acps.13175
- Vergouwen, D. P. C., Rothova, A., Berge, J. C. T., Verdijk, R. M., van Laar, J. A. M., Vingerling, J. R., et al. (2020). Current insights in the pathogenesis of scleritis. *Exp. Eye Res.* 197:108078. doi: 10.1016/j.exer.2020.108078
- Vignesh, A. P., and Srinivasan, R. (2015). Ocular manifestations of rheumatoid arthritis and their correlation with anti-cyclic citrullinated peptide antibodies. *Clin. Ophthalmol.* 9, 393–397. doi: 10.2147/OPHTH.S77210
- Wakefield, D., Di Girolamo, N., Thureau, S., Wildner, G., and McCluskey, P. (2013). Scleritis: Immunopathogenesis and molecular basis for therapy. *Prog. Retin. Eye Res.* 35, 44–62. doi: 10.1016/j.preteyeres.2013.02.004
- Xu, H., Zhao, H., Fan, D., Liu, M., Cao, J., Xia, Y., et al. (2020). Interactions between gut microbiota and immunomodulatory cells in rheumatoid arthritis. *Mediators Inflamm.* 2020, 1–14. doi: 10.1155/2020/1430605
- Yang, W., and Cong, Y. (2021). Gut microbiota-derived metabolites in the regulation of host immune responses and immune-related inflammatory diseases. *Cell. Mol. Immunol.* 18, 866–877. doi: 10.1038/s41423-021-00661-4
- Yang, Y., and Jobin, C. (2017). Novel insights into microbiome in colitis and colorectal cancer. *Curr. Opin. Gastroenterol.* 33, 422–427. doi: 10.1097/MOG.0000000000000399
- Ye, Z., Zhang, N., Wu, C., Zhang, X., Wang, Q., Huang, X., et al. (2018). A metagenomic study of the gut microbiome in Behcet's disease. *Microbiome* 6:135. doi: 10.1186/s40168-018-0520-6

**Conflict of Interest:** The authors declare that the research was conducted in the absence of any commercial or financial relationships that could be construed as a potential conflict of interest.

**Publisher's Note:** All claims expressed in this article are solely those of the authors and do not necessarily represent those of their affiliated organizations, or those of the publisher, the editors and the reviewers. Any product that may be evaluated in this article, or claim that may be made by its manufacturer, is not guaranteed or endorsed by the publisher.

Copyright © 2022 Li, Yang, Zhao, Bai and Liu. This is an open-access article distributed under the terms of the Creative Commons Attribution License (CC BY). The use, distribution or reproduction in other forums is permitted, provided the original author(s) and the copyright owner(s) are credited and that the original publication in this journal is cited, in accordance with accepted academic practice. No use, distribution or reproduction is permitted which does not comply with these terms.



# Intestinal Microbiota Participates in the Protective Effect of HO-1/BMMSCs on Liver Transplantation With Steatotic Liver Grafts in Rats

Mengshu Yuan<sup>1</sup>, Ling Lin<sup>1</sup>, Huan Cao<sup>1</sup>, Weiping Zheng<sup>2,3</sup>, Longlong Wu<sup>4</sup>, Huaiwen Zuo<sup>1</sup>, Xiaorong Tian<sup>1</sup> and Hongli Song<sup>2,5\*</sup>

<sup>1</sup> Tianjin First Central Hospital Clinic Institute, Tianjin Medical University, Tianjin, China, <sup>2</sup> Department of Organ Transplantation, Tianjin First Central Hospital, Tianjin, China, <sup>3</sup> National Health Commission (NHC) Key Laboratory of Critical Care Medicine, Tianjin, China, <sup>4</sup> School of Medicine, Nankai University, Tianjin, China, <sup>5</sup> Tianjin Key Laboratory of Organ Transplantation, Tianjin, China

## OPEN ACCESS

### Edited by:

Cong-Qiu Chu,  
Oregon Health and Science University,  
United States

### Reviewed by:

Li Ma,  
Shanghai Children's Hospital, China  
Xue-Tao Yan,  
Shenzhen Bao'an Maternal and Child  
Health Hospital, China

### \*Correspondence:

Hongli Song  
hlsong26@163.com;  
songhl@tmu.edu.cn

### Specialty section:

This article was submitted to  
Microbial Symbioses,  
a section of the journal  
Frontiers in Microbiology

**Received:** 27 March 2021

**Accepted:** 03 May 2022

**Published:** 10 June 2022

### Citation:

Yuan M, Lin L, Cao H, Zheng W, Wu L,  
Zuo H, Tian X and Song H (2022)  
Intestinal Microbiota Participates in the  
Protective Effect of HO-1/BMMSCs  
on Liver Transplantation With Steatotic  
Liver Grafts in Rats.  
Front. Microbiol. 13:905567.  
doi: 10.3389/fmicb.2022.905567

The present study aimed to explore whether heme oxygenase-1 (HO-1)-modified bone marrow mesenchymal stem cells (BMMSCs) have a protective effect on liver transplantation with steatotic liver grafts in rats, and to determine the role of the intestinal microbiota in such protection. HO-1/BMMSCs were obtained by transduction of *Hmox1* gene [encoding heme oxygenase (HO-1)]-encoding adenoviruses into primary rat BMMSCs. Steatotic livers were obtained by feeding rats a high-fat diet, and a model of liver transplantation with steatotic liver grafts was established. The recipients were treated with BMMSCs, HO-1/BMMSCs, or neither, via the portal vein. Two time points were used: postoperative day 1 (POD 1) and POD 7. The results showed that under the effect of HO-1/BMMSCs, the degree of steatosis in the liver grafts was significantly reduced, and the level of liver enzymes and the levels of pro-inflammatory cytokines in plasma were reduced. The effect of HO-1/BMMSCs was better than that of pure BMMSCs in the prolongation of the rats' postoperative time. In addition, HO-1/BMMSCs promoted the recovery of recipients' intestinal structure and function, especially on POD 7. The intestinal villi returned to normal, the expression of tight junction proteins was restored, and intestinal permeability was reduced on POD 7. The intestinal bacterial of the LT group showed significantly weakened energy metabolism and overgrowth. On POD 1, the abundance of *Akkermansiaceae* was higher. On POD 7, the abundance of *Clostridiaceae* increased, the level of lipopolysaccharide increased, the intestinal mucosal barrier function was destroyed, and the levels of several invasive bacteria increased. When treated with HO-1/BMMSCs, the energy metabolism of intestinal bacteria was enhanced, and on POD 1, levels bacteria that protect the intestinal mucosa, such as *Desulfovibrionaceae*, increased significantly. On POD 7, the changed intestinal microbiota improved lipid metabolism and increased the levels of butyrate-producing bacteria, such as *Lachnospiraceae*. In conclusion, HO-1/BMMSCs have protective effects on

steatotic liver grafts and the intestinal barrier function of the recipients. By improving lipid metabolism and increasing the abundance of butyrate-producing bacteria, the changed intestinal microbiota has a protective effect and prolongs the recipients' survival time.

**Keywords:** bone marrow mesenchymal stem cells, liver transplantation, steatotic liver graft, tight junction (TJ), intestinal permeability, intestinal microbiota

## INTRODUCTION

Liver transplantation is the most effective treatment for end-stage liver disease and liver failure. The shortage of donor livers and the deterioration of the quality of donor livers restricts the widespread application of liver transplantation. With changes in lifestyle and the normalization of high-fat and high-sugar diets, the global incidence of fatty liver has reached as high as 25% (Sheka et al., 2020). As a result, the use of steatotic donor livers (especially moderately steatotic livers) is increasingly common in liver transplantation, accounting for 30 and 20% of cadaveric and living donor livers, respectively (Jackson et al., 2020). However, grafts using severely steatotic livers will directly affect the postoperative survival time of liver transplant recipients (Hughes and Humar, 2021). Therefore, to improve the quality of life and prolong the survival time of liver transplantation recipients, it is very important to develop a method of repairing steatotic liver grafts.

Mesenchymal stem cells (MSCs) have the potential for self-replication and multi-directional differentiation, and can be inserted into injured tissues to replace damaged cells. Their paracrine effects have been used in tissue repair, regeneration, and immune regulation of the body (Yang et al., 2014; Mahruf-Yorgov et al., 2017; Sun et al., 2020b). Bone marrow mesenchymal stem cells (BMMSCs) have been transfected with genes such as *HMOX1* [encoding heme oxygenase-1 (HO-1)] to form HO-1/BMMSCs, which could increase the activity and efficiency of BMMSCs. Increasing the local survival time of BMMSCs, and enhancing their anti-apoptotic, anti-inflammatory, and anti-oxidative stress functions, can also improve their repair and immune regulation capabilities (Zheng et al., 2017; Chen et al., 2019; Sun et al., 2020a). However, studies on stem cells and steatotic liver transplantation are few and lack detail.

The liver-gut axis plays an important role in the occurrence and development of non-alcoholic fatty liver disease, and portal blood flow and bile acids exert a bridge function to connect the liver and the intestines (Adolph et al., 2018; Albillos et al., 2020). Dysbiosis and an impaired intestinal mucosal barrier lead to bacterial translocation and the entry of their metabolites into the bloodstream, causing chronic low-grade inflammation throughout the body, and are closely related to the occurrence and development of non-alcoholic fatty liver disease (Lang and Schnabl, 2020; Tilg et al., 2020; Yang et al., 2020). Microbially-induced differences might impact the course of cholestasis and modulate liver injury (Juanola et al., 2021). Emerging data demonstrate that gut-derived lipopolysaccharide, gut microbiota-associated bile acids, and other bacterial metabolites, such as short-chain fatty acids and tryptophan metabolites, might play multifaceted roles in liver

injury and regeneration (Zheng and Wang, 2021). In addition, the gut microbial signature of impaired inhibitory control, which is associated with addictive disorders that can lead to cirrhosis, is distinct from cirrhosis-related cognitive impairment (Bajaj et al., 2021). At the same time, the intestinal microbiota is also involved in the repair of recipients after liver transplantation (Mu et al., 2019; Nakamura et al., 2019; Sharpton et al., 2021). Therefore, the present study sought to determine whether HO-1/BMMSCs could protect steatotic liver grafts and play a role in alterations of the intestinal microbiota, aiming to explore the relationship between liver transplantation with steatotic liver grafts and the intestinal microbiota under the action of HO-1/BMMSCs. We believe that the results will provide a favorable foundation and research direction to improve the prognosis of steatotic liver transplantation.

## MATERIALS AND METHODS

### Animals and Steatotic Liver Grafts Model

The experiments were performed using specific pathogen-free (SPF) rats (China Food and Drug Administration, Beijing, China). Male SD rats, 6–7 weeks old, weighing 180–200 g, were fed a high-fat diet (15% fat, 15% sucrose, 10% egg yolk powder, 1% cholesterol, 0.2% bile salts, 58.8% basal diet, Chinese food Drug Administration, Beijing, China). After 12 weeks, they had reached a weight of 450–500 g, and liver oil red and hematoxylin and eosin (H&E) staining were used to estimate whether the rat livers were steatotic. The steatotic livers were used as grafts. Male SD rats were fed with a normal basal diet for 22–24 weeks until they weighed 450–500 g, at which point, they were used as the steatotic liver transplant recipients. All animal experiments followed the Guidelines for the Care and Use of Laboratory Animals and were approved by the Animal Ethics Committee of Nankai University (Permit number: 2021-SYDWLL-000331).

### BMMSCs Culture, Preparation, and Identification of HO-1/BMMSCs

Isolation, culture, identification, and gene transfection of BMMSCs were performed as previously described (Yin et al., 2017). Bone marrow contents and BMMSCs were obtained from rat femurs and tibias by repeated pipetting. HO-1/BMMSCs were obtained by transfecting BMMSCs with adenoviral vectors (Ad/HO-1; Shanghai Jikai Gene, Shanghai, China) expressing Green fluorescent protein (GFP) and/or *Hmox1* constructs. The molecular biological functions of the cells were identified by inducing adipogenic and osteogenic differentiation *in vitro*. Cell phenotyping was performed using flow cytometry to identify cluster of differentiation (CD)29, CD90, RT1A (rat MHC class I antibody), CD34, CD45 and RT1B (rat MHC



class II antibody) (BioLegend, San Diego, CA, USA) expression. Immunofluorescence, western blotting, and quantitative real-time reverse transcription PCR (qRT-PCR) were used to detect the expression of HO-1 in cells.

## Establishment of the Rat Liver Transplantation Model

Liver transplantation was performed as described previously (Cao et al., 2020). Rats were anesthetized, the liver was exposed, and heparin (1 U/g) was injected. After 10 min of heparinization, the diaphragm was incised, the thoracic artery was clamped using an arterial clip, the heart was compressed, and cardiac arrest was induced. The abdominal cavity was then covered with warm saline at 37°C for 30 min. During this period, a temperature-sensing probe was placed in the rats' abdominal cavity to detect and maintain the body temperature between 35 and 37°C. According to the suggestion by Kamada and Calne (Kamada and Calne, 1979), the same surgeon performed all the operations. The duration of the anhepatic phase was  $30 \pm 1$  min.

According to the different treatment methods of the steatotic donor livers, recipients were divided into four groups, namely the sham operation group (Sham group), the liver transplantation with steatotic liver grafts group (LT group), the LT + BMSCs treated group (BM group), and the LT + HO-1/BMSCs treated group (HBM group). The steatotic liver grafts in the BM group were perfused with about  $1 \times 10^7$  BMSCs *via* the portal vein, and those in the HBM group were perfused with about  $1 \times 10^7$  HO-1/BMSCs. Five animals in the Sham group were used for blood, liver, and intestinal histopathological specimens, and ileocecal feces (about 0.2 g) collection. Ten animals in each experimental group were used for blood, liver, and intestinal histopathological specimens, and ileocecal feces (about 0.2 g) collection on post operational day (POD) 1 ( $n = 5$  in each group) and POD 7 ( $n = 5$  in each group), respectively. Twenty-four ( $n = 6$  in each group) animals were used for survival analysis; 40 animals ( $n = 10$  in each group) were used for biochemical analysis; and three animals were used for BMSC *in vivo* tracking.

## Establishment of an Injury Model of Steatotic IAR20 Cells

After stimulating steatosis of IAR20 cells (National Infrastructure of Cell Line Resource, Beijing, China) with 100  $\mu$ M palmitic acid (Sigma-Aldrich, St. Louis, MO, USA) and 200  $\mu$ M oleic acid (Sigma), lipopolysaccharide (LPS) at 10  $\mu$ g/mL used to treat the steatotic IAR20 cells for 24 h to establish the steatosis hepatocyte injury model. According to the different treatment methods of the IAR20 cells, they were divided into four groups: ① The control group; ② the LPS group (steatotic IAR20 cells stimulated with 10  $\mu$ g/mL LPS for 24 h); ③ the LBM group (after obtaining the LPS-injured steatotic IAR20 cell model,  $1 \times 10^6$  BMSCs/well were added, and co-cultured for 24 h); and ④ the LHM group (after obtaining the LPS-injured steatosis IAR20 cell model,  $1 \times 10^6$  HO-1/BMSCs/well were added, and co-cultured for 24 h). The activity of IAR20 cells and the mRNA and protein levels of Toll-like receptor 4 (TLR4) were determined.

## Establishment of an Injury Model of Intestinal Epithelial Cells

The 10  $\mu$ g/mL LPS was used to treat IEC-6 and Caco-2 cells (National Infrastructure of Cell Line Resource, Beijing, China) for 24 h to establish intestinal epithelial cell injury models. After obtaining the LPS-injured intestinal epithelial cell model,  $1 \times 10^6$  BMSCs were added to the upper layer of a 0.8- $\mu$ m Transwell chamber (Corning Inc., Corning, NY, USA), and the lower layer comprised intestinal epithelial cells. The cells in the chambers were co-cultured for 24 h, to rule out the role of MSCs in direct contact with intestinal epithelial cells. The activity of intestinal epithelial cells and the levels of tight junction proteins were determined. According to the different treatment methods of intestinal epithelial cells, they were divided into the same for groups as the injury model of steatotic IAR20 cells.

## Liver Biochemical Examination

Plasma was taken and an automatic biochemical analyzer (Cobas 800, Roche, Basel, Switzerland) was used to detect serum alanine aminotransferase (ALT), aspartate aminotransferase (AST), alkaline phosphatase (ALP), glutamyl transpeptidase (GGT), total bilirubin (TBil), and serum albumin (ALB). The assays were carried out according to the instrument manual.

## Histopathology

The liver tissue of the left lateral lobe, with a size of  $2 \times 2 \times 1$  cm<sup>3</sup>, and ileum tissue at about 6–8 cm away from the ileocecal area were sampled, completely immersed in 10% neutral formalin solution, fixed for 48 h, and then embedded in paraffin. Serial 3  $\mu$ m sections were obtained and stained using hematoxylin and eosin (H&E).

## Transmission Electron Microscopy (TEM)

Fresh ileocecal intestinal tissue was cut into  $1 \times 1 \times 2$  mm<sup>3</sup>, preserved with 2.5% glutaraldehyde, fixed with epoxy resin, and cut into ultrathin sections. The sections were observed using a transmission electron microscope (HT7800, Hitachi, Tokyo, Japan).

## Enzyme-Linked Immunosorbent Assay (ELISA)

Whole blood samples were kept at 4°C for 30 min, centrifuged at 4°C (500  $\times g$  for 20 min), and the supernatant was taken and stored in a  $-80^\circ\text{C}$  refrigerator. Measurements of serum interleukin-1 $\beta$  (IL-1 $\beta$ ), IL-6, IL-10, tumor necrosis factor- $\alpha$  (TNF- $\alpha$ ), diamine oxidase (DAO), D-lactic acid (D-LA), and LPS levels were carried out using ELISA kits (Multisciences Biotech Co., Hangzhou, China) according to the manufacturer's instructions.

## Immunofluorescence

Rat ileum samples taken at about 2–3 cm away from the ileocecal region were collected, placed in optimal cutting temperature compound (OCT) for embedding, and immediately placed in a  $-80^\circ\text{C}$  refrigerator for long-term storage. Frozen tissues were sectioned, fixed, and sealed, and then incubated with anti-zona occludens 1 (ZO-1) (1:250) and anti-Occludin (1:250) (Cell

Signaling Technology, Danvers, MA, USA) primary antibodies at 4°C overnight in the dark. Next day, the sections were incubated secondary antibodies (1:250) at room temperature for 60 min in the dark, and then the nuclei were counterstained using 4',6-diamidino-2-phenylindole (DAPI) solution by incubation in the dark for 5 min. The sections were stored at 4°C, and photographed under a fluorescence microscope.

## Western Blotting

Total protein was extracted by high performance liquid chromatography into radioimmunoprecipitation assay (RIPA) buffer with added phenylmethanesulfonyl fluoride (PMSF). The total protein concentration was determined using a bicinchoninic acid (BCA) assay. The proteins were separated by electrophoresis using sodium dodecyl sulfate-polyacrylamide gel electrophoresis (SDS-PAGE), transferred to polyvinylidene fluoride (PVDF) membranes, and blocked using 5% skim milk for 1 h. The membranes were then incubated with primary antibody overnight at 4°C. The primary antibodies used included those recognizing: TLR4 (1:1000) and  $\beta$ -actin (1:3000) (Multisciences Biotech Co., Hangzhou, China). After overnight incubation, the membranes were rinsed with TBST buffer (Tris buffer, NaCl, and Tween 20) and incubated with the corresponding secondary antibodies (1:2000) for 1 h at room temperature. Membranes were scanned using the ChemiDoc XRS+ imaging system (Bio-Rad, Hercules, CA, USA), and the gray values of the immunoreactive protein bands were analyzed using ImageJ 7.0 software (NIH, Bethesda, MD, USA). Relative protein expression levels were calculated in comparison with the level of  $\beta$ -actin.

## Quantitative Real-Time Reverse Transcription Polymerase Chain Reaction (qRT-PCR)

Total RNA from liver and intestinal tissues was extracted using the TRIzol reagent (Takara Biotechnology, Shiga, Japan), and cDNA was produced from the total RNA using a cDNA reverse transcription kit (Takara Biotechnology) according to the manufacturer's instructions. The cDNA was used as the template in the qPCR step of the qRT-PCR protocol.  $\beta$ -actin was used as an internal control. Data processing was performed using the  $2^{-\Delta\Delta CT}$  method for relative quantification (Livak and Schmittgen, 2001).

## Cell Counting Kit 8 (CCK8) Assay

10  $\mu$ g/mL LPS was used to treat IAR20, Caco-2, and IEC-6 cells for 24 hours in 96-well plates. The cells were then assayed using a CCK8 kit according to the manufacturer's instructions (Solarbio, Beijing, China). After the reaction was completed, the absorbance was measured at 450 nm using a microplate reader, and the cell viability was calculated:

$$\text{Cell viability(\%)} = \frac{(\text{experimental group} - \text{blank})}{(\text{control group} - \text{blank})}$$

## 16S rRNA Sequencing

About 0.2 g of fresh fecal samples were collected from the rats in each group, placed in a closed sterile cryopreservation tube, and stored in liquid nitrogen. High-throughput sequencing of the 16S rDNA gene V3-V4 region was carried out by Beijing Boao Jingdian Co., Ltd. (Beijing, China) using the Illumina NovaSeq sequencing platform. Cutadapt (version 1.18) was used to trim and filter the original sequences to get the optimized number of clean tags. Clustering was performed according to 97% similarity sequences using USEARCH (Version 11.0.667) software to obtain the species distribution information of each sample. Based on the operational taxonomic units (OTU) analysis results, the species richness information of each sample was obtained.

The QIIME software was used to analyze the abundance information at different classification levels in the Silva database. The Rarefaction curve, species accumulation curves, and alpha diversity reflected by the Shannon index were analyzed using the Mothur software. Beta diversity analysis, reflected by principal component analysis (PCA) used the vegan and GUniFrac packages in R. In the LEfSe (Linear Discriminant Analysis (LDA) Effect Size) analysis, the nonparametric factor Kruskal–Wallis rank-sum test and the Wilcoxon rank sum test were used to analyze the differences between groups. We used the PICRUST (Phylogenetic Investigation of Communities by Reconstruction of Unobserved States) software to predict the relative abundance of microbial functional categories in samples from 16S rDNA gene sequencing data. The R package limma was used to test the significant difference between the two groups for the prediction results of PICRUST2.

## Data Analysis

SPSS 13.0 (SPSS GmbH, Munich, Germany) and GraphPad 8.0 (GraphPad Software, Inc., San Diego, CA, USA) were used for statistical analysis. Data are presented as the mean  $\pm$  the standard deviation. One-way analysis of variance (ANOVA) was used to test the significance of the data. Count data were expressed as percentages (%) and the chi-squared test was used to assess data significance. Survival analysis was performed using Kaplan–Meier survival curves and log-rank tests (Mantel–Cox). Pearson's correlation method was used to determine the correlation coefficient ( $r$ ) between groups.  $P < 0.05$  was considered statistically significant.

## RESULTS

### Phenotypic and Functional Identification of BMMSCs and HO-1/BMMSCs

BMMSCs are adherent growing cells, and there was no morphological change after transfection with Ad/HO-1, showing typical long fusiform or spindle shapes, and a swirling arrangement (**Supplementary Figure 1A**). Furthermore, HO-1/BMMSCs were osteogenic (**Supplementary Figure 1B**) and adipogenic (**Supplementary Figure 1C**). Flow cytometry results showed more than 98% CD29, CD90, and RT1A positivity, and more than 98% CD34, CD45, and RT1B negativity (**Supplementary Figures 1D–F**). Red fluorescence, indicating expression of HO-1 in BMMSCs (**Supplementary Figure 1G**)

and HO-1/BMMSCs (**Supplementary Figure 1H**), was significantly higher in HO-1/BMMSCs than that in BMMSCs. The HO-1 protein level HO-1/BMMSCs was significantly higher than that in BMMSCs ( $P < 0.05$ ), and the mRNA level of HO-1 gene (*Hmox1*) was also significantly higher than that in BMMSCs ( $P < 0.05$ ) (**Supplementary Figure 1I**). Hence, HO-1 was successfully transfected into BMMSCs without affecting the molecular biological properties of BMMSCs.

## Morphology, Cell Distribution, and Survival Rate of Recipients Under the Function of HO-1/BMMSCs

Morphological changes of transplanted livers in each group were as follows: normal rat livers appeared red with sharp edges (**Figure 1A**), had almost no oil red staining positive areas (**Figure 1B**), and only a small amount of fat in the mesentery (**Figure 1C**). By contrast, the steatotic liver graft's capsule was tense and smooth, generally yellow, with dull edges and a greasy appearance (**Figure 1D**); the positive area of oil red staining was significantly increased (**Figure 1E**), and obvious fat is seen in the mesentery (**Figure 1F**), indicating that steatotic liver grafts were successfully established.

The distribution of MSCs in the liver were as follows: on POD 7, the expression of HO-1 protein (**Figures 1G,H**) and mRNA (**Figure 1I**) in the liver tissue of the HBM group increased significantly ( $P < 0.05$ ), which indirectly indicated that HO-1/BMMSCs were present in the liver and persisted. In the frozen sections of the steatotic liver grafts, an obvious red fluorescence signal for BMMSCs was observed, indicating that both BMMSCs and HO-1/BMMSCs could colonize the transplanted liver (**Figure 1J**).

From the survival curve, the median survival time of the HBM group was the longest ( $>60$  d), while the median survival time of the LT group was the shortest (16 d). The median survival time of the BM group was 29 days, which was slightly higher than that of the LT group, but significantly lower than that of the HBM group ( $P < 0.05$ ). Therefore, HO-1/BMMSCs could significantly prolong the survival time of steatotic liver transplantation recipients, and their effect was significantly better than that of BMMSCs alone (**Figure 1K**).

## HO-1/BMMSCs Can Improve the Function of the Steatotic Liver and Reduce Inflammation

Liver histology showed lipid droplets in more than 90% of hepatocytes in the Sham group, indicating mixed steatosis. On POD 1, hepatic sinusoids in the LT group were narrowed, with obvious congestion or even necrosis, and fewer lipid droplets and severe infiltration of inflammatory cells were seen. In the BM and HBM groups, obvious congestion of hepatic sinusoids, vesicular steatosis, and inflammatory cell infiltration were observed, but to a lesser extent than in the LT group. On POD 7, large areas of liver tissue necrosis were seen in the LT group; whereas, in the BM group, there was mild steatosis, and the liver cords were neatly arranged. In the HBM group, the liver cords were

neatly arranged without lipid droplets or inflammatory cell infiltration (**Figure 2A**).

Liver function tests showed that on POD 1, ALT, AST, ALP, GGT, and TBiL levels increased rapidly in the LT group (**Figure 2B**); the BM and HBM groups had lower levels of these markers than the LT group, but higher than those in the Sham group ( $P < 0.05$ ). On POD 7, the levels of AST and ALT in the LT group decreased, but ALP, GGT, and TBiL levels continued to increase; ALB was in a state of decline ( $P < 0.05$ ). All indexes in the BM and HBM groups were improved compared with those in the LT group, and the improvement in the HBM group was significantly greater than that in the BM group on POD 7 ( $P < 0.05$ ).

These results suggested that MSCs can improve the histology and functions of steatotic liver grafts, and the effect of HO-1/BMMSCs was better than that of BMMSCs alone over time.

For inflammation, the level of TLR4 in the liver tissue in the LT group was the highest after liver transplantation, and on POD 7 was higher than that of POD 1; the level of TLR4 in the HBM group was the lowest on POD 7 (**Figure 2C**). The qRT-PCR results also confirmed that the *Tlr4* mRNA level in the LT group was significantly increased (**Figure 2D**). Detection of inflammatory factors showed that on POD 1, compared with those in the Sham group, the levels of IL-1 $\beta$ , TNF- $\alpha$ , and IL-6 in the LT group were the highest; while the levels of IL-1 $\beta$ , TNF- $\alpha$ , and IL-6 in the BM and HBM groups increased, but not significantly compared with those in the LT group. The level of IL-10 increased; however, there was no statistical difference between the BM and HBM groups ( $P > 0.05$ ) (**Figure 2E**). On POD 7, the levels of TNF- $\alpha$ , IL-1 $\beta$ , and IL-6 in the LT group were still high. Compared with those in the LT group, the levels of TNF- $\alpha$ , IL-1 $\beta$ , and IL-6 in the BM and HBM groups decreased, with the decrease being most significant in the HBM group ( $P < 0.05$ ). The level of IL-10 increased most significantly in the HBM group ( $P < 0.05$ ). The mRNA results showed the same patterns (**Figure 2F**). Hence, inflammatory factors are involved in the pathological process after liver transplantation, and MSCs reduced the hepatic inflammatory response after steatotic liver transplantation and prolonged postoperative time. The anti-inflammatory function of HO-1/BMMSCs was significantly better than that of BMMSCs.

## The Effect of HO-1/BMMSCs on the Structure and Function of Recipient Intestines

In terms of intestinal histology, the intestinal villi in the Sham group were neat. In the LT group, on POD 1, the intestinal villi were obviously destroyed, the villi were broken, and the villus epithelium was detached; on POD 7, the villous epithelium was still obviously detached. In the BM and HBM groups, severe detachment of the villous epithelium was seen on POD 1; on POD 7, the intestinal villi were regularly arranged, and there was no intestinal villus breakage or detachment of the villous epithelium (**Figure 3A**). In the Sham group, the microvilli of the intestinal epithelial cells were neat, the tight junctions between the intestinal epithelial cells were intact, desmosomes were



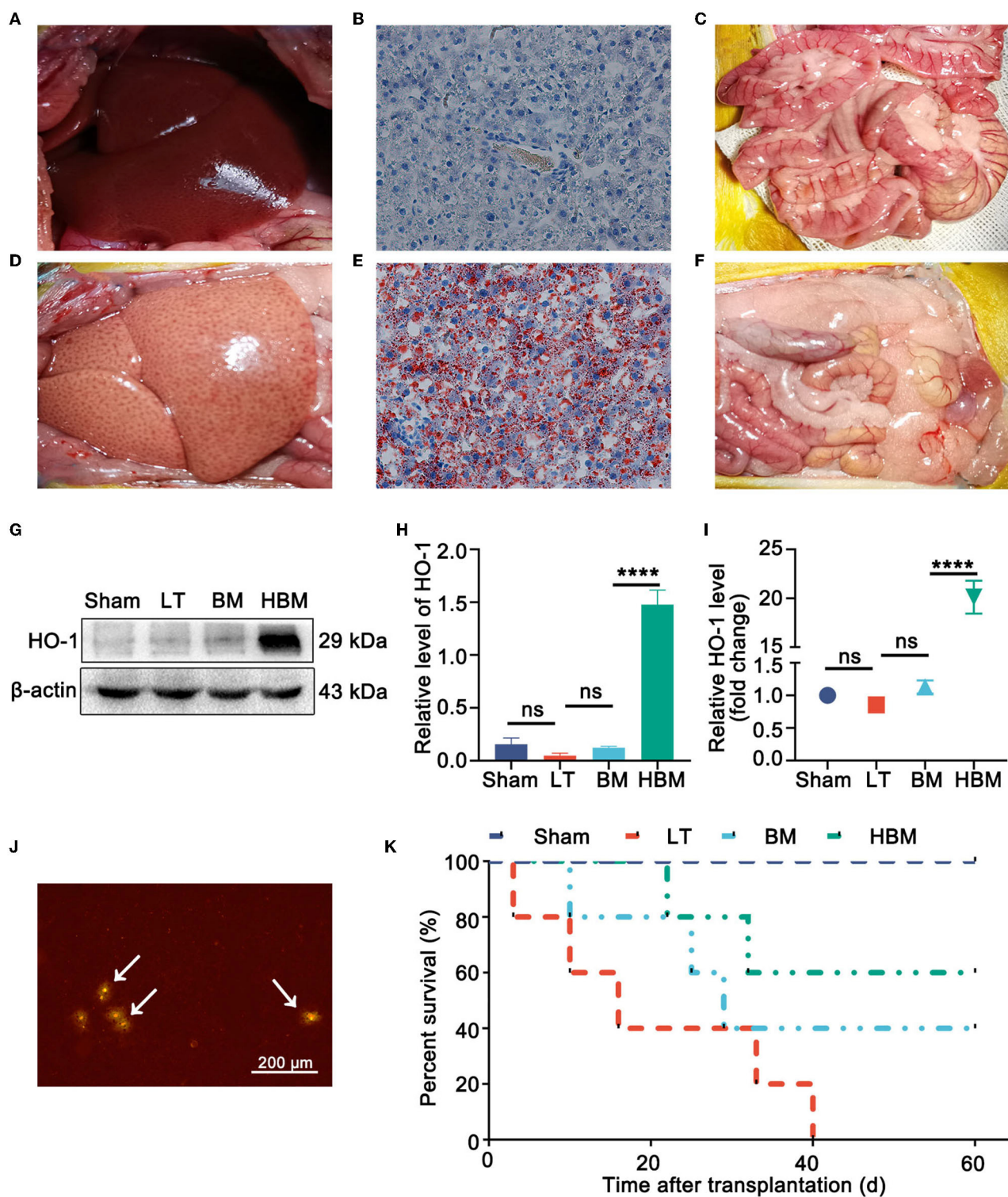


**FIGURE 1 |** Steatotic liver graft morphology, stem cell distribution, and recipient survival. **(A)** Normal rat liver. **(B)** Oil red staining of a normal liver. **(C)** Normal rat gut. **(D)** Rat steatotic graft liver. **(E)** Oil red staining of steatotic liver grafts ( $\times 200$ ). **(F)** Fat in the intestine of a donor rat. **(G,H)** On POD 7, the level of the HO-1 protein was the highest in the HBM group. **(I)** On POD 7, the expression of *Hmox1* mRNA was obvious in the HBM group. **(J)** Liver tissue frozen section of a steatotic donor liver ( $\times 40$ ). GFP/BMMSCs colonization in the hepatic sinusoids could be observed by fluorescence microscopy. Arrows point to BMMSCs. **(K)** Survival time after liver transplantation for the steatotic donor livers. The median survival times of the Sham, LT, BM, and HBM groups were >60, 16, 29, and 60 d, respectively. \* $P < 0.05$ , \*\* $P < 0.01$ , \*\*\* $P < 0.001$ , \*\*\*\* $P < 0.0001$ .

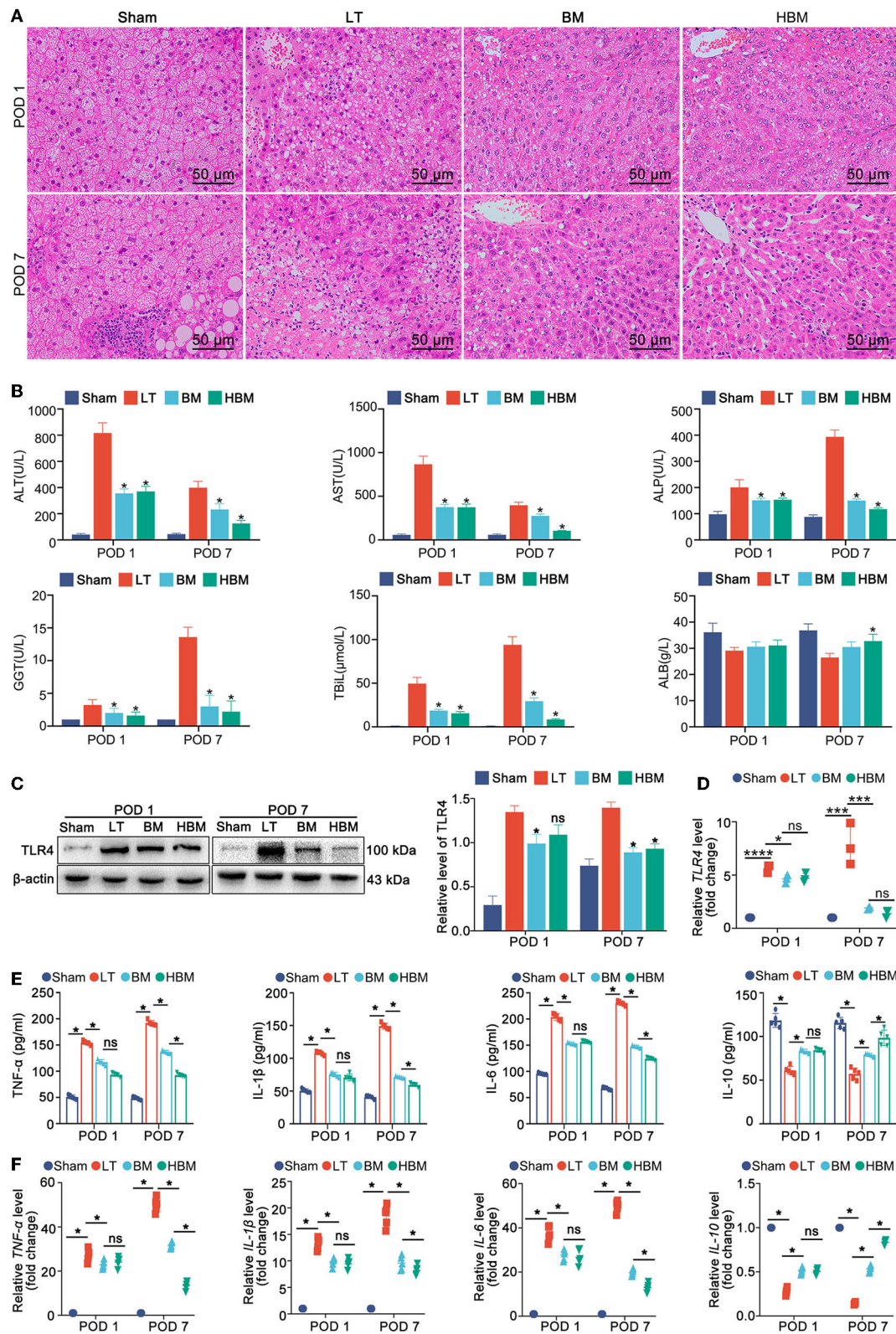


**FIGURE 2 |** Changes in the steatotic liver graft histology, liver biochemical examination, and plasma inflammatory indexes in each group. **(A)** Histopathology of transplanted livers at different time points (H&E staining,  $\times 200$ ). **(B)** Transplanted liver function. On POD 1, the ALT level in the LT group ( $817.20 \pm 77.63$  U/L) was significantly higher than that in the BM group ( $355.70 \pm 34.04$  U/L) and the HBM group ( $370.60 \pm 38.63$  U/L) ( $P < 0.05$ ), while the difference between the BM group (Continued)



**FIGURE 2** | and the HBM group was not statistically significant. On POD 7, the ALT level in the LT group ( $399.20 \pm 47.56$  U/L) was still significantly higher than that in the BM ( $232.60 \pm 43.92$  U/L) and HBM groups ( $126.00 \pm 23.50$  U/L), with a significant difference ( $P < 0.05$ ). Changes in AST, ALP, GGT, and TBIL levels were similar to those of ALT (\* $P < 0.05$  vs. LT group). **(C)** TLR4 levels in the liver tissues of each group. Among them, the level on POD 7 in the LT group was the highest. **(D)** The expression of *Tlr4* mRNA in the liver tissue of each group. The hepatic *Tlr4* mRNA level was the highest on POD 7 in the LT group and the lowest on POD 7 in the HBM group. **(E)** Changes in the levels inflammatory factors IL-1 $\beta$ , TNF- $\alpha$ , IL-6, and IL-10 in serum. On POD 1, the LT group had the highest levels of IL-1 $\beta$ , TNF- $\alpha$ , and IL-6. On POD 7, the levels of TNF- $\alpha$ , IL-1 $\beta$ , and IL-6 were still higher in the LT group, while their levels in the HBM group decreased the most. \* $P < 0.05$ . **(F)** Changes of *Il1b*, *Tnfa*, *Il6*, and *Il10* mRNA in serum. \* $P < 0.05$ , \*\* $P < 0.01$ , \*\*\* $P < 0.001$ , \*\*\*\* $P < 0.001$ .

present, and the intercellular space had not widened. However, in the LT group, on POD 1, the microvilli of the intestinal mucosal epithelial cells became short, sparse, and broken, and showed serious cell loss; on POD 7, intestinal epithelial cell necrosis was seen. In the BM and HBM groups, the intact tight junctions were still visible on POD 1, and on POD 7, the tight junctions were more intact.

On POD 1, the expression levels of the tight junction proteins ZO-1 and Occludin in the LT group were low and interrupted, while their expression levels in the BM and HBM groups were slightly higher than those in the LT group, and interruption was not obvious. On POD 7, the tight junction proteins ZO-1 and Occludin in the LT group were still at a low level, even lower than that of POD 1; whereas, their expression levels in BM and HBM groups were higher than those on POD 1, and the HBM group showed a more significant increase than the BM group (Figure 3B).

In terms of intestinal function, the plasma D-LA, DAO, and LPS levels in each group increased significantly on POD 1, with the largest increase being observed the LT group ( $P < 0.05$ ), indicating that the LT group had increased intestinal permeability. There was no significant difference between the BM and HBM groups ( $P > 0.05$ ). On POD 7, D-LA and LPS levels had increased further in the LT group, and DAO was in a stable state; while the D-LA, DAO, and LPS levels in BM group had stabilized, and those in the HBM group showed a downward trend ( $P < 0.05$ ) (Figure 3C).

Hence, after liver transplantation with steatotic liver grafts, the intestinal mucosal structure was destroyed and the intestinal permeability continued to increase. MSCs could slightly improve intestinal permeability. Over time, the effect of HO-1/BMMSCs on intestinal permeability was better.

The detection of proteins and mRNAs showed that on POD 1, the expression of tight junction protein was the highest in the Sham group and the lowest in the LT group ( $P < 0.05$ ). Among the groups, there was no difference in expression between the BM and HBM groups. On POD 7, their expression levels in the LT group remained the lowest among the groups; whereas, their expression levels in the BM and HBM groups increased, with the HBM group showing the most significant increase ( $P < 0.05$ ; Figures 3D–F). The mRNA results showed the same patterns (Figures 3G,H;  $P < 0.05$ ).

Hence, after liver transplantation with steatotic liver grafts, the intestinal mucosal structure is destroyed and the expression of tight junction proteins is reduced. Meanwhile, MSCs can reduce the damage to the recipients' intestinal tissue and promote

the recovery of the recipients' intestinal tight junction proteins. The effect of HO-1/BMMSCs was better than that of BMMSCs over time.

### Effects of HO-1/BMMSCs on Injured Intestinal Epithelial Cells and Steatotic Hepatocytes *in vitro*

In the steatosis IAR20 cell model, after stimulation by LPS on steatotic cells (Figure 4A), the degree of steatosis increased (Figure 4B), while the degree of steatosis decreased significantly after co-culture with BMMSCs and HO-1/BMMSCs (Figures 4C,D). LPS stimulation decreased cell viability (Figure 4E) and increased TLR4 protein and mRNA levels (Figures 4F,G). After co-culture with BMMSCs and HO-1/BMMSCs, cell viability increased significantly, and the level of TLR4 was decreased. These results indicated that MSCs could reduce the degree of steatosis and inhibit the TLR4 inflammatory response induced by LPS.

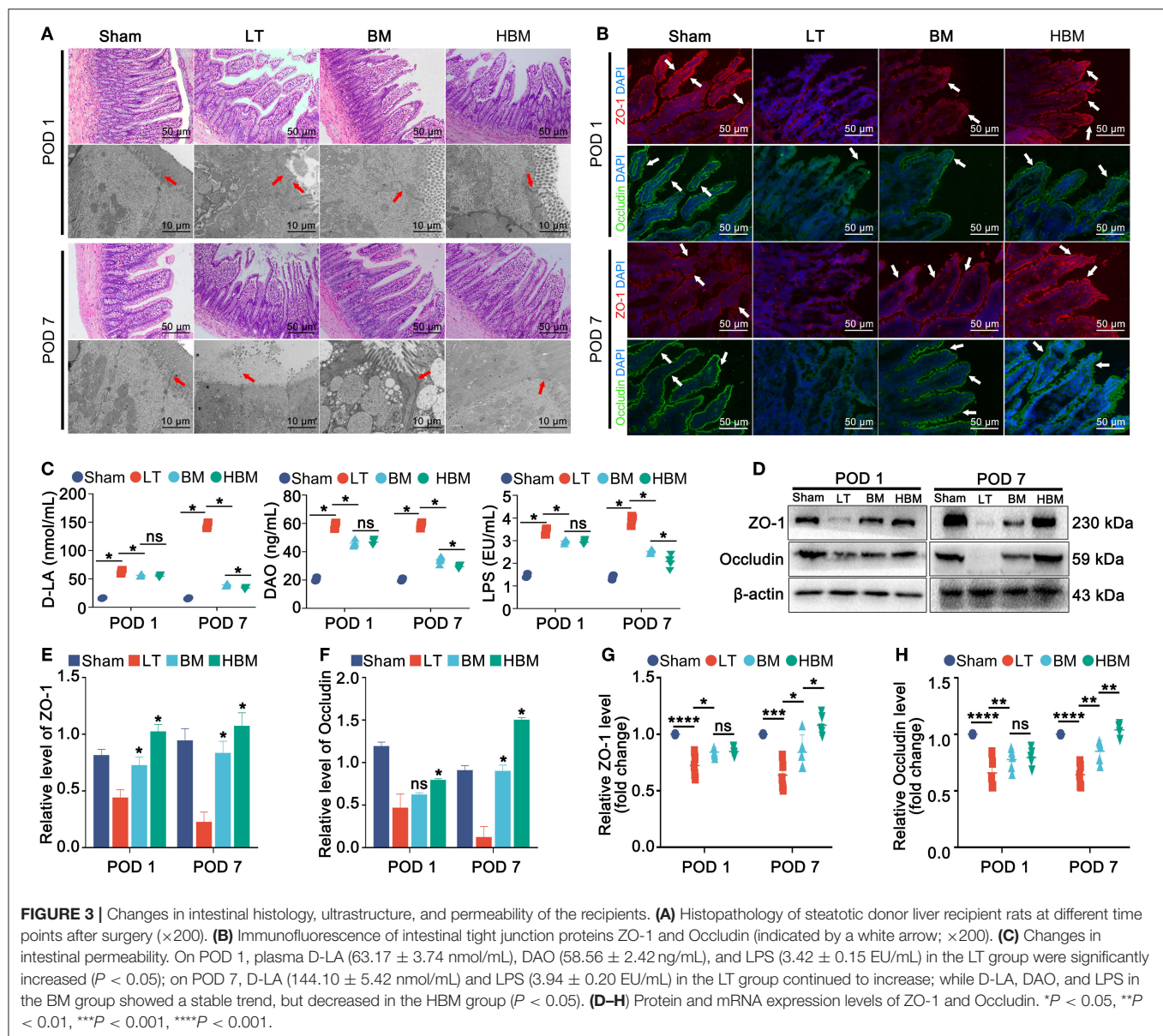
After LPS acted on IEC-6 and Caco-2 cells for 24 h, the activity of intestinal epithelial cells decreased significantly (Figure 4H), and tight junction protein (ZO-1 and Occludin) levels were significantly reduced (Figures 4I–M). Under the indirect effect of BMMSCs and HO-1/BMMSCs, the viability of IEC-6 and Caco-2 cells increased significantly ( $P < 0.05$ ), and the protein and mRNA expressions of tight junction proteins ZO-1 and Occludin also increased. This suggested that MSCs can repair damaged intestinal epithelial cells through paracrine action, improve cell viability, and enhance the expression of tight junction proteins.

### Effects of HO-1/BMMSCs on the Intestinal Microbiota of Recipients

To further explore whether the effect of HO-1/BMMSCs in repairing steatotic liver grafts is related to the intestinal microbiota, we investigated the changes in the gut microbiota of recipient rats under different conditions using 16S rRNA gene sequencing.

#### The Predominant Bacteria of the Recipients in all Groups

At the phylum level, *Firmicutes*, *Bacteroidota*, *Desulfobacterota*, *Proteobacteria*, *Verrucomicrobiota*, and *Spirochaetta* had the highest abundance in all groups. *Firmicutes/Bacteroidota* decreased on POD 1, while *Firmicutes/Bacteroidota* increased on POD 7 (Figures 5A,B). At the family level, *Lachnospiraceae*, *Oscillospiraceae*, *Muribaculaceae*, *Lactobacillaceae*, and *Prevotellaceae* were the most abundant microbiota in all groups.



## Species Diversity

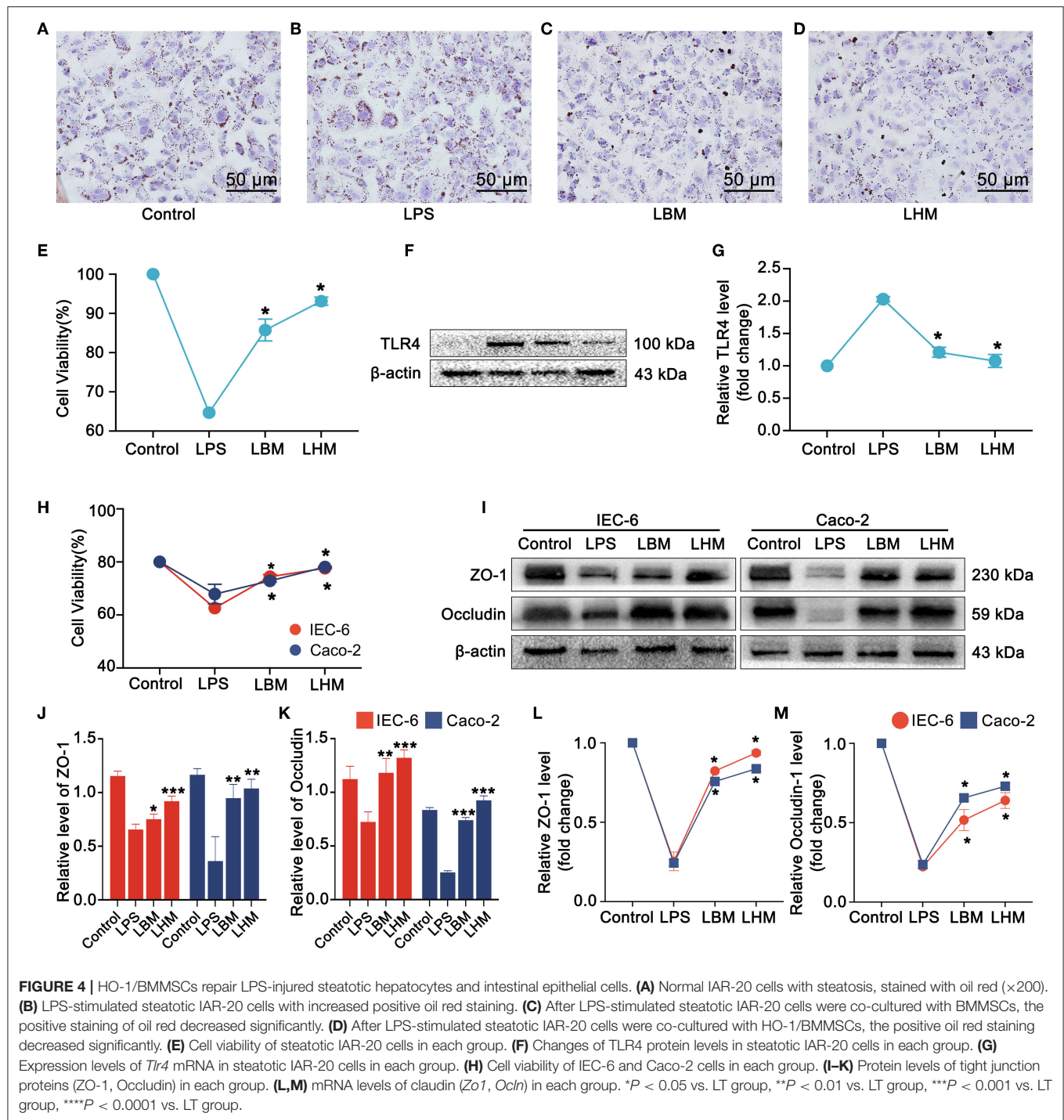
Rarefaction and Specaccum curves (**Supplementary Figures 2A,B**) indicated that the amount of sample sequencing data was reasonable and could be analyzed. Alpha diversity reflects the species diversity within each group. Shannon's index of alpha diversity showed that the number of OTUs in the Sham group was significantly lower than that in the other groups, especially on POD 7 ( $P < 0.05$ ) (**Supplementary Figure 2C**). This suggested that liver transplantation with steatotic live grafts led to an increase in the species diversity of the recipient intestinal microbiota. Beta diversity aims to compare how similar in different samples are in terms of species diversity. Based on the PCA analysis, compared with the Sham group, the other groups were farther away from it (**Supplementary Figure 2D**), and

the similarity of the beta diversity of intestinal microbiota decreased significantly, indicating that liver transplantation with steatotic liver grafts significantly changed the intestinal microbiota composition.

## Differences in the Microbiota in Each Group

We used Lefse (Line Discriminant Analysis (LDA) Effect Size) analysis (LDA Score greater than the set value of 4.0) to screen out species with significant differences in abundance between groups (biomarkers). At the family level, on POD 1, compared with the Sham group, the abundances of *Akkermansiaceae*, *Oscillospiraceae*, *Prevotellaceae*, and *Ruminococcaceae* in the LT group were higher; while the abundances of *Lactobacillaceae*, *Muribaculaceae*, and *Staphylococcaceae* decreased significantly ( $P < 0.05$ ). Compared with those in the LT group, the BM group

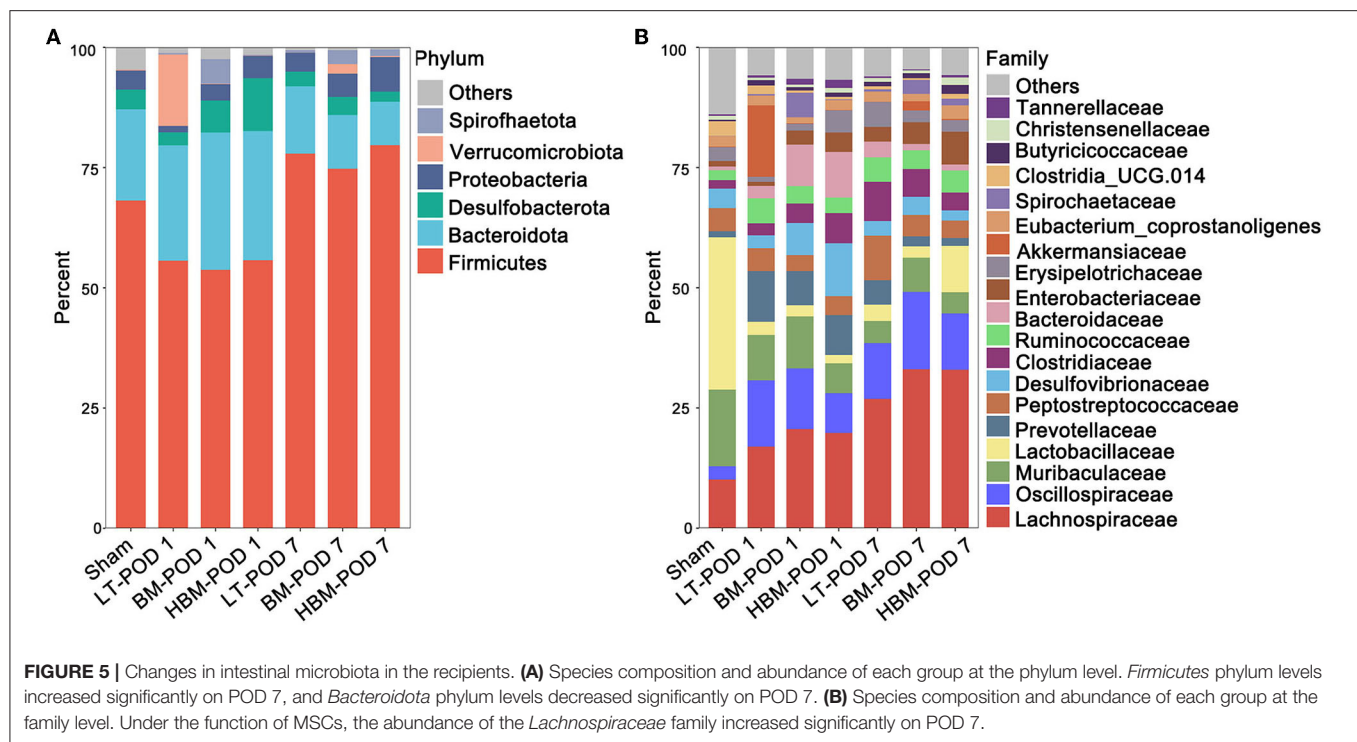




showed an increased abundance of *Desulfovibrionaceae*, while *Akkermansiaceae* and *Oscillospiraceae* had lower abundances ( $P < 0.05$ ). Compared with those in the BM group, the HBM group had lower abundances of *Spirochaetaceae* and *Muribaculaceae* (Figure 6A). This suggested that on POD 1, the increased intestinal microbiota of BMMSCs and HO-1/BMMSCs is mainly

*Desulfovibrionaceae*, which might be involved in the repair of intestinal mucosal function.

On POD 7, the abundances of *Lachnospiraceae*, *Oscillospiraceae*, *Clostridiaceae*, *Peptostreptococcaceae*, and *Ruminococcaceae* were higher in the LT group compared with those in the Sham group, while the abundances of



*Lactobacillaceae* and *Muribaculaceae* remained low ( $P < 0.05$ ). Compared with those in the LT group, the abundances of *Lachnospiraceae*, *Spirochaetaceae*, and *Akkermansiaceae* increased in the BM group, while the abundances of *Peptostreptococcaceae*, *Prevotellaceae*, and *Clostridiaceae* decreased; *Oscillospiraceae* (*Colidextribacter*) richness also decreased ( $P < 0.05$ ; **Figure 6B**). These results suggested that on POD 7, MSCs mainly increased the levels of butyrate-producing bacteria, such as *Lactobacillaceae* and *Akkermansiaceae*, and bacteria that improved fat metabolism, and HO-1/BMMSCs further increased the levels butyrate-producing bacteria, such as *Blautia*.

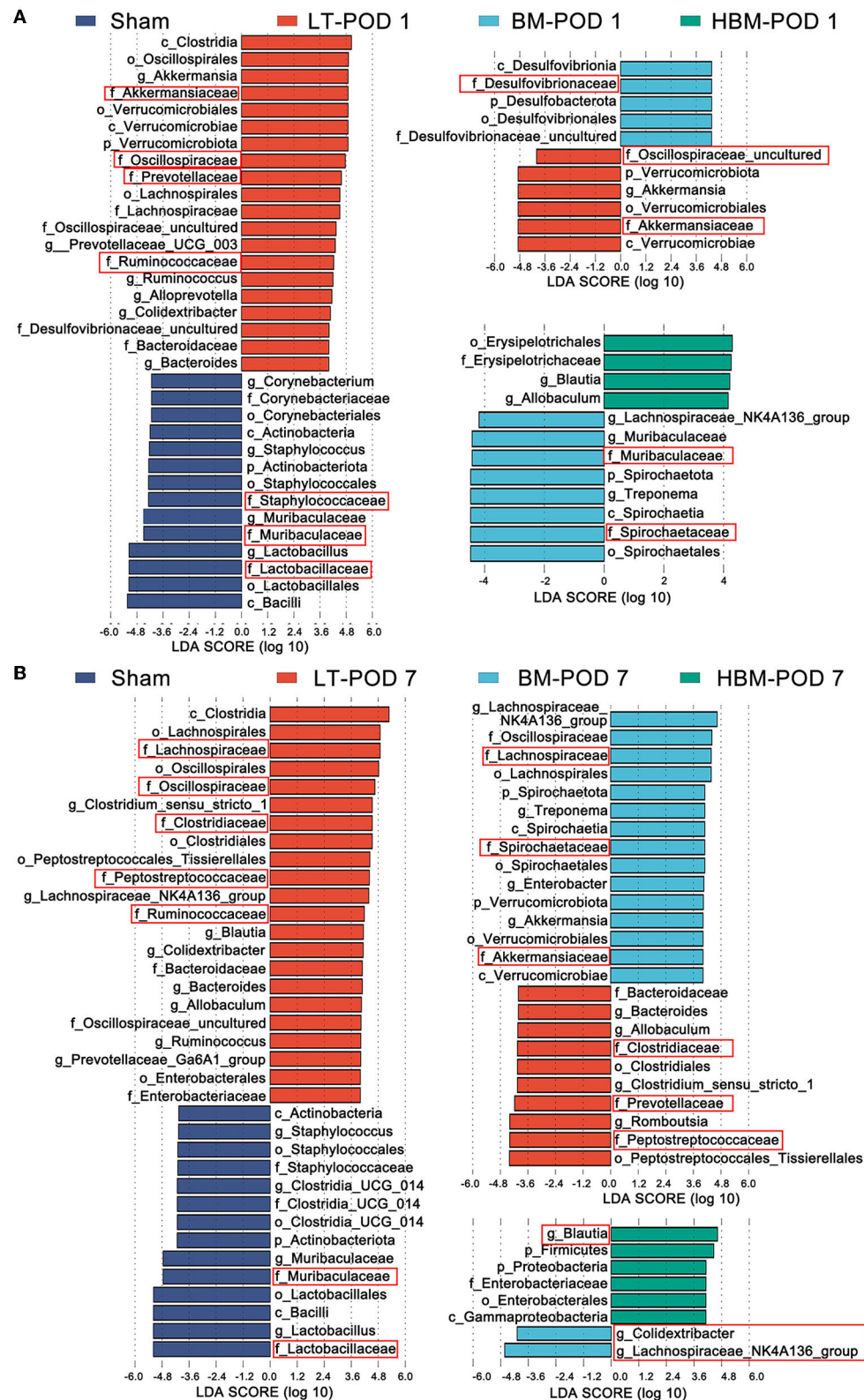
## The Intestinal Microbiota Is Involved in the Protective Effect of HO-1/BMMSCs on Recipients

For the intestinal microbiota, the PICRUSt function prediction (**Figure 7A**) results showed the pathway changes of each group for carbohydrate metabolism, lipid metabolism, glycan biosynthesis and metabolism, membrane transport, cell motility, and infectious disease: bacterial. For short-chain fatty acid metabolism pathways: Pyruvate metabolism, Propanoate metabolism, and Butanoate metabolism were significantly enhanced on POD 7 in the HBM group, and were higher than those of the BM group ( $P < 0.05$ ), whereas on POD 7, there were no significant differences between the BM and LT groups (**Figure 7B**). Fatty acid degradation in the Fatty acid metabolism pathway and the Biosynthesis of unsaturated fatty acids pathway were significantly enhanced on POD 7 in the HBM group ( $P < 0.05$ ; **Figure 7C**), and were significantly higher than those of the BM group. However, there was no statistical difference

between the BM and LT groups. For pathways associated with pathogen-related molecular patterns: Peptidoglycan biosynthesis was significantly enhanced on POD 7 in the LT, BM, and HBM groups (**Figure 7D**); Lipopolysaccharide biosynthesis was highest on POD 1 in HBM group, and significantly decreased on POD 7 in the BM and HBM groups, and declined the most in the HBM group (**Figure 7D**). In Membrane transport pathways related to bacterial pathogenicity, the Bacterial secretion system was significantly increased on POD 7 in the LT, BM, and HBM groups. For the pathways related to bacterial uptake of nutrients, Phosphotransferase system (PTS) and ABC transporters were significantly increased in BM and HBM groups on POD 7, and were significantly enhanced in the HBM group compared with that in the BM group ( $P < 0.05$ ; **Figure 7E**). For pathways related to bacterial motility: Flagellar assembly and Bacterial chemotaxis were strongest on POD 7 in the BM group. Meanwhile, these two bacterial motility pathways were enhanced in the LT and HBM groups compared with those in the Sham group, but there was no statistical difference between them (**Figure 7F**). Among bacterial infectious diseases, *Staphylococcus aureus* infection was significantly decreased in the LT, BM, and HBM groups and Bacterial invasion of epithelial cells was highest on POD 7 in the LT group; however, there was no statistical difference between the BM and HBM groups (**Figure 7G**).

## DISCUSSION

Although steatotic donor livers account for a large proportion of the donor liver pool, the risk of post-transplantation recipient mortality, early primary graft dysfunction, and primary nonfunction in recipients with steatotic liver grafts is significantly





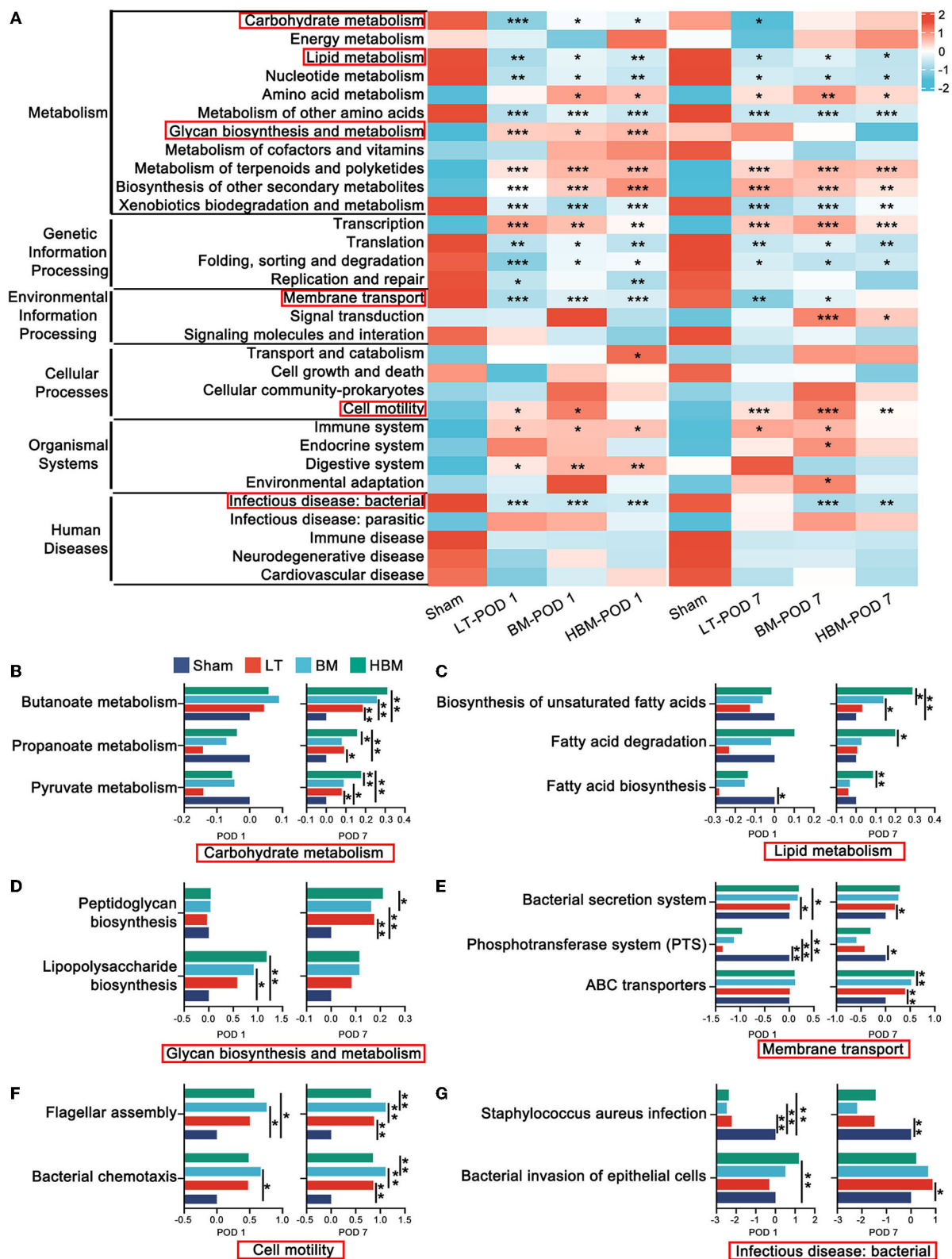


**FIGURE 7 |** PICRUSt functional prediction of changes in the intestinal microbiota. **(A)** Six main pathways at level 1 and 31 main pathways at level 2. Among them, carbohydrate metabolism, lipid metabolism, glycan biosynthesis and metabolism, membrane transport, cell motility, and bacterial infection disease play an important role in the repair process involved in the steatotic transplanted liver (the important secondary pathways are in the red box). **(B)** The expression levels of genes related

(Continued)

**FIGURE 7 |** (C) Pyruvate metabolism, Propanoate metabolism, and Butanoate metabolism in the carbohydrate metabolism groups were highest in the HBM group. (C) The expression levels of genes related to Fatty acid degradation and the Biosynthesis of unsaturated fatty acids in each group in fat metabolism were the highest on POD 7 in the HBM group. (D) In glycan biosynthesis and metabolism, the expression levels of genes in the Lipopolysaccharide biosynthesis groups showed the most significant decrease in the HBM group. (E) Membrane transport pathways in each group were significantly enhanced in the BM and HBM groups. (F) For flagellar assembly in cell motility, the expression levels of genes related to Bacterial chemotaxis in each group were the strongest on POD 7 in the BM group. (G) The expression levels of genes related to Bacterial invasion of epithelial cells in each group of bacterial infection disease were the highest level on POD 7 in the LT group. \* $P < 0.05$ , \*\* $P < 0.01$ , \*\*\* $P < 0.001$ , \*\*\*\* $P < 0.001$ .

higher than that of non-steatotic livers grafts (McCormack et al., 2011; Croome et al., 2020; Chen et al., 2021). Therefore, acquiring an understanding of the damage repair mechanism of steatotic liver grafts is significant to improve and optimize the prognosis of steatotic liver transplantation. In this study, we investigated whether the intestinal microbiota plays an important role in the repair of steatotic liver grafts by HO-1/BMMSCs and explored a new way to repair steatotic liver grafts.

MSCs play an important role in the repair and regeneration of tissue and organ damage and good results have been achieved in organ transplantation and repair (Yang et al., 2014; Yin et al., 2017, 2019; Cao et al., 2020; Tian et al., 2021). Our research group has verified that HO-1-modified BMMSCs have anti-inflammatory, anti-oxidative, anti-apoptotic, and delayed rejection functions in transplant recipients, and are more effective than BMMSCs alone. Activity in the diseased part is related to prolonging its duration of function (Cao et al., 2020; Tian et al., 2021). However, there is no relevant research on the effect of MSCs on steatotic liver transplantation. This study aimed to observe the effect of HO-1/BMMSCs on recipients after steatotic liver transplantation in rats, and on this basis, to observe the effect of the intestinal microbiota.

Hepatic sinusoidal microcirculation disturbance is one of the main reasons why steatotic liver grafts are more susceptible to ischemia-reperfusion injury, which causes primary graft nonfunction and other complications (Teramoto et al., 1993). Compared with a normal liver, the degree of stenosis of hepatic sinusoids in steatotic liver grafts can reach 50% (Ijaz et al., 2003). In this experiment, we established a stable steatotic liver transplantation model and directly infused MSCs into the portal vein. On POD 1, we found that the degree of liver congestion, steatosis, and inflammatory cell infiltration decreased in the MSC groups. On POD 7, the degree of repair exerted by HO-1/BMMSCs to the steatotic liver grafts was significantly better than that of BMMSCs, i.e., there was no congestion in the hepatic sinusoids, the fatty infiltration almost disappeared, and the degree of inflammatory cell infiltration was significantly reduced. Meanwhile, HO-1/BMMSCs could significantly inhibit the expression of TLR4 and pro-inflammatory factors in steatotic livers grafts. This demonstrated that HO-1/BMMSCs have more advantages in improving the prognosis and survival rate of steatotic liver transplant recipients in rats compared with BMMSCs alone.

D-LA is a metabolite of various intestinal bacteria and cannot be rapidly degraded. DAO is mainly concentrated in the small intestinal mucosal villi. LPS is a major component of gram-negative bacteria and is released after enterobacterial cell death. Therefore, plasma D-LA, DAO, and LPS levels might partly

reflect changes in gastrointestinal permeability and intestinal mucosal barrier function (Cai et al., 2019). During steatotic liver transplantation, portal vein blood flow is blocked (30 min), and severe congestion of the mesentery, ischemia, and hypoxia of the intestinal wall tissue, and further damage to the intestinal mucosal structure, occur, i.e., villi breakage and detachment of the villus epithelium (Deng et al., 2021a,b). We found that plasma D-LA, DAO, and LPS levels increased significantly after liver transplantation with steatotic liver grafts compared with those without surgery, while the levels of ZO-1 and Occludin, the key proteins of intestinal tight junctions, decreased significantly, indicating that there might be dysbacteriosis and intestinal mucosal damage. When MSCs were administered, the levels of D-LA, DAO, and LPS decreased significantly, while ZO-1 and Occludin levels increased significantly, and the effect of HO-1/BMMSCs was the most obvious with time. This indicated that HO-1/BMMSCs could reduce intestinal mucosal damage and protect intestinal permeability indirectly after the restoration of the sinusoidal microcirculation of the steatotic liver grafts, and their effects were more durable than those of BMMSCs.

*In vitro* experiments showed that LPS could reduce the activity of steatotic IAR20 cells, aggravate the degree of steatosis, and increase the expression of TLR4. Moreover, LPS reduced the expression of tight junction proteins ZO-1 and Occludin, and increased intestinal permeability. However, after treatment with MSCs, the activity of IAR20 cells increased, the degree of cellular steatosis was decreased, and the expression of TLR4 decreased significantly. The activities of IEC-6 and Caco-2 cells increased, and the expression of tight junction proteins also increased. These results indicated that in steatotic liver cells, MSCs could reduce the degree of steatosis and the expression of TLR4, which would decrease the inflammatory response of the transplanted liver. Moreover, MSCs also reduced the damage caused by LPS on intestinal epithelial cells through a paracrine effect.

The intestinal microbiota plays an important role in the alleviation of steatotic liver grafts (Bäckhed et al., 2004; Le Roy et al., 2013; Safari and Gérard, 2019). Modulating the gut microbiome is a promising therapeutic approach in nonalcoholic fatty liver disease (NAFLD; Lee et al., 2020). Probiotics has been used to prevent and treat NAFLD (Khan et al., 2021). The interplay between the gut microbiota, the intestinal barrier, the immune system, and the liver is complex (Martín-Mateos and Albillos, 2021). To further explore whether the recipient's intestinal microbiota has any effect on the recipients after steatotic liver transplantation, we investigated the intestinal microbiota of the recipients on POD 1 and POD 7. The results showed that the pathogenic bacteria in the recipients' intestinal microbiota increased significantly in

the LT group over time, while in the BMMSCs and HO-1/BMMSCs groups, there were significant increases in the number of bacteria with increased lipid metabolism and butyrate production.

On POD 1, the abundance of anaerobic bacteria *Akkermansiaceae* increased significantly after steatotic liver transplantation. *Akkermansiaceae* use mucins in the mucus layer of the intestine as a source of carbon and nitrogen. *Akkermansiaceae* are closely related to the intestinal health of the body and pathological states such as obesity (Plovier et al., 2017), and are involved in the repair of damaged intestinal epithelium, antagonize pathogenic bacteria, and consolidate the function of new intestinal epithelium (Reunanen et al., 2015). Rao et al. (2021) found that obese mice treated with *A. muciniphila* eliminated hepatic steatosis, inflammation, and liver injury through regulating the metabolism of L-aspartate. However, on POD 1 after steatotic liver transplantation, the intestinal villi were significantly disrupted, edema and the infiltration of inflammatory cells led to a significant increase in *Akkermansiaceae* under conditions of low nutritional status. Intestinal epithelial cells were damaged, tight junctions were destroyed, intestinal resistance was weakened, bacterial metabolism was weakened, and overgrowth occurred, such that the increased abundance of *Akkermansiaceae* did not play a significant protective role in the intestinal mucus layer, but instead promoted the decomposition of the mucus layer. Inflammatory bacteria (e.g., *Ruminococcus*, *Bacteroides*, and *Erysipelotrichaceae*; Kaakoush, 2015; Hall et al., 2017; Miyauchi et al., 2020; Henke et al., 2021) enhance the invasive intestinal epithelial cell response, which in turn allows LPS and a large number of bacterial metabolites to enter the portal vein. This indicated that the increase of bacterial diversity after steatotic liver transplantation did not protect the recipients, but because of the enhanced ability of bacteria to invade the epithelium, the metabolites entered the liver through the portal vein and aggravated the inflammatory response of the steatotic liver grafts.

Under the function of MSCs, the levels of butyrate-producing bacteria, such as *Desulfovibrionaceae*, *Lachnospiraceae*, and *Blautia*, increased; the levels of bacteria that improved lipid metabolism, such as *Akkermansiaceae*, increased; and the levels of obesity-causing bacteria, such as *Peptostreptococcaceae*, *Prevotellaceae*, and *Erysipelotrichaceae*, decreased. Over time, the effect of HO-1/BMMSCs on the levels of these bacteria was the most significant. *Desulfovibrionaceae* produces LPS and is strongly associated with obesity and metabolic syndrome (Zhang et al., 2021); however, studies also have shown that the H<sub>2</sub>S produced by *Desulfovibrionaceae* is an important mediator of gastrointestinal mucosal defense repair and reduction of systemic inflammation (Wallace et al., 2018). Therefore, the abundance of *Desulfovibrionaceae* increased on POD 1, which might have a repairing effect on the intestinal mucosa, while on POD 7, its abundance decreased, resulting in less LPS, which can enter the liver and activate the TLR4 pathway (Xiong et al., 2017). In addition, the abundance of *Akkermansiaceae* increased and microbiota associated with obesity and hyperlipidemia (*Peptostreptococcaceae*, *Prevotellaceae*, and *Erysipelotrichales*)

decreased (Castonguay-Paradis et al., 2020; Sookoian et al., 2020). These microbiota alterations could improve glucose tolerance, insulin resistance, and protect the intestinal mucosa (Plovier et al., 2017).

The phylum *Firmicutes* can metabolize dietary fiber to butyrate, and *Spirochaetes* and *Proteobacteria* are also potential butyrate-producing bacteria (Fu et al., 2019). Butyrate is not only an energy source for colon cells, but also regulates genes epigenetically by inhibiting histone deacetylases, modulates intestinal immunity and inflammatory responses (Singhal et al., 2021), maintains and improves intestinal function, plays a role in reducing obesity, and has an important role in improving insulin resistance (Koh et al., 2016; Morrison and Preston, 2016; Fu et al., 2019). More importantly, butyrate reduction was associated with reduced numbers of tight junctions and increased intestinal permeability (Tripathi et al., 2018). MSCs could significantly increase the abundance of *Lachnospiraceae* in the class *Clostridia*. *Lachnospiraceae* are important butyrate-producing bacteria (Berger et al., 2021), which not only produce butyrate, with multifaceted effects on host metabolism and immune function, but also generate peptide antibiotics and convert primary bile acids to secondary bile acids, which promote the microbial community's response to drug-resistant pathogens (Sorbara et al., 2020). HO-1/BMMSCs could also increase the abundance of the butyrate-producing bacteria, *Blautia* (Wang et al., 2020), over time. Therefore, under the action of MSCs, LPS production was reduced, bacterial metabolism was enhanced, especially the metabolism of lipid and butyrate production. The effect of HO-1/BMMSCs on these beneficial parameters was more obvious with time. In addition, the protective effect of the microbiota on intestinal epithelial tight junction proteins would reduce the chance of bacteria and their metabolites entering the portal vein, thereby reducing the inflammatory response of the steatotic liver grafts.

All of these results indicated that the liver microcirculation is impaired after steatotic liver transplantation. Although the portal vein is opened after transplantation, the portal vein pressure might still be high in the short term after transplantation; therefore, mesenteric congestion cannot be effectively relieved. However, MSCs can reduce the degree of steatosis, alleviate the inflammatory response of the liver, and restore the microcirculation of the donor liver as soon as possible, which might reduce the portal venous pressure, reduce mesenteric congestion, and maintain the integrity of the intestinal barrier function, which could regulate the intestinal microbiota, and reduce the abundance of pathogenic bacteria. Importantly, the effects of BMMSCs optimized with HO-1 were more pronounced and longer-lasting over time than those of BMMSCs alone. Thus, HO-1/BMMSCs can better improve lipid metabolism, increase butyrate-producing bacteria, and help to repair steatotic liver grafts.

## CONCLUSION

HO-1/BMMSCs can accelerate lipid metabolism, reduce the inflammatory response, and improve the degree of congestion

and steatosis of the steatotic liver grafts. In addition, HO-1/BMMSCs can protect the intestinal epithelial barrier and regulate intestinal microbiota homeostasis, reduce LPS in the blood, and increase the abundance of bacteria that improve lipid metabolism and butyrate production, thereby exerting a protective effect on steatotic liver grafts. Thus, HO-1/BMMSCs have a beneficial effect on the long-term survival of recipients.

This study had limitations: there was no research on the production and excretion of bile acids, which are important because the metabolism of bile salts by the intestinal microbiota can regulate the consumption of intestinal fat and can also affect the composition of the intestinal microbiota. In addition, the specific changes of portal pressure and the role of liver Kupffer cells also require further study.

## DATA AVAILABILITY STATEMENT

The data presented in the study are deposited in the NCBI SRA database, accession number: PRJNA817803.

## ETHICS STATEMENT

All animal experiments followed the Guidelines for the Care and Use of Laboratory Animals and were approved by the Animal Ethics Committee of Nankai University (Permit Number: 2021-SYDWLL-000331).

## REFERENCES

- Adolph, T. E., Grander, C., Moschen, A. R., and Tilg, H. (2018). Liver-microbiome axis in health and disease. *Trends Immunol.* 39, 712–723. doi: 10.1016/j.it.2018.05.002
- Albillos, A., De Gottardi, A., and Rescigno, M. (2020). The gut-liver axis in liver disease: pathophysiological basis for therapy. *J. Hepatol.* 72, 558–577. doi: 10.1016/j.jhep.2019.10.003
- Bäckhed, F., Ding, H., Wang, T., Hooper, L. V., Koh, G. Y., Nagy, A., et al. (2004). The gut microbiota as an environmental factor that regulates fat storage. *Proc. Natl. Acad. Sci. U. S. A.* 101, 15718–15723. doi: 10.1073/pnas.0407076101
- Bajaj, J. S., Shamsaddini, A., Fagan, A., McGeorge, S., Gavis, E., Sikaroodi, M., et al. (2021). Distinct gut microbial compositional and functional changes associated with impaired inhibitory control in patients with cirrhosis. *Gut Microb.* 13:1953247. doi: 10.1080/19490976.2021.1953247
- Berger, K., Burleigh, S., Lindahl, M., Bhattacharya, A., Patil, P., Ståhlbrand, H., et al. (2021). Xylooligosaccharides increase and in mice on a high-fat diet, with a concomitant increase in short-chain fatty acids, especially butyric acid. *J. Agri. Food Chem.* 69, 3617–3625. doi: 10.1021/acs.jafc.0c06279
- Cai, J., Chen, H., Weng, M., Jiang, S., and Gao, J. (2019). Diagnostic and clinical significance of serum levels of D-lactate and diamine oxidase in patients with Crohn's disease. *Gastroenterol. Res. Practice* 2019:8536952. doi: 10.1155/2019/8536952
- Cao, H., Yang, L., Hou, B., Sun, D., Lin, L., Song, H.-L., et al. (2020). Heme oxygenase-1-modified bone marrow mesenchymal stem cells combined with normothermic machine perfusion to protect donation after circulatory death liver grafts. *Stem Cell Res. Ther.* 11:218. doi: 10.1186/s13287-020-01736-1
- Castonguay-Paradis, S., Lacroix, S., Rochefort, G., Parent, L., Perron, J., Martin, C., et al. (2020). Dietary fatty acid intake and gut microbiota determine circulating endocannabinoid signaling beyond the effect of body fat. *Sci. Rep.* 10:15975. doi: 10.1038/s41598-020-72861-3

## AUTHOR CONTRIBUTIONS

All authors have contributed to the study conception and design, commented on previous versions of the manuscript, and read and approved the final manuscript. HS conceived and designed experiments. MY, LL, HC, and HS conducted the experiments and obtained the results. WZ, LW, HZ, XT, and HS sorted and analyzed the results. MY and HS wrote the draft, extensively revised, formatted, and submitted versions of the manuscript.

## FUNDING

The work was supported by the National Natural Science Foundation of China (Nos. 82070639, 81670574, 81441022, and 81270528).

## ACKNOWLEDGMENTS

We thank Key Laboratory of Emergency and Care Medicine of Ministry of Health and Tianjin Key Laboratory of Organ Transplantation for allowing this work to progress in their laboratories.

## SUPPLEMENTARY MATERIAL

The Supplementary Material for this article can be found online at: <https://www.frontiersin.org/articles/10.3389/fmicb.2022.905567/full#supplementary-material>

- Chen, M., Chen, Z., Lin, X., Hong, X., Ma, Y., Huang, C., et al. (2021). Application of ischaemia-free liver transplantation improves prognosis of patients with steatotic donor livers - a retrospective study. *Transpl. Int.* 34, 1261–1270. doi: 10.1111/tri.13828
- Chen, X., Wu, S., Tang, L., Ma, L., Wang, F., Feng, H., et al. (2019). Mesenchymal stem cells overexpressing heme oxygenase-1 ameliorate lipopolysaccharide-induced acute lung injury in rats. *J. Cell. Physiol.* 234, 7301–7319. doi: 10.1002/jcp.27488
- Croome, K. P., Mathur, A. K., Mao, S., Aqel, B., Piatt, J., Senada, P., et al. (2020). Perioperative and long-term outcomes of utilizing donation after circulatory death liver grafts with macrosteatosis: a multicenter analysis. *Am. J. Transpl.* 20, 2449–2456. doi: 10.1111/ajt.15877
- Deng, F., Hu, J.-J., Yang, X., Sun, Q.-S., Lin, Z.-B., Zhao, B.-C., et al. (2021a). Gut microbial metabolite pravastatin attenuates intestinal ischemia/reperfusion injury through promoting IL-13 release from type II innate lymphoid cells IL-33/ST2 signaling. *Front. Immunol.* 12:704836. doi: 10.3389/fimmu.2021.704836
- Deng, F., Zhao, B.-C., Yang, X., Lin, Z.-B., Sun, Q.-S., Wang, Y.-F., et al. (2021b). The gut microbiota metabolite capsate promotes Gpx4 expression by activating to inhibit intestinal ischemia reperfusion-induced ferroptosis. *Gut Microbes* 13:1902719. doi: 10.1080/19490976.2021.1902719
- Fu, X., Liu, Z., Zhu, C., Mou, H., and Kong, Q. (2019). Nondigestible carbohydrates, butyrate, and butyrate-producing bacteria. *Crit. Rev. Food Sci. Nutr.* 59, S130–S152. doi: 10.1080/10408398.2018.1542587
- Hall, A. B., Yassour, M., Sauk, J., Garner, A., Jiang, X., Arthur, T., et al. (2017). A novel *Ruminococcus gnavus* clade enriched in inflammatory bowel disease patients. *Genome Med.* 9:103. doi: 10.1186/s13073-017-0490-5
- Henke, M. T., Brown, E. M., Cassilly, C. D., Vlamakis, H., Xavier, R. J., and Clardy, J. (2021). Capsular polysaccharide correlates with immune response to the human gut microbe. *Proc. Natl. Acad. Sci. U. S. A.* 118:2007595. doi: 10.1073/pnas.2007595118



- Hughes, C. B., and Humar, A. (2021). Liver transplantation: current and future. *Abdominal Radiol.* 46, 2–8. doi: 10.1007/s00261-019-02357-w
- Ijaz, S., Yang, W., Winslet, M. C., and Seifalian, A. M. (2003). Impairment of hepatic microcirculation in fatty liver. *Microcirculation* 10, 447–456. doi: 10.1038/sj.mn.7800206
- Jackson, K. R., Motter, J. D., Haugen, C. E., Holscher, C., Long, J. J., Massie, A. B., et al. (2020). Temporal trends in utilization and outcomes of steatotic donor livers in the United States. *Am. J. Transplant.* 20, 855–863. doi: 10.1111/ajt.15652
- Juanola, O., Hassan, M., Kumar, P., Yilmaz, B., Keller, I., Simillion, C., et al. (2021). Intestinal microbiota drives cholestasis-induced specific hepatic gene expression patterns. *Gut Microbes* 13:1911534. doi: 10.1080/19490976.2021.1911534
- Kaakoush, N. O. (2015). Insights into the role of erysipelotrichaceae in the human host. *Front. Cell. Infect. Microbiol.* 5:84. doi: 10.3389/fcimb.2015.00084
- Kamada, N., and Calne, R. Y. (1979). Orthotopic liver transplantation in the rat. Technique using cuff for portal vein anastomosis and biliary drainage. *Transplantation* 28, 47–50. doi: 10.1097/00007890-197907000-00011
- Khan, A., Ding, Z., Ishaq, M., Bacha, A. S., Khan, I., Hanif, A., et al. (2021). Understanding the effects of gut microbiota dysbiosis on nonalcoholic fatty liver disease and the possible probiotics role: recent updates. *Int. J. Biol. Sci.* 17, 818–833. doi: 10.7150/ijbs.56214
- Koh, A., De Vadder, F., Kovatcheva-Datchary, P., and Bäckhed, F. (2016). From dietary fiber to host physiology: short-chain fatty acids as key bacterial metabolites. *Cell* 165, 1332–1345. doi: 10.1016/j.cell.2016.05.041
- Lang, S., and Schnabl, B. (2020). Microbiota and fatty liver disease—the known, the unknown, and the future. *Cell Microbe* 28, 233–244. doi: 10.1016/j.chom.2020.07.007
- Le Roy, T., Llopis, M., Lepage, P., Bruneau, A., Rabot, S., Bevilacqua, C., et al. (2013). Intestinal microbiota determines development of non-alcoholic fatty liver disease in mice. *Gut* 62, 1787–1794. doi: 10.1136/gutjnl-2012-303816
- Lee, N. Y., Yoon, S. J., Han, D. H., Gupta, H., Youn, G. S., Shin, M. J., et al. (2020). Lactobacillus and *Pedococcus ameliorate* progression of non-alcoholic fatty liver disease through modulation of the gut microbiome. *Gut Microbes* 11, 882–899. doi: 10.1080/19490976.2020.1712984
- Livak, K. J., and Schmittgen, T. D. (2001). Analysis of relative gene expression data using real-time quantitative PCR and the 2(-Delta Delta C(T)) method. *Methods* 25, 402–408. doi: 10.1006/meth.2001.1262
- Mahrouf-Yorgov, M., Augeul, L., Da Silva, C. C., Jourdan, M., Rigolet, M., Manin, S., et al. (2017). Mesenchymal stem cells sense mitochondria released from damaged cells as danger signals to activate their rescue properties. *Cell Death Differentiat.* 24, 1224–1238. doi: 10.1038/cdd.2017.51
- Martin-Mateos, R., and Albillos, A. (2021). The role of the gut-liver axis in metabolic dysfunction-associated fatty liver disease. *Front. Immunol.* 12:660179. doi: 10.3389/fimmu.2021.660179
- Mccormack, L., Dutkowski, P., El-Badry, A. M., and Clavien, P.-A. (2011). Liver transplantation using fatty livers: always feasible? *J. Hepatol.* 54, 1055–1062. doi: 10.1016/j.jhep.2010.11.004
- Miyauchi, E., Kim, S.-W., Suda, W., Kawasumi, M., Onawa, S., Taguchi-Atarashi, N., et al. (2020). Gut microorganisms act together to exacerbate inflammation in spinal cords. *Nature* 585, 102–106. doi: 10.1038/s41586-020-2634-9
- Morrison, D. J., and Preston, T. (2016). Formation of short chain fatty acids by the gut microbiota and their impact on human metabolism. *Gut Microbes* 7, 189–200. doi: 10.1080/19490976.2015.1134082
- Mu, J., Chen, Q., Zhu, L., Wu, Y., Liu, S., Zhao, Y., et al. (2019). Influence of gut microbiota and intestinal barrier on enterogenic infection after liver transplantation. *Curr. Med. Res. Opin.* 35, 241–248. doi: 10.1080/03007995.2018.1470085
- Nakamura, K., Kageyama, S., Ito, T., Hirao, H., Kadono, K., Aziz, A., et al. (2019). Antibiotic pretreatment alleviates liver transplant damage in mice and humans. *J. Clin. Invest.* 129, 3420–3434. doi: 10.1172/JCI127550
- Plovier, H., Everard, A., Druart, C., Depommier, C., Van Hul, M., Geurts, L., et al. (2017). A purified membrane protein from *Akkermansia muciniphila* or the pasteurized bacterium improves metabolism in obese and diabetic mice. *Nat. Med.* 23, 107–113. doi: 10.1038/nm.4236
- Rao, Y., Kuang, Z., Li, C., Guo, S., Xu, Y., Zhao, D., et al. (2021). Gut *Akkermansia muciniphila* ameliorates metabolic dysfunction-associated fatty liver disease by regulating the metabolism of L-aspartate via gut-liver axis. *Gut Microbes* 13:1927633. doi: 10.1080/19490976.2021.1927633
- Reunanen, J., Kainulainen, V., Huuskonen, L., Ottman, N., Belzer, C., Huhtinen, H., et al. (2015). *Akkermansia muciniphila* adheres to enterocytes and strengthens the integrity of the epithelial cell layer. *Appl. Environ. Microbiol.* 81, 3655–3662. doi: 10.1128/AEM.04050-14
- Safari, Z., and Gérard, P. (2019). The links between the gut microbiome and non-alcoholic fatty liver disease (NAFLD). *Cell. Mol. Life Sci.* 76, 1541–1558. doi: 10.1007/s00018-019-03011-w
- Sharpton, S. R., Schnabl, B., Knight, R., and Loomba, R. (2021). Current concepts, opportunities, and challenges of gut microbiome-based personalized medicine in nonalcoholic fatty liver disease. *Cell Metabol.* 33, 21–32. doi: 10.1016/j.cmet.2020.11.010
- Sheka, A. C., Adeyi, O., Thompson, J., Hameed, B., Crawford, P. A., and Ikramuddin, S. (2020). Nonalcoholic steatohepatitis: a review. *J. Am. Med. Assoc.* 323, 1175–1183. doi: 10.1001/jama.2020.22298
- Singhal, R., Donde, H., Ghare, S., Stocke, K., Zhang, J., Vadhanam, M., et al. (2021). Decrease in acetyl-CoA pathway utilizing butyrate-producing bacteria is a key pathogenic feature of alcohol-induced functional gut microbial dysbiosis and development of liver disease in mice. *Gut Microbes* 13:1946367. doi: 10.1080/19490976.2021.1946367
- Sookoian, S., Salatiello, A., Castaño, G. O., Landa, M. S., Fijalkowky, C., Garaycoechea, M., et al. (2020). Intrahepatic bacterial metatranscriptomic signature in non-alcoholic fatty liver disease. *Gut* 69, 1483–1491. doi: 10.1136/gutjnl-2019-318811
- Sorbara, M. T., Littmann, E. R., Fontana, E., Moody, T. U., Kohout, C. E., Gjonbalaj, M., et al. (2020). Functional and genomic variation between human-derived isolates of lachnospiraceae reveals inter- and intra-species diversity. *Cell Host Microbe* 28:5. doi: 10.1016/j.chom.2020.05.005
- Sun, D., Cao, H., Yang, L., Lin, L., Hou, B., Zheng, W., et al. (2020a). MiR-200b in heme oxygenase-1-modified bone marrow mesenchymal stem cell-derived exosomes alleviates inflammatory injury of intestinal epithelial cells by targeting high mobility group box 3. *Cell Death Dis.* 11:480. doi: 10.1038/s41419-020-2685-8
- Sun, D., Yang, L., Cao, H., Shen, Z.-Y., and Song, H.-L. (2020b). Study of the protective effect on damaged intestinal epithelial cells of rat multilineage-differentiating stress-enduring (Muse) cells. *Cell Biol. Int.* 44, 549–559. doi: 10.1002/cbin.11255
- Teramoto, K., Bowers, J. L., Kruskal, J. B., and Clouse, M. E. (1993). Hepatic microcirculatory changes after reperfusion in fatty and normal liver transplantation in the rat. *Transplantation* 56, 1076–1082. doi: 10.1097/00007890-199311000-00005
- Tian, X., Cao, H., Wu, L., Zheng, W., Yuan, M., Li, X., et al. (2021). Heme oxygenase-1-modified bone marrow mesenchymal stem cells combined with normothermic machine perfusion repairs bile duct injury in a rat model of DCD liver transplantation via activation of peribiliary glands through the Wnt pathway. *Stem Cells Int.* 2021:9935370. doi: 10.1155/2021/9935370
- Tilg, H., Zmora, N., Adolph, T. E., and Elinav, E. (2020). The intestinal microbiota fuelling metabolic inflammation. *Nat. Rev. Immunol.* 20, 40–54. doi: 10.1038/s41577-019-0198-4
- Tripathi, A., Debelius, J., Brenner, D. A., Karin, M., Loomba, R., Schnabl, B., et al. (2018). The gut-liver axis and the intersection with the microbiome. *Nat. Rev. Gastroenterol. Hepatol.* 15, 397–411. doi: 10.1038/s41575-018-0011-z
- Wallace, J. L., Motta, J.-P., and Buret, A. G. (2018). Hydrogen sulfide: an agent of stability at the microbiome-mucosa interface. *Am. J. Physiol.* 314, G143–G149. doi: 10.1152/ajpgi.00249.2017
- Wang, J., Qian, T., Jiang, J., Yang, Y., Shen, Z., Huang, Y., et al. (2020). Gut microbial profile in biliary atresia: a case-control study. *J. Gastroenterol. Hepatol.* 35, 334–342. doi: 10.1111/jgh.14777
- Xiong, X., Ren, Y., Cui, Y., Li, R., Wang, C., and Zhang, Y. (2017). Obeticholic acid protects mice against lipopolysaccharide-induced liver injury and inflammation. *Biomed. Pharmacother.* 96, 1292–1298. doi: 10.1016/j.biopha.2017.11.083
- Yang, X., Lu, D., Zhuo, J., Lin, Z., Yang, M., and Xu, X. (2020). The gut-liver axis in immune remodeling: new insight into liver diseases. *Int. J. Biol. Sci.* 16, 2357–2366. doi: 10.7150/ijbs.46405
- Yang, Y., Song, H.-L., Zhang, W., Wu, B.-J., Fu, N.-N., Zheng, W.-P., et al. (2014). Reduction of acute rejection by bone marrow mesenchymal

- stem cells during rat small bowel transplantation. *PLoS ONE* 9:e114528. doi: 10.1371/journal.pone.0114528
- Yin, M., Shen, Z., Yang, L., Zheng, W., and Song, H. (2019). Protective effects of CXCR3/HO-1 gene-modified BMMSCs on damaged intestinal epithelial cells: role of the p38-MAPK signaling pathway. *Int. J. Mol. Med.* 43, 2086–2102. doi: 10.3892/ijmm.2019.4120
- Yin, M.-L., Song, H.-L., Yang, Y., Zheng, W.-P., Liu, T., and Shen, Z.-Y. (2017). Effect of genes modified bone marrow mesenchymal stem cells on small bowel transplant rejection. *World J. Gastroenterol.* 23, 4016–4038. doi: 10.3748/wjg.v23.i22.4016
- Zhang, X., Coker, O. O., Chu, E. S., Fu, K., Lau, H. C. H., Wang, Y.-X., et al. (2021). Dietary cholesterol drives fatty liver-associated liver cancer by modulating gut microbiota and metabolites. *Gut* 70, 761–774. doi: 10.1136/gutjnl-2019-319664
- Zheng, W.-P., Zhang, B.-Y., Shen, Z.-Y., Yin, M.-L., Cao, Y., and Song, H.-L. (2017). Biological effects of bone marrow mesenchymal stem cells on hepatitis B virus *in vitro*. *Mol. Med. Rep.* 15, 2551–2559. doi: 10.3892/mmr.2017.6330
- Zheng, Z., and Wang, B. (2021). The gut-liver axis in health and disease: the role of gut microbiota-derived signals in liver injury and regeneration. *Front. Immunol.* 12:775526. doi: 10.3389/fimmu.2021.775526

**Conflict of Interest:** The authors declare that the research was conducted in the absence of any commercial or financial relationships that could be construed as a potential conflict of interest.

**Publisher's Note:** All claims expressed in this article are solely those of the authors and do not necessarily represent those of their affiliated organizations, or those of the publisher, the editors and the reviewers. Any product that may be evaluated in this article, or claim that may be made by its manufacturer, is not guaranteed or endorsed by the publisher.

Copyright © 2022 Yuan, Lin, Cao, Zheng, Wu, Zuo, Tian and Song. This is an open-access article distributed under the terms of the Creative Commons Attribution License (CC BY). The use, distribution or reproduction in other forums is permitted, provided the original author(s) and the copyright owner(s) are credited and that the original publication in this journal is cited, in accordance with accepted academic practice. No use, distribution or reproduction is permitted which does not comply with these terms.



# Fermented Soy and Fish Protein Dietary Sources Shape Ileal and Colonic Microbiota, Improving Nutrient Digestibility and Host Health in a Piglet Model

Ying Li<sup>1,2†</sup>, Yunsheng Han<sup>3†</sup>, Qingyu Zhao<sup>1,2</sup>, Chaohua Tang<sup>1,2</sup>, Junmin Zhang<sup>1,2\*</sup> and Yuchang Qin<sup>1,2\*</sup>

<sup>1</sup> State Key Laboratory of Animal Nutrition, Institute of Animal Sciences of Chinese Academy of Agricultural Sciences, Beijing, China, <sup>2</sup> Scientific Observing and Experiment Station of Animal Genetic Resources and Nutrition in North China of Ministry of Agriculture and Rural Affairs, Institute of Animal Science of Chinese Academy of Agricultural Sciences, Beijing, China, <sup>3</sup> Key Laboratory of Feed Biotechnology, Ministry of Agriculture and Rural Affairs, Feed Research Institute of Chinese Academy of Agricultural Sciences, Beijing, China

## OPEN ACCESS

### Edited by:

Yubin Luo,  
Sichuan University, China

### Reviewed by:

Shimeng Huang,  
Jiangsu Academy of Agricultural  
Sciences, China  
Md. Abul Kalam Azad,  
Institute of Subtropical Agriculture  
(CAS), China

### \*Correspondence:

Junmin Zhang  
zhjmxms@sina.com  
Yuchang Qin  
qinyuchang@caas.cn

<sup>†</sup> These authors have contributed  
equally to this work

### Specialty section:

This article was submitted to  
Microbial Symbioses,  
a section of the journal  
Frontiers in Microbiology

Received: 02 April 2022

Accepted: 30 May 2022

Published: 22 June 2022

### Citation:

Li Y, Han Y, Zhao Q, Tang C,  
Zhang J and Qin Y (2022) Fermented  
Soy and Fish Protein Dietary Sources  
Shape Ileal and Colonic Microbiota,  
Improving Nutrient Digestibility  
and Host Health in a Piglet Model.  
Front. Microbiol. 13:911500.  
doi: 10.3389/fmicb.2022.911500

Suitable protein sources are essential requirements for piglet growth and health. Typically, intestinal microbiota co-develops with the host and impact its physiology, which make it more plastic to dietary protein sources at early stages. However, the effects of fermented soybean meal (FSB) and fish meal (FM) on foregut and hindgut microbiota, and their relationship with nutrient digestion and host health remain unclear. In this study, we identified interactions between ileac and colonic microbiota which were reshaped by FSB and FM, and assessed host digestibility and host health in a piglet model. Eighteen weaned piglets (mean weight = 8.58 ± 0.44 kg) were divided into three dietary treatments, with six replicates/treatment. The level of dietary protein was 16%, with FSB, FM, and a mixture of fermented soybean meal and fish meal (MFSM) applied as protein sources. During days 1–14 and 1–28, diets containing MFSM generated higher piglet body weight and average daily gain, but lower feed to weight gain ratios when compared with the FM diet ( $P < 0.05$ ). Piglets in MFSM and FM groups had lower apparent total tract digestibility (ATTD) of crude protein (CP) compared with the FSB group ( $P < 0.05$ ). Serum immunoglobulins (IgM and IgG) in MFSM and FM groups were significantly higher on day 28, but serum cytokines (interleukin-6 and tumor necrosis factor- $\alpha$ ) were significantly lower than the FSB group on days 14 and 28 ( $P < 0.05$ ). When compared with FSB and FM groups, dietary MFSM significantly increased colonic acetic acid and butyric acid levels ( $P < 0.05$ ). Compared with the FM and MFSM groups, the FSB diet increased the relative abundance of ileac *Lactobacillus* and *f\_Lactobacillaceae*, which were significant positively correlated with CP ATTD ( $P < 0.05$ ). Compared with the FSB group, the relative abundance of *f\_Peptostreptococcaceae* and *Romboutsia* in MFSM or FM groups were increased and were significant positively correlated with total carbohydrate (TC) ATTD ( $P < 0.05$ ). Piglets fed FSB had higher  $\alpha$ -diversity in colonic microbiota when compared with other groups ( $P < 0.05$ ). The

relative abundance of colonic *unidentified\_Clostridiales* and *Romboutsia* in MFSM and FSB groups were significantly higher than in the FM group ( $P < 0.05$ ). Dietary MFSM or FM increased the relative abundance of colonic *Streptococcaceae* and *Streptococcus*, but decreased the relative abundance of *Christensenellaceae* when compared with the FSB group ( $P < 0.05$ ). These bacteria showed a significantly positive correlation with serum cytokine and immunoglobulin levels ( $P < 0.05$ ). Therefore, dietary FSB improved CP digestibility by increasing the relative abundance of ileac *f\_Lactobacillaceae* and *Lactobacillus*, while dietary MFSM benefited TC digestibility by increasing *f\_Peptostreptococcaceae* and *Romboutsia*. Dietary MFSM and FM enhanced immunoglobulin secretion by increasing colonic *f\_Streptococcaceae* and *Streptococcus* prevalence, while dietary FSB promoted cytokine production by increasing microbiota diversity and *Romboutsia* and *Christensenellaceae*. Our data provide a theoretical dietary basis for young animals using plant and animal protein sources.

**Keywords:** fermented soybean meal, fish meal, growth performance, ileac and colonic microbiota, apparent total tract digestibility, serum immunity

## INTRODUCTION

Dietary protein is a fundamental source of amino acids for mammals, and an essential requirement for physiological organ function and neurodevelopment in early life stages. In the gastrointestinal tract, dietary proteins interplay with a variety of substrates. Most are digested as peptides and amino acids by proteinases in the small intestine. Others enter the hindgut to undergo microbial fermentation (Walker et al., 2005; Blachier et al., 2007). High protein levels and poor protein digestibility in diets increase protein influx into the hindgut, cause excess fermentation, and release toxic metabolites which are detrimental to the host (Yao et al., 2016; Zhang and Piao, 2022). Thus, reducing dietary protein levels and optimizing existing protein sources may be effective in reducing abnormal fermentation processes in the hindgut.

In the pig industry, weaned piglets often experience a transition from highly digestible milk to solid protein diets which induce intestinal disorders and cause diarrhea or even death (Hu et al., 2020). The piglet model is suitable to investigate the effects of dietary protein sources on gut microbiota and health as they are susceptible to protein levels and quality (Li et al., 2019b). Fish meal (FM) has long been used as an ideal dietary protein source for animal production as it contains a balanced source of indispensable amino acids, and a rich source of long-chain omega-3 fatty acids, vitamins, and minerals (Zhang et al., 2018a). Soybean meal is derived from plant proteins and is considered an excellent protein source approximately equivalent to animal proteins, and it rates as 1.0 on the protein digestibility corrected amino acid score scale (Hasler and Clare, 2002). Low protein diets with balanced amino acids can reduce diarrhea incidence and maintain intestinal health without affecting piglet performance (Wang et al., 2018). Reducing crude protein levels by 3% could shift colonic microbiota in pigs, decrease the relative abundance of *Streptococcus* but increase the relative abundance of *Sarcina*, *Coprococcus*, and *Peptostreptococcaceae* (Zhou et al., 2016). Fermentation improves soybean meal quality

by decreasing anti-nutritional factors, such as protease inhibitors, and enhancing free amino acid and small peptide levels (Seo and Cho, 2016; Zhang et al., 2016). Also, fermented soybean meal (FSB) administration decreases the incidence of diarrhea in pigs by inhibiting intestinal pathogen colonization (Kiers et al., 2010).

The gastrointestinal tract contains a dense, dynamic, and highly complex microbial community, equating to appropriately  $10^{14}$  microbes and comprising thousands of individual species (Collins et al., 2012). Swine intestinal microbiota co-develop with the host and play important roles in nutrient digestion, absorption, metabolism, and intestinal health protection (Li et al., 2019b). Microbiota composition is in flux, but over time, diversity increases and converges toward an adult-like microbiota, with features in increasing overall number of taxa and functional genes (Koenig et al., 2011; Rodriguez et al., 2015). During early life stages, this microbial colonization period appears critical for both current- and whole-life health as the microbiota are more plastic and dynamic than in adults. Generally, the intestinal microbiota are resilient to changes in dietary protein sources (Rist et al., 2013). However, little is known about the effects of FSB and FM on host foregut and hindgut microbiota, while their relationship with nutrient digestion and host health remains unclear.

Therefore, we hypothesized that diets containing FSB and FM could alter ileal and colonic microbiota and contribute to host digestibility and health in early life. To this end, we used a piglet model to investigate dietary effects on growth performance and ileal and colonic microbial structures, and to understand the relationship between microbiota, nutrient digestibility, and serum immunity. Our data provide a theoretical dietary basis for young animals using different protein sources for overall health.

## MATERIALS AND METHODS

### Ethical Considerations

This study was conducted in accordance with the “Guidelines on Welfare and Ethical Review for Laboratory Animals” (GB/T



35892-2018), and it was approved by the Institutional Animal Care and Use Committee of the Institute of Animal Science of the Chinese Academy of Agricultural Sciences, Beijing, China (IAS2019-25).

## Materials

High-quality FSB was selected based on our previous study (Li et al., 2019c). Firstly, three FSB samples were selected from ten representative samples, based on the evaluation of crude protein (CP), amino acids, acid soluble proteins, and anti-nutrient factors, including glycinin,  $\beta$ -conglycinin, and trypsin inhibitors. The highest quality FSB was then selected based on dry matter (DM) and CP digestibility, and *in vitro* amino acid evaluation. FSB was fermented using a combination of *Bacillus subtilis*, *Lactobacillus plantarum*, and *Saccharomyces cerevisiae* at  $\geq 10^9$  CFU/mL,  $\geq 10^{10}$  CFU/mL, and  $\geq 10^9$  CFU/mL concentrations, respectively. Also, imported fishmeal (Peru) containing 68.5% CP was selected as a high-quality FM source.

## Animals, Diets, and Experimental Design

Eighteen crossbred male weaned piglets (Duroc  $\times$  Landrace  $\times$  Yorkshire, weaned at 28 days), with an average body weight (BW =  $8.58 \pm 0.44$  kg), were randomly allocated to three groups, consisting of six replicates, with one piglet/replicate. FSB ( $n = 6$ ), FM ( $n = 6$ ), and a mixture of fermented soybean meal and fish meal (MFSM,  $n = 6$ ) were used as protein sources. To meet National Research Council (2012) nutrient requirements for 7–11 kg pigs, a non-medicated basal diet in mashed form was formulated, with CP levels at 16% in accordance with a previous study (Chen et al., 2018; Table 1). All diets contained equal standardized ileal digestible (SID) lysine, methionine, threonine, tryptophan, leucine, isoleucine, and valine, using added crystalline amino acids. Piglets were housed alone in one pen (1.8 m  $\times$  0.8 m) with a hard plastic, fully-slotted floor. Adjacent pens were separated by a closed baffle. Piglets were housed in an environmentally controlled room (28–30 and 25–28°C between days 1–14 and 15–28, respectively). The study lasted 28 days, during which time meals were provided twice daily at 08:00 and 16:00 h, and pigs had *ad libitum* access to food and water.

## Sample Collection and Measurements

### Growth Performance

Taking each piglet as one unit, BW was recorded at study commencement and every fortnight. The feed intake of each piglet was recorded daily using an electronic feeding system (MXCD-15B, Yangzhou, China). Then, average daily feed intake (ADFI), average daily gain (ADG), and feed to weight gain ratios (F/G) were calculated between days 1–14, 15–28, and 1–28.

### Apparent Total Tract Digestibility

Representative 1 kg feed samples were collected at study end and stored at 4°C. Between days 25 and 28, approximately 200 g fresh feces from each pen was collected twice a day at 7:00 and 16:00, and immediately frozen at  $-20^\circ\text{C}$ . Feces was pooled by pen, dried at  $65^\circ\text{C}$  for 72 h, and ground down to pass

**TABLE 1** | Ingredients and chemical composition of experimental diets (as-fed basis).

Ingredient (%)	Diet treatments <sup>§</sup>		
	FSB	FM	MFSM
Corn	65.27	76.77	69.18
Fermented soybean meal	23.50	0.00	15.25
Fish meal	0.00	14.00	5.00
Soybean oil	4.50	4.50	4.50
Dicalcium phosphate	1.50	0.20	1.00
Limestone	0.60	0.10	0.55
Sodium chloride	0.27	0.07	0.20
Glucose	2.00	2.00	2.00
L-Lysine-HCl	0.69	0.61	0.66
DL-Methionine	0.20	0.04	0.14
L-Threonine	0.28	0.30	0.28
L-Tryptophan	0.07	0.10	0.08
L-Leucine	0.00	0.14	0.02
L-Isoleucine	0.13	0.22	0.16
L-Valine	0.28	0.25	0.27
Chromium oxide	0.20	0.20	0.20
Vitamin and mineral premix <sup>†</sup>	0.50	0.50	0.50
Total	100.00	100.00	100.00
<b>Nutrient composition (%)<sup>‡</sup></b>			
Digestible energy (MJ/kg)	14.59	14.77	14.65
Crude protein	16.21	16.27	16.28
Calcium	0.75	0.75	0.79
Total phosphorus	0.66	0.66	0.65
Available phosphorus	0.39	0.48	0.42
SID* Lysine	1.35	1.35	1.35
SID* Methionine	0.39	0.39	0.39
SID* Threonine	0.79	0.79	0.79
SID* Tryptophan	0.22	0.22	0.22
SID* Leucine	1.35	1.35	1.35
SID* Isoleucine	0.69	0.69	0.69
SID* Valine	0.86	0.86	0.86

<sup>†</sup>A vitamin-mineral premix provided the following nutrients per kg of diet: Vitamin A, 2200 IU; Vitamin D3, 220 IU; Vitamin E, 16 IU; Vitamin K3, 0.5 mg; Vitamin B12, 0.02 mg; Riboflavin, 4 mg; Niacin, 30 mg; Pantothenic acid, 12 mg; Choline chloride, 600 mg; Folic acid, 0.3 mg; Vitamin B1, 1.5 mg; Vitamin B6, 7 mg; Biotin, 0.08 mg; Zn, 100 mg; Mn, 4 mg; Fe, 105 mg; Cu, 6 mg; I, 0.14 mg; Se, 0.3 mg.

<sup>‡</sup>Nutrient levels were calculated.

\*SID, standardized ileal digestible.

<sup>§</sup>FSB, fermented soybean meal diet; FM, fish meal; MFSM, mixture of fermented soybean meal and fish meal diet.

through a 1 mm sieve for analysis. DM, CP, ether extract (EE), and ash in feed and fecal samples were measured according to the Association of Official Analytical Chemists (AOAC, 2012). Chromium (Cr) levels in feed and feces were measured using an atomic absorption spectrophotometer (AAS) (TAS-990super, Beijing, China) based on a method by Williams et al. (1962). In addition, organic matter (OM) and total carbohydrates (TCs) were calculated using the following equations:  $\text{OM} = 1 - \text{ash}$  and  $\text{TC} = \text{DM} - \text{CP} - \text{EE} - \text{ash}$  (Gerritsen et al., 2010).  $\text{ATTD}_{\text{nutrient}} = 1 - (\text{Cr}_{\text{diet}} \times \text{Nutrient}_{\text{feces}}) / (\text{Cr}_{\text{feces}} \times \text{Nutrient}_{\text{diet}})$  (Long et al., 2017).

## Serum Immune Globulin and Inflammatory Cytokines

On the morning of days 14 and 28, after fasting overnight, 5 mL blood samples were collected from piglets via jugular vein puncture into a vacutainer. After 2 h, bloods were centrifuged at  $3,000 \times g$  at  $4^{\circ}\text{C}$  for 10 min to recover serum, and stored at  $-20^{\circ}\text{C}$ . Serum immunoglobulin A (IgA), IgG, IgM, interleukin- $1\beta$  (IL- $1\beta$ ), IL-6, and tumor necrosis factor- $\alpha$  (TNF- $\alpha$ ) levels were determined using enzyme-linked immunosorbent assays (Shanghai Enzyme-linked Biotechnology, Co., Ltd., Shanghai, China) following manufacturer's instructions.

## Ileal and Colonic Microbiota

After fasting overnight on day 28, piglets were humanely slaughtered 5 min after anesthetic injection. Ileal and colonic chyme was collected into 5 mL centrifuge tubes, snap frozen in liquid nitrogen, and stored at  $-80^{\circ}\text{C}$ . Bacterial genomic DNA was extracted from ileal and colonic chyme samples (Qiagen DNA stool mini kit, Hilden, Germany). DNA quantity and quality were assessed by NanoDrop 2000 spectrophotometer (Thermo Fisher Scientific, Waltham, MA United States) and 1% agarose gels, respectively. The V3–V4 hypervariable region of 16S rRNA was amplified using specific primers (forward 5'-ACTCCTACGGGAGGAGCA-3' and reverse 5'-GGACTACHVGGGTWTCTAAT-3') which contained barcodes. Polymerase chain reaction (PCR) was conducted in a total volume of 20  $\mu\text{L}$ , including  $1 \times$  FastPfu buffer, 250  $\mu\text{M}$  dNTP, 0.2  $\mu\text{M}$  each primer, 1 U FastPfu polymerase (Beijing TransGen Biotech, Beijing, China), and 10 ng template DNA. Thermal cycling parameters: initial denaturation at  $98^{\circ}\text{C}$  for 1 min, followed by 30 cycles of  $98^{\circ}\text{C}$  for 10 s, annealing at  $50^{\circ}\text{C}$  for 30 s, elongation at  $72^{\circ}\text{C}$  for 30 s, and a final extension at  $72^{\circ}\text{C}$  for 5 min. PCR products were electrophoresed on 2% agarose gels and purified using a Qiagen gel extraction kit (Qiagen, Hilden, Germany). Sequencing libraries were constructed using TruSeq<sup>®</sup> DNA PCR-Free Sample Preparation Kit (Illumina, California, CA, United States) according to manufacturer's recommendations, and index codes were added. Library quality was assessed using the Qubit V.2.0 Fluorometer (Thermo Fisher Scientific, Waltham, MA United States). Qualified DNA libraries were loaded into a NovaSeq platform, capable of  $2 \times 250$  bp paired-end sequencing (Novogene, Beijing, China).

## Biodiversity Analysis

Paired-end reads were generated and merged using FLASH software (V1.2.7)<sup>1</sup>. Operational taxonomic units with 97% identity were gathered using Uparse (ver. 7.1)<sup>2</sup>. Taxonomic annotations were performed using the Mothur algorithm (70% confidence) in the Silva Database<sup>3</sup>. Alpha-diversity was analyzed using Chao<sup>4</sup>, ACE<sup>5</sup>, Shannon<sup>6</sup>, and Simpson<sup>7</sup>

indices. Beta-diversity was visualized using Non-Metric Multi-Dimensional Scaling (NMDS) plots combined with Bray-Curtis distances.

## Statistical Analysis

Data were analyzed using one-way analysis of variance using comparative averages in SPSS 22.0 (IBM Corp., Armonk, NY, United States). Differences between treatment means for growth performance, ATTD, and serum immune indices were analyzed using Duncan's multiple-range and least significant difference *post hoc* tests. Data were expressed as the mean  $\pm$  standard deviation (SD). Correlations between differential gut microbiota and immune indices, and corresponding *P*-values were estimated using Spearman correlation analyzes using gplot and psych packages, respectively. *P*-values  $< 0.05$  (\*) were statistically significant and *P*-values  $< 0.01$  (\*\*) were extremely significant.

# RESULTS

## Growth Performance

Dietary MFSM and FSB generated significantly higher piglet BWs on day 14 and ADG between days 1–14 ( $P < 0.05$ ; **Table 2**). Dietary MFSM generated significantly higher piglet BWs on day 28 and ADG between days 1–28 ( $P < 0.05$ ) when compared to FM animals. Between days 1–14, ADFI in the FSB group was significantly higher than the FM group ( $P < 0.05$ ). Also, when compared to the FM group, piglets in FSB and MFSM groups had significantly lower F/G ratios between days 1–14 ( $P < 0.05$ ), and piglets in the MFSM group had significantly lower F/G ratios between days 1–28 ( $P < 0.05$ ).

## Apparent Total Tract Digestibility

Apparent total tract digestibility (ATTD) of DM and TC were not influenced by dietary protein sources ( $P > 0.05$ ; **Table 3**). FSB-fed piglets had significantly higher CP ATTD than other groups ( $P < 0.05$ ), whereas FSB and FM piglets had significantly higher OM ATTD than MFSM animals ( $P < 0.05$ ). The EE ATTD in FM animals was significantly higher than MFSM and FSB groups ( $P < 0.05$ ), and EE ATTD in the FSB group was significantly higher than the MFSM group ( $P < 0.05$ ).

## Serum Immune Globulins and Inflammatory Cytokines

On day 14, in MFSM and FM groups, serum IgA levels were higher ( $P < 0.05$ ) and serum IL-6 and TNF- $\alpha$  levels were lower ( $P < 0.05$ ) than the FSB group (**Table 4**). Serum IgG levels in the FM group were significantly increased and serum IL- $1\beta$  levels in the MFSM group significantly decreased when compared with the FSB group ( $P < 0.05$ ). On day 28, when compared with the FSB group, MFSM and FM piglets had significantly higher serum IgG and IgM levels ( $P < 0.05$ ) and lower serum IL- $1\beta$ , IL-6, and TNF- $\alpha$  levels ( $P < 0.05$ ). Piglets in the MFSM group had higher serum IgA levels than FSB and FM groups, and higher serum IgM levels than the FM group ( $P < 0.05$ ).

<sup>1</sup><http://ccb.jhu.edu/software/FLASH/>

<sup>2</sup><http://drive5.com/uparse/>

<sup>3</sup><http://www.arb-silva.de/>

<sup>4</sup><http://www.mothur.org/wiki/Chao>

<sup>5</sup><http://www.mothur.org/wiki/Ace>

<sup>6</sup><http://www.mothur.org/wiki/Shannon>

<sup>7</sup><http://www.mothur.org/wiki/Simpson>

## Microbiota Diversity in the Ileum and Colon

In total, 2,294,708 effective sequences were generated from piglet gut microbiota samples, with an average 69,537 sequences/sample. Alpha-diversity analyzes showed varied community richness between groups in terms of colonic bacterial communities; the Chao 1 index in FSB animals was higher than FM and MFSM groups, and both Observed\_species and ACE indices in the FSB group were higher than those in the MFSM group ( $P < 0.05$ ; Table 5). However, no significant differences

**TABLE 2 |** The effects of different protein dietary sources on weaned piglet growth and development.

Item	Dietary treatments <sup>1</sup>			P-value
	FSB	FM	MFSM	
Body weight (kg)				
Initial	8.47 ± 0.47	8.65 ± 0.46	8.61 ± 0.47	0.78
Day 14	12.13 ± 0.54 <sup>a</sup>	11.19 ± 0.86 <sup>b</sup>	12.32 ± 0.23 <sup>a</sup>	0.01
Day 28	18.61 ± 1.37 <sup>ab</sup>	17.48 ± 1.74 <sup>b</sup>	19.89 ± 1.20 <sup>a</sup>	0.04
Day 1–14				
ADFI (g) <sup>2</sup>	446.98 ± 55.53 <sup>a</sup>	367.29 ± 38.19 <sup>b</sup>	410.75 ± 42.98 <sup>ab</sup>	0.03
ADG (g) <sup>2</sup>	228.55 ± 39.75 <sup>a</sup>	158.75 ± 36.27 <sup>b</sup>	232.25 ± 32.05 <sup>a</sup>	0.01
F/G <sup>2</sup>	1.99 ± 0.33 <sup>b</sup>	2.38 ± 0.41 <sup>a</sup>	1.78 ± 0.07 <sup>b</sup>	0.01
Day 15–28				
ADFI (g)	719.94 ± 98.35	730.73 ± 68.27	762.88 ± 73.37	0.64
ADG (g)	415.64 ± 76.09	393.13 ± 69.44	472.88 ± 66.2	0.17
F/G	1.75 ± 0.18	1.89 ± 0.26	1.62 ± 0.07	0.08
Day 1–28				
ADFI (g)	581.58 ± 56.25	549.01 ± 41.84	586.81 ± 58.05	0.42
ADG (g)	320.8 ± 51.1 <sup>ab</sup>	275.94 ± 42.14 <sup>b</sup>	352.56 ± 48.51 <sup>a</sup>	0.04
F/G	1.84 ± 0.23 <sup>ab</sup>	2.01 ± 0.17 <sup>a</sup>	1.68 ± 0.06 <sup>b</sup>	0.01

<sup>a,b</sup> Different superscript letters in a row indicate a significant difference ( $P < 0.05$ ).

<sup>1</sup>FSB, fermented soybean meal; FM, fish meal; MFSM, mixture of fermented soybean meal and fish meal.

<sup>2</sup>ADFI, average daily feed intake; ADG, average daily gain; F/G, feed to weight gain ratio.

<sup>3</sup>Data were the mean of six replicates with one piglet each.

**TABLE 3 |** The effects of different protein dietary sources on nutrient apparent total tract digestibility (ATTD) in weaned pigs.

Item (%)	Dietary treatments <sup>1</sup>			P-value
	FSB	FM	MFSM	
DM <sup>2</sup>	87.82 ± 0.36	88.24 ± 0.36	87.34 ± 0.60	0.06
CP <sup>2</sup>	85.39 ± 0.77 <sup>a</sup>	82.29 ± 0.87 <sup>b</sup>	81.7 ± 0.71 <sup>b</sup>	<0.01
EE <sup>2</sup>	74.63 ± 1.14 <sup>b</sup>	78.94 ± 2.29 <sup>a</sup>	71.97 ± 0.47 <sup>c</sup>	<0.01
OM <sup>2</sup>	89.98 ± 0.33 <sup>a</sup>	89.91 ± 0.32 <sup>a</sup>	89.24 ± 0.45 <sup>b</sup>	0.04
TC <sup>2</sup>	92.08 ± 0.21	92.52 ± 0.29	92.12 ± 0.48	0.19

<sup>a–c</sup> Different superscript letters in a row indicate a significant difference ( $P < 0.05$ ).

<sup>1</sup>FSB, fermented soybean meal; FM, fish meal; MFSM, mixture of fermented soybean meal and fish meal.

<sup>2</sup>DM, dry matter; CP, crude protein; EE, ether extract; OM, organic matter; TC, total carbohydrate.

<sup>3</sup>Data were the mean of four replicates with one piglet each.

**TABLE 4 |** The effects of different protein dietary sources on serum immunity in weaned piglets.

Item	Dietary treatments <sup>1</sup>			P-value
	FSB	FM	MFSM	
14 days				
IgA <sup>2</sup> (μg/mL)	70.22 ± 13.68 <sup>b</sup>	91.00 ± 17.60 <sup>a</sup>	100.05 ± 9.25 <sup>a</sup>	0.01
IgG <sup>2</sup> (mg/mL)	5.41 ± 0.77 <sup>b</sup>	6.33 ± 0.50 <sup>a</sup>	6.12 ± 0.57 <sup>ab</sup>	0.05
IgM <sup>2</sup> mg/mL)	2.05 ± 0.22	2.18 ± 0.30	2.34 ± 0.41	0.32
IL-1β <sup>2</sup> (pg/mL)	119.24 ± 10.44 <sup>a</sup>	107.00 ± 15.87 <sup>ab</sup>	99.37 ± 14.65 <sup>b</sup>	0.07
IL-6 <sup>2</sup> (pg/mL)	290.57 ± 14.86 <sup>a</sup>	251.38 ± 18.46 <sup>b</sup>	247.31 ± 10.58 <sup>b</sup>	<0.01
TNF-α <sup>2</sup> (pg/mL)	62.60 ± 3.08 <sup>a</sup>	53.21 ± 5.22 <sup>b</sup>	53.93 ± 4.04 <sup>b</sup>	<0.01
28 days				
IgA (μg/mL)	88.19 ± 14.29 <sup>b</sup>	100.53 ± 13.47 <sup>b</sup>	127.50 ± 13.54 <sup>a</sup>	<0.01
IgG (mg/mL)	5.67 ± 0.64 <sup>b</sup>	6.86 ± 0.59 <sup>a</sup>	7.37 ± 0.57 <sup>a</sup>	<0.01
IgM (mg/mL)	1.90 ± 0.27 <sup>c</sup>	2.68 ± 0.23 <sup>b</sup>	3.22 ± 0.22 <sup>a</sup>	<0.01
IL-1β (pg/mL)	123.59 ± 10.31 <sup>a</sup>	90.25 ± 17.15 <sup>b</sup>	79.97 ± 15.89 <sup>b</sup>	<0.01
IL-6 (pg/mL)	279.70 ± 19.13 <sup>a</sup>	219.23 ± 20.16 <sup>b</sup>	217.13 ± 20.06 <sup>b</sup>	<0.01
TNF-α (pg/mL)	58.00 ± 3.57 <sup>a</sup>	49.10 ± 5.58 <sup>b</sup>	44.82 ± 5.81 <sup>b</sup>	<0.01

<sup>a–c</sup> Different superscript letters in a row indicate a significant difference ( $P < 0.05$ ).

<sup>1</sup>FSB, fermented soybean meal; FM, fish meal; MFSM, mixture of fermented soybean meal and fish meal.

<sup>2</sup>IgA, immunoglobulin A; IgG, immunoglobulin G; IgM, immunoglobulin M; IL-1β, interleukin-1β; IL-6, interleukin-6; TNF-α, tumor necrosis factor-α.

<sup>3</sup>Data were the mean of six replicates with one piglet each.

**TABLE 5 |** The effects of different protein dietary sources on bacterial α-diversity indices in piglets.

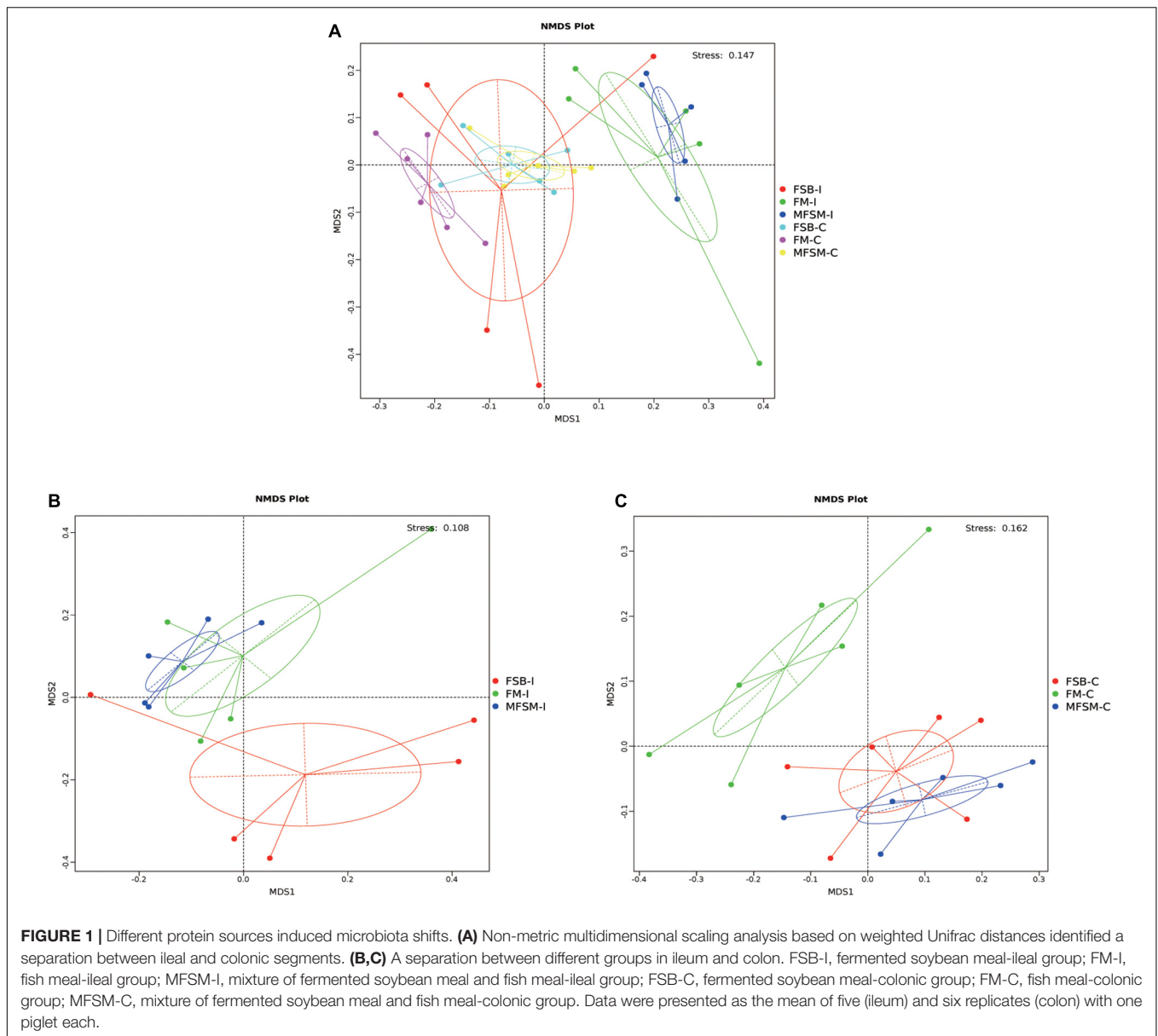
Item (%)	Dietary treatments <sup>1</sup>			P-value
	FSB	FM	MFSM	
Ileum				
Observed_species	502 ± 91	484 ± 91	457 ± 153	0.57
Shannon	3.86 ± 0.62	3.31 ± 0.41	3.28 ± 0.79	0.19
Simpson	0.791 ± 0.141	0.777 ± 0.054	0.708 ± 0.149	0.33
Chao 1	577 ± 121	568 ± 101	528 ± 158	0.58
ACE	597 ± 122	590 ± 114	541 ± 159	0.54
Colon				
Observed_species	698 ± 61 <sup>a</sup>	646 ± 49 <sup>ab</sup>	617 ± 52 <sup>b</sup>	0.05
Shannon	5.65 ± 0.57	5.47 ± 0.72	5.45 ± 0.48	0.59
Simpson	0.924 ± 0.040	0.912 ± 0.063	0.932 ± 0.025	0.48
Chao 1	768 ± 62 <sup>a</sup>	702 ± 40 <sup>b</sup>	677 ± 54 <sup>b</sup>	0.03
ACE	773 ± 62 <sup>a</sup>	709 ± 40 <sup>ab</sup>	687 ± 52 <sup>b</sup>	0.03

<sup>a,b</sup> Different superscript letters in a row indicate a significant difference ( $P < 0.05$ ).

<sup>1</sup>FSB, fermented soybean meal; FM, fish meal; MFSM, mixture of fermented soybean meal and fish meal.

<sup>2</sup>Data were the mean of five replicates (ileum) and six replicates (colon) with one piglet each.

in alpha diversity were observed in the ileum ( $P > 0.05$ ). Beta-diversity NMDS analysis based on Bray-Curtis distances showed microbial communities were well separated between the ileum and colon (Figure 1A), and among groups in the ileum (Figure 1B) and colon (Figure 1C). Thus, piglet gut microbiota composition was shaped by different protein sources.

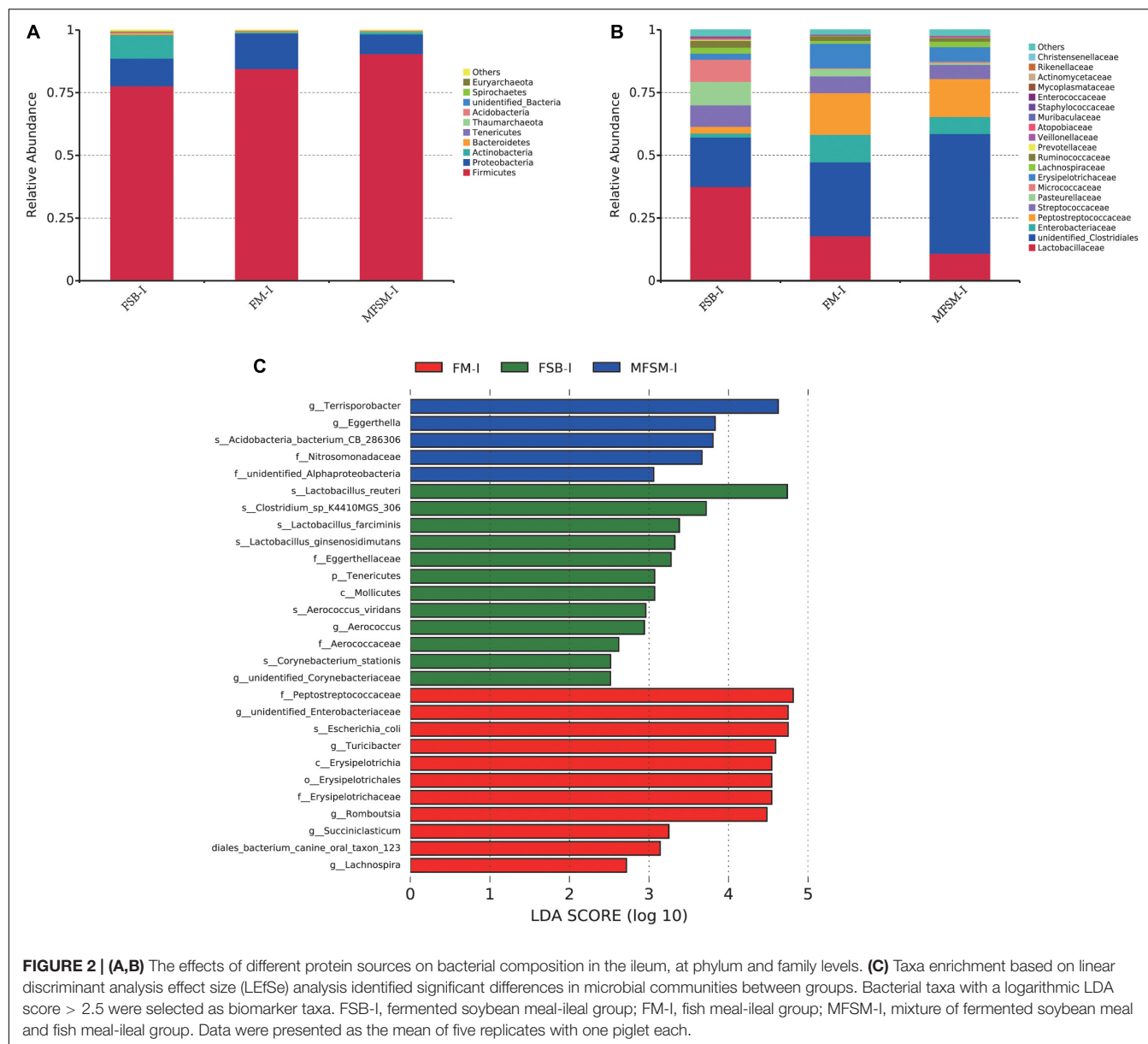


## Ileal and Colonic Bacterial Community Structures

In the ileum, *Firmicutes*, *Proteobacteria*, and *Actinobacteria* were the three major bacterial phyla accounting for >95% of total ileal bacterial communities (**Figure 2A**). The relative abundance of *Firmicutes* in the MFSM-ileal (MFSM-I) group was 90.49%, and was higher than the 84.54 and 77.64% levels in FM-ileal (FM-I) and FSB-ileal (FSB-I) groups ( $P > 0.05$ ), respectively. The relative abundance of *Proteobacteria* in the MFSM-I group was 7.87%, and was lower than the 14.17 and 11.08% levels in FM-I and FSB-I groups ( $P > 0.05$ ), respectively. The relative abundance of *Actinobacteria* in FM-I and MFSM-I groups was 0.43 and 0.94%, respectively, but lower than the 9.40% in the FSB-I group ( $P > 0.05$ ).

At the family level, the relative abundance of *Lactobacillaceae* decreased from 37.54 to 17.85 and 10.85% (FSB-I group to FM-I and MFSM-I groups, respectively), while *unidentified\_Clostridiales* levels were opposite, with increases from 19.72 to 29.46 and 47.79%, respectively ( $P > 0.05$ ; **Figure 2B**). When compared with FSB-I and MFSM-I groups, the FM-I group showed an increased relative abundance of *Enterobacteriaceae*, from 1.55 and 6.77 to 11.01%, respectively ( $P > 0.05$ ). The relative abundance of *Peptostreptococcaceae* in MFSM-I and FM-I groups was 16.62 and 15.13% higher, respectively, than the 2.68% in the FSB-I group ( $P > 0.05$ ). The relative abundance of *Pasteurellaceae* was lowest in the MFSM-I group at 0.77%, in comparison with FSB-I and FM-I groups at 9.36 and 2.96%, respectively ( $P > 0.05$ ).





Linear discriminant analysis effect size showed that FM-I piglets had a higher relative abundance of the genera, *unidentified\_Enterobacteriaceae*, *Turicibacter*, *Romboutsia*, *Succiniciasticum*, and *Lachnospira* when compared with FSB-I and MFSM-I piglets (**Figure 2C**). *Lactobacillus\_reuteri*, *Lactobacillus\_farciminis*, *Lactobacillus\_ginsenosidimutans*, and *Clostridium\_sp\_K4410MGS\_306* were dominant bacteria in the FSB-I group when compared with the other groups, whereas the relative abundance of *Terrisporobacter* and *Eggerthella* was significantly increased in the MFSM-I group when compared with FM-I and FSB-I groups.

In the colon, *Firmicutes* was the most predominant phylum, with a relative abundance of 90.04, 79.74, and 85.36%, respectively, in FSB-colonic (FSB-C), FM-colonic (FM-C), and MFSM-colonic (MFSM-C) groups (**Figure 3A**). The relative

abundance of *Actinobacteria* (5.02%) and *Bacteroidetes* (6.82%) in the FM-C group was higher than FSB-C (1.12 and 3.55%, respectively) and MFSM-C (1.04 and 4.01%, respectively) groups ( $P < 0.05$ ).

At the family level, when compared with the FM-C group, both FSB-C and MFSM-C groups had a significantly increased relative abundance of *unidentified\_Clostridiales* and *Peptostreptococcaceae* ( $P < 0.05$ ; **Figures 3B–D**). The relative abundance of *Streptococcaceae* in the FM-C group was higher, and the relative abundance of *Atopobiaceae*, *Veillonellaceae*, and *Christensenellaceae* in the MFSM-C group was lower than the FSB-C group ( $P < 0.05$ ).

Of the 35 most dominant colonic genera, the relative abundance of *Butyricoccus*, *Romboutsia*, *unidentified\_Clostridiales*, *Terrisporobacter*, and *Sarcina* in

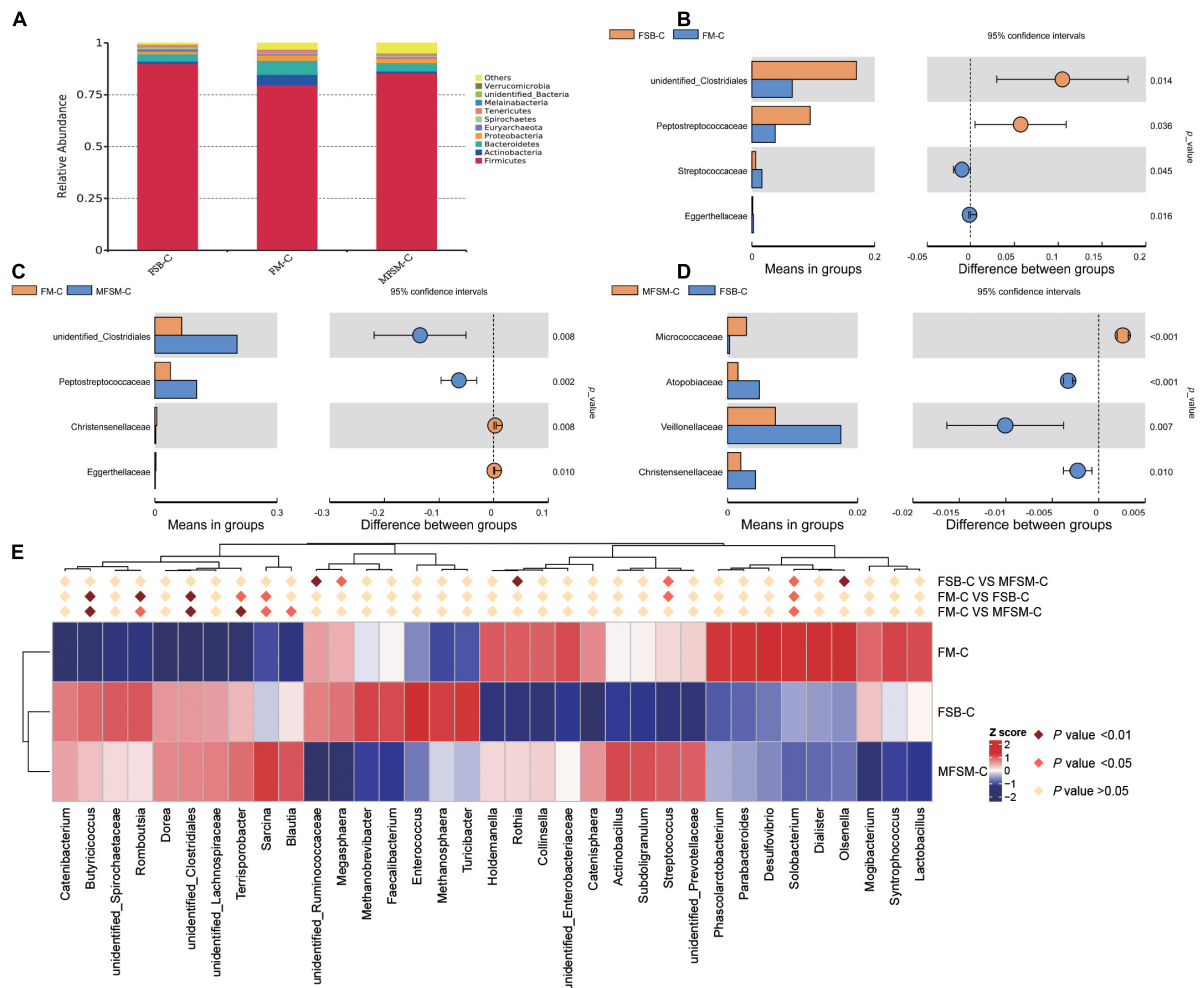


**FIGURE 3 |** The effects of different protein sources on bacterial compositions in the colon, at phylum, family, and genus levels. **(A)** Distribution of colonic bacteria at the phylum level. **(B–D)** Statistical analysis of differences at the family level; t-tests were used to test for significant differences;  $P < 0.05$  indicates a significant difference. **(E)** In the top 35 genera, Metastat was used to test for significant differences in genera relative abundance; deep pink diamonds indicate  $P < 0.05$  and dark pink diamonds indicate  $P < 0.01$  between two groups. FSB-C, fermented soybean meal-colonic group; FM-C, fish meal-colonic group; MFSM-C, mixture of fermented soybean meal and fish meal-colonic group. Data were presented as the mean of six replicates with one piglet each.

MFSM-C and FSB-C groups was significantly higher than the FM-C group ( $P < 0.05$ ; **Figure 3E**). When compared with the FSB-C group, the MFSM-C group had a significantly decreased relative abundance of *unidentified\_Ruminococcaceae*, *Olsenella*, and *Megasphaera* ( $P < 0.05$ ), but a significantly increased relative abundance of *Rothia* ( $P < 0.05$ ). The relative abundance of *Streptococcus* and *Solobacterium* in the FSB-C group was lower than MFSM-C and FM-C groups ( $P < 0.05$ ), while the relative abundance of *Solobacterium* in the FSB-C group was higher than the MFSM-C group ( $P < 0.05$ ).

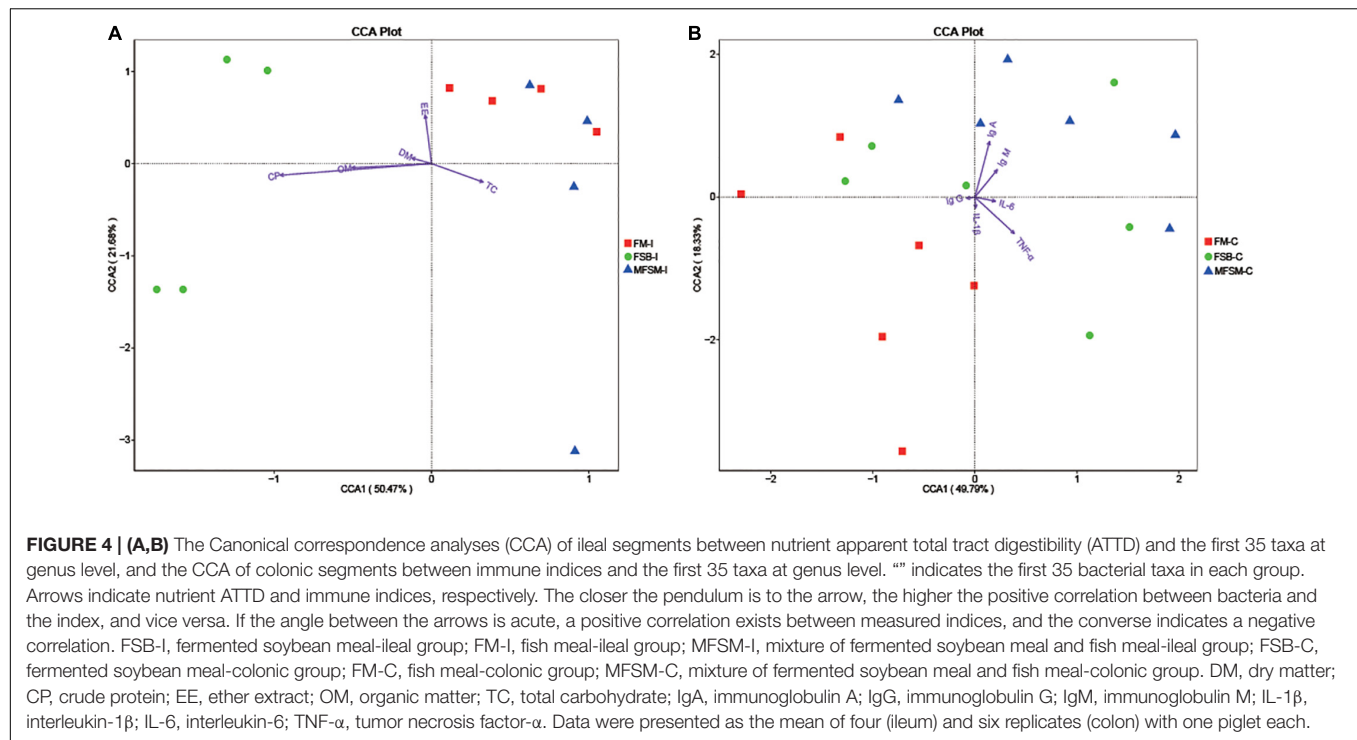
## Correlations Between Gut Microbiota and Apparent Total Tract Digestibility or Immune Parameters

Canonical correspondence analyses (CCA) suggested TC ATTD was negatively correlated with DM, CP, OM, and EE ATTD, and

serum IgG was negatively correlated with IgA, IgM, IL-6, and TNF- $\alpha$  (**Figure 4**). Ileal microbes in FSB piglets were positively correlated with CP, OM, and DM ATTD. Ileal microbes in MFSM piglets were positively correlated with TC ATTD, and FM group microbes were positively correlated with EE ATTD.

Colonic microbes in the MFSM group were positively correlated with serum IgA and IgM levels, but negatively correlated with IL-1 $\beta$  and TNF- $\alpha$ . Colonic microbes in FM animals were positively correlated with serum IgG and IL-1 $\beta$ , and FSB group microbes were positively correlated with IL-6 and TNF- $\alpha$  levels.

A Spearman correlation matrix was used to explore relationships between predominant families and genera (35 most dominant genera) and ATTD or host immunity (**Figures 5, 6**). *F\_unidentified\_Clostridiales* and *unidentified\_Clostridiales* were significantly negatively correlated with CP and OM ATTD ( $P < 0.05$ ). *Unidentified\_Enterobacteriaceae*,



*f\_Peptostreptococcaceae*, *f\_Erysipelotrichaceae*, and *Romboutsia* were significantly negatively correlated with CP ATTD, while *f\_Lactobacillaceae*, *Lactobacillus*, and *Proteus* were significantly positively correlated with CP ATTD ( $P < 0.05$ ). *F\_Peptostreptococcaceae* and *Romboutsia* showed significantly positive correlations with TC ATTD, but *Dialister*, *Olsenella*, and *Solobacterium* showed significantly negative correlations with TC ATTD ( $P < 0.05$ ).

From statistical analyzes, colonic microbiota was more affected by protein sources than ileum microbiota, therefore, only correlations between colonic microbiota and immunity indices were investigated. *Megasphaera*, *unidentified\_Ruminococcaceae*, and *f\_Christensenellaceae* were significantly positively correlated with TNF- $\alpha$ , but negatively correlated with IgA ( $P < 0.05$ ). *F\_Streptococcaceae* and *Streptococcus* were significantly positively correlated with IgG, but significantly negatively correlated with IL-6 and IL-1 $\beta$  ( $P < 0.05$ ). *Pasteurella* was significantly positively correlated with IgA and IgM, but negatively correlated with IL-6 and TNF- $\alpha$ . Also, *Proteus* was significantly positively correlated with IgM, but negatively correlated with IL-1 $\beta$  ( $P < 0.05$ ). *Romboutsia* was positively correlated with IL-6 and TNF- $\alpha$ , *Turicibacter* positively correlated with TNF- $\alpha$ , and *Rothia* negatively correlated with IL-6 and TNF- $\alpha$  ( $P < 0.05$ ).

## Short Chain Fatty Acid Levels in the Colon

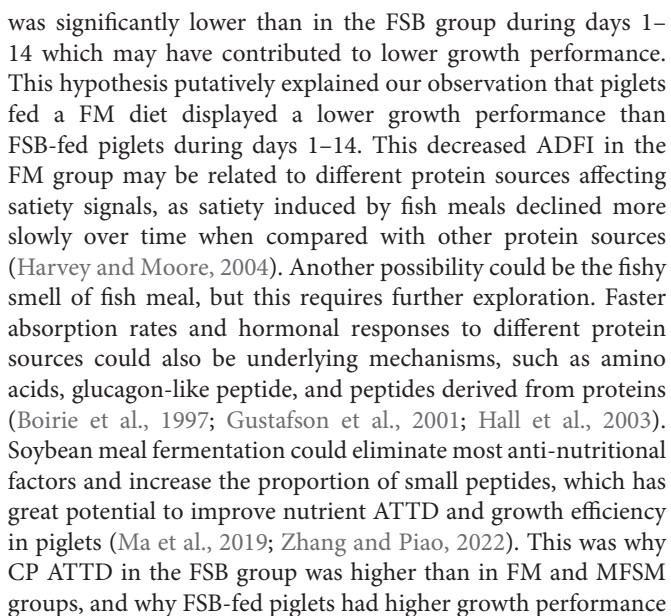
Acetic and butyric acid levels in MFSM animals were significantly higher than levels in FSB and FM groups ( $P < 0.05$ ; Table 6). Propionic acid levels in the MFSM group were significantly higher than those in the FSB group ( $P < 0.05$ ). In terms

of branched chain fatty acids, no significant differences were identified between groups ( $P > 0.05$ ).

## DISCUSSION

Given that high-quality protein and protein restriction can effectively decrease the amounts of proteins flowing into the hindgut, and decreased the risk of aberrant fermentation in the hindgut. Based on previous studies, no negative effects were reported on piglet growth performance when dietary CP levels were reduced by 3–4%, in contrast to the 2012 NRC recommendation of 20.5% in some piglet models (Liu et al., 2012; Gloaguen et al., 2014; Sirtori et al., 2014; Bandsma et al., 2015; Kalantar-Zadeh et al., 2016). Thus, in this study, a low-protein diet, with balanced amino acids, was used to determine interactions between dietary protein, gut microbiota, host digestibility, and health.

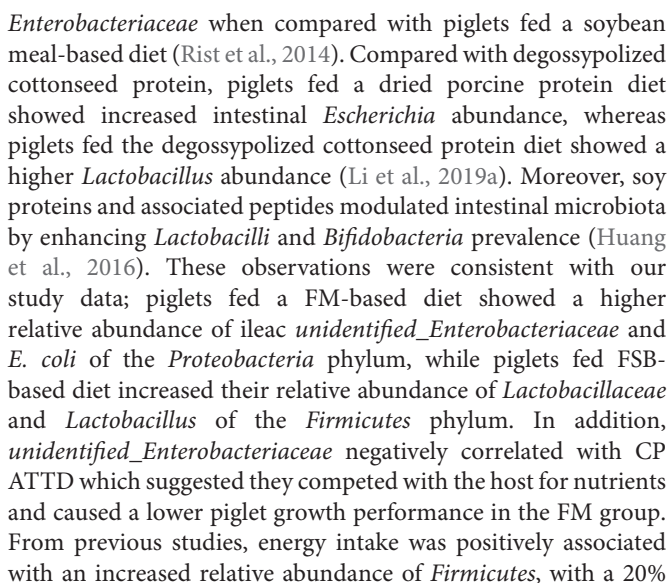
In our study, piglets fed a combination of FSB and FM had higher BW and ADG but a lower feed to weight gain ratio than piglets fed a single protein source, indicating piglets in the MFSM group had a higher growth rate when compared with other diets. This observation was consistent with a previous study; a combined soybean meal and fish meal diet significantly increased ADG and feed conversion ratios in piglets when compared with soybean meal or fermented soybean meal diets (Ma et al., 2019). Similarly, when compared with soy protein isolate or zein as the single dietary protein source, combination diets of soy meal, fish meal, and whey powder significantly increased piglet ADG and ADFI (Qi, 2011). A possible reason could be that ADFI was affected by different protein sources; ADFI in the FM group



than FM-fed piglets at certain phases. However, EE ATTD in the FM group was higher than in other groups, which may explain why there was no significance in growth parameters in later phases among the three groups. Additionally, a higher piglet growth rate in the MFSM group may be attributed to the mixture of protein sources which reduced malnutrition risks and improved intestinal dysfunction (Engelsmann et al., 2022).

Most dietary nutrients are fully digested and absorbed at the end of the ileum, whereas undigested complex fragments are fermented in the hindgut (Zhang et al., 2018b). During this process, microbes promote nutrient application, and the protein sources can shape the composition of intestinal microbiota (Wu et al., 2022). The *Proteobacteria* phylum, as facultative anaerobes, cannot consume fiber, but can interfere with host nutrition by metabolizing fermentation products to carbon dioxide in the presence of oxygen (Litvak et al., 2018). As reported, the primary bacteria implicated in protein metabolism in the small intestine are: *Escherichia coli*, *Streptococcus*, *Mitsuokella*, and *Succinivibrio dextrinosolvens* (Ma et al., 2017). Piglets fed a highly digestible casein-based diet showed an increased abundance of





increase in abundance associated with an additional energy harvest of 628 kJ (Hildebrandt et al., 2009; Reiner et al., 2018). These reports agreed with our data suggesting that FSB and FM combinations increased the relative abundance of *Firmicutes* and accelerated piglet growth. This positive correlation was also observed in previous piglet models (Pedersen et al., 2013; Mach et al., 2015), and in our study, was evidenced as a higher piglet growth performance in the MFSM group. Combined CCA and Spearman correlation analyzes indicated that *f\_Lactobacillaceae*, *Lactobacillus*, and *Proteus* were dominant microbes in FSB animals and promoted CP digestibility, whereas *f\_Peptostreptococcaceae* and *Romboutsia* were the main bacteria in MFSM animals and benefited TC digestibility. These bacteria may positively affect piglet growth performance.

Along the intestinal tract, between the ileum and colon, considerable variations in *Bacteroidetes*, *Actinobacteria*, *Firmicutes*, and *Proteobacteria* were observed. We showed that oxygen-tolerant *Proteobacteria*, such as *Enterobacteriaceae* grew well and were abundant in the ileum, but were dramatically

**TABLE 6 |** The effects of different protein sources on colonic short chain fatty acid (SCFA) levels in weaned piglets.

Item ( $\mu\text{Mol/g}$ )	Dietary treatment <sup>1</sup>			P-value
	FSB	FM	MFSM	
Acetic acid	48.56 $\pm$ 3.92 <sup>b</sup>	47.75 $\pm$ 5.3 <sup>b</sup>	56.83 $\pm$ 4.87 <sup>a</sup>	0.02
Propionic acid	18.74 $\pm$ 1.21 <sup>b</sup>	21.38 $\pm$ 1.16 <sup>ab</sup>	23.54 $\pm$ 3.77 <sup>a</sup>	0.03
Butyric acid	9.97 $\pm$ 0.63 <sup>b</sup>	11.07 $\pm$ 2.83 <sup>b</sup>	13.79 $\pm$ 1.59 <sup>a</sup>	0.02
Isobutyric acid	0.91 $\pm$ 0.13	0.89 $\pm$ 0.08	0.96 $\pm$ 0.06	0.51
Isovaleric acid	1.11 $\pm$ 0.07	1.19 $\pm$ 0.06	1.28 $\pm$ 0.17	0.09
Valeric acid	2.79 $\pm$ 0.59	3.23 $\pm$ 0.85	3.76 $\pm$ 0.72	0.15

<sup>a,b</sup> Different superscript letters in a row indicate a significant difference ( $P < 0.05$ ).

<sup>1</sup>FSB, fermented soybean meal; FM, fish meal; MFSM, mixture of fermented soybean meal and fish meal.

<sup>2</sup>Data were the mean of five replicates (ileum) and six replicates (colon) with one piglet each.

decreased in the colon, while oxygen-sensitive *Bacteroidetes* adapting to a low oxygen environment were significantly increased in the colon. This observation agreed with a previous study showing that spatial changes in bacterial composition occurred as a result of altered microenvironments (Zhang et al., 2018b). Our colonic microbial composition data were consistent with previous findings showing that *Lactobacillaceae*, *Peptostreptococcaceae*, *Veillonellaceae*, *Ruminococcaceae*, *Clostridiales*, and *Lachnospiraceae* involving in *Firmicutes*, and *Prevotellaceae* belonging to *Bacteroidetes* were dominated taxa in the large intestine (Gill et al., 2006; Claus et al., 2011; Zhang et al., 2018b). These microbial abundance is important for complex carbohydrate digestion, amino acid biotransformation in the host.

Using excretory enzymes, *Clostridia* processes undigested dietary proteins and complex carbohydrates to produce amino acids and SCFAs (Zhu et al., 2017; Zhang et al., 2018b). Amino acids are further fermented via deamination in the colon to produce SCFAs and ammonia (Cummings and Macfarlane, 2010), which are key energy sources for colocytes. In our study, the relative abundance of *Clostridiales* in FSB and MFSM groups was higher than the FM group, while the relative abundance of *Enterobacteriaceae* was highest in the FM group when compared with the other groups. As previously reported, a host-protective mechanism against intestinal infection involves resistance between the obligate anaerobic *Clostridia* and the facultative anaerobic *Enterobacteriaceae* (Spees et al., 2013). *Clostridiales*, including *Clostridium butyrate*, stimulated immunoglobulins secretion in mice and Peyer's patch cell (Murayama et al., 1995; Wang et al., 1996). Immunoglobulins provide passive immune protection in early life by enhancing anti-bacterial, anti-infective, and anti-viral capabilities. In our study, serum IgA on day 14 and serum IgG or IgM on day 28 in FM and MFSM groups were higher than the FSB group. Bai et al. (2016) reported that feeding soy protein and raffinose combinations markedly increased cecum IgA levels. Gut bacteria and various antigens may be involved in these changes. In our study, the relative abundance of *Streptococcus* involved in *f.Streptococcaceae* in FM-C and MFSM-C groups was significantly higher than

the FSB-C group, with immunoglobulins positively correlated with *f.Streptococcaceae*, *Streptococcus*, *Pasteurella*, and *Proteus*. When combined with data from the previous study, even though *Streptococcus* is generally considered a pathogen, a modest increase in their numbers could increase IL-10 levels (Bartholomeus et al., 2014). Interleukin 10 secreted by Th2 cells stimulate B lymphocyte proliferation and generate IgG antibodies (Chang et al., 2018). These results indicated that those microbes might be the under antigens for maintaining higher immunoglobulins to protect against infection when they are in an extremely lower relative abundance.

During piglet production, weaning stress may induce intestinal disorders with increased pro-inflammatory cytokine secretion such as IL-1 $\beta$ , IL-6, and TNF- $\alpha$ , which cause growth retardation (Bomba et al., 2014; Xiong et al., 2019). Our results showed that both FM and MFSM diets significantly decreased pro-inflammatory cytokine levels when compared with the FSB diet, indicating FM alleviated host inflammatory responses in weaned piglets. This observation may be associated with microbial diversity and composition. Theoretically, highly diverse gut microbiota reflect microbial maturity, which increases with age (Turnbaugh et al., 2007). In a previous report on children, microbial diversification was a gradual process, whereas the premature formation of an adult-type microbiota negatively affected host immune function (Maynard et al., 2012; Nylund et al., 2013). This observation accorded with our study; FSB diets enhanced host inflammatory responses by increasing microbial diversity. Distinct to microbial diversity, a study showed that dietary protein sources were major factors influencing microbial composition (Rist et al., 2013). *Romboutsia* is a bacterial genus of the family *Peptostreptococcaceae*, and are generally associated with protective leukocyte antigen haplotypes in autoimmune disease (Russell et al., 2019). *Turicibacter* was shown to have a strong association with immune function, as in the intestine, *Turicibacter* was almost abolished in innate and adaptive immunodeficiency mouse models (Dorottya and Richard, 2011; Dimitriu et al., 2013). At the family level, *Christensenellaceae* was positively correlated with gut metabolites implicated in protein catabolism (Waters and Ley, 2019). In our study, these bacteria were strongly correlated with serum TNF- $\alpha$  and IL-6 levels, suggesting that dietary FSB-enhanced host inflammation responses may be associated with these bacteria. This was distinct to dietary FM and the combined MFSM, which increased immunoglobulin secretion.

*Clostridiales* and *Peptostreptococcus* are predominant bacteria in the large intestine of healthy humans, and they produce SCFAs and are key drivers of amino acid utilization, including lysine, threonine, proline, and glutamate (Abdallah et al., 2020). When compared with animal protein sources, soy protein intake could induce more carbohydrate metabolism and generate SCFAs (Zhu et al., 2017). The role of SCFAs in immunity is well characterized; most studies show that SCFAs sustain a balance between commensal microbes and pathogen immunity by modulating Tregs and IL-10-producing T cells, and suppressing inflammatory cytokines (Singh et al., 2014). This regulatory mechanism is associated with SCFA-G protein coupled receptors

or their histone deacetylase inhibiting ability (Ara et al., 2016). These observations agreed with our data showing that a combined MFSM diet increased SCFA levels in the colon, and had lower inflammation cytokines with tolerance to *Streptococcus*, *Pasteurella*, and *Proteus*. Another reason for this could be related to tryptophan metabolism by *Peptostreptococcus* and *Clostridiales* (Abdallah et al., 2020). Indole is a predominant tryptophan metabolite which reduces severe inflammation induced by lipopolysaccharide via IL-22 up-regulation, and also enhances aryl hydrocarbon receptor activation (Shijie et al., 2018). Thus, dietary FSB and FM sources affected host health by shaping different microbiota phenotypes, and combined dietary MFSM appeared to demonstrate better tolerance to commensals.

## CONCLUSION

Diets containing MFSM significantly increased piglet growth performance when compared with FM-fed piglets, while diets containing FSB significantly increased CP ATTD when compared with MFSM and FM groups. Dietary MFSM and FM significantly enhanced serum immunoglobulin secretion and decreased serum cytokine production when compared with dietary FSB. Dietary FSB shaped the ileac microbiota, accelerated *f\_Lactobacillaceae* and *Lactobacillus* prevalence, and increased CP digestibility, whereas dietary MFSM shaped the ileac microbiota, accelerated *f\_Peptostreptococcaceae* and *Romboutsia* prevalence, and benefited TC digestibility. These microbiota phenotypes shaped by MFSM diets contributed to piglet growth performance. MFSM and FM diets also shaped a more tolerant phenotype in dominant microbiota, increasing the relative abundance of colonic *f\_Streptococcaceae* and *Streptococcus* and enhancing immunoglobulin secretion. In contrast, dietary FSB shaped a more diverse microbiota phenotype, increasing the relative abundance of *Christensenellaceae* and *Romboutsia* and

enhancing inflammation cytokine production. Therefore, dietary MFSM shaped particular microbiota, improving nutrient ATTD and host health which helped weaned piglets overcome weanling stress. Our study provides a theoretical basis for the application of different protein sources to the diets of young animals.

## DATA AVAILABILITY STATEMENT

The datasets generated for this study can be found in the NCBI sequence read archive, accession number: PRJNA648691.

## ETHICS STATEMENT

The animal study was reviewed and approved by Institutional Animal Care and Use Committee of the Institute of Animal Science of the Chinese Academy of Agricultural Sciences.

## AUTHOR CONTRIBUTIONS

YQ and JZ: conceptualization, methodology, and project administration. YL and YH: animal experiments, chemical analysis, and data collection. YH: writing original draft. QZ, CT, and JZ: finished writing review. All authors agreed to the final manuscript and approved the submitted version.

## FUNDING

This work was supported by the National Key Research and Development Program of China (2021YFD1300301), the Agricultural Science and Technology Innovation Program (ASTIP-IAS12), and the Special Basic Research Fund for Central Public Research Institutes (1610382022010).

## REFERENCES

- Abdallah, A., Elemba, E., Zhong, Q., and Sun, Z. (2020). Gastrointestinal interaction between dietary amino acids and gut microbiota: with special emphasis on host nutrition. *Curr. Protein Pept. Sci.* 21, 785–798. doi: 10.2174/1389203721666200212095503
- AOAC (2012). *Official Methods of Analysis*, 19th Edn. Arlington, VA: Association of Official Analytical Chemists.
- Ara, K., Filipe, D. V., Petia, K.-D., and Fredrik, B. (2016). From dietary fiber to host physiology: short-chain fatty acids as key bacterial metabolites. *Cell* 165, 1332–1345. doi: 10.1016/j.cell.2016.05.041
- Bai, G., Ni, K., Tsuruta, T., and Nishino, N. (2016). Dietary casein and soy protein isolate modulate the effects of raffinose and fructooligosaccharides on the composition and fermentation of gut microbiota in rats. *J. Food Sci.* 81, H2093–H2098. doi: 10.1111/1750-3841.13391
- Bandsma, R., Ackerley, C., Koulajian, K., Zhang, L., Zutphen, T. V., Dijk, T. V., et al. (2015). A low-protein diet combined with low-dose endotoxin leads to changes in glucose homeostasis in weanling rats. *Am. J. Physiol. Endocrinol. Metab.* 309, E466–E473. doi: 10.1152/ajpendo.00090.2015
- Bartholomeus, V., Marjolein, M., Zoetendal, E. G., Wells, J. M., Michiel, K., and Benoit, F. (2014). Immunomodulatory properties of *Streptococcus* and *Veillonella* isolates from the human small intestine microbiota. *PLoS One* 9:e114277. doi: 10.1371/journal.pone.0114277
- Blachier, F., Mariotti, F., and Tomé, J.-F. H. (2007). Effects of amino acid-derived luminal metabolites on the colonic epithelium and physiopathological consequences. *Amino Acids* 33, 547–562. doi: 10.1007/s00726-006-0477-9
- Boirie, Y., Dangin, M., Gachon, P., Vasson, M. P., Maubois, J. L., and Beaufre, B. (1997). Slow and fast dietary proteins differently modulate postprandial protein accretion. *Proc. Natl. Acad. Sci. U.S.A.* 94, 14930–14935. doi: 10.1073/pnas.94.26.14930
- Bomba, L., Minuti, A., Moisa, S. J., Trevisi, E., Eufemi, E., Lizier, M., et al. (2014). Gut response induced by weaning in piglet features marked changes in immune and inflammatory response. *Funct. Integr. Genomics* 14, 657–671. doi: 10.1007/s10142-014-0396-x
- Chang, M., Zhao, Y., Qin, G., and Zhang, X. (2018). Fructo-oligosaccharide alleviates soybean-induced anaphylaxis in piglets by modulating gut microbes. *Front. Microbiol.* 9:2769. doi: 10.3389/fmicb.2018.02769
- Chen, X., Song, P., Fan, P., He, T., Jacobs, D., Levesque, C. L., et al. (2018). Moderate dietary protein restriction optimized gut microbiota and mucosal barrier in growing pig model. *Front. Cell. Infect. Microbiol.* 8:246. doi: 10.3389/fcimb.2018.00246
- Claus, S. P., Ellero, S. L., Berger, B., Krause, L., Bruttin, A., Molina, J., et al. (2011). Colonization-induced host-gut microbial metabolic interaction. *mBio* 2, e00271–e00210. doi: 10.1128/mBio.00271-10

- Collins, S. M., Surette, M., and Bercik, P. (2012). The interplay between the intestinal microbiota and the brain. *Nat. Rev. Microbiol.* 10, 735–742. doi: 10.1038/nrmicro2876
- Cummings, J. H., and Macfarlane, G. T. (2010). The control and consequences of bacterial fermentation in the human colon. *J. Appl. Microbiol.* 70, 443–459. doi: 10.1111/j.1365-2672.1991.tb02739.x
- Dimitriu, P. A., Boyce, G., Samarakoon, A., Hartmann, M., Johnson, P., and Mohn, W. W. (2013). Temporal stability of the mouse gut microbiota in relation to innate and adaptive immunity. *Environ. Microbiol. Rep.* 5, 200–210. doi: 10.1111/j.1758-2229.2012.00393.x
- Dorotya, N.-S., and Richard, K. (2011). Colonic mucosal DNA methylation, immune response, and microbiome patterns in Toll-like receptor 2-knockout mice. *Gut Microbes* 2, 178–182. doi: 10.4161/gmic.2.3.16107
- Engelsmann, M. N., Jensen, L. D., van der Heide, M. E., Hedemann, M. S., Nielsen, T. S., and Norgaard, J. V. (2022). Age-dependent development in protein digestibility and intestinal morphology in weaned pigs fed different protein sources. *Animal* 16:100439. doi: 10.1016/j.animal.2021.100439
- Gerritsen, A. R., Van Dijk, B. A. J., Rethy, B. K., and Bikker, A. P. (2010). The effect of blends of organic acids on apparent faecal digestibility in piglets. *Livest. Sci.* 134, 246–248. doi: 10.1016/j.livsci.2010.06.154
- Gill, S. R., Pop, M., DeBoy, R. T., Eckburg, P. B., Turnbaugh, P. J., Samuel, B. S., et al. (2006). Metagenomic analysis of the human distal gut microbiome. *Science* 312, 1355–1359. doi: 10.1007/s00726-006-0477-9
- Gloaguen, M., Floc'H, N. L., Corrent, E., Primot, Y., and Milgen, J. V. (2014). The use of free amino acids allows formulating very low crude protein diets for piglets. *J. Anim. Sci.* 92:637. doi: 10.2527/jas.2013-6514
- Gustafson, D. R., McMahon, D. J., Morrey, J., and Nan, R. (2001). Appetite is not influenced by a unique milk peptide: caseinomacropptide (CMP). *Appetite* 36, 157–163. doi: 10.1006/appe.2000.0392
- Hall, W. L., Millward, D. J., Long, S. J., and Morgan, L. M. (2003). Casein and whey exert different effects on plasma amino acid profiles, gastrointestinal hormone secretion and appetite. *Br. J. Nutr.* 89, 239–248. doi: 10.1079/BJN2002760
- Harvey, A. G., and Moore, S. E. (2004). Dietary proteins in the regulation of food intake and body weight in humans. *J. Nutr.* 134, 974S–979S. doi: 10.1111/j.1365-277X.2004.00513.x
- Hasler, and Clare, M. (2002). The cardiovascular effects of soy products. *J. Cardiovasc. Nurs.* 16, 75–76. doi: 10.1097/00005082-200207000-00006
- Hildebrandt, M. A., Hoffmann, C., Sherrill-Mix, S., Keilbaugh, S. A., Hamady, M., Chen, Y., et al. (2009). High-fat diet determines the composition of the murine gut microbiome independently of obesity. *Gastroenterology* 137, P1716–P1724.e2. doi: 10.1053/j.gastro.2009.08.042
- Hu, R., He, Z., Liu, M., Tan, J., Zhang, H., Hou, D. X., et al. (2020). Dietary protocathechuic acid ameliorates inflammation and up-regulates intestinal tight junction proteins by modulating gut microbiota in LPS-challenged piglets. *J. Anim. Sci. Biotechnol.* 11:92. doi: 10.1186/s40104-020-00492-9
- Huang, H., Krishnan, H. B., Pham, Q., Yu, L. L., and Wang, T. T. (2016). Soy and gut microbiota: interaction and implication for human health. *J. Agric. Food Chem.* 64, 8695–8709. doi: 10.1021/acs.jafc.6b03725
- Kalantar-Zadeh, K., Moore, L. W., Tortorici, A. R., Chou, J. A., St-Jules, D. E., Aoun, A., et al. (2016). North American experience with low protein diet for non-dialysis-dependent chronic kidney disease. *BMC Nephrol.* 17:90. doi: 10.1186/s12882-016-0304-9
- Kiers, J. L., Meijer, J. C., Nout, M. J. R., Rombouts, F. M., and Meulen, J. V. D. (2010). Effect of fermented soya beans on diarrhoea and feed efficiency in weaned piglets. *J. Appl. Microbiol.* 95, 545–552. doi: 10.1046/j.1365-2672.2003.02011.x
- Koenig, J. E., Spor, A., Scalfone, N., Fricker, A. D., Stombaugh, J., Knight, R., et al. (2011). Succession of microbial consortia in the developing infant gut microbiome. *Proc. Natl. Acad. Sci. U.S.A.* 108, 4578–4585. doi: 10.1016/j.jynpm.2011.07.111
- Li, R., Chang, L., Hou, G., Song, Z., Fan, Z., He, X., et al. (2019a). Colonic microbiota and metabolites response to different dietary protein sources in a piglet model. *Front. Nutr.* 6:151. doi: 10.3389/fnut.2019.00151
- Li, R., Hou, G., Jiang, X., Song, Z., Fan, Z., Hou, D. X., et al. (2019b). Different dietary protein sources in low protein diets regulate colonic microbiota and barrier function in a piglet model. *Food Funct.* 10, 6417–6428. doi: 10.1039/c9fo01154d
- Li, Y., Han, Y., Zhao, Q., Tang, C., Zhang, T., Zhang, J., et al. (2019c). Comparative analysis of main nutrients, anti-nutritional factors and in vitro digestibility between soybean meal and fermented soybean meal. *China's Feed* 23, 76–81. doi: 10.15906/j.cnki.cn11-2975/s.20192318
- Litvak, Y., Byndloss, M. X., and Baumber, A. J. (2018). Colonocyte metabolism shapes the gut microbiota. *Science* 362, 1017–1017. doi: 10.1126/science.aat9076
- Liu, X. D., Wu, X., Yin, Y. L., Liu, Y. Q., Geng, M. M., Yang, H. S., et al. (2012). Effects of dietary L-arginine or N-carbamylglutamate supplementation during late gestation of sows on the miR-15b/16, miR-221/222, VEGFA and eNOS expression in umbilical vein. *Amino Acids* 42, 2111–2119. doi: 10.1007/s00726-011-0948-5
- Long, S. F., Xu, Y. T., Pan, L., Wang, Q. Q., Wang, C. L., Wu, J. Y., et al. (2017). Mixed organic acids as antibiotic substitutes improve performance, serum immunity, intestinal morphology and microbiota for weaned piglets. *Anim. Feed Sci. Technol.* 235, 23–32. doi: 10.1016/j.anifeedsci.2017.08.018
- Ma, N., Tian, Y., Wu, Y., and Ma, X. (2017). Contributions of the interaction between dietary protein and gut microbiota to intestinal health. *Curr. Protein Pept. Sci.* 18, 795–808. doi: 10.2174/1389203718666170216153505
- Ma, X., Shang, Q., Hu, J., Liu, H., Brökner, C., and Piao, X. (2019). Effects of replacing soybean meal, soy protein concentrate, fermented soybean meal or fish meal with enzyme-treated soybean meal on growth performance, nutrient digestibility, antioxidant capacity, immunity and intestinal morphology in weaned pigs. *Livest. Sci.* 225, 39–46. doi: 10.1016/j.livsci.2019.04.016
- Mach, N., Berri, M., Estellé, J., Levenez, F., Lemonnier, G., Denis, C., et al. (2015). Early-life establishment of the swine gut microbiome and impact on host phenotypes. *Environ. Microbiol. Rep.* 7, 554–569. doi: 10.1111/1758-2229.12285
- Maynard, C. L., Elson, C. O., Hatton, R. D., and Weaver, C. T. (2012). Reciprocal interactions of the intestinal microbiota and immune system. *Nature* 489, 231–241. doi: 10.1038/nature11551
- Murayama, T. I., Mita, N., Tanaka, M., and Kitajo, T. (1995). Effects of orally administered *Clostridium butyricum* MIYAIRI 588 on mucosal immunity in mice. *Vet. Immunol. Immunopathol.* 48, 333–342. doi: 10.1016/0165-2427(95)05437-B
- National Research Council (2012). *Nutrient Requirements of Swine*. 11th Edn. Washington, DC: National Academy Press.
- Nylund, L., Satokari, R., Nikkilä, J., Rajilić-Stojanović, M., Kalliomäki, M., Erika Isolauri, et al. (2013). Microarray analysis reveals marked intestinal microbiota aberrancy in infants having eczema compared to healthy children in at-risk for atopic disease. *BMC Microbiol.* 13:12. doi: 10.1186/1471-2180-13-12
- Pedersen, R., Andersen, A. D., Mølbak, L., Stagsted, J., and Boye, M. (2013). Changes in the gut microbiota of cloned and non-cloned control pigs during development of obesity: gut microbiota during development of obesity in cloned pigs. *BMC Microbiol.* 13:30. doi: 10.1186/1471-2180-13-30
- Qi, H. W. (2011). *Effects of Dietary Protein Sources on Intestinal Micro-Cological Environment and Health in Weaned Piglets*. Ph.D. thesis Sichuan, CTU: Sichuan Agriculture university.
- Reiner, J., Duc Son, L., Turnbaugh, P. J., Cathy, T., Clifton, B., Gordon, J. I., et al. (2018). Energy-balance studies reveal associations between gut microbes, caloric load, and nutrient absorption in humans. *Am. J. Clin. Nutr.* 94, 58–65. doi: 10.3945/ajcn.110.010132
- Rist, V. T. S., Weiss, E., Eklund, M., and Mosenthin, R. (2013). Impact of dietary protein on microbiota composition and activity in the gastrointestinal tract of piglets in relation to gut health: a review. *Animal* 7, 1067–1078. doi: 10.1017/S1751731113000062
- Rist, V. T. S., Weiss, E., Sauer, N., Mosenthin, R., and Eklund, M. (2014). Effect of dietary protein supply originating from soybean meal or casein on the intestinal microbiota of piglets. *Anaerobe* 25, 72–79. doi: 10.1016/j.anaerobe.2013.10.003
- Rodríguez, J. M., Murphy, K., Stanton, C., Ross, R. P., Kober, O. I., Juge, N., et al. (2015). The composition of the gut microbiota throughout life, with an emphasis on early life. *Microb. Ecol. Health Dis.* 26:26050. doi: 10.3402/mehd.v26.26050
- Russell, J. T., Roesch, L., Rdborg, M., Ilonen, J., and Ludvigsson, J. (2019). Genetic risk for autoimmunity is associated with distinct changes in the human gut microbiome. *Nat. Commun.* 10:3621. doi: 10.1038/s41467-019-11460-x
- Seo, S.-H., and Cho, S.-J. (2016). Changes in allergenic and antinutritional protein profiles of soybean meal during solid-state fermentation with *Bacillus subtilis*. *LWT Food Sci. Technol.* 70, 208–212. doi: 10.1016/j.lwt.2016.02.035



- Shijie, G., Saisai, C., Yuan, L., Zhengshun, W., Xin, M., Xuemei, J., et al. (2018). Fecal microbiota transplantation reduces susceptibility to epithelial injury and modulates tryptophan metabolism of microbial community in a piglet model. *J. Crohns Colitis* 12:11. doi: 10.1093/ecco-jcc/jjy103
- Singh, N., Gurav, A., Sivaprakasam, S., Brady, E., Padia, R., Shi, H., et al. (2014). Activation of Gpr109a, receptor for niacin and the commensal metabolite butyrate, suppresses colonic inflammation and carcinogenesis. *Immunity* 40, 128–139. doi: 10.1016/j.immuni.2013.12.007
- Sirtori, F., Crovetto, A., Acciaioli, A., Pugliese, C., Bozzi, R., Campodoni, G., et al. (2014). Effect of dietary protein level on carcass traits and meat properties of Cinta Senese pigs. *Animal* 8, 1987–1995. doi: 10.1017/S1751731114002006
- Spees, A. M., Lopez, C. A., Kingsbury, D. D., Winter, S. E., and Bäuml, A. J. (2013). Colonization resistance: battle of the bugs or ménage à trois with the host? *PLoS Pathog.* 9:e1003730. doi: 10.1371/journal.ppat.1003730
- Turnbaugh, P. J., Ley, R. E., Hamady, M., Fraser-Liggett, C. M., and Gordon, J. I. (2007). The human microbiome project: exploring the microbial part of ourselves in a changing world. *Nature* 449:804. doi: 10.1038/nature06244
- Walker, A. W., Duncan, S. H., McWilliam Leitch, E. C., Child, M. W., and Flint, H. J. (2005). pH and peptide supply can radically alter bacterial populations and short-chain fatty acid ratios within microbial communities from the human colon. *Appl. Environ. Microbiol.* 71, 3692–3700. doi: 10.1128/AEM.71.7.3692-3700.2005
- Wang, G. R., Chen, H. Y., Chen, C. H., Yeh, M. Y., and Mikami, Y. (1996). Immunopotentiating activity of *Clostridium butyricum* in mice. *Proc. Natl. Sci. Counc. Repub. China B* 20, 101–109.
- Wang, Y., Zhou, J., Wang, G., Cai, S., Zeng, X., and Qiao, S. (2018). Advances in low-protein diets for swine. *J. Anim. Sci. Biotechnol.* 9:60. doi: 10.1186/s40104-018-0276-7
- Waters, J. L., and Ley, R. E. (2019). The human gut bacteria Christensenellaceae are widespread, heritable, and associated with health. *BMC Biol.* 17:83. doi: 10.1186/s12915-019-0699-4
- Williams, C. H., David, D. J., and Iismaa, O. (1962). The determination of chromic oxide in faeces samples by atomic absorption spectrophotometry. *J. Agric. Sci.* 59, 381–385. doi: 10.1017/s002185960001546x
- Wu, S., Bhat, Z. F., Gounder, R. S., Mohamed Ahmed, I. A., Al-Juhaimi, F. Y., Ding, Y., et al. (2022). Effect of dietary protein and processing on gut microbiota—a systematic review. *Nutrients* 14:453. doi: 10.3390/nu14030453
- Xiong, W., Ma, H., Zhang, Z., Jin, M., Wang, J., Xu, Y., et al. (2019). Icaritin enhances intestinal barrier function by inhibiting NF- $\kappa$ B signaling pathways and modulating gut microbiota in a piglet model. *RSC Adv.* 9, 37947–37956. doi: 10.1039/c9ra07176h
- Yao, C. K., Muir, J. G., and Gibson, P. R. (2016). Review article: insights into colonic protein fermentation, its modulation and potential health implications. *Aliment. Pharmacol. Ther.* 43, 181–196. doi: 10.1111/apt.13456
- Zhang, C., Rahimnejad, S., Wang, Y. R., Lu, K., Kai, S., Ling, W., et al. (2018a). Substituting fish meal with soybean meal in diets for Japanese seabass (*Lateolabrax japonicus*): effects on growth, digestive enzymes activity, gut histology, and expression of gut inflammatory and transporter genes. *Aquaculture* 483, 173–182. doi: 10.1016/j.aquaculture.2017.10.029
- Zhang, L., Wu, W., Lee, Y.-K., Xie, J., and Zhang, H. (2018b). Spatial heterogeneity and co-occurrence of mucosal and luminal microbiome across swine intestinal tract. *Front. Microbiol.* 9:48. doi: 10.3389/fmicb.2018.00048
- Zhang, L., and Piao, X. (2022). Different dietary protein sources influence growth performance, antioxidant capacity, immunity, fecal microbiota and metabolites in weaned piglets. *Anim. Nutr.* 8, 71–81. doi: 10.1016/j.aninu.2021.06.013
- Zhang, Y. T., Yu, B., Lu, Y. H., Wang, J., and Liang, J. B. (2016). Optimization of the fermentation conditions to reduce anti-nutritive factors in soybean meal. *J. Food Process. Preserv.* 41:e13114. doi: 10.1111/jfpp.13114
- Zhou, L., Fang, L., Sun, Y., Su, Y., and Zhu, W. (2016). Effects of the dietary protein level on the microbial composition and metabolomic profile in the hindgut of the pig. *Anaerobe* 38, 61–69. doi: 10.1016/j.anaerobe.2015.12.009
- Zhu, Y., Shi, X., Lin, X., Ye, K., Xu, X., Li, C., et al. (2017). Beef, chicken, and soy proteins in diets induce different gut microbiota and metabolites in rats. *Front. Microbiol.* 8:1395. doi: 10.3389/fmicb.2017.01395

**Conflict of Interest:** The authors declare that the research was conducted in the absence of any commercial or financial relationships that could be construed as a potential conflict of interest.

**Publisher's Note:** All claims expressed in this article are solely those of the authors and do not necessarily represent those of their affiliated organizations, or those of the publisher, the editors and the reviewers. Any product that may be evaluated in this article, or claim that may be made by its manufacturer, is not guaranteed or endorsed by the publisher.

Copyright © 2022 Li, Han, Zhao, Tang, Zhang and Qin. This is an open-access article distributed under the terms of the Creative Commons Attribution License (CC BY). The use, distribution or reproduction in other forums is permitted, provided the original author(s) and the copyright owner(s) are credited and that the original publication in this journal is cited, in accordance with accepted academic practice. No use, distribution or reproduction is permitted which does not comply with these terms.



## OPEN ACCESS

## EDITED BY

Yubin Luo,  
Sichuan University, China

## REVIEWED BY

Weizhong Li,  
J. Craig Venter Institute (La Jolla),  
United States  
Ratnakar Deole,  
Oklahoma State University,  
United States

## \*CORRESPONDENCE

Lin Tang  
tanglin@zzu.edu.cn  
Suying Ding  
fccdingsy@zzu.edu.cn

## SPECIALTY SECTION

This article was submitted to  
Microbiome in Health and Disease,  
a section of the journal  
Frontiers in Cellular and  
Infection Microbiology

RECEIVED 18 May 2022

ACCEPTED 06 July 2022

PUBLISHED 29 July 2022

## CITATION

Sheng S, Yan S, Chen J, Zhang Y,  
Wang Y, Qin Q, Li W, Li T, Huang M,  
Ding S and Tang L (2022) Gut  
microbiome is associated with  
metabolic syndrome accompanied by  
elevated gamma-glutamyl  
transpeptidase in men.  
*Front. Cell. Infect. Microbiol.* 12:946757.  
doi: 10.3389/fcimb.2022.946757

## COPYRIGHT

© 2022 Sheng, Yan, Chen, Zhang,  
Wang, Qin, Li, Li, Huang, Ding and Tang.  
This is an open-access article  
distributed under the terms of the  
Creative Commons Attribution License  
(CC BY). The use, distribution or  
reproduction in other forums is  
permitted, provided the original  
author(s) and the copyright owner(s)  
are credited and that the original  
publication in this journal is cited, in  
accordance with accepted academic  
practice. No use, distribution or  
reproduction is permitted which does  
not comply with these terms.

# Gut microbiome is associated with metabolic syndrome accompanied by elevated gamma-glutamyl transpeptidase in men

Shifeng Sheng<sup>1</sup>, Su Yan<sup>1,2</sup>, Jingfeng Chen<sup>1</sup>, Yuheng Zhang<sup>1</sup>,  
Youxiang Wang<sup>1,2</sup>, Qian Qin<sup>1</sup>, Weikang Li<sup>1</sup>, Tiantian Li<sup>1</sup>,  
Meng Huang<sup>1</sup>, Suying Ding<sup>1,2\*</sup> and Lin Tang<sup>3\*</sup>

<sup>1</sup>Health Management Center, The First Affiliated Hospital of Zhengzhou University, Zhengzhou, China, <sup>2</sup>College of Public Health, Zhengzhou University, Zhengzhou, China, <sup>3</sup>Department of Nephropathy, The First Affiliated Hospital of Zhengzhou University, Zhengzhou, China

It is predicted that by 2035, metabolic syndrome (MS) will be found in nearly more than half of our adult population, seriously affecting the health of our body. MS is usually accompanied by the occurrence of abnormal liver enzymes, such as elevated gamma-glutamyl transpeptidase (GGT). More and more studies have shown that the gut microbiota is involved in MS; however, the correlation between gut microbiota and MS with elevated GGT has not been studied comprehensively. Especially, there are few reports about its role in the physical examination of the population of men with MS and elevated GGT. By using the whole-genome shotgun sequencing technology, we conducted a genome-wide association study of the gut microbiome in 66 participants diagnosed as having MS accompanied by high levels of GGT (case group) and 66 participants with only MS and normal GGT level (control group). We found that the number of gut microbial species was reduced in participants in the case group compared to that of the control group. The overall microbial composition between the two groups is of significant difference. The gut microbiota in the case group is characterized by increased levels of "harmful bacteria" such as *Megamonas hypermegale*, *Megamonas funiformis*, *Megamonas unclassified*, *Klebsiella pneumoniae*, and *Fusobacterium mortiferum* and decreased levels of "beneficial bacteria" such as *Faecalibacterium prausnitzii*, *Eubacterium eligens*, *Bifidobacterium longum*, *Bifidobacterium pseudocatenulatum*, *Bacteroides dorei*, and *Alistipes putredinis*. Moreover, the pathways of POLYAMSYN-PWY, ARG+POLYAMINE-SYN, PWY-6305, and GOLPDLAT-PWY were also increased in the case group, which may play a role in the elevation of GGT by producing amine, polyamine, putrescine, and endogenous alcohol. Taken together, there are apparent changes in the composition of the gut microbiome in men with MS and

abnormal GGT levels, and it is high time to discover specific gut microbiome as a potential therapeutic target in that population. More in-depth studies of relevant mechanism could offer some new methods for the treatment of MS with elevated GGT.

#### KEYWORDS

metabolic syndrome, glutamyl transpeptidase, gut microbiota, metagenomics, metabolic pathway, polyamine, endogenous alcohol

## 1 Introduction

Metabolic syndrome (MS) is a complex group of metabolic diseases in the pathological state characterized by abdominal obesity, hypertension, insulin resistance, and hyperlipidemia, defined by the World Health Organization (WHO) (Saklayen, 2018). At present, the prevalence of MS is increasing all over the world, and it has become a major problem endangering public health and seriously affecting the quality of life. The International Diabetes Federation (IDF) has reported that approximately 25% of the total world population is suffering from MS (Saklayen, 2018). It is predicted that the prevalence of MS will increase to 53% by 2035 (Engin, 2017). MS is also a cause of lipid deposition in hepatocytes and is closely associated with hepatocyte necrosis and dysfunction. Studies have found that elevated gamma-glutamyl transpeptidase (GGT) is closely related to atherosclerosis, cardiovascular disease, and impaired glucose tolerance (Franzini et al., 2013) and can predict the risk of diabetes, hypertension, MS, and cardiovascular disease independently (Onat et al., 2012; Yadav et al., 2017; Shiraishi et al., 2019). The possible reason is that GGT not only participated in the hydrolysis of extracellular glutathione but also is a marker of oxidative stress and subclinical inflammation (Alissa, 2018), both of which are considered as important mechanisms for atherosclerosis and the occurrence of MS. However, the current focus of the prevention and treatment of MS is just improvement of lifestyle and comprehensive control of various metabolic abnormal factors and lacks a specific treatment plan. Hence, it is high time to further

study the mechanism of MS with elevated GGT and further explore effective treatment measures.

In recent years, with the quick development of high-throughput sequencing technology, the close association between intestinal microbiota and MS has gradually attracted our attention. Glycolipid metabolism disorders, oxidative stress, and inflammatory reactions in the process of MS can cause the alteration of intestinal microbiota, and the disturbances of intestinal microbiota can also accelerate the progression of MS. Studies have shown that the intestinal microbiota is an “energy metabolism organ” of our host (Ley et al., 2006; Sadik et al., 2010), and it can affect the metabolism of various nutrients such as sugar, fat, and protein and maintain the normal function of the intestinal mucosa (Anhe et al., 2015). The possible mechanisms that gut microbiota is involved in MS are as follows: firstly, it can regulate the immune system and balance the immune response of our body (Furusawa et al., 2013); secondly, it may mediate low-grade inflammation by producing lipopolysaccharide (LPS) (Org et al., 2017); last but not the least, it can digest and utilize substances that the host cannot use and promote the absorption of polysaccharides (Lindheim et al., 2017). At present, the treatment of MS lacks specific multitarget therapeutic drugs. Thus, improving metabolic disorders through different methods may be a new treatment method, such as the regulation of the gut microbiota. Yet, research on whether the increase of GGT in patients with MS is related to the intestinal microbiota is rare, especially in the male physical examination population. In this study, asymptomatic physical examination population was selected as the research object to observe the characteristics of the gut microbiota of MS patients with elevated GGT. It may provide new therapeutic targets and personalized prevention strategies for the clinical treatment of MS with abnormal GGT level.

## 2 Materials and methods

### 2.1 Study design

A total of 1 770 subjects were examined in our study from January 2018 to May 2019, and the Ethics Committee from the First

**Abbreviations:** MS, metabolic syndrome; WC, waist circumference; BMI, body mass index; FBG, fasting plasma glucose; SBP, systolic blood pressure; DBP, diastolic blood pressure; ALT, alanine aminotransferase; AST, aspartate aminotransferase; GGT, gamma-glutamyl transpeptidase; TBIL, total bilirubin; ALB, albumin; TC, total cholesterol; TG, triglyceride; LDL, low-density lipoprotein; HDL, high-density lipoprotein; Crea, serum creatinine; SUA, serum uric acid; WBC, white blood cell; PLT, platelet; NEUT, absolute value of neutrophil; MON, monocyte absolute value; BASO, absolute basophil; SCFAs, short-chain fatty acids; LPS, lipopolysaccharide; MAFLD, metabolic-associated fatty liver disease; IDF, International Diabetes Federation; LPS, lipopolysaccharide; CKD, chronic kidney disease; MAM, microbial anti-inflammatory molecule.

Affiliated Hospital of Zhengzhou University approved this study (Approval numbers: 2018-KY-56 and 2018-KY-90). Inclusion criteria are as follows: 1) age >18 years; 2) clinically diagnosed MS and elevated GGT level (the exact level of GGT is 50 U/L) according to relevant guidelines (Grundt et al., 2005; Hsieh et al., 2009). Exclusion criteria are as follows: 1) other factors that affect liver enzymes such as hepatitis B/C, autoimmune, and alcohol or drug-induced hepatitis (all of the subjects were prohibited from alcohol consumption at least 3 days before the exsanguination); 2) women in pregnancy or lactation; 3) subjects who were being treated with antibiotics, microbiota regulators, yogurt, probiotics, or proton pump inhibitors within the past 2 months; 4) subjects with diabetes, hypertension, coronary atherosclerotic heart disease, hyperthyroidism, hypothyroidism, Cushing syndrome, and so on. A total of 69 people and 75 participants were randomly enrolled in the case group (MS with elevated GGT level) and control group (MS with normal GGT level), respectively. Three women in the case group and nine women in the control group were excluded. The flow diagram is shown in Figure 1A and their profile is summarized in Table 1.

## 2.2 Measurement data and laboratory tests

The height, weight, waist circumference (Computerized body scale, SK-X80), and blood pressure (OMRON Medical automatic electronic blood pressure monitor, HBP-9021) were measured by trained staff, and body mass index (BMI) ( $\text{kg}/\text{m}^2$ ) was calculated as  $\text{weight}/\text{height}^2$ . All blood samples were examined by UniCel DxI 800 Immunoassay System from Beckman Coulter: alanine aminotransferase (ALT), aspartate aminotransferase (AST), gamma-glutamyl transpeptidase (GGT), fasting blood glucose (FBG), total bilirubin (TBIL), low-density lipoprotein (LDL),

high-density lipoprotein (HDL), triglyceride (TG), total cholesterol (TC), albumin (ALB), serum creatinine (Crea), serum uric acid (SUA), white blood cell (WBC), monocyte absolute value (MO), absolute value of neutrophil (NEUT), absolute basophil (BASO), and platelet (PLT).

Meanwhile, a Toshiba Color Doppler Ultrasound System (APLI0500 TUS-A500, Japan) was applied to scan the abdomen by a linear array probe with a frequency of 5–12 MHz. Two mid-level or above sonographers jointly cooperate with each other to observe the changes of the echo in the near and far fields of the liver and structure of the intrahepatic ducts, then determine whether the liver cells have steatosis, that is, metabolic-associated fatty liver disease (MAFLD).

## 2.3 Stool sample collection

About 1 g of feces specimens were obtained from recruited participants before 10 o'clock on the day, and the microbial sample preservation tubes were immediately stored in  $-20^\circ\text{C}$  and then transferred to  $-80^\circ\text{C}$  refrigerator for frozen preservation within 30 min.

## 2.4 Microbiota composition and function profiling

According to the manufacturer's instructions, we extracted DNA from 132 stool samples using a MagPure Stool DNA KF kit B (Magen, China). Qubit Fluorometer was used for the quantification of DNA, prepped with the Qubit dsDNA BR Assay kit (Invitrogen, USA). All genomic DNA was broken to form random fragments by ultrasound and be selected. The

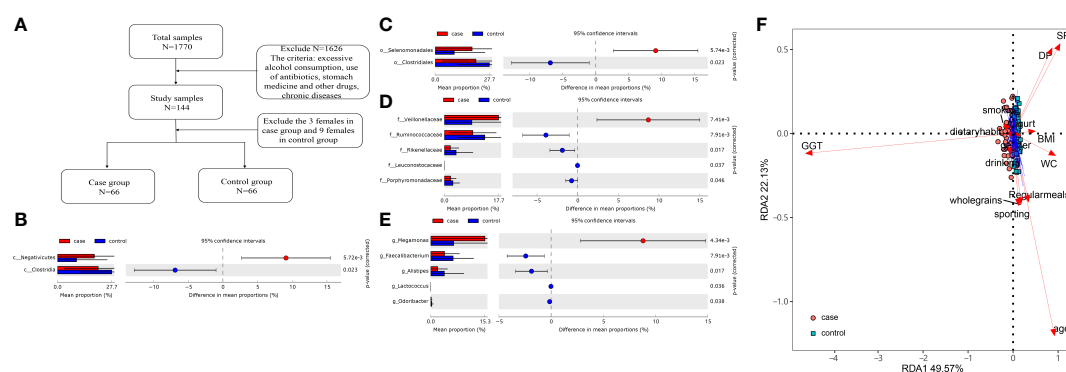




TABLE 1 The major characteristics and laboratory test results in male patients of the case and control groups.

Feature	Control (n = 66)	Case (n = 66)	P
Age	45.26 ± 8.11	43.47 ± 8.83	0.23
WC	94.93 ± 4.92	97.15 ± 8.31	0.09
SBP	138.70 ± 14.91	143.05 ± 13.02	0.08
DBP	88.47 ± 10.55	91.65 ± 10.29	0.08
BMI	28.47 ± 1.90	28.93 ± 2.78	0.27
WBC	6.34 ± 1.41	6.97 ± 1.35	0.01*
PLT	221.71 ± 45.67	240.3 ± 60.64	0.04*
NEUT	3.77 ± 1.02	4.08 ± 1.00	0.08
MON	0.37 ± 0.11	0.47 ± 0.12	<0.01**
BASO	0.03 ± 0.02	0.04 ± 0.02	0.016*
ALT	30.82 ± 13.02	46.89 ± 36.9	<0.01**
AST	21.58 ± 5.58	29.55 ± 17.21	<0.01**
GGT (U/L)	31.02 ± 9.66	96.00 ± 47.88	<0.01**
ALB	48.74 ± 2.46	48.94 ± 2.69	0.645
TBIL	12.16 ± 4.09	12.96 ± 6.65	0.41
Crea	75.21 ± 11.71	73.14 ± 11.05	0.30
SUA	376.67 ± 97.02	392.79 ± 76.31	0.29
TC	4.79 ± 0.87	5.19 ± 0.85	0.01*
TG	2.51 ± 1.09	3.33 ± 2.52	0.02*
HDL	1.13 ± 0.26	1.15 ± 0.26	0.62
LDL	2.99 ± 0.75	3.18 ± 0.78	0.15
FBG	6.46 ± 2.02	6.68 ± 2.02	0.53
MAFLD	NO 11; YES 55	NO 5; YES 61	0.11
Regular meals	NO 15; YES 51	NO 25; YES 41	0.058
Dietary habit	mix19; meatarian 44; vegetarian 3	mix 15; meatarian 36; vegetarian 15	0.01*
Wholegrains	NO 21; YES 45	NO 33; YES 33	0.034*
Yogurt	NO 36; YES 30	NO 41; YES 25	0.377
Smoking	NO 38; YES 28	NO 28; YES 38	0.082
Drinking	NO 20; YES 46	NO 19; YES 50	0.434
Sporting	not 19; rarely 24; frequently 23	not 21; rarely 28; frequently 17	0.52

WC, waist circumference; BMI, body mass index; DBP, diastolic blood pressure; SBP, systolic blood pressure; FBG, fasting blood glucose; AST, aspartate aminotransferase; ALT, alanine aminotransferase; GGT, gamma-glutamyl transpeptidase; ALB, albumin; TBIL, total bilirubin; SUA, serum uric acid; Crea, serum creatinine; TC, total cholesterol; TG, triglyceride; LDL, low-density lipoprotein; HDL, high-density lipoprotein; WBC, white blood cell; NEUT, absolute value of neutrophil; MO, monocyte absolute value; BASO, absolute basophil; PLT, platelet; MAFLD, metabolic-associated fatty liver disease. \* $P < 0.05$  and \*\* $P < 0.01$ .

selected fragments were then amplified and purified to obtain probe-anchored synthesis technology (cPAS) (MGI2000, MGI, Shenzhen, China). The final library sequenced on BGISEQ-500 platform (BGI-Shenzhen, China) was formed after formatting and identified by quality control. Hybrid sequences such as food genome sequence, low-quality sequence, and human genome sequence were eliminated by performing the sequencing data as the qualitative control. MetaPhlAn2 with default settings was applied to classify and annotate the metagenome of the sequencing library and generate the standard gut microbial profiling species at all levels such as bacteria, archaea, viruses, and eukaryotes (Truong et al., 2015). The NCBI.nlm.nih.gov database (National Center for Biotechnology Information, 2014 Edition) and HUMAnN2 (the HMP Unified Metabolic Analysis

Network 2) were used to annotate the non-redundant gene set and the functional genes into Kyoto Encyclopedia of Genes and Genomes (KEGG) metabolic pathway and generated the composition of the metabolic pathway (Fang et al., 2018; Li et al., 2021).

## 2.5 Statistical analysis

R (version 4.0.5) was used for the statistical analyses. Laboratory test, demography, bacterial species, and pathways were analyzed by standardized statistical tests. Categorical variables were represented by counts, and chi-square tests were used for differential analyses. Continuous variables were expressed

as means  $\pm$  standard deviation ( $\bar{x} \pm s$ ). Normality tests and homogeneity tests were used for the analysis of between-group differences, and  $P \geq 0.05$  was selected as the normal and homogeneity variances. The Student's t-test or Mann–Whitney test was used for analyzing the normal and homogeneous results, respectively, and  $P < 0.05$  was regarded as statistically significant. The permutational multivariate analysis of variance (PERMANOVA) and redundancy analysis (RDA) were performed by us to confirm whether elevated GGT level was the most important influencing factor between the two groups. The package of “ADE4” in R program was applied to perform the principal coordinate analysis (PCoA), and the package of “vegan” was used to obtain Shannon, Gini, Hellinger, Jensen–Shannon divergence (JSD), and Bray indexes for each sample. STAMP (version 2.1.3) was used to analyze the difference in the microbiome at the phylum through species levels and pathways. Welch's t-test and multiple test correction using the Benjamini–Hochberg false discovery rate (FDR) were applied to calculate the difference between two groups. The species with low occurrence rates and expression levels (positivity rates  $< 10\%$ ) were removed. The correlations between gut microbiota and covariates were analyzed by Spearman correlation method and the “corrplot” package was used for visualization.

### 3 Results

#### 3.1 Clinical characteristics

There were 66 MS patients with elevated GGT (case group) and 66 MS patients with normal GGT (control group) in our cross-sectional cohort study. The level of GGT accompanied by

ALT, AST, WBC, MON, BASO, PLT, TC, TG, Dietary habit, and Wholegrains in the case group were significantly higher than those in the control group. Moreover, the incidence of MAFLD in the case and control groups is 92.42% and 83.33%, respectively (Table 1).

#### 3.2 Analysis of factors affecting the gut microbiota in the species level

First, we use multivariate variance (PERMANOVA) to analyze the response factor to gut microbiota changes in the species level and use a distance matrix (Bray–Curtis distance) to decompose the total variance. The interpretation degree of different grouping factors on sample differences was analyzed, and permutation tests were used to analyze whether different response variables had a significant impact on bacterial community structure. Specifically, we analyzed the basic information of the included population (i.e., GGT level, Regular meals, Dietary habit, Wholegrains, Yogurt, Smoking, Drinking, Sporting, Age, WC, BMI, SBP, DBP) *via* PERMANOVA. Both univariate and multivariate analyses showed that the GGT level had the greatest effect on participants' gut microbiota structure ( $P < 0.05$ , Table 2).

#### 3.2 Differences in the microbiota at all levels

Together, 16 phyla, 25 classes, 37 orders, 76 families, and 170 genera were found. The differences in the microbiota were calculated by STAMP from the level of phylum to species.

TABLE 2 The influence of the basic attributes of the participants on the gut microbiome in the species level.

Phenotype	Single factor			Multifactor		
	F. Model	Variation ( $R^2$ )	Pr ( $>F$ )	F. Model	Variation ( $R^2$ )	Pr ( $>F$ )
GGT	2.807	0.021	0.004	2.815	0.021	0.002
Regular meals	0.989	0.008	0.402	1.186	0.009	0.261
Dietary habit	0.523	0.004	0.933	0.457	0.003	0.967
Wholegrains	0.711	0.005	0.74	0.874	0.007	0.534
Yogurt	0.933	0.007	0.471	1.04	0.008	0.357
Smoking	1.025	0.008	0.393	0.623	0.005	0.86
Drinking	0.881	0.007	0.583	0.708	0.005	0.75
Sporting	0.739	0.006	0.704	0.896	0.007	0.511
Age	1.382	0.011	0.172	1.405	0.011	0.156
WC	1.083	0.008	0.337	1.25	0.009	0.228
SP	1.175	0.009	0.282	1.171	0.009	0.248
DP	1.081	0.008	0.338	0.955	0.007	0.483
BMI	1.04	0.008	0.378	1.812	0.014	0.048

WC, waist circumference; BMI, body mass index; DBP, diastolic blood pressure; SBP, systolic blood pressure; GGT, gamma-glutamyl transpeptidase.

Benjamini–Hochberg FDR was used for the correction of Welch’s t-test and multiple tests. In total, 2 classes, 2 orders, 5 families, and 5 genera (Figures 1B–E) showed a difference between the two groups. We also constructed the RDA diagram to show the relevance between the microbiome and subjects’ individual attributes and cohort (Figure 1F). The RDA was applied to reflect the samples and response factors on the same two-dimensional ranking map from which the relationship between the sample distribution and the basic characteristics of the host can be seen intuitively.

### 3.4 Community diversity in the case and control groups

At the species level, we applied alpha and beta diversity to evaluate the community diversity. In Figures 2A, B, the alpha diversity by Shannon index and Gini index showed a significant difference between the case and control groups ( $P < 0.05$ ). In the species-level beta diversity, Bray distance, Hellinger distance, and Jensen–Shannon divergence (JSD) distance were calculated, and all of them showed significant differences ( $P < 0.05$ , Figures 2C–E).

## 3.5 The gut microbiome characteristics in different groups and the association with clinical index

### 3.5.1 The gut microbiome characteristics in different groups

Seventeen species showed a significant difference between the two groups at the species level ( $P < 0.05$ ; Figure 3A). A total of 7 species including *Megamonas hypermegale*, *Megamonas funiformis*, *Megamonas unclassified*, *Fusobacterium mortiferum*, *Sutterella wadsworthensis*, *Bacteroides thetaiotaomicron*, and *Klebsiella pneumoniae* were enriched in the case group; 10 species including *Bifidobacterium longum*, *Bifidobacterium pseudocatenulatum*, *Faecalibacterium prausnitzii*, *Bacteroides dorei*, *Alistipes putredinis*, *Clostridium sp\_L2\_50*, *Ruminococcus gnavus*, *Paraprevotella unclassified*, *Eubacterium eligens*, and *Veillonella parvula* were enriched in the control group.

### 3.5.2 Association between the gut microbiota and clinical index

We used Spearman’s correlation analysis to explore the correlation between the abundance of species and participants’

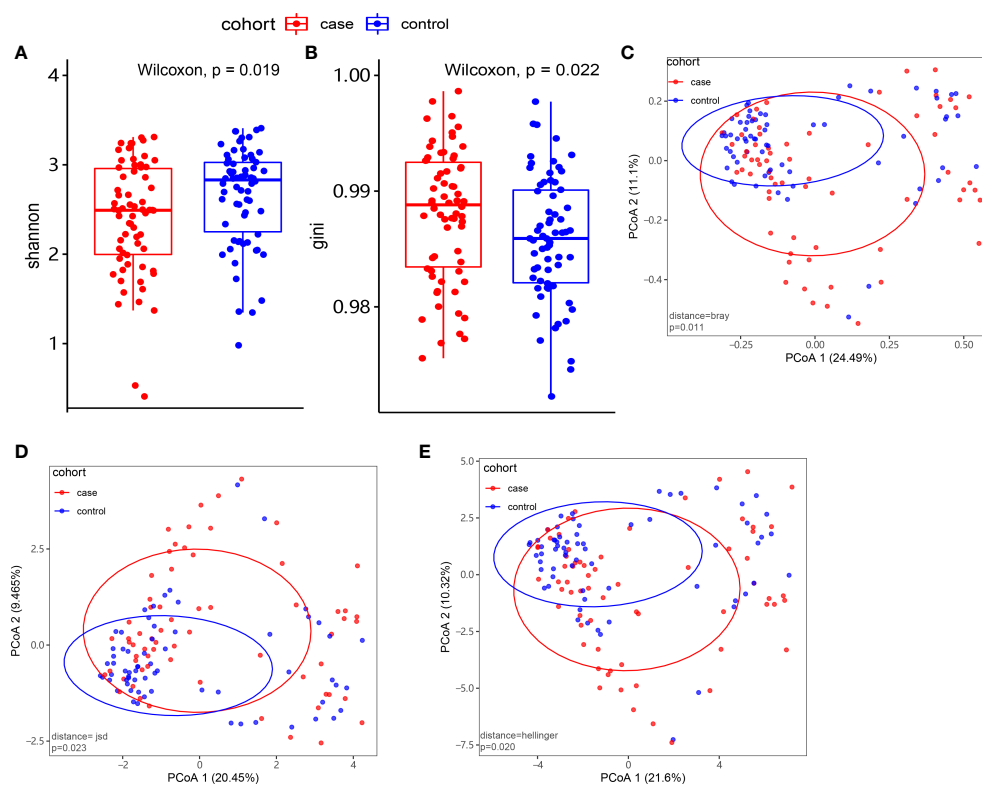


**FIGURE 2**  
Microbiome composition and diversity. (A, B) Alpha diversity by Shannon and Gini indexes between the case group (N = 66) and control group (N = 66). (C–E) Beta diversity by Bray, Hellinger, and Jensen–Shannon divergence (JSD) indexes between the two groups.

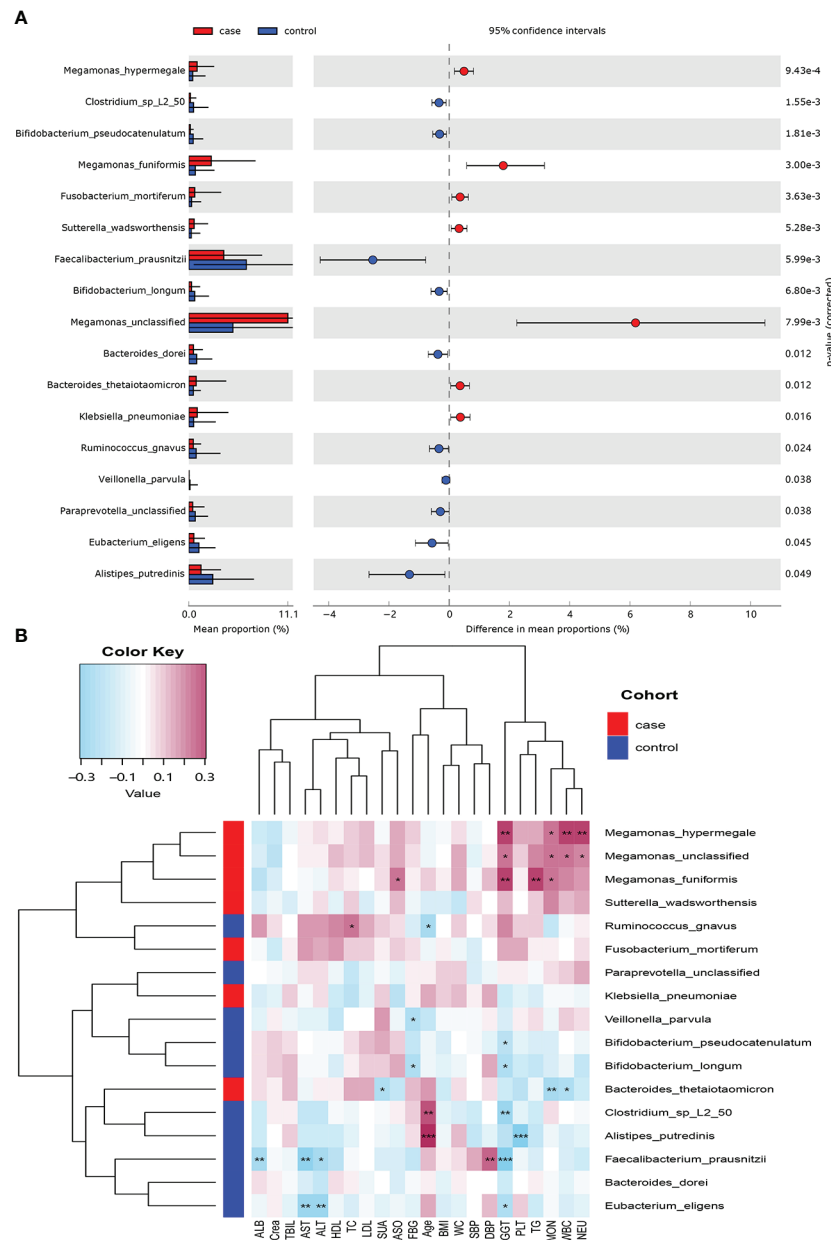


FIGURE 3

Microbiome difference between the case and control groups and the correlation with clinical index ( $P$ -value  $_{corrected} < 0.05$ ). (A) The relative abundance of bacterial species with significant difference between the two groups. (B) Correlation matrix of the bacterial species and clinical index. Blue cell color represented a negative correlation; red cell color represented a positive correlation.  $*P < 0.05$ ,  $**P < 0.01$ , and  $***P < 0.001$ .

features. Except ALB, TBIL, and Crea, most of the gut microbiota enriched in the case group had positive relationships with these clinical indexes, such as *M. hypermegale*, *M. funiformis*, *Megamonas* unclassified, *S. wadsworthensis*, and *F. mortiferum*; especially *M. hypermegale*, *M. funiformis*, and *Megamonas* unclassified had a significantly positive correlation with the marker of inflammation (i.e., NEU, WBC, and MOC) and metabolic

indicators (i.e., TG and GGT). While those microbiomes enriched in the control group had negative correlations with most clinical indexes, such as *B. longum*, *B. pseudocatenulatum*, *F. prausnitzii*, *B. dorei*, *A. putredinis*, *Clostridium* sp\_L2\_50, and *E. eligens*, especially *F. prausnitzii* and *E. eligens* had the most negative association with liver enzymes (GGT, ALT, and AST); *A. putredinis* was highly negatively correlated with PLT (Figure 3B).



## 3.6 Functional shifts in the microbiome characteristics in the case and control groups

### 3.6.1 The functional shifts from the contrast of different subjects

A total of 494 microbial MetaCyc pathways were applied to construct the function profile. Forty-one pathways showed a significant difference between the two groups after removing the low occurrence rate pathways (positivity rates < 10%), and 16 were enriched in the case group (Figure 4). Within these 16 pathways, three were for biosynthesis of amine and polyamine (ARG+POLYAMINE-SYN, POLYAMSYN-PWY, and PWY-6305) and one was for their degradation (GLCMANNANAUT-PWY); one was for fermentation of hexitols to lactic acid, formic acid, ethanol, and acetic acid (P461-PWY); one was for inositol degradation (PWY-7237); two pathways were in charge of producing the precursor metabolite and energy (PWY-5690 and GLYCOCAT-PWY); one was responsible for guanosine nucleotide degradation (PWY-6608); one was for glycerol degradation (GOLPDLAT-PWY); and the others were for biosynthesis (PWY0-162, PWY-7371, PWY0-1586, and PWY-5188). For the pathways enriched in

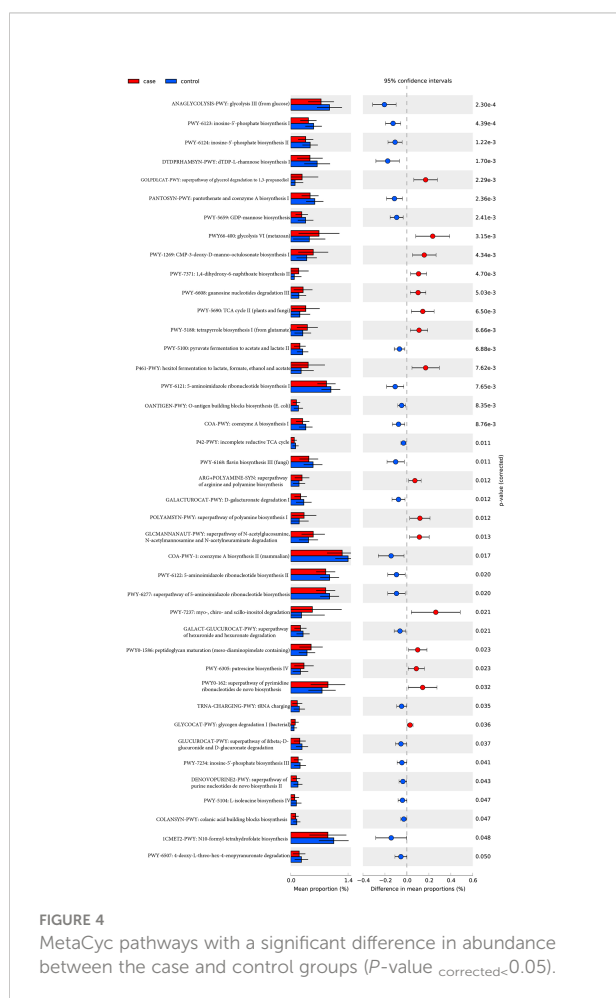
the control group, six were related to nucleoside and nucleotide biosynthesis process (DENOVPURINE2-PWY, PWY-6121, PWY-6122, PWY-6123, PWY-6124, and PWY-7234); five were for biosynthesis of cofactor, carrier, and vitamin, which make large contributions to the Tricarboxylic acid cycle (TCA cycle) and redox reactions (1CMET2-PWY, COA-PWY-1, COA-PWY, PANTOSYN-PWY, and PWY-6168); seven were responsible for degradation of carbohydrates and generation of precursor metabolites and energy (ANAGLYCOLYSIS-PWY, GALACT-GLUCUROCAT-PWY, PWY-5100, GALACTUROCAT-PWY, GLUCUROCAT-PWY, P42-PWY, and PWY-6507); four were for carbohydrate biosynthesis (COLANSYN-PWY, DTDPRHAMSYN-PWY, OANTIGEN-PWY, and PWY-5659); one was for amino acid synthesis (PWY-5104); and one was for tRNA charging (TRNA-CHARGING-PWY).

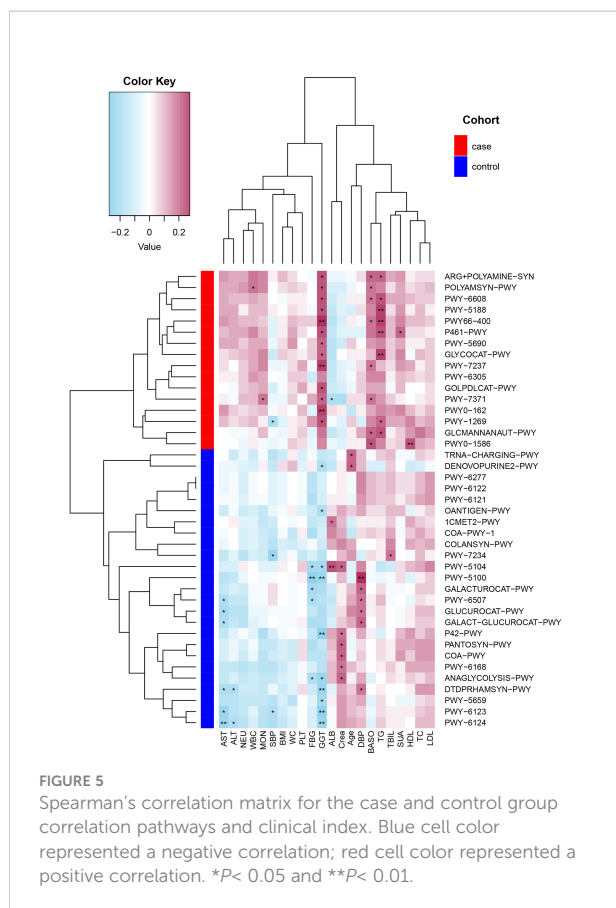
### 3.6.2 Relationship between functional shifts in the microbiome and the clinical index

Spearman's correlation analyses explored the relationships between functional shifts and clinical index, and then we constructed the heatmaps ( $P < 0.05$ , Figure 5). Except ALB and Crea, the most enriched pathways in the case group had positive associations with the clinical index, especially PWY-5188, PWY66-400, P461-PWY, and GLYCOCAT-PWY had a significant difference with GGT and TG, while the most enriched pathways in the control group had a negative relationship with FBG, liver function, and inflammation indexes.

### 3.6.3 Relationship between functional shifts and microbiome characteristics

Spearman's correlation analyses were used to analyze the relationships between functional shifts and microbiome characteristics ( $P < 0.05$ ), and then we constructed the heatmaps (Figure 6). Apparently, *Megamonas* species and *F. Mortiferum*, enriched in the case group, had significantly positive relationships with all pathways enriched in the case group (especially the pathways that were responsible for the biosynthesis of amine, polyamine, and putrescine, such as POLYAMSYN-PWY, ARG+POLYAMINE-SYN, and PWY-6305; the biosynthesis of 1,4-dihydroxy-6-naphthoate such as PWY-7371; and the degradation of glycerol and myo-, chiro-, and scillo-inositol, such as GOLPDLAT-PWY and PWY-7237) and negative relationships with most pathways enriched in the control group. *F. prausnitzii*, *E. eligens*, *B. dorei*, *V. parvula*, *B. longum*, and *B. pseudocatenulatum*, enriched in the control group, had highly positive correlations with most pathways that were enriched in the control group, especially *F. prausnitzii* had the most significantly positive relationships with those pathways responsible for degradation of

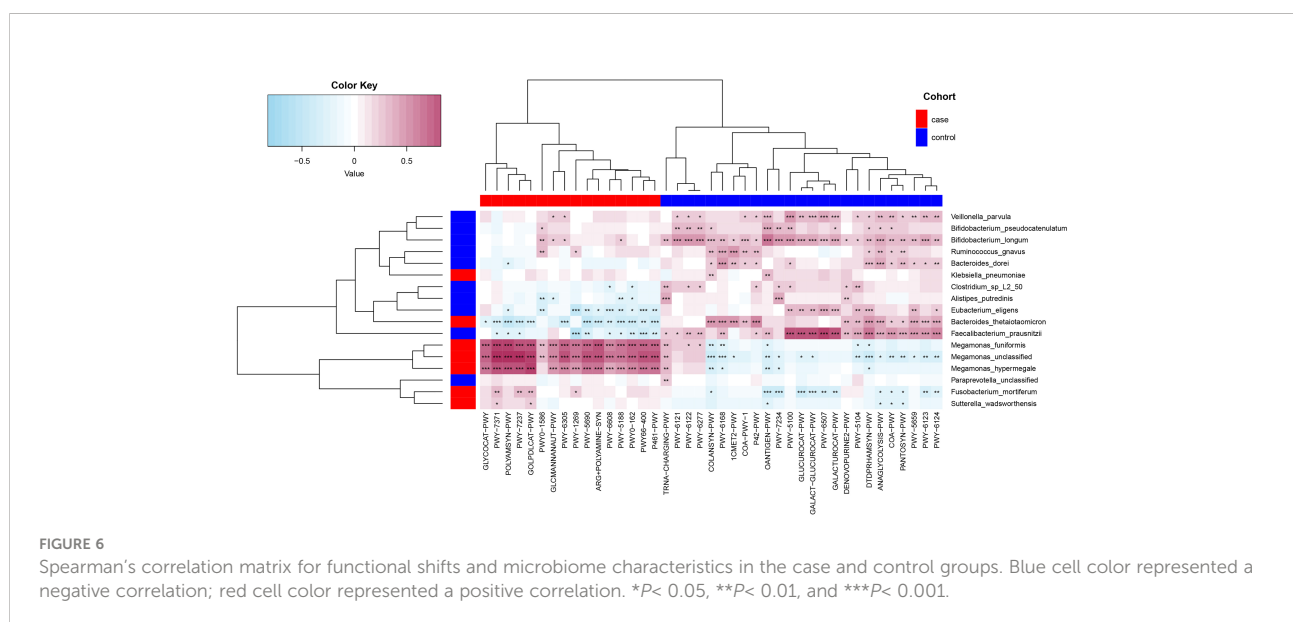




carbohydrates and generation of precursor metabolites and energy (GALACT-GLUCUROCAT-PWY, PWY-5100, GALACTUROCAT-PWY, GLUCUROCAT-PWY, PWY-6507, and ANAGLYCOLYSIS-PWY).

## 4 Discussion

A growing number of studies have shown that disruption of normal state gut microbiota is involved in the pathogenesis and development of multiple chronic low-grade inflammatory diseases, e.g., diabetes (Qin et al., 2012), obesity (Ley et al., 2006), hypertension (Manco et al., 2010), and liver cirrhosis (Qin et al., 2014), and the role of gut microbiome in MS has been gradually elucidated in recent years. Glycolipid metabolism disorders, oxidative stress, and inflammatory reactions in the process of MS can cause the alteration of gut microbiome, and the disturbance in the gut microbiota can also accelerate the progression of MS. At present, the treatment of MS still lacks specific multitarget therapeutic drugs. However, it may be a potential treatment method to regulate the gut microbiota and improve metabolic disorders through different methods. GGT is a direct marker of hepatic insulin resistance that can reflect the degree of hepatic fat deposition (Doi et al., 2007). Studies have shown that the increase in visceral fat is likely to be the main reason for the increase in liver enzyme levels (Pacífico et al., 2011). In addition, GGT is also involved in the oxidation stress response, which may mediate a chronic inflammatory process in MS. However, the research on whether the elevated GGT in patients with MS is related to the gut microbiota has been rarely reported, especially in the male physical examination population. According to our results, it is speculated that there may be some targeted gut microbiota biomarkers that can act as easy, safe, and non-invasive diagnostic tools, which could be used as a complement to traditional diagnostic methods for MS with abnormal GGT levels.



In our study, the level of GGT along with another two liver function indicators (ALT and AST), inflammation factors (WBC, MON, BASO, and PLT), and plasma lipid index (TC and TG) in the case group was obviously higher than that of the control group. Moreover, the level of SBP, DBP, and NEUT in the case group was slightly, but not significantly, higher than that of the control group. Increasing research has proven that the level of liver transaminase is related to the risk of MS (Chen et al., 2016; Kim and Han, 2018). A high level of primary GGT and the GGT value increase over time were both regarded as independent predictors of MS (Yadav et al., 2017). Just as Park et al. (2013) found that elevated liver enzymes were associated with hypertriglyceridemia, hypertension, etc., and there was an obvious dose-response correlation with the number of MS components. In addition, Oh et al. (2006) suggested that patients with metabolic abnormalities should pay much attention to the monitoring and analysis of liver enzyme levels even if they are not enough to diagnose MS. Even liver enzymes within the normal range are also related to the pathogenesis of MS (Steinvil et al., 2010; Zhang et al., 2014). Moreover, the incidence of MAFLD in the case group and control group is 92.42% and 83.33%, respectively. MAFLD is generally considered to be the liver manifestation of MS (Chen et al., 2020). The latest epidemiological data show that the prevalence of MAFLD in China rose from 25.4% in 2008–2010 to 32.3% in 2015–2018, of which 14%–25% MAFLD patients progressed to advanced fibrosis, and the prevalence of MAFLD in overweight and obese population was as high as 52.27% (Zhou et al., 2019), which is much lower than the result of this study, which may be due to region, diet, small population base, etc. Studies have shown that MAFLD and MS are mutually causal; these metabolic factors jointly promote diabetes, atherosclerosis, chronic kidney disease (CKD), coronary heart disease, liver cirrhosis, and the incidence of extrahepatic malignant tumors (Chalasani et al., 2018; Silva et al., 2018; Targher et al., 2020). Therefore, early prevention and intervention of the metabolism-related risks of MAFLD and MS are very important. Of course, the exact mechanism needs to be further studied urgently.

In this study, PERMANOVA was also used to analyze the basic information of the including population, and it was discovered that GGT was the most important influencing factor on the intestinal microbial structure. In terms of gut microbiome, not only the diversity of bacteria in the case group reduced obviously, but the microbial community was of obvious difference from that of the control group. Reduced diversity of microbiota was one of the main types of intestinal disease related to ecological imbalance (Requena et al., 2018) and was documented in many diseases, such as inflammatory bowel disease (IBD) (Frank et al., 2007), autoimmune hepatitis (Wei et al., 2020), and type 1 diabetes (Kostic et al., 2015). Researchers had shown that people with a

reduction of microbial richness are more likely to develop chronic low-grade inflammation (Le Chatelier et al., 2013; Cotillard et al., 2013). Requena et al. (2018) once noticed that the microbiome diversity had close association with our health, and our result showed that the gut microbiota status has transformed significantly from MS to the development of MS with elevated GGT. We found that elevated GGT levels had significant effects on the gut microbiota, and the diversities of alpha and beta differed significantly. At the species level, compared with that of the control group, the relative abundance of *M. hypermegale*, *M. funiformis*, *Megamonas* unclassified, *F. mortiferum*, *S. wadsworthensis*, *B. Thetaiotaomicron*, and *K. pneumoniae* in the case group increased; *B. longum*, *B. pseudocatenulatum*, *F. prausnitzii*, *B. dorei*, *A. putredinis*, *Clostridium* sp\_L2\_50, *R. gnavus*, *Paraprevotella* unclassified, *E. eligens*, and *V. parvula* decreased. Interestingly, most of the gut microbes enriched in the case group (especially the *Megamonas*) showed significantly positive correlations with inflammatory markers (WBC, NEU, MON, and PLT), and the gut microbes in the control group had a negative correlation with them.

We found that the typical butyrate-producing gut microbiota such as *E. eligens* and *F. prausnitzii* were increased in the control group. Not only could they protect against inflammation by producing butyrate, a short-chain fatty acid (SCFA), but contribute to the gut integrity (Morrison and Preston, 2016). *In vitro* cell experiments have shown that *E. eligens* can strongly promote the generation of an anti-inflammatory cytokine, that is, interleukin (IL)-10 (Chung et al., 2017). *F. prausnitzii* is one of the most common bacteria in our intestinal microbiota (Lopez-Siles et al., 2017), and it was discovered to produce a microbial anti-inflammatory molecule (MAM), which can inhibit the pathway of nuclear factor (NF)- $\kappa$ B *in vitro* (Sokol et al., 2008; Quevrain et al., 2016; Breyner et al., 2017; Ganesan et al., 2018). This is consistent with our finding that *E. eligens* and *F. prausnitzii* were negatively correlated with inflammatory indicators. Moreover, *F. prausnitzii* had significant positive correlations with the pathways responsible for the generation of precursor metabolites and energy (GALACT-GLUCUROCAT-PWY, PWY-5100, GALACTUROCAT-PWY, GLUCUROCAT-PWY, PWY-6507, and ANAGLYCOLYSIS-PWY). *A. putredinis* decreases in both compensated and decompensated liver cirrhosis patients (Shao et al., 2018), and it was discovered to increase with the intakes of cruciferous vegetable in human body (Li et al., 2009). *B. dorei* has the effect of anti-influenza by enhancing the expression of earlier interferon, regulating the balance of pro- or anti-inflammatory cytokines, and reconstructing the composition of the gut microbiome (Song et al., 2021). *B. dorei* can also reduce the production of LPS, and treatment with live *B. dorei* may help prevent coronary artery disease (Yoshida et al., 2018) and treat obesity (Yoshida et al., 2021). Hence, *B. dorei* could be regarded as a new probiotic for the prevention and treatment of some clinical disease. Compositionally,

bacteria belonging to *Bifidobacterium* genera were discovered to be enriched in or excited by the prebiotic in the lean microbiome, intimating the potential effect in leanness (Aguirre et al., 2016). Many studies have informed the anti-obesity effect of *Bifidobacterium* spp. (Ma et al., 2008; Yin et al., 2010; An et al., 2011), and some of them have been used as prebiotics in several diseases due to their immune-modulatory action. The bile acid excretion in feces was significantly increased in rats fed yogurt including *B. pseudocatenulatum* or *B. longum* (Al-Sheraji et al., 2012). *B. pseudocatenulatum* may ameliorate the gut homeostasis and impede the gut-derived complication in chronic liver disease (Moratalla et al., 2016). *B. longum* LTBL16, with a strong antioxidant activity, is a bacterial strain of potential probiotic isolated from Chinese healthy centenarians in Bama (Huang et al., 2020). *B. longum* 51A can protect mice against intestinal damage that was caused by irinotecan (Quintanilha et al., 2022). Taken together, the common feature of the above intestinal microbiota is that they are all generally considered “beneficial bacteria”. Most of them also showed the anti-inflammatory or anti-obesity effect in different studies, and the MS with elevated GGT is also a process of chronic low-grade inflammatory response, and there may be some link existing between these bacteria and this process. However, more further studies are required for exploring the exact relationship between them. This is an interesting direction worth exploring.

Numerous studies have confirmed the gut microbial community of obesity (Chiu et al., 2014; Maya-Lucas et al., 2019; Chen et al., 2020; Crovesy et al., 2020; Duan et al., 2021; Palmas et al., 2021), prediabetes (Zhang et al., 2013), primary aldosteronism (Liu et al., 2021), CKD, and hemodialysis patients (Lun et al., 2019), and dogs that have aggressive and phobic behavior (Mondo et al., 2020) exhibited an obvious increase in the *Megamonas* abundance, genera that are associated with not only inflammation (Hiippala et al., 2016; Ling et al., 2016; Lan et al., 2021) but also the metabolism of primary bile acids and abdominal pain in humans (Sakon et al., 2008; Yusof et al., 2017; Aleman et al., 2018). Moreover, members of *Megamonas* can produce acetic and propionic acids, which have been discovered to be substrates for the formation of lipogenesis and cholesterol in rodents (Conterno et al., 2011); more lipogenesis and cholesterol accumulation may lead to abnormal liver function. Especially the *Megamonas* species had highly positive correlations with the pathways responsible for the biosynthesis of amine, polyamine, and putrescine, such as POLYAMSYN-PWY, ARG+POLYAMINE-SYN, and PWY-6305 in this study. Studies have shown that the relative abundance of *Fusobacterium ulcerans* in hyperuricemia (Sheng et al., 2021) and post colorectal cancer surgery (Schmitt et al., 2021) was higher than that in the control group. As is known to all, *K. pneumoniae*, a Gram-negative pathogen bacterium of, is related to lots of opportunistic community-acquired infections. In anaerobic or aerobic conditions, *K. pneumoniae* can grow rapidly and produce high amounts of alcohol. High titers of 2,3-butanediol or 1,3-propanediol are the natural product of *K. pneumoniae*, and under

micro-aerobic conditions, lactic acid is the main end product of fermentation, accompanied by some by-products such as ethanol, acetoin, acetic acids, formic acids, and succinic acids. In a previous Chinese cohort, researchers found that *K. pneumoniae* was associated with more than 60% of individuals with fatty liver disease (FLD), a precursor stage of liver cirrhosis and hepatocellular carcinoma. In addition, they proposed in some FLDs, the change in the gut microbiota can drive the condition by producing excess endogenous alcohol (Yuan et al., 2019). Moreover, they also showed that *K. pneumoniae* may lead to FLD via the production of endogenous ethanol, which is mediated by the pathway of 2,3-butanediol (Li et al., 2021). Consistent with previous research, our result showed that *K. pneumoniae* was enriched in the case group, and it has a positive correlation with GOLPDLCAT-PWY pathway, a super pathway for the degradation of glycerol to 1,3-propanediol. GGT is the most classic and sensitive indicator of alcoholic liver injury; accordingly, we can assume that *K. pneumoniae* may cause liver damage by producing high amounts of endogenous alcohol through the 1,3-propanediol pathway. There may exist some link between *K. pneumoniae* and abnormal liver function. Now, the gut microbiota has received much attention as a non-invasive biomarker for the prevention, diagnosis, and treatment of FLD (Sharpton et al., 2021). Fecal markers have been proposed for the diagnosis and prevention of colorectal and breast cancer subtypes (Yu et al., 2017; Banerjee et al., 2018). Hence, high-throughput sequencing of the above microbiota in feces may help in predicting the risk of abnormal liver enzymes in MS. This study provides a new direction on the diagnosis, prevention, and treatment of MS with elevated GGT.

This research selects the technology of whole-genome shotgun sequencing and chooses the population of asymptomatic physical examination as the study object to explore the disruption of gut microbiota in men with MS accompanied by abnormal GGT level, which are the highlights of the study. Our research also has limitations, such as this is a cross-sectional study, not detecting more inflammatory factors and bacterial metabolites, the gender in the two groups is male adult.

In summary, this research showed the alterations of structural and functional gut microbiome in men with MS accompanied by elevated GGT, which were characterized by increased levels of “harmful bacteria” such as *M. hypermegale*, *M. funiformis*, *Megamonas* unclassified, *K. pneumoniae*, and *F. mortiferum* and decreased levels of “beneficial bacteria” such as *F. prausnitzii*, *E. eligens*, *B. longum*, *B. pseudocatenulatum*, *B. dorei*, and *A. putredinis*. Moreover, the pathways of POLYAMSYN-PWY, ARG+POLYAMINE-SYN, PWY-6305, and GOLPDLCAT-PWY were also increased, which may play a role in the elevation of GGT by producing amine, polyamine, putrescine, and endogenous alcohol. Generally, the potential mechanisms underlying the gut microbiome and GGT accumulation link still need further exploration. The novel associations could provide novel direction for specific microbiome-targeted therapy.



## Data availability statement

The datasets presented in this study can be found in online repositories. The names of the repository/repositories and accession number(s) can be found below: <https://db.cngb.org/>, CNP0003031.

## Ethics statement

The study was approved by the ethics committee from the First Affiliated Hospital of Zhengzhou University (Number: 2018-KY-56 and 2018-KY-90). The patients/participants provided their written informed consent to participate in this study.

## Author contributions

Conceptualization, LT, SD, and SS. Data analysis, SY, JC, and YW. Samples collection, QQ, YZ, WL, TL, and MH. Original drafting, SS. Review and editing, LT and SD. Visualization, JC and SY. Project administration, LT and SD. All authors have read and agreed to submit the manuscript.

## Funding

This study was equally supported and funded by Henan Province Medical Science and Technology Research Plan (LHGJ20200311), Chinese National Science and Technology

Major Project (2018ZX10305410), and Henan Province Key Scientific Research Projects of Universities (21A320035).

## Acknowledgments

The authors sincerely thank all participants or patients enrolled in this research. We also gratefully thank the clinicians and nurses from The First Affiliated Hospital of Zhengzhou University who assisted us with the questionnaire and sample collections, and TopEdit ([www.topedit.com](http://www.topedit.com)) for basic language editing of this manuscript.

## Conflict of interest

The authors declare that the research was conducted in the absence of any commercial or financial relationships that could be construed as a potential conflict of interest.

## Publisher's note

All claims expressed in this article are solely those of the authors and do not necessarily represent those of their affiliated organizations, or those of the publisher, the editors and the reviewers. Any product that may be evaluated in this article, or claim that may be made by its manufacturer, is not guaranteed or endorsed by the publisher.

## References

- Aguirre, M., Bussolo, D. S. C., and Venema, K. (2016). The gut microbiota from lean and obese subjects contribute differently to the fermentation of arabinogalactan and inulin. *PLoS One* 11 (7), e159236. doi: 10.1371/journal.pone.0159236
- Aleman, J. O., Bokulich, N. A., Swann, J. R., Walker, J. M., De Rosa, J. C., Battaglia, T., et al. (2018). Fecal microbiota and bile acid interactions with systemic and adipose tissue metabolism in diet-induced weight loss of obese postmenopausal women. *J. Transl. Med.* 16 (1), 244. doi: 10.1186/s12967-018-1619-z
- Alissa, E. M. (2018). Relationship between serum gamma-glutamyltransferase activity and cardiometabolic risk factors in metabolic syndrome. *J. Family Med. Prim. Care* 7 (2), 430–434. doi: 10.4103/jfmpc.jfmpc\_194\_17
- Al-Sheraji, S. H., Ismail, A., Manap, M. Y., Mustafa, S., Yusof, R. M., and Hassan, F. A. (2012). Hypocholesterolaemic effect of yoghurt containing bifidobacterium pseudocatenulatum G4 or bifidobacterium longum BB536. *Food Chem.* 135 (2), 356–361. doi: 10.1016/j.foodchem.2012.04.120
- Anhe, F. F., Roy, D., Pilon, G., Dufour, S., Matamoros, S., Varin, T. V., et al. (2015). A polyphenol-rich cranberry extract protects from diet-induced obesity, insulin resistance and intestinal inflammation in association with increased akkermansia spp. population in the gut microbiota of mice. *Gut* 64 (6), 872–883. doi: 10.1136/gutjnl-2014-307142
- An, H. M., Park, S. Y., Lee, D. K., Kim, J. R., Cha, M. K., Lee, S. W., et al. (2011). Antiobesity and lipid-lowering effects of bifidobacterium spp. in high fat diet-induced obese rats. *Lipids Health Dis.* 10, 116. doi: 10.1186/1476-511X-10-116
- Banerjee, S., Tian, T., Wei, Z., Shih, N., Feldman, M. D., Peck, K. N., et al. (2018). Distinct microbial signatures associated with different breast cancer types. *Front. Microbiol.* 9. doi: 10.3389/fmicb.2018.00951
- Breyner, N. M., Michon, C., de Sousa, C. S., Vilas, B. P., Chain, F., Azevedo, V. A., et al. (2017). Microbial anti-inflammatory molecule (MAM) from faecalibacterium prausnitzii shows a protective effect on DNBS and DSS-induced colitis model in mice through inhibition of NF-kappaB pathway. *Front. Microbiol.* 8. doi: 10.3389/fmicb.2017.00114
- Chalasani, N., Younossi, Z., Lavine, J. E., Charlton, M., Cusi, K., Rinella, M., et al. (2018). The diagnosis and management of nonalcoholic fatty liver disease: Practice guidance from the American association for the study of liver diseases. *Hepatology* 67 (1), 328–357. doi: 10.1002/hep.29367
- Chen, S., Guo, X., Yu, S., Zhou, Y., Li, Z., and Sun, Y. (2016). Metabolic syndrome and serum liver enzymes in the general chinese population. *Int. J. Environ. Res. Public Health* 13 (2), 223. doi: 10.3390/ijerph13020223
- Chen, X., Sun, H., Jiang, F., Shen, Y., Li, X., Hu, X., et al. (2020). Alteration of the gut microbiota associated with childhood obesity by 16S rRNA gene sequencing. *PeerJ* 8, e8317. doi: 10.7717/peerj.8317
- Chen, C., Zhu, Z., Mao, Y., Xu, Y., Du, J., Tang, X., et al. (2020). HbA1c may contribute to the development of non-alcoholic fatty liver disease even at normal-range levels. *Biosci. Rep.* 40 (1), BSR20193996. doi: 10.1042/BSR20193996
- Chiu, C. M., Huang, W. C., Weng, S. L., Tseng, H. C., Liang, C., Wang, W. C., et al. (2014). Systematic analysis of the association between gut flora and obesity through high-throughput sequencing and bioinformatics approaches. *BioMed. Res. Int.* 2014, 906168. doi: 10.1155/2014/906168
- Chung, W., Meijerink, M., Zeuner, B., Holck, J., Louis, P., Meyer, A. S., et al. (2017). Prebiotic potential of pectin and pectic oligosaccharides to promote anti-inflammatory commensal bacteria in the human colon. *FEMS Microbiol. Ecol.* 93 (11), fix127. doi: 10.1093/femsec/fix127

- Conterno, L., Fava, F., Viola, R., and Tuohy, K. M. (2011). Obesity and the gut microbiota: Does up-regulating colonic fermentation protect against obesity and metabolic disease? *Genes Nutr.* 6 (3), 241–260. doi: 10.1007/s12263-011-0230-1
- Cotillard, A., Kennedy, S. P., Kong, L. C., Prifti, E., Pons, N., Le Chatelier, E., et al. (2013). Dietary intervention impact on gut microbial gene richness. *Nature* 500 (7464), 585–588. doi: 10.1038/nature12480
- Crovesy, L., Masterson, D., and Rosado, E. L. (2020). Profile of the gut microbiota of adults with obesity: A systematic review. *Eur. J. Clin. Nutr.* 74 (9), 1251–1262. doi: 10.1038/s41430-020-0607-6
- Doi, Y., Kubo, M., Yonemoto, K., Ninomiya, T., Iwase, M., Tanizaki, Y., et al. (2007). Liver enzymes as a predictor for incident diabetes in a Japanese population: The hisayama study. *Obes. (Silver. Spring)*. 15 (7), 1841–1850. doi: 10.1038/oby.2007.218
- Duan, M., Wang, Y., Zhang, Q., Zou, R., Guo, M., and Zheng, H. (2021). Characteristics of gut microbiota in people with obesity. *PLoS One* 16 (8), e255446. doi: 10.1371/journal.pone.0255446
- Engin, A. (2017). The definition and prevalence of obesity and metabolic syndrome. *Adv. Exp. Med. Biol.* 960, 1–17. doi: 10.1007/978-3-319-48382-5\_1
- Fang, C., Zhong, H., Lin, Y., Chen, B., Han, M., Ren, H., et al. (2018). Assessment of the cPAS-based BGISEQ-500 platform for metagenomic sequencing. *Gigascience* 7 (3), 1–8. doi: 10.1093/gigascience/gix133
- Frank, D. N., St, A. A., Feldman, R. A., Boedeker, E. C., Harpaz, N., and Pace, N. R. (2007). Molecular-phylogenetic characterization of microbial community imbalances in human inflammatory bowel diseases. *Proc. Natl. Acad. Sci. U. S. A.* 104 (34), 13780–13785. doi: 10.1073/pnas.0706625104
- Fransini, M., Fornaciari, I., Rong, J., Larson, M. G., Passino, C., Emdin, M., et al. (2013). Correlates and reference limits of plasma gamma-glutamyltransferase fractions from the framingham heart study. *Clin. Chim. Acta* 417, 19–25. doi: 10.1016/j.cca.2012.12.002
- Furusawa, Y., Obata, Y., Fukuda, S., Endo, T. A., Nakato, G., Takahashi, D., et al. (2013). Commensal microbe-derived butyrate induces the differentiation of colonic regulatory T cells. *Nature* 504 (7480), 446–450. doi: 10.1038/nature12721
- Ganesan, K., Chung, S. K., Vanamala, J., and Xu, B. (2018). Causal relationship between diet-induced gut microbiota changes and diabetes: A novel strategy to transplant faecalibacterium prausnitzii in preventing diabetes. *Int. J. Mol. Sci.* 19 (12), 3720. doi: 10.3390/ijms19123720
- Grundy, S. M., Cleeman, J. I., Daniels, S. R., Donato, K. A., Eckel, R. H., Franklin, B. A., et al. (2005). Diagnosis and management of the metabolic syndrome: An American heart Association/National heart, lung, and blood institute scientific statement. *Circulation* 112 (17), 2735–2752. doi: 10.1161/CIRCULATIONAHA.105.169404
- Hiippala, K., Kainulainen, V., Kalliomaki, M., Arkkila, P., and Satokari, R. (2016). Mucosal prevalence and interactions with the epithelium indicate commensalism of *sutterella* spp. *Front. Microbiol.* 7. doi: 10.3389/fmicb.2016.01706
- Hsieh, M. H., Ho, C. K., Hou, N. J., Hsieh, M. Y., Lin, W. Y., Yang, J. F., et al. (2009). Abnormal liver function test results are related to metabolic syndrome and BMI in Taiwanese adults without chronic hepatitis b or c. *Int. J. Obes. (Lond)*. 33 (11), 1309–1317. doi: 10.1038/sj.ijo.2009.172
- Huang, G., Pan, H., Zhu, Z., and Li, Q. (2020). The complete genome sequence of *bifidobacterium longum* LTBL16, a potential probiotic strain from healthy centenarians with strong antioxidant activity. *Genomics* 112 (1), 769–773. doi: 10.1016/j.ygeno.2019.05.015
- Kim, H. R., and Han, M. A. (2018). Association between serum liver enzymes and metabolic syndrome in Korean adults. *Int. J. Environ. Res. Public Health* 15 (8), 1658. doi: 10.3390/ijerph15081658
- Kostic, A. D., Gevers, D., Siljander, H., Vatanen, T., Hyötyläinen, T., Hamalainen, A. M., et al. (2015). The dynamics of the human infant gut microbiome in development and in progression toward type 1 diabetes. *Cell Host Microbe* 17 (2), 260–273. doi: 10.1016/j.chom.2015.01.001
- Lan, R., Wan, Z., Xu, Y., Wang, Z., Fu, S., Zhou, Y., et al. (2021). Taurine reprograms mammary-gland metabolism and alleviates inflammation induced by streptococcus uberis in mice. *Front. Immunol.* 12. doi: 10.3389/fimmu.2021.696101
- Le Chatelier, E., Nielsen, T., Qin, J., Prifti, E., Hildebrand, F., Falony, G., et al. (2013). Richness of human gut microbiome correlates with metabolic markers. *Nature* 500 (7464), 541–546. doi: 10.1038/nature12506
- Ley, R. E., Turnbaugh, P. J., Klein, S., and Gordon, J. I. (2006). Microbial ecology: Human gut microbes associated with obesity. *Nature* 444 (7122), 1022–1023. doi: 10.1038/4441022a
- Li, F., Hullar, M. A., Schwarz, Y., and Lampe, J. W. (2009). Human gut bacterial communities are altered by addition of cruciferous vegetables to a controlled fruit- and vegetable-free diet. *J. Nutr.* 139 (9), 1685–1691. doi: 10.3945/jn.109.108191
- Li, N. N., Li, W., Feng, J. X., Zhang, W. W., Zhang, R., Du, S. H., et al. (2021). High alcohol-producing *klebsiella pneumoniae* causes fatty liver disease through 2,3-butanediol fermentation pathway *in vivo*. *Gut. Microbes* 13 (1), 1979883. doi: 10.1080/19490976.2021.1979883
- Li, A., Li, T., Gao, X., Yan, H., Chen, J., Huang, M., et al. (2021). Gut microbiome alterations in patients with thyroid nodules. *Front. Cell Infect. Microbiol.* 11. doi: 10.3389/fcimb.2021.643968
- Lindheim, L., Bashir, M., Munzker, J., Trummer, C., Zachhuber, V., Leber, B., et al. (2017). Alterations in gut microbiome composition and barrier function are associated with reproductive and metabolic defects in women with polycystic ovary syndrome (PCOS): A pilot study. *PLoS One* 12 (1), e168390. doi: 10.1371/journal.pone.0168390
- Ling, Z., Jin, C., Xie, T., Cheng, Y., Li, L., and Wu, N. (2016). Alterations in the fecal microbiota of patients with HIV-1 infection: An observational study in a Chinese population. *Sci. Rep.* 6, 30673. doi: 10.1038/srep30673
- Liu, Y., Jiang, Q., Liu, Z., Shen, S., Ai, J., Zhu, Y., et al. (2021). Alteration of gut microbiota relates to metabolic disorders in primary aldosteronism patients. *Front. Endocrinol. (Lausanne)*. 12. doi: 10.3389/fendo.2021.667951
- Lopez-Siles, M., Duncan, S. H., Garcia-Gil, L. J., and Martinezmedina, M. (2017). Faecalibacterium prausnitzii: From microbiology to diagnostics and prognostics. *ISME J.* 11 (4), 841–852. doi: 10.1038/ismej.2016.176
- Lun, H., Yang, W., Zhao, S., Jiang, M., Xu, M., Liu, F., et al. (2019). Altered gut microbiota and microbial biomarkers associated with chronic kidney disease. *Microbiologyopen* 8 (4), e678. doi: 10.1002/mbo3.678
- Ma, X., Hua, J., and Li, Z. (2008). Probiotics improve high fat diet-induced hepatic steatosis and insulin resistance by increasing hepatic NKT cells. *J. Hepatol.* 49 (5), 821–830. doi: 10.1016/j.jhep.2008.05.025
- Manco, M., Putignani, L., and Bottazzo, G. F. (2010). Gut microbiota, lipopolysaccharides, and innate immunity in the pathogenesis of obesity and cardiovascular risk. *Endocr. Rev.* 31 (6), 817–844. doi: 10.1210/er.2009-0030
- Maya-Lucas, O., Murugesan, S., Nirmalkar, K., Alcaraz, L. D., Hoyo-Vadillo, C., Pizano-Zarate, M. L., et al. (2019). The gut microbiome of Mexican children affected by obesity. *Anaerobe* 55, 11–23. doi: 10.1016/j.anaerobe.2018.10.009
- Mondo, E., Barone, M., Soverini, M., D'Amico, F., Cocchi, M., Petrulli, C., et al. (2020). Gut microbiome structure and adrenocortical activity in dogs with aggressive and phobic behavioral disorders. *Heliyon* 6 (1), e3311. doi: 10.1016/j.heliyon.2020.e03311
- Moratalla, A., Gomez-Hurtado, I., Moya-Perez, A., Zapater, P., Peiro, G., Gonzalez-Navajas, J. M., et al. (2016). Bifidobacterium pseudocatenulatum CECT7765 promotes a TLR2-dependent anti-inflammatory response in intestinal lymphocytes from mice with cirrhosis. *Eur. J. Nutr.* 55 (1), 197–206. doi: 10.1007/s00394-015-0837-x
- Morrison, D. J., and Preston, T. (2016). Formation of short chain fatty acids by the gut microbiota and their impact on human metabolism. *Gut. Microbes* 7 (3), 189–200. doi: 10.1080/19490976.2015.1134082
- Oh, S. Y., Cho, Y. K., Kang, M. S., Yoo, T. W., Park, J. H., Kim, H. J., et al. (2006). The association between increased alanine aminotransferase activity and metabolic factors in nonalcoholic fatty liver disease. *Metabolism* 55 (12), 1604–1609. doi: 10.1016/j.metabol.2006.07.021
- Onat, A., Can, G., Ornek, E., Cicek, G., Ayhan, E., and Dogan, Y. (2012). Serum gamma-glutamyltransferase: Independent predictor of risk of diabetes, hypertension, metabolic syndrome, and coronary disease. *Obes. (Silver. Spring)*. 20 (4), 842–848. doi: 10.1038/oby.2011.136
- Org, E., Blum, Y., Kasela, S., Mehrabian, M., Kuusisto, J., Kangas, A. J., et al. (2017). Relationships between gut microbiota, plasma metabolites, and metabolic syndrome traits in the METSIM cohort. *Genome Biol.* 18 (1), 70. doi: 10.1186/s13059-017-1194-2
- Pacifico, L., Nobili, V., Anania, C., Verdecchia, P., and Chiesa, C. (2011). Pediatric nonalcoholic fatty liver disease, metabolic syndrome and cardiovascular risk. *World J. Gastroenterol.* 17 (26), 3082–3091. doi: 10.3748/wjg.v17.i26.3082
- Palmas, V., Pisanu, S., Madau, V., Casula, E., Deledda, A., Cusano, R., et al. (2021). Gut microbiota markers associated with obesity and overweight in Italian adults. *Sci. Rep.* 11 (1), 5532. doi: 10.1038/s41598-021-84928-w
- Park, E. Y., Lim, M. K., Oh, J. K., Cho, H., Bae, M. J., Yun, E. H., et al. (2013). Independent and supra-additive effects of alcohol consumption, cigarette smoking, and metabolic syndrome on the elevation of serum liver enzyme levels. *PLoS One* 8 (5), e63439. doi: 10.1371/journal.pone.0063439
- Qin, J., Li, Y., Cai, Z., Li, S., Zhu, J., Zhang, F., et al. (2012). A metagenome-wide association study of gut microbiota in type 2 diabetes. *Nature* 490 (7418), 55–60. doi: 10.1038/nature11450
- Qin, N., Yang, F., Li, A., Prifti, E., Chen, Y., Shao, L., et al. (2014). Alterations of the human gut microbiome in liver cirrhosis. *Nature* 513 (7516), 59–64. doi: 10.1038/nature13568

- Quevrain, E., Maubert, M. A., Michon, C., Chain, F., Marquant, R., Tailhades, J., et al. (2016). Identification of an anti-inflammatory protein from faecalibacterium prausnitzii, a commensal bacterium deficient in crohn's disease. *Gut* 65 (3), 415–425. doi: 10.1136/gutjnl-2014-307649
- Quintanilha, M. F., Miranda, V. C., Souza, R. O., Gallotti, B., Cruz, C., Santos, E. A., et al. (2022). Bifidobacterium longum subsp. longum 5(1A) attenuates intestinal injury against irinotecan-induced mucositis in mice. *Life Sci.* 289, 120243. doi: 10.1016/j.lfs.2021.120243
- Requena, T., Martinez-Cuesta, M. C., and Pelaez, C. (2018). Diet and microbiota linked in health and disease. *Food Funct.* 9 (2), 688–704. doi: 10.1039/c7fo01820g
- Sadik, R., Björnsson, E., and Simren, M. (2010). The relationship between symptoms, body mass index, gastrointestinal transit and stool frequency in patients with irritable bowel syndrome. *Eur. J. Gastroenterol. Hepatol.* 22 (1), 102–108. doi: 10.1097/MEG.0b013e32832fd9b
- Saklayen, M. G. (2018). The global epidemic of the metabolic syndrome. *Curr. Hypertens. Rep.* 20 (2), 12. doi: 10.1007/s11906-018-0812-z
- Sakon, H., Nagai, F., Morotomi, M., and Tanaka, R. (2008). Sutterella parvirubra sp. nov. and megamonas funiformis sp. nov., isolated from human faeces. *Int. J. Syst. Evol. Microbiol.* 58 (Pt 4), 970–975. doi: 10.1099/ijs.0.65456-0
- Schmitt, F., Schneider, M., Mathejczyk, W., Weigand, M. A., Figueiredo, J. C., Li, C. I., et al. (2021). Postoperative complications are associated with long-term changes in the gut microbiota following colorectal cancer surgery. *Life (Basel)*. 11 (3), 246. doi: 10.3390/life11030246
- Shao, L., Ling, Z., Chen, D., Liu, Y., Yang, F., and Li, L. (2018). Disorganized gut microbiome contributed to liver cirrhosis progression: A meta-Omics-Based study. *Front. Microbiol.* 9. doi: 10.3389/fmicb.2018.03166
- Sharpton, S. R., Schnabl, B., Knight, R., and Loomba, R. (2021). Current concepts, opportunities, and challenges of gut microbiome-based personalized medicine in nonalcoholic fatty liver disease. *Cell Metab.* 33 (1), 21–32. doi: 10.1016/j.cmet.2020.11.010
- Sheng, S., Chen, J., Zhang, Y., Qin, Q., Li, W., Yan, S., et al. (2021). Structural and functional alterations of gut microbiota in males with hyperuricemia and high levels of liver enzymes. *Front. Med. (Lausanne)*. 8. doi: 10.3389/fmed.2021.779994
- Shiraishi, M., Tanaka, M., Okada, H., Hashimoto, Y., Nakagawa, S., Kumagai, M., et al. (2019). Potential impact of the joint association of total bilirubin and gamma-glutamyltransferase with metabolic syndrome. *Diabetol. Metab. Syndr.* 11, 12. doi: 10.1186/s13098-019-0408-z
- Silva, F. P., Inada, A. C., Ribeiro, F. M., Granja, A. D., Freitas, K. C., Avellaneda, G. R., et al. (2018). An overview of novel dietary supplements and food ingredients in patients with metabolic syndrome and non-alcoholic fatty liver disease. *Molecules* 23 (4), 877. doi: 10.3390/molecules23040877
- Sokol, H., Pigneur, B., Watterlot, L., Lakhdari, O., Bermudez-Humaran, L. G., Gratadoux, J. J., et al. (2008). Faecalibacterium prausnitzii is an anti-inflammatory commensal bacterium identified by gut microbiota analysis of crohn disease patients. *Proc. Natl. Acad. Sci. U. S. A.* 105 (43), 16731–16736. doi: 10.1073/pnas.0804812105
- Song, L., Huang, Y., Liu, G., Li, X., Xiao, Y., Liu, C., et al. (2021). A novel immunobiotics bacteroides dorei ameliorates influenza virus infection in mice. *Front. Immunol.* 12. doi: 10.3389/fimmu.2021.828887
- Steinvil, A., Shapira, I., Ben-Bassat, O. K., Cohen, M., Vered, Y., Berliner, S., et al. (2010). The association of higher levels of within-normal-limits liver enzymes and the prevalence of the metabolic syndrome. *Cardiovasc. Diabetol.* 9, 30. doi: 10.1186/1475-2840-9-30
- Targher, G., Byrne, C. D., and Tilg, H. (2020). NAFLD and increased risk of cardiovascular disease: Clinical associations, pathophysiological mechanisms and pharmacological implications. *Gut* 69 (9), 1691–1705. doi: 10.1136/gutjnl-2020-320622
- Truong, D. T., Franzosa, E. A., Tickle, T. L., Scholz, M., Weingart, G., Pasolli, E., et al. (2015). MetaPhlAn2 for enhanced metagenomic taxonomic profiling. *Nat. Methods* 12 (10), 902–903. doi: 10.1038/nmeth.3589
- Wei, Y., Li, Y., Yan, L., Sun, C., Miao, Q., Wang, Q., et al. (2020). Alterations of gut microbiome in autoimmune hepatitis. *Gut* 69 (3), 569–577. doi: 10.1136/gutjnl-2018-317836
- Yadav, D., Lee, M. Y., Kim, J. Y., Ryu, H., Huh, J. H., Bae, K. S., et al. (2017). Combined effect of initial and longitudinal increases in gamma-glutamyltransferase on incident metabolic syndrome: ARIRANG study. *Yonsei. Med. J.* 58 (4), 763–769. doi: 10.3349/ymj.2017.58.4.763
- Yin, Y. N., Yu, Q. F., Fu, N., Liu, X. W., and Lu, F. G. (2010). Effects of four bifidobacteria on obesity in high-fat diet induced rats. *World J. Gastroenterol.* 16 (27), 3394–3401. doi: 10.3748/wjg.v16.i27.3394
- Yoshida, N., Emoto, T., Yamashita, T., Watanabe, H., Hayashi, T., Tabata, T., et al. (2018). Bacteroides vulgatus and bacteroides dorei reduce gut microbial lipopolysaccharide production and inhibit atherosclerosis. *Circulation* 138 (22), 2486–2498. doi: 10.1161/CIRCULATIONAHA.118.033714
- Yoshida, N., Yamashita, T., Osone, T., Hosooka, T., Shinohara, M., Kitahama, S., et al. (2021). Bacteroides spp. promotes branched-chain amino acid catabolism in brown fat and inhibits obesity. *iScience* 24 (11), 103342. doi: 10.1016/j.isci.2021.103342
- Yuan, J., Chen, C., Cui, J., Lu, J., Yan, C., Wei, X., et al. (2019). Fatty liver disease caused by high-Alcohol-Producing klebsiella pneumoniae. *Cell Metab.* 30 (4), 675–688. doi: 10.1016/j.cmet.2019.08.018
- Yu, J., Feng, Q., Wong, S. H., Zhang, D., Liang, Q. Y., Qin, Y., et al. (2017). Metagenomic analysis of faecal microbiome as a tool towards targeted non-invasive biomarkers for colorectal cancer. *Gut* 66 (1), 70–78. doi: 10.1136/gutjnl-2015-309800
- Yusuf, N., Hamid, N., Ma, Z. F., Lawenko, R. M., Wan, M. W., Collins, D. A., et al. (2017). Exposure to environmental microbiota explains persistent abdominal pain and irritable bowel syndrome after a major flood. *Gut. Pathog.* 9, 75. doi: 10.1186/s13099-017-0224-7
- Zhang, X., Mu, Y., Yan, W., Ba, J., and Li, H. (2014). Alanine aminotransferase within reference range is associated with metabolic syndrome in middle-aged and elderly Chinese men and women. *Int. J. Environ. Res. Public Health* 11 (12), 12767–12776. doi: 10.3390/ijerph111212767
- Zhang, X., Shen, D., Fang, Z., Jie, Z., Qiu, X., Zhang, C., et al. (2013). Human gut microbiota changes reveal the progression of glucose intolerance. *PLoS One* 8 (8), e71108. doi: 10.1371/journal.pone.0071108
- Zhou, F., Zhou, J., Wang, W., Zhang, X. J., Ji, Y. X., Zhang, P., et al. (2019). Unexpected rapid increase in the burden of NAFLD in China from 2008 to 2018: A systematic review and meta-analysis. *Hepatology* 70 (4), 1119–1133. doi: 10.1002/hep.30702



## OPEN ACCESS

## EDITED BY

Cong-Qiu Chu,  
Oregon Health and Science University,  
United States

## REVIEWED BY

Feng Zhang,  
Affiliated Hospital of Jiangnan  
University, China  
Suleiman Joseph Bagi,  
Akanu Ibiam Federal  
Polytechnic, Nigeria

## \*CORRESPONDENCE

Fang He  
hf18602880124@163.com  
Haoming Tian  
hmtian999@126.com

<sup>†</sup>These authors have contributed  
equally to this work

## SPECIALTY SECTION

This article was submitted to  
Microbial Symbioses,  
a section of the journal  
Frontiers in Microbiology

RECEIVED 30 March 2022

ACCEPTED 14 July 2022

PUBLISHED 15 August 2022

## CITATION

Jin J, Wang J, Cheng R, Ren Y, Miao Z,  
Luo Y, Zhou Q, Xue Y, Shen X, He F and  
Tian H (2022) Orlistat and ezetimibe  
could differently alleviate the high-fat  
diet-induced obesity phenotype by  
modulating the gut microbiota.  
*Front. Microbiol.* 13:908327.  
doi: 10.3389/fmicb.2022.908327

## COPYRIGHT

© 2022 Jin, Wang, Cheng, Ren, Miao,  
Luo, Zhou, Xue, Shen, He and Tian.  
This is an open-access article  
distributed under the terms of the  
[Creative Commons Attribution License  
\(CC BY\)](https://creativecommons.org/licenses/by/4.0/). The use, distribution or  
reproduction in other forums is  
permitted, provided the original  
author(s) and the copyright owner(s)  
are credited and that the original  
publication in this journal is cited, in  
accordance with accepted academic  
practice. No use, distribution or  
reproduction is permitted which does  
not comply with these terms.

# Orlistat and ezetimibe could differently alleviate the high-fat diet-induced obesity phenotype by modulating the gut microbiota

Jin Jin<sup>1†</sup>, Jiani Wang<sup>2†</sup>, Ruyue Cheng<sup>2</sup>, Yan Ren<sup>1</sup>,  
Zhonghua Miao<sup>2</sup>, Yating Luo<sup>2</sup>, Qingqing Zhou<sup>2</sup>, Yigui Xue<sup>3</sup>,  
Xi Shen<sup>2</sup>, Fang He<sup>2\*</sup> and Haoming Tian<sup>1\*</sup>

<sup>1</sup>Department of Endocrinology and Metabolism, West China Hospital of Sichuan University, Chengdu, Sichuan, China, <sup>2</sup>Department of Nutrition and Food Hygiene, West China School of Public Health and West China Fourth Hospital, Sichuan University, Chengdu, Sichuan, China, <sup>3</sup>Frontier Medical Service Training Battalion of Army Military Medical University, Changji Hui Autonomous Prefecture, Xinjiang, China

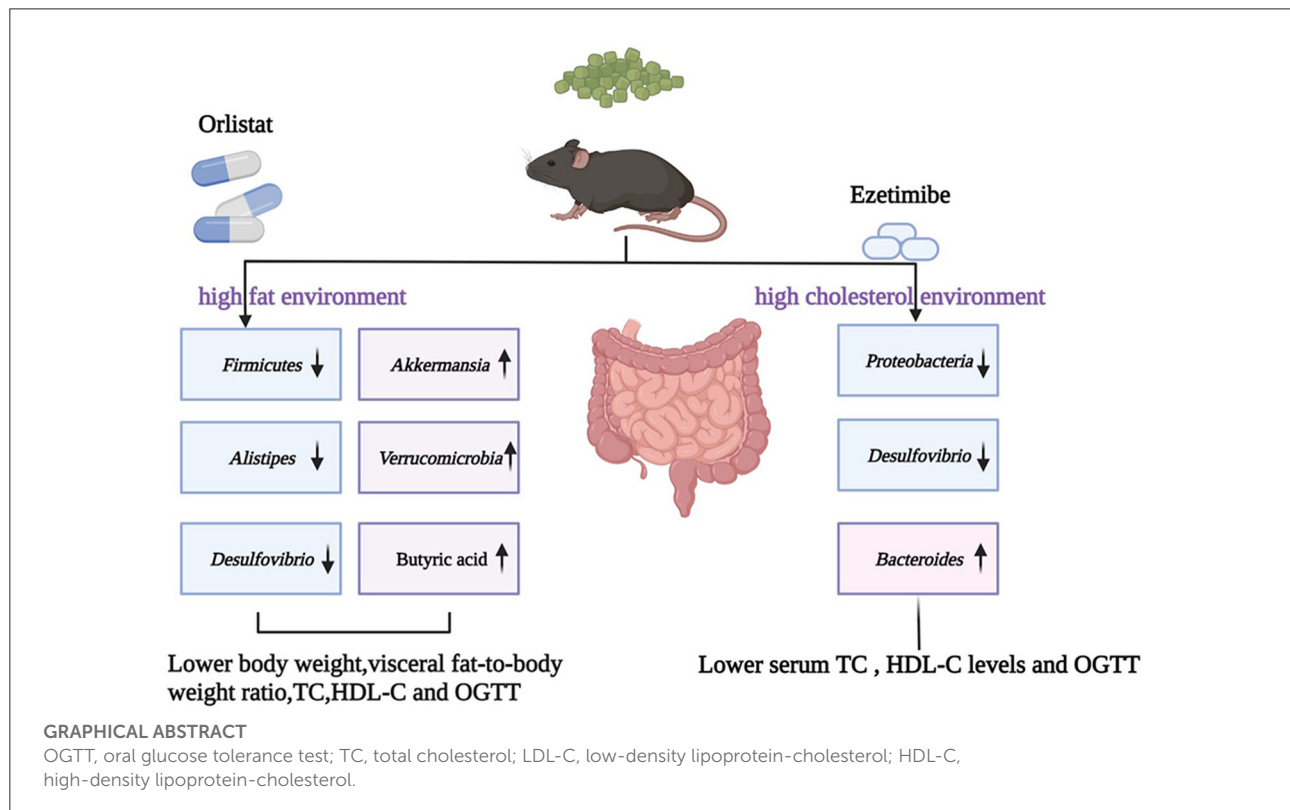
This study aimed to evaluate the possible anti-obesity effects of orlistat and ezetimibe and determine the mechanism by which they alter the composition of gut microbiota and short-chain fatty acids (SCFAs) in mice with a high-fat diet (HFD)-induced obesity. Eighty male, specific pathogen-free C57BL/6J mice aged 3 weeks were divided into four groups ( $n = 20$ ). The NCD group was fed with a normal diet, and the HFD, HFD+ORL, and HFD+EZE groups were fed with HFD for 20 weeks. From the 13th week onward, the HFD+ORL and HFD+EZE groups were administered with orlistat and ezetimibe, respectively. The glucose and lipid metabolism of the tested mice were evaluated by analyzing blood biochemical indicators during the intervention. Furthermore, the changes in the structure of the fecal microbiota and the fecal SCFA content were analyzed by 16S rRNA sequencing and gas chromatography-mass spectrometry, respectively. HFD induced the obesity phenotype in mice. Compared to the HFD group, the body weight, visceral fat-to-body weight ratio, serum total cholesterol (TC), high-density lipoprotein-cholesterol (HDL-C), and oral glucose tolerance test (OGTT) of the HFD+ORL group significantly decreased, whereas fecal butyric acid levels significantly increased. Ezetimibe intervention significantly reduced the OGTT, serum TC, and HDL-C levels only. The  $\alpha$ -diversity of the gut microbiota significantly decreased after intervention with orlistat and ezetimibe. Orlistat altered the relative abundance of some bacteria in the fecal microbiota. The populations of *Firmicutes*, *Alistipes*, and *Desulfovibrio* decreased, whereas those of *Verrucomicrobia* and *Akkermansia* significantly increased. Ezetimibe caused changes only in some low-abundance bacteria, as manifested by a decrease in *Proteobacteria* and *Desulfovibrio*, and an increase in *Bacteroides*. The administration of orlistat and ezetimibe can characteristically influence the body weight and serum lipid metabolism, and glucolipid levels in diet-induced obese mice and is accompanied by significant changes in the gut microbiota and SCFAs. These results suggest that the two drugs might exert their own specific anti-obesity



effects by modulating the gut microbiota in a different manner. The enhanced health-promoting effect of orlistat might result from its stronger ability to alter the gut microbiota and SCFAs, at least partly.

## KEYWORDS

gut microbiota, SCFAs, orlistat, ezetimibe, obesity



## Introduction

Over the past few decades, obesity has become a growing global public health problem. Nearly 2 billion adults worldwide are overweight, and more than half of them are classified as obese (Hoffman et al., 2021). According to the World Health Organization statistics, at least 280,000 people died due to overweight or obesity (Hussain et al., 2020). The Report on Nutrition and Chronic Disease Status of Chinese Residents (2020) showed that the overweight and obesity rate of Chinese adult residents exceeded 50%. Based on current trends, the projections suggested an increase in the prevalence of obesity to 40% in adult women, 60% in adult men, and 25% in children by the year 2050 (Milano et al., 2020). Obesity is often accompanied by other metabolic diseases, such as hyperlipidemia, hypercholesterolemia, cardiovascular

disease, liver steatosis, and type 2 diabetes mellitus (T2DM), all of which increase the risk of death (Mayoral et al., 2020). Therefore, the effective control of overweight and obesity is of great significance to preventing and controlling chronic noncommunicable diseases in the world, particularly in China.

Although the influence of diet, lifestyle, and genetics on the occurrence and progression of obesity is well-known, new research suggests that the gut microbiota may be involved in the pathogenesis of obesity. Observations made in the past 20 years indicated that the gut microbiota might contribute to the metabolic health of the human host. When the intestinal microbiota is abnormal, it may cause various common metabolic disorders, including obesity, T2DM, nonalcoholic liver disease, and dyslipidemia (Fan and Pedersen, 2021). The majority of microorganisms that inhabit humans reside within the intestines and are influenced by the host's mode of birth, lifestyle,

medication, and genetics (Lynch and Pedersen, 2016). As early as 2005, Gordon's research team discovered that obesity would change the ecology of the gut microbiota, and the obvious gut microbial feature of obese people shows a significant increase in *Firmicutes*/Bacteroides (Ley et al., 2005; Voigt et al., 2014). Since then, more and more evidence has shown that interventions aimed at regulating the intestinal microbiota (such as probiotics, prebiotics, and fecal microbiota transplantation) are effective and have a comprehensive effect on obesity (Lynch and Pedersen, 2016; López-Moreno et al., 2020; Sergeev et al., 2020; Yu et al., 2020).

Oral medication is one of the approaches to fight obesity and its complications in humans. In clinical practice, orlistat or ezetimibe is often used to treat obesity or hypercholesterolemia. Orlistat is an oral over-the-counter anti-obesity drug approved by the US Food and Drug Administration for chronic weight management. Studies have shown that orlistat loses 2.9% of the total body weight after subtracting a placebo for at least 12 months (Tak and Lee, 2021). Orlistat induces weight loss by inhibiting lipase in the mucosa of the stomach, small intestine, and pancreas, thereby preventing triglycerides (TGs) from being broken down into fatty acids and absorbed in the intestine (Son and Kim, 2020). Ezetimibe is a lipid-lowering drug that inhibits the intestinal absorption of dietary and bile cholesterol without affecting the absorption of fat-soluble nutrients. It is clinically used to treat hypercholesterolemia (Kosoglou et al., 2005). Both drugs act on the gastrointestinal tract, causing TGs or cholesterol to accumulate in the intestinal tract, respectively (Lynch and Pedersen, 2016). A growing number of studies have shown that the gut microbiota is involved in the metabolism of many drugs and can modulate their effectiveness and side effects (Zimmermann et al., 2019; Klünemann et al., 2021).

The main nutrient source of intestinal microbes is complex carbohydrates that are not digested by upstream digestive tract enzymes. These carbohydrates can be fermented by the intestinal microbiota to produce metabolites, such as short-chain fatty acids (SCFAs). Previous studies have shown that a high-fat diet (HFD) and a high-cholesterol diet can change the gut microbiota differently and its metabolites, including SCFAs and bile acids (Liang et al., 2021). Moreover, orlistat and ezetimibe have limited effects on the gut microbiota of obese patients in Xinjiang in a previous study (Jin et al., 2021). At present, little is known about the identity of the bacterial population that ultimately participates in lipid and cholesterol metabolism, and its underlying mechanism is still unclear.

Therefore, this study selected an HFD to induce obesity in mice and used orlistat and ezetimibe to intervene in obese mice. The changes in body weight, blood glucose, blood lipids, liver function, intestinal microbiota, and other indicators were observed to find the core microorganisms that respond to orlistat and ezetimibe and determine the contribution of the gut microbiota to host metabolism.

## Materials and methods

### Mice

Eighty male, specific pathogen-free C57BL/6J mice aged 3 weeks were purchased from Beijing Huafukang Bioscience Co., Ltd. (approval no. SCXK2019-0008) and kept at the Laboratory Animal Center of West China Second Hospital of Sichuan University (approval no. SYXK2018-209) at an ambient temperature of 20–26°C, relative area minimum static pressure difference of 10 Pa, noise  $\leq 60$  dB (a), day and night alternate time of 12 h, and free drinking water and feed. This experimental design was approved by the Ethics Committee of West China Second Hospital of Sichuan University. All experimental procedures were carried out in accordance with the guidelines for animal experiments of West China School of Public Health of Sichuan University and the guidelines of the Experimental Animal Center of West China Second Medical College of Sichuan University.

### HFD feed and orlistat and ezetimibe treatment

Eighty 3-week-old male C57BL/6J mice were randomly divided into four groups with 20 mice in each group: NCD, HFD, HFD+ORL, and HFD+EZE groups. The NCD group was fed a normal diet, and the other three groups were fed with HFD (D12492; Research Diets, New Brunswick, NJ, USA). From the 13th week onward, the HFD+ORL group was given orlistat (approval no. H20123131; Zhien Pharmaceutical, Chongqing, China) by gavage, and the HFD+EZE group was given ezetimibe (approval no. H20160181; MSD Pharma Pte. Ltd., Gateway West Singapore) by gavage until the 20th week. The dose of ezetimibe and orlistat was 10 and 120 mg/kg/day, respectively. The drug was dissolved in normal saline and intragastrically administered at 0.2 ml each time, once daily. The NCD and HFD groups were given the same volume of normal saline.

### Body weight, organ indexes, and visceral fat-to-body weight ratio

The body weight of mice was measured once weekly until the end of the experiment. Mice were anesthetized by CO<sub>2</sub> and killed by cervical dislocation. The liver, spleen, pancreas, gonadal fat, perirenal fat, and mesenteric fat were collected and weighed. The organ indexes and visceral fat-to-body weight ratio of mice were calculated. Organ index = organ weight (mg)/body weight of mice (g). Visceral fat-to-body weight ratio = fat weight (g)/mice body weight (g)  $\times 100\%$ .

## Fasting blood glucose (FBG) and oral glucose tolerance test (OGTT)

Fasting blood glucose was measured once monthly. After fasting for 12 h, FBG was measured by using Roche Accu-Chek Active test strips (approval no. 20182401933; Roche Diabetes Care GmbH, Mannheim, Germany). OGTT was determined before and at the end of the experiment. After fasting for 12 h, FBG (0 min) was determined by a Roche blood glucose meter, and each mouse was given a 2.0 g/kg glucose solution quickly. The blood glucose values at 30, 60, 90, and 120 min after administration were determined, and the area under the blood glucose curve (AUC) was calculated.  $AUC = 15 \times (GLU0 + 2GLU30 + 2GLU60 + 2GLU90 + GLU120)$ .

## Detection of serum biochemical indicators, insulin, leptin, and adiponectin

At the end of the experiment, blood samples were collected and kept at room temperature for 2 h. Blood was centrifuged at  $2,000 \times g$  for 20 min, and the supernatant was absorbed and centrifuged again for 5 min to obtain the serum. The serum was kept at  $-80^{\circ}\text{C}$  for later use. The serum total cholesterol (TC), TG, high-density lipoprotein-cholesterol (HDL-C), low-density lipoprotein-cholesterol (LDL-C), alanine aminotransferase (ALT), aspartate transaminase (AST), total bilirubin (TBIL), direct bilirubin (DBIL), albumin (ALB), and  $\gamma$ -glutamyl transpeptidase ( $\gamma$ -GT) were detected by Wuhan Servicebio Biotechnology Co., Ltd. Mouse Ins1/insulin-1 enzyme-linked immunosorbent assay (ELISA) kit (Millipore), mouse/rat leptin Quantikine ELISA kit (R&D Systems), and mouse adiponectin/Acrp30 Quantikine ELISA kit (R&D Systems) were used to determine the serum insulin, leptin, and adiponectin content in strict accordance with the instructions provided in the kit.

## DNA extraction of fecal bacteria

At the end of the experiment, a sterile stool collection box was used to collect the fecal samples of mice. The samples were stored in a sterile EP tube and preserved at  $-80^{\circ}\text{C}$ . Fecal bacterial DNA was extracted according to the TIANamp fecal DNA kit (Tiangen Biotech Co., Ltd., Beijing, China).

## 16S rRNA encoding gene sequencing and bioinformatics analysis

To ensure the accuracy of high-throughput sequencing results, the extracted fecal DNA was tested for purity and

concentration and sent to Chengdu Basebio Biotechnology Co., Ltd. for high-throughput sequencing with Illumina MiSeq (Illumina, Inc., Foster City, CA, USA). Illumina high-throughput sequencing results were converted into raw sequencing data after base calling using bcl2fastq (version 1.8.4). Reads with missing barcodes, incorrect barcodes, or conflicting barcode pairs were discarded, and mismatches of more than three per primer were cut off using Trimmomatic (version 0.36). Splice double-ended sequences were analyzed using FLASH (version 1.2.11), which should overlap by at least 10 base pairs, and a maximum of two base mismatches was allowed. After this, the sequences were defined as high-quality sequences.

Chimeric sequences were detected and removed, and the operational taxonomic unit (OTU) was clustered using Usearch (version 11) UNOISE3 algorithm. Usearch was used to compare to the RDP (Release\_16) database, and OTU sequences were annotated to obtain taxonomy information for each OTU. Taxonomic assignments were considered reliable when bootstrap confidence values exceeded 0.75. Phylogenetic tree construction was conducted using the USEARCH cluster\_aggd command.

Subsequently, the  $\alpha$ -diversity indexes (Observed\_OTUs, Chao1, ACE, Fisher, Shannon, and Simpson indexes) were calculated based on the species abundance of each sample in the OTU list using the summary.single command in Mothur. The  $\beta$ -diversity was identified by a principal coordinates analysis (PCoA) using R language PCoA for statistical analysis and graphing. Colony structure statistical analysis and species richness analysis used QIIME to generate species abundance tables and multisample species distribution maps at different taxonomic levels (phylum, class, order, family, and genus) based on the results of the OTU table. Finally, R (version 3.4.1) was used to visualize the statistical results.

## Fecal SCFA analysis

Fecal SCFA analysis was conducted using gas chromatography-mass spectrometry (GC-MS). An Agilent HP-INNOWax GC-MS (Agilent Technologies, Inc., Santa Clara, CA, USA) was used for quantification. To 50 mg of sample, 50  $\mu\text{L}$  of 15% phosphoric acid (China National Pharmaceutical Group Co., Ltd., Beijing, China), 100  $\mu\text{L}$  of 125  $\mu\text{g/mL}$  internal standard solution (isohexanoic acid, >98%; Sigma), and 400  $\mu\text{L}$  of ether (China National Pharmaceutical Group) were added and homogenized for 1 min and centrifuged at  $4^{\circ}\text{C}$  at 12,000 rpm for 10 min, and the supernatant was taken for the test. Acetic acid (AA, >99.5%), propionic acid (PA, >99.0%), isobutyric acid (IBA, >99.0%), butyric acid (BA, >99.0%), isovaleric acid (IVA, >99.0%), and valeric acid (VA, >98.0%) were purchased from Sigma. Caproic acid (CA,  $\geq 99.5\%$ ) was purchased from Aladdin Shanghai Biochemical Technology (Shanghai, China).

## Statistical analysis

The IBM SPSS Statistics software package version 19.0 (Statistical Package for the Social Sciences, Chicago, IL, USA) and GraphPad Prism 8.0 (GraphPad Software, Inc., San Diego, CA, USA) were used to analyze the experimental data. The experimental results were expressed as the mean  $\pm$  standard deviation. One-way analysis of variance or the Kruskal–Wallis nonparametric test was used to compare multiple groups of independent samples, followed by a *post-hoc* least significant difference and Bonferroni test. All tests were two-tailed.  $P < 0.05$  indicated a statistically significant difference. The correlations between the abundance of key OTUs and phenotypes were assessed using Spearman's correlation analysis.

## Results

### Body weight, organ index, and visceral fat-to-body weight ratio

In the first 12 weeks of the experiment, the body weight of the HFD, HFD+EZE, and HFD+ORL groups was significantly higher than the NCD group. After orlistat intervention, the body weight of the HFD+ORL group was significantly lower than the HFD group. However, there was no significant difference in body weight between the HFD and HFD+EZE groups after ezetimibe intervention (Figure 1A). The spleen index of the HFD+EZE group was lower than the NCD group. The pancreas index of the HFD, HFD+EZE, and HFD+ORL groups was lower than the NCD group. The liver index of the HFD, HFD+EZE, and HFD+ORL groups was significantly lower than the NCD group (Figure 1B). Visceral fat tissue accumulation (including the mesenteric fat tissue, gonadal fat tissue, and the perirenal fat tissue) in the HFD and HFD+EZE groups was greater than in the NCD group. However, visceral fat accumulation in the HFD+ORL group was significantly less than in the HFD group (Figure 1C).

### Alterations in blood glucose levels

There was no significant difference in FBG levels between groups at the 0th and 1st month of the experiment. On the 3rd, 4th, and 5th months of the experiment, the FBG levels of the HFD group were higher than the NCD group. A month after ezetimibe intervention (4th month), the FBG levels of the HFD+EZE group were still significantly higher than the NCD group, which decreased significantly in the 5th month and were lower than the HFD group and similar to the NCD group. Two months after orlistat intervention (5th month), the FBG levels of the HFD+ORL group were significantly lower than the HFD group, which was similar to the NCD group (Figure 1D).

As shown in Figure 1E, the blood glucose of the four groups increased to the highest levels at 30 min, and the blood glucose levels of the HFD and HFD+EZE groups were significantly higher than the NCD group at all time points. However, the blood glucose level of the HFD+ORL group was lower than the HFD group at all time points. Moreover, the AUC of the HFD and HFD+EZE groups was significantly higher than the NCD group, and the AUC of the HFD+ORL group was significantly lower than the HFD group and similar to the NCD group (Figure 1F).

### Detection of serum lipid and hormones

The blood lipid composition of each group is shown in Figure 2. After 20 weeks of intervention, the serum TG, TC, LDL-C, and HDL-C levels of HFD-fed mice were significantly higher than mice fed with a normal diet (Figures 2A–D). After orlistat and ezetimibe intervention, compared to the HFD group, no significant difference was found in TG and LDL-C; however, the serum TC and HDL-C levels significantly decreased (Figures 2A–D). As shown in Figures 2E–G, the serum leptin, adiponectin, and insulin levels in HFD-fed mice were significantly higher than in the NCD group. There was no significant difference in the serum leptin, adiponectin, and insulin levels between the HFD and HFD+EZE groups. Conversely, the serum leptin and adiponectin levels in the HFD+ORL group were significantly lower than in the HFD group, although the serum insulin levels between the HFD and HFD+ORL groups were similar.

### Detection of liver function

The serum liver function indexes of mice are shown in Figure 3. The serum ALT levels in HFD-fed mice were significantly lower than in mice fed with a normal diet, and the ALT levels in the HFD+ORL group were significantly lower than in the HFD group (Figure 3A). However, there were no significant differences in AST and  $\gamma$ -GT among groups (Figures 3B,C). Besides, the serum DBIL and TBIL levels in the HFD+ORL group were significantly higher than in the NCD group (Figures 3D,E). Moreover, the serum TBA levels in the HFD+ORL group were significantly lower than in the NCD and HFD groups (Figure 3F). The serum ALB levels were significantly lower than in the NCD group (Figure 3G).

### Fecal SCFA analysis

Compared to the NCD group, AA, PA, BA, IBA, and VA in the HFD group significantly decreased, AA in the HFD+EZE and HFD+ORL groups significantly decreased, BA



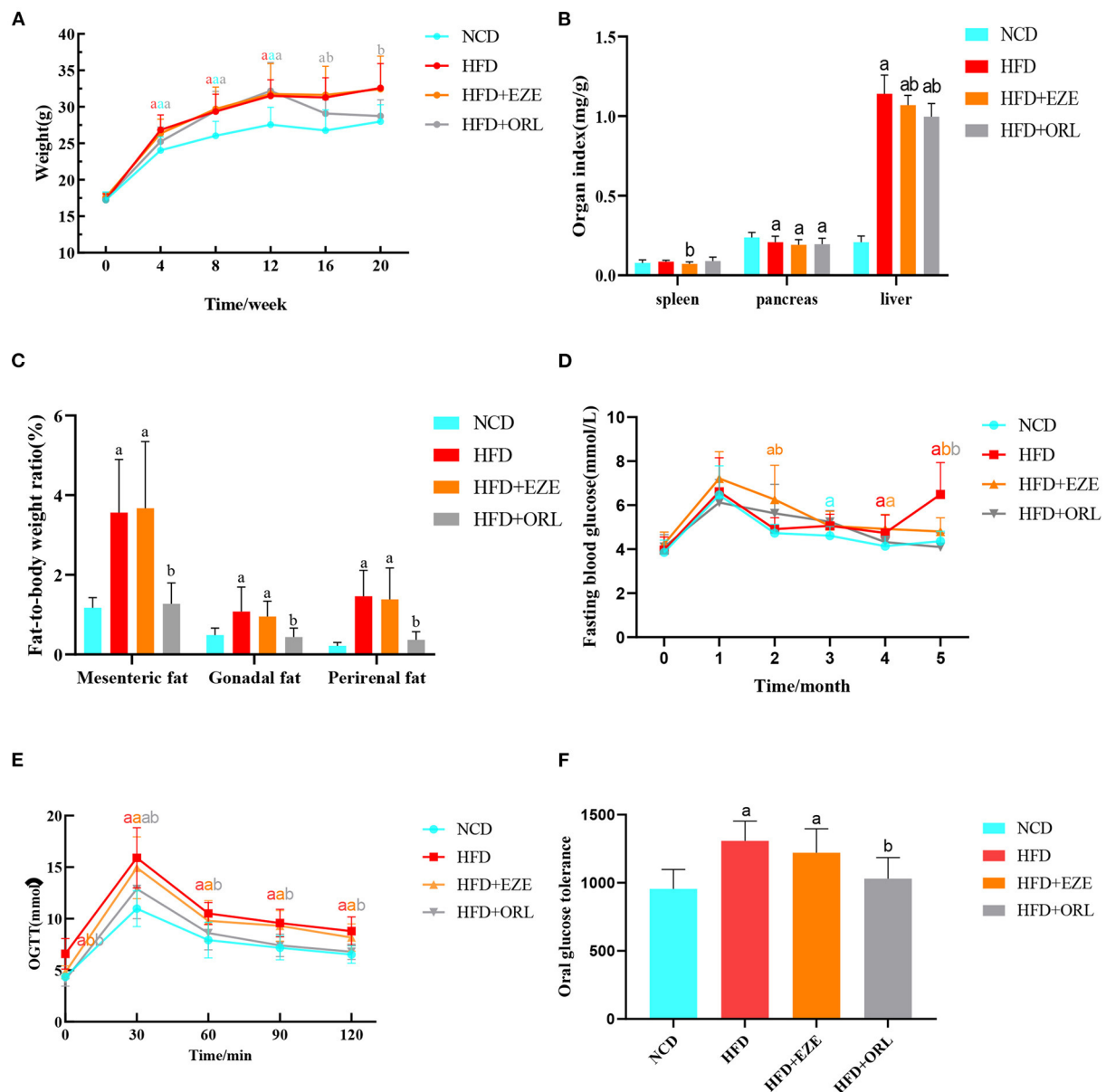


FIGURE 1

Body weight, organ indexes, visceral fat-to-body weight ratio, and the glucose response of mice. (A) The body weight of mice in different groups. (B) Organ (spleen, pancreas, and liver) indexes of mice. (C) Visceral fat-to-body weight ratios of mice. (D) Determination of fasting blood glucose levels of mice each month. (E) An oral glucose tolerance test (OGTT) was performed on mice in the 20th week. (F) Area under the oral glucose tolerance curve of mice. a:  $P < 0.05$  compared with the NCD group. b:  $P < 0.05$  compared with the HFD group. a in red: HFD group compared with NCD group. a in orange: HFD+EZE group compared with NCD group. a in gray: HFD+ORL group compared with NCD group. b in orange: HFD+EZE group compared with HFD group. b in gray: HFD+ORL group compared with HFD group. NCD, normal diet; HFD, high-fat diet; HFD+EZE, high-fat diet and intervention of ezetimibe; HFD+ORL, high-fat diet and intervention of orlistat;  $n = 19$ –20 per group.

in the HFD+EZE group significantly decreased, and VA and IVA in the HFD+ORL group significantly decreased. Compared to the HFD group, SCFAs in the HFD+EZE group did not change significantly (Figures 4A–G). However, BA and CA in the HFD+ORL group significantly increased, which was significantly higher than in the HFD groups (Figures 4D,G).

## Modifications in the composition of the fecal microbiota after orlistat treatment

The  $\alpha$ -diversity indexes of HFD-fed mice, including ACE, Chao1, Observed\_OTUs, Shannon, Simpson, and PD\_whole\_tree index, were all significantly decreased compared

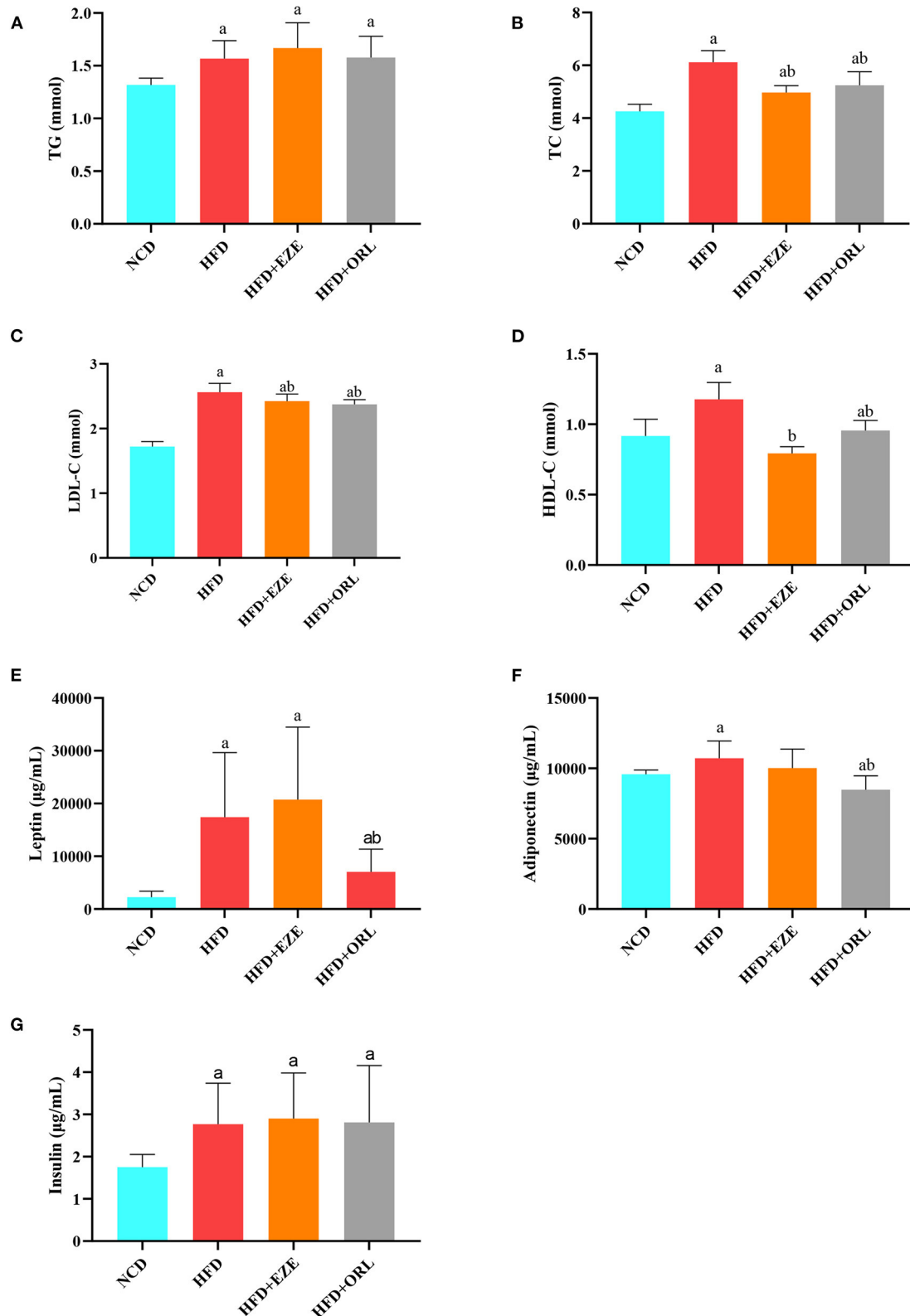


**FIGURE 2**  
Serum biochemical parameters of mice at week 20. **(A)** Triglyceride (TG) levels. **(B)** Total cholesterol (TC) levels. **(C)** Low-density lipoprotein-cholesterol (LDL-C) levels. **(D)** High-density lipoprotein-cholesterol (HDL-C) levels. **(E)** Leptin levels. **(F)** Adiponectin levels. **(G)** Insulin levels. a:  $P < 0.05$  compared with the NCD group. b:  $P < 0.05$  compared with the HFD group. NCD, normal diet; HFD, high-fat diet; HFD+EZE, high-fat diet and intervention of ezetimibe; HFD+ORL, high-fat diet and intervention of orlistat;  $n = 10$  per group.

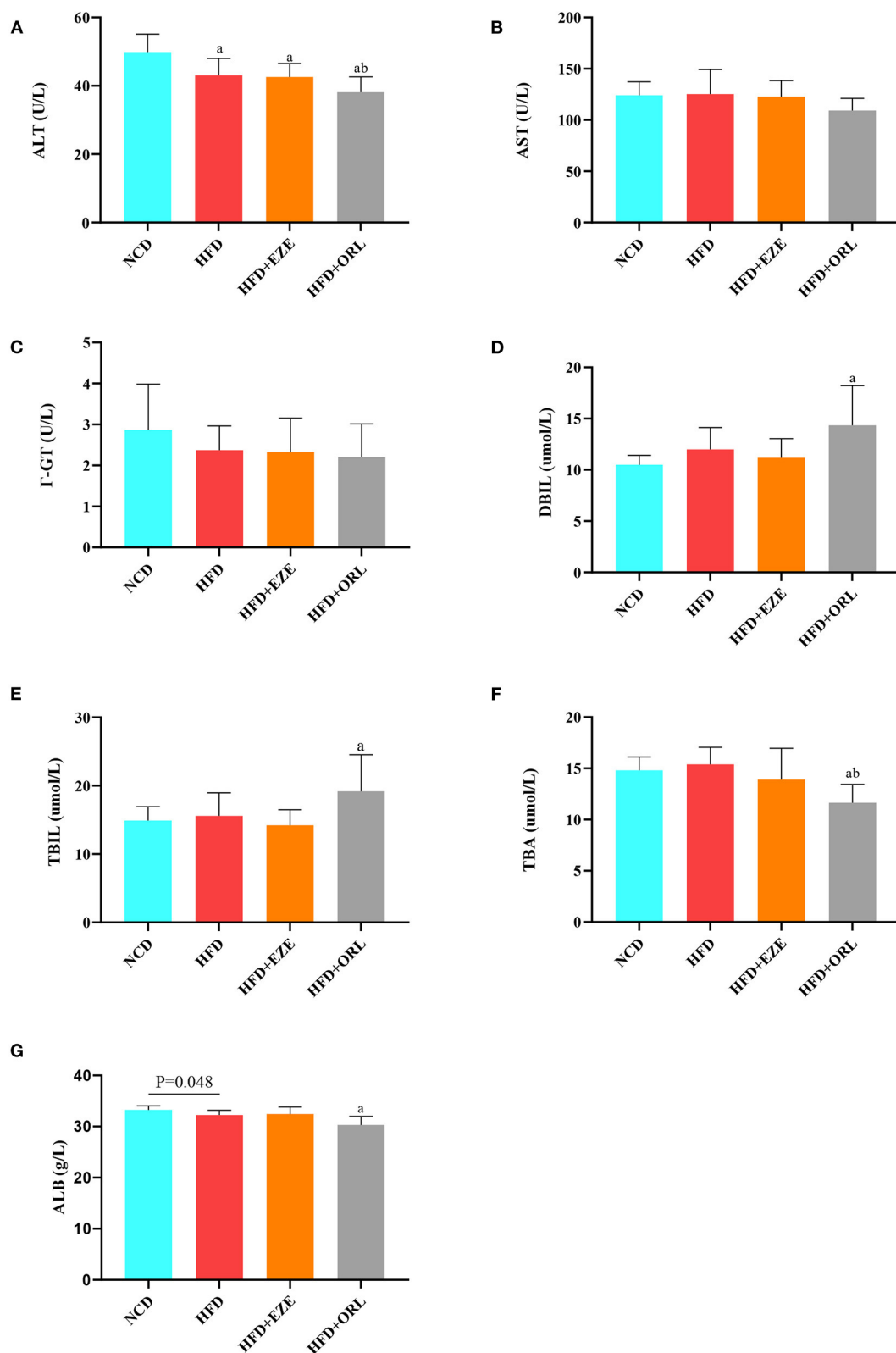


FIGURE 3

Liver function levels of mice in different groups. (A) Serum alanine aminotransferase (ALT) levels; (B) serum aspartate aminotransferase (AST) levels; (C) serum  $\Gamma$ -glutamyl transpeptidase ( $\Gamma$ -GT) levels; (D) serum direct bilirubin (DBIL) levels; (E) serum total bilirubin (TBIL) levels; (F) serum total bile acid (TBA) levels; and (G) serum albumin (ALB) levels. a:  $P < 0.05$  compared with the NCD group. b:  $P < 0.05$  compared with the HFD group. NCD, normal diet; HFD, high-fat diet; HFD+EZE, high-fat diet and intervention of ezetimibe; HFD+ORL, high-fat diet and intervention of orlistat;  $n = 10$  per group.

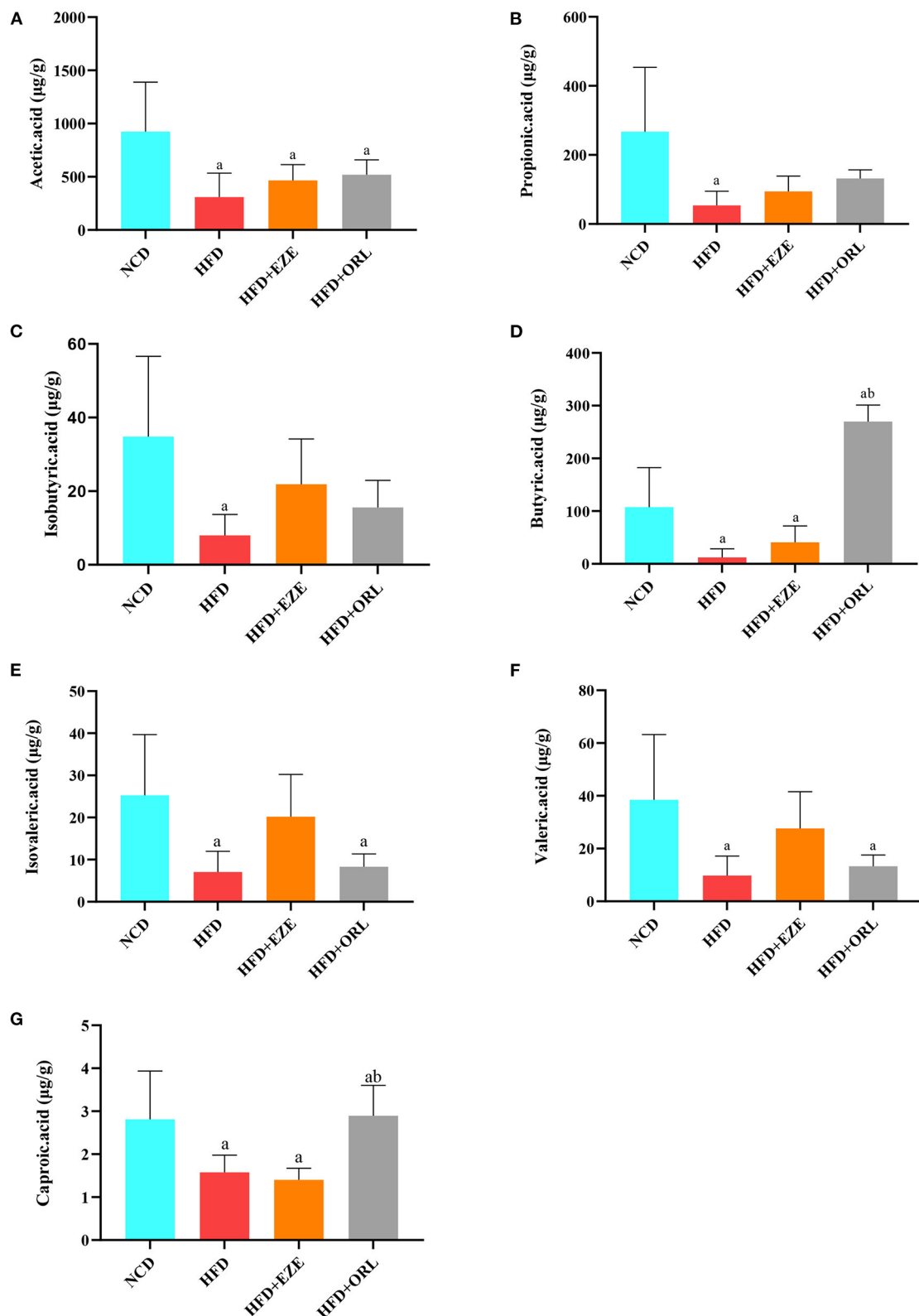


FIGURE 4

Fecal short-chain fatty acid (SCFA) levels of mice in different groups (μg/g wet weight of feces). (A) Acetic acid levels in fecal samples. (B) Propionic acid levels in fecal samples. (C) Fecal isobutyric acid levels. (D) Fecal butyric acid levels. (E) Fecal isovaleric acid levels. (F) Fecal valeric acid levels. (G) Fecal caproic acid levels. a:  $P < 0.05$  compared with the NCD group. b:  $P < 0.05$  compared with the HFD group. NCD, normal diet; HFD, high-fat diet; HFD+EZE: high-fat diet and intervention of ezetimibe; HFD+ORL: high-fat diet and intervention of orlistat;  $n = 6$  per group.



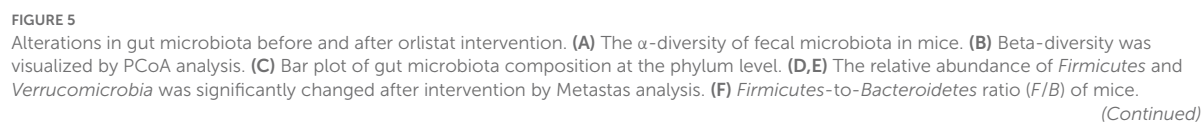


FIGURE 5

(G) Bar plot of gut microbiota composition at the genus level. (H–J) The relative abundance of *Alistipes*, *Akkermansia*, and *Desulfovibrio* was significantly changed after orlistat intervention by Metastat analysis. \* $p < 0.05$ . LCBD, Local contributions to beta-diversity; LCBD values represent the degree of uniqueness of the sampling units in terms of community composition. NCD, normal diet; HFD, high-fat diet; HFD+ORL, high-fat diet and intervention of orlistat;  $n = 6$  per group.

TABLE 1 PERMANOVA analysis of gut microbiota based on weighted Unifrac distance.

Groups compared	P-values	P-adjust
HFD+ORL vs. HFD	0.00	0.01*
HFD+ORL vs. NCD	0.01	0.01*
HFD vs. NCD	0.01	0.01*

\* $P < 0.05$ . NCD, normal diet; HFD, high-fat diet; HFD+ORL, high-fat diet and intervention of orlistat; subject to the adjusted  $P$ -value,  $n = 6$  per group.

to mice fed with a normal diet. After orlistat intervention, the Chao1, Observed\_OTUs, Shannon, and Simpson indexes were significantly lower than the HFD group (Figure 5A). The PCoA analysis based on the weighted Unifrac distance showed that the principal component 1 separated the NCD group from the HFD group and the HFD+ORL component, and its interpretation was 75.82%. The HFD and HFD+ORL groups were not completely separated, and the axis contribution rate was 15.32% (Figure 5B). The PERMANOVA analysis also showed that the beta-diversity of the HFD+ORL group was significantly different from the remaining two groups (Table 1).

After 8 weeks of orlistat intervention, at the phylum level, the five main bacterial phyla in the NCD group were *Bacteroidetes*, *Firmicutes*, *Verrucomicrobia*, *Proteobacteria*, and *Actinobacteria* in order of relative abundance; the five main bacterial phyla of the HFD group were *Firmicutes*, *Proteobacteria*, *Bacteroidetes*, *Actinobacteria*, and *Deferribacteres*; and the five main bacterial phyla of the HFD+ORL group were *Firmicutes*, *Proteobacteria*, *Verrucomicrobia*, *Bacteroidetes*, and *Actinobacteria* (Figure 5C). Compared to the NCD group, *Firmicutes* in the HFD group significantly increased, and *Verrucomicrobia* significantly decreased; however, compared to the HFD group, *Firmicutes* in the HFD+ORL group significantly reduced (Figure 5D), and *Verrucomicrobia* significantly increased (Figure 5E). After HFD intervention, the *F/B* of the HFD group increased significantly. After orlistat intervention, although the *F/B* value showed a decreasing trend, the difference was not statistically significant (Figure 5F).

At the genus level, the five major bacterial genera in the NCD group were *Barnesiella*, *Lactobacillus*, *Akkermansia*, *Alistipes*, and *Prevotella* in order of relative abundance; the five major bacterial genera in the HFD group were *Desulfovibrio*, *Lactobacillus*, *Oscillibacter*, *Olsenella*, and

*Lactococcus*; and the five main bacterial genera in the HFD+ORL group were *Clostridium* XI, *Akkermansia*, *Parasutterella*, *Clostridium sensu stricto*, and *Escherichia/Shigella* in order (Figure 5G). Compared to the NCD group, the relative abundance of *Alistipes* and *Akkermansia* significantly decreased (Figures 5H,I), and the relative abundance of *Desulfovibrio* significantly increased in the HFD group (Figure 5J); however, compared to the HFD group, the relative abundance of *Alistipes* and *Desulfovibrio* in the HFD+ORL group significantly decreased (Figures 5H,J), and the relative abundance of *Akkermansia* significantly increased (Figure 5I).

## Modifications in the composition of the fecal microbiota after ezetimibe treatment

After ezetimibe intervention, the ACE, Chao1, and Observed\_OTUs indexes continued to decline (Figure 6A). The PCoA analysis based on the weighted Unifrac distance showed that principal component 1 separated the NCD group from the HFD group, and its interpretation was 46.05%, whereas principal component 2 separated the NCD group from the other two groups, and the axis contribution rate was 39.57%. Among them, the area where the HFD and HFD+EZE groups gather overlapped (Figure 6B). The PERMANOVA analysis showed that the beta-diversity of the HFD group was significantly different from that of the NCD group, while there was no significant difference between the HFD+EZE group and the other two groups (Table 2).

After 8 weeks of ezetimibe intervention, at the phylum level, the five main bacterial phyla of the HFD+EZE group were *Firmicutes*, *Bacteroidetes*, *Proteobacteria*, *Verrucomicrobia*, and *Deferribacteres* (Figure 6C). Compared to the HFD group, only the relative abundance of *Proteobacteria* was significantly reduced (Figure 6D). After HFD intervention, the *F/B* of the HFD group increased significantly. There was no difference in the *F/B* value between the HFD+EZE and the HFD and NCD groups (Figure 6E).

At the genus level, the five main bacterial genera in the HFD+EZE group were *Bacteroides*, *Akkermansia*, *Desulfovibrio*, *Acetatifactor*, and *Oscillibacter* (Figure 6F). Compared to the HFD group, the relative abundance of *Desulfovibrio* significantly decreased (Figure 6G), and the relative abundance of *Bacteroides* significantly increased in the HFD+EZE group (Figure 6H).

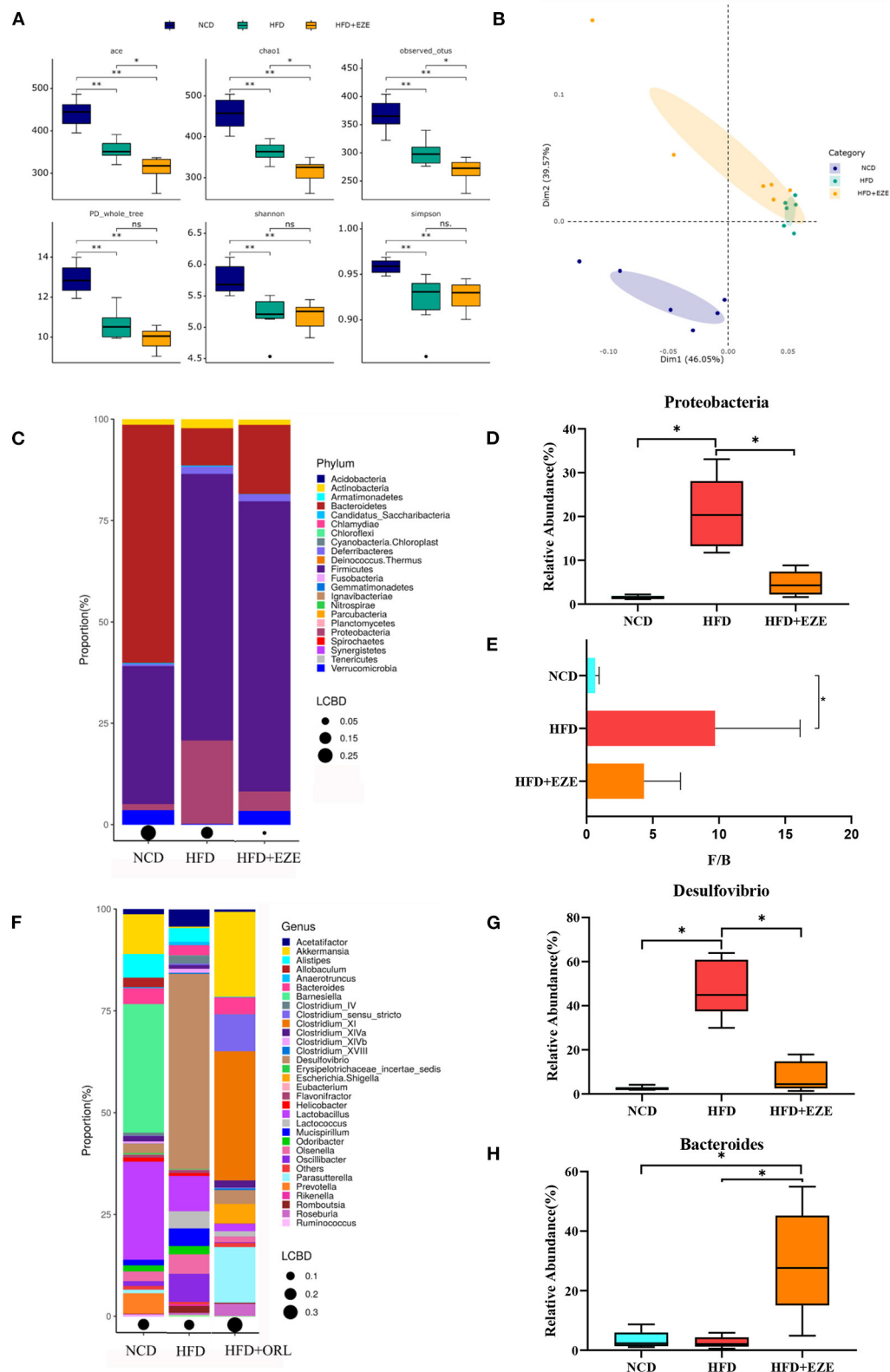


FIGURE 6

Alterations in gut microbiota before and after ezetimibe intervention. (A) The  $\alpha$ -diversity of fecal microbiota in mice. (B) Beta-diversity was visualized by PCoA analysis. (C) Bar plot of gut microbiota composition at the phylum level. (D) The relative abundance of *Proteobacteria* was significantly decreased after intervention by Metastats analysis. (E) *Firmicutes*-to-*Bacteroidetes* ratio (F/B) of mice. (F) Bar plot of gut microbiota composition at the genus level. (G) The relative abundance of *Desulfovibrio* was significantly decreased after intervention by Metastats analysis. (H) The relative abundance of *Bacteroides* was significantly decreased after intervention by Metastats analysis.

(Continued)

FIGURE 6

composition at the genus level. (G,H) The relative abundance of *Desulfovibrio* was significantly decreased and that of *Bacteroides* was significantly increased after ezetimibe intervention by Metastats analysis. \* $p < 0.05$ . LCBD, Local contributions to beta-diversity, LCBD values represent the degree of uniqueness of the sampling units in terms of community composition. NCD, normal diet; HFD, high-fat diet; HFD+ORL, high-fat diet and intervention of orlistat;  $n = 6$  per group.

TABLE 2 PERMANOVA analysis of gut microbiota based on weighted Unifrac distance.

Groups compared	P-values	P-adjust
HFD+EZE vs. HFD	0.03	0.06
HFD+EZE vs. NCD	0.17	0.17
HFD vs. NCD	0.01	0.02 *

\* $P < 0.05$ . NCD, normal diet; HFD, high-fat diet; HFD+ORL, high-fat diet and intervention of orlistat; subject to the adjusted  $P$ -value,  $n = 6$  per group.

## Correlation between body weight, FBG, OGTT, serum lipid, and orlistat-responded microbes

In the NCD group, *Firmicutes* was positively correlated with the body weight and TC and negatively correlated with FBG, *Clostridium XI* was negatively correlated with FBG and OGTT, *Akkermansia* was positively correlated with FBG and negatively correlated with TC, *Desulfovibrio* was positively correlated with TC and HDL-C and negatively correlated with OGTT, *Alistipes* was positively correlated with OGTT and negatively correlated with TC and HDL-C, *Verrucomicrobia* was positively correlated with FBG and negatively correlated with TC, and *Lactobacillus* was positively correlated with TC and negatively correlated with FBG and OGTT (Figure 7A). In the HFD group, *Firmicutes* was positively correlated with TC, *Actinobacteria* was positively correlated with HDL-C and negatively correlated with TG; *Clostridium XI* was negatively correlated with TG; *Akkermansia* was positively correlated with body weight, FBG, and TG; and *Verrucomicrobia* was positively correlated with body weight, FBG, and TG (Figure 7B). In the HFD+ORL group, *Clostridium XI* was negatively correlated with body weight and TC, *Akkermansia* was negatively correlated with FBG, *Alistipes* was positively correlated with TG and HDL-C, *Verrucomicrobia* was negatively correlated with FBG, and *Lactobacillus* was positively correlated with FBG (Figure 7C).

## Correlation between body weight, FBG, OGTT, serum lipid, and ezetimibe-responded microbes

In the NCD group, *Proteobacteria* was negatively correlated with OGTT; *Bacteroides* was positively correlated with FBG and

OGTT and negatively correlated with TC (Figure 8A). In the HFD group, *Bacteroides* was positively correlated with HDL-C (Figure 8B). In the HFD+EZE group, *Firmicutes* was positively correlated with HDL-C, *Actinobacteria* was positively correlated with TG and negatively correlated with LDL-C, *Akkermansia* was negatively correlated with LDL-C, and *Desulfovibrio* was negatively correlated with TG and HDL-C (Figure 8C).

## Discussion

In this study, HFD was successfully used to induce a typical obesity phenotype. In addition, the gut microbiota of mice fed with an HFD was disordered. Studies have shown that the gut microbiota, combined with factors related to diet and genetic susceptibility or changes in the gut microbiota related to itself, may be an active driver of obesity (Cox and Blaser, 2013; Shapiro et al., 2017). Many experiments on germ-free mice have found that the obese phenotype can be transferred by gut microbes (Fei and Zhao, 2013; Scheithauer et al., 2020). Similar to most studies (Zhou et al., 2021), in this study, the  $\alpha$ -diversity of the gut microbiota of the HFD group decreased, leading to disorders in the gut microbiota. Turnbaugh (Turnbaugh et al., 2006) and other studies have shown that obesity is related to the relative abundance of *Bacteroides* and *Firmicutes* in the gut microbiota. Turnbaugh et al. believed that microbial communities with larger  $F/B$  values are more capable of converting heat from food into fat (Turnbaugh et al., 2009). Other data in humans and rodents revealed that obesity was associated with dysbacteria characterized by an enhanced representation of *Firmicutes* and a reduced representation of *Bacteroidetes* (Rooks et al., 2014; Bian et al., 2022). Similarly, in this study, the  $F/B$  value of the HFD group significantly increased, indicating that the HFD transformed the intestinal microbiota of mice into an obesity phenotype. However, there is controversy about the relationship between the  $F/B$  ratio and obesity. Some studies discovered that  $F/B$  was positively correlated with obesity, but other studies did not observe any modifications in this parameter or even reported a decreased  $F/B$  ratio in obese animals and humans (Magne et al., 2020). Therefore, although the present study found that a high-fat diet resulted in a higher  $F/B$  ratio, suggesting a possible association between an increased  $F/B$  and obesity, the association between  $F/B$  and obesity remains to be further studied due to the limitation of animal study.

Fiber fermentation by the gut microbiota yields SCFAs that are either absorbed by the gut epithelium to participate in



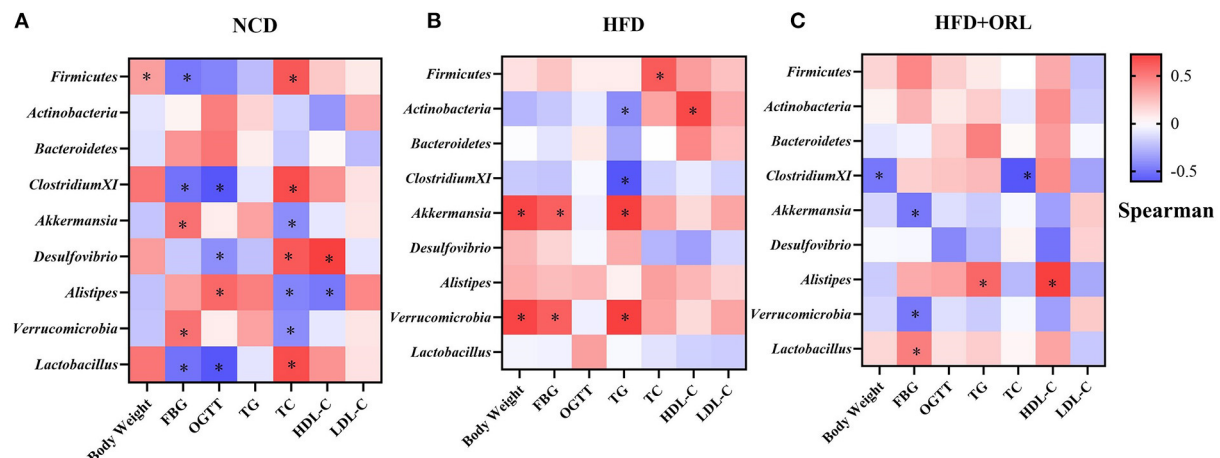


**FIGURE 7**  
Correlations between orlistat responsive core microbes and phenotypes. **(A)** Heatmap of the correlations between orlistat responsive core microbes and phenotypes in the NCD group. **(B)** Heatmap of the correlations between orlistat responsive core microbes and phenotypes in the HFD group. **(C)** Heatmap of the correlations between orlistat responsive core microbes and phenotypes in the HFD+ORL group. \* Indicates that the correlations are statistically significant. Blue indicates the negative correlations, while red indicates the positive correlations. FBG, fasting blood glucose; OGTT, oral glucose tolerance test; TG, triglyceride; TC, total cholesterol; LDL-C, low-density lipoprotein-cholesterol; HDL-C, high-density lipoprotein-cholesterol.

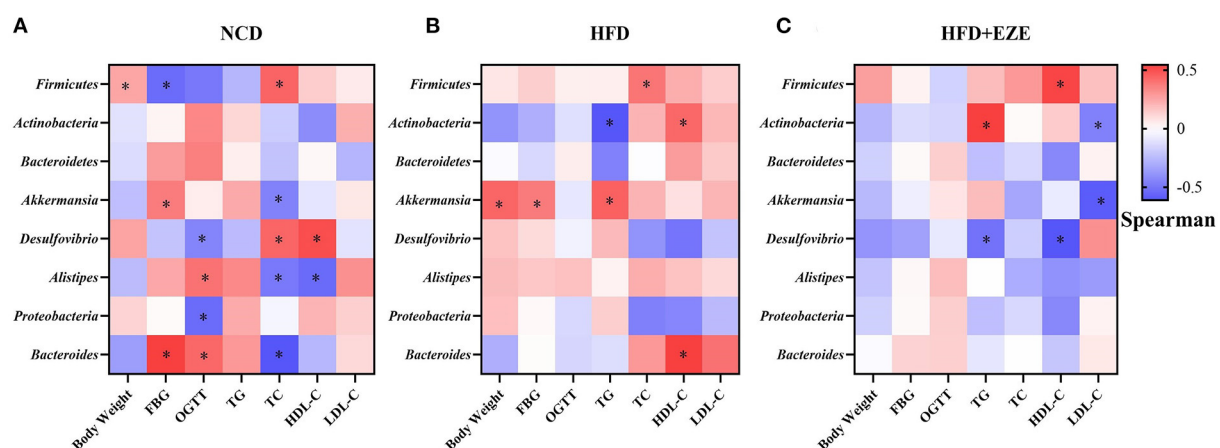


**FIGURE 8**  
Correlations between ezetimibe responsive core microbes and phenotypes. **(A)** Heatmap of the correlations between ezetimibe responsive core microbes and phenotypes in the NCD group. **(B)** Heatmap of the correlations between ezetimibe responsive core microbes and phenotypes in the HFD group. **(C)** Heatmap of the correlations between ezetimibe responsive core microbes and phenotypes in the HFD+EZE group. \*Indicated that the correlations were statistically significant. Blue indicated the negative correlations, while red indicated the positive correlations. FBG, fasting blood glucose; OGTT, oral glucose tolerance test; TG, Triglyceride; TC, total cholesterol; LDL-C, low-density lipoprotein-cholesterol; HDL-C, high-density lipoprotein-cholesterol.

a variety of physiologic processes or excreted in feces (de la Cuesta-Zuluaga et al., 2018). Several western epidemiological studies have found that the concentration of total SCFAs and SCFAs of several subtypes in feces are positively correlated with the prevalence of obesity (Schwartz et al., 2010; Patil et al., 2012; Teixeira et al., 2013; Fernandes et al., 2014; Rahat-Rozenbloom et al., 2014; de la Cuesta-Zuluaga et al., 2018). On the contrary,

in animal experiments, it was found that an HFD reduced the concentration of AA in feces (Yamamura et al., 2021). In this study, we found that the concentration of SCFA of various subtypes of the tested mice in the HFD group decreased. In light of the previous studies, the results of this study demonstrated again that the fecal SCFAs could be deeply involved in obesity, and the decreased fecal SCFAs might be one of the important

pathological features of diet-induced obesity. The decrease in fecal SCFAs may be related to the decrease in the abundance of SCFAs-producing bacteria in the intestine. Bacterial species belonging to the genera *Bacteroides* and *Prevotella* produce acetate and propionate (Koh et al., 2016). The decrease in AA content may be caused by the decrease in the abundance of *Prevotella* and *Akkermansia muciniphila* in this study.

In this study, orlistat significantly reduced the weight gain of mice induced by HFD, significantly reduced the serum TC and HDL-C levels, and improved dyslipidemia. In addition, orlistat also reduced blood glucose and glucose tolerance and improved metabolic disorders in mice. Moreover, the level of adiponectin in the mice of the high-fat diet group was increased, and orlistat decreased the level of adiponectin. Our previous study also found that a high-fat diet can increase serum adiponectin levels in obese mice (Kang et al., 2021). We inferred that this may result from the significant increase in visceral fat caused by the long-term high-fat diet in this study, thereby secreting more adipokine, such as adiponectin. However, the orlistat intervention reversed the abnormal increase in adiponectin levels, which might be a negative feedback phenomenon caused by the significantly reduced visceral fat. These results were well consistent with the previous studies in which orlistat has been demonstrated to exhibit significant anti-obesity effects clinically. One of the key underlying mechanisms is by inhibiting the absorption of dietary fat. However, whether the anti-obesity effects of orlistat are related to the gut microbiota and its metabolites is unclear.

In the Xenical in the Prevention of Diabetes in Obese Subjects Study, a longitudinal study of patients using orlistat, the mean weight loss from baseline was significantly greater with orlistat (5.8 kg) than with placebo (3.0 kg) after 4 years of treatment (Torgerson et al., 2004). In addition, orlistat also decreased blood lipid levels (Son and Kim, 2020). Singh et al. conducted a meta-analysis of all randomized controlled trials  $\geq 1$  year with five anti-obesity drugs and found that orlistat significantly reduced body weight (Singh and Singh, 2020). *Firmicutes*, *Bacteroides*, and *Actinobacteria* have been documented to be associated with obesity (Ke et al., 2020). HFD consumption is linked with a decrease in *Bacteroidetes*, which exerts immunomodulatory effects on the host, and a higher abundance of *Firmicutes*, which plays a role in energy resorption and obesity (Everard et al., 2014). Other studies have demonstrated a higher abundance of *Actinobacteria* in obese subjects (Turnbaugh et al., 2009). Therefore, orlistat reduced the body weight of obese mice, which may be related to the accumulation of dietary fat in the colon and reduced the abundance of *Firmicutes*. However, no significant effect on *Bacteroides* and *Actinomycetes* was found in this study.

In this study, the microbial diversity, dominant bacteria, and fecal SCFAs were altered after orlistat intervention. These results were consistent with Ke et al. who performed an orlistat intervention study in obese mice (Ke et al., 2020). In this

study, some bacterial populations and alpha-diversity were modified by orlistat, presenting as increased *Firmicutes* and *Akkermansia* and a reduction of the  $\alpha$ -diversity index, and decreased *Desulfovibrio* and *Alistipes*. The  $\alpha$ -diversity index reflects the richness and uniformity of the gut microbiota, and the microbial diversity was normally negatively related to the disease occurrence in adulthood. In our previous population study, we found that overweight and obese individuals in Xinjiang had significantly lower alpha-diversity levels of the gut microbiota (Jin et al., 2021). Our results showed that HFD consumption caused significantly decreased microbial diversity and richness, and orlistat treatment further reduced it. This may be due to the fact that the high triglyceride environment in the gut caused by orlistat use is not conducive to the growth of certain gut microbes, which further reduces the alpha-diversity of gut microbiota. Murphy et al. found a greater abundance of *Desulfovibrio* (species) in people who subsequently had diabetes (Murphy et al., 2017). Besides, in a metagenome-wide association study, sulfate-reducing *Desulfovibrio* species were more prevalent in the gut microbiota of Chinese people with T2DM (Qin et al., 2012). *A. muciniphila* is a promising candidate among the next-generation beneficial microbes that have been identified. Indeed, *A. muciniphila* is inversely associated with obesity, diabetes, cardiometabolic diseases, and low-grade inflammation (Cani and de Vos, 2017). In the present study, *Akkermansia* was negatively correlated with FBG after the intervention of orlistat, which indicated *Akkermansia* may be related to the hypoglycemic effect of orlistat. *Alistipes* is a relatively new genus that belongs to the phylum *Bacteroidetes*, which is highly relevant in dysbiosis and disease (Parker et al., 2020). This study found that *Alistipes* decreased after orlistat intervention, the abundance of which was negatively correlated with obesity, lipid, and glucose homeostasis parameters (Garcia-Ribera et al., 2020). Another population study also found that the abundance of *Alistipes* was negatively correlated with body mass index (Lv et al., 2019). In the present study, we found that *Alistipes* was negatively correlated with TC and HDL-C levels in the NCD group and positively correlated with HDL-C levels after the intervention of orlistat. Studies have shown that *Alistipes* is related to certain diseases, such as anxiety, myalgic encephalomyelitis/chronic fatigue syndrome, depression, pervasive developmental disorder not otherwise specified, and colorectal cancer. In contrast, in terms of pathogenicity, it was believed that their presence is correlated with the promotion of healthy phenotypes, such as colitis, autism spectrum disorder, and various liver and cardiovascular fibrotic disorders (Parker et al., 2020).

The BA bacteria are distributed in the colon and cecum, mainly *Firmicutes*, including *Fusobacterium*, *Eubacterium*, *Clostridium*, and *Roseburia* (Louis and Flint, 2009). Although the relative abundance of *Firmicutes* decreased after orlistat intervention, *Firmicutes* are still the main bacteria in this study. Besides, this study found that *Clostridium sensu stricto* and

*Clostridium XI* significantly increased after orlistat intervention. Moreover, *Clostridium XI* has been found to be negatively correlated with body weight and TC after orlistat intervention. This result indicated that *Clostridium XI* might be a keystone that is associated with the hypolipidemic efficacy of orlistat, which implies that the depletion of this genera might facilitate orlistat to improve lipid metabolism and obesity. A large number of phylogenetic studies based on the 16S rRNA gene sequencing indicated that *Clostridium* should be restricted to *Clostridium I* as the narrow sense *Clostridium* (*Clostridium sensu stricto*) (Galperin et al., 2016). *Clostridium sensu stricto* is sufficiently close to the type species *Clostridium butyricum* (Lawson and Rainey, 2016). Pan et al. found that supplementation with *C. butyricum* can restore the gut microbiota composition and enhance butyrate production in feces (Pan et al., 2021). *Clostridium XI* is the phylogenetic cluster containing *Clostridium difficile* and is considered a harmful bacterium in the intestine. In this study, *Clostridium XI* and *Clostridium sensu stricto* may be the most important factors in increasing BA. Moreover, *Desulfovibrio* has been confirmed to have acetate and butyrate as metabolites (Dubinski et al., 2021). The changes in BA-producing bacteria in this study were complex, manifested as an increase in *Clostridium XI* and *Clostridium sensu stricto* and a decrease in *Desulfovibrio*, *Clostridium XIVa*, and *Clostridium XVIII*, which ultimately led to an increase in BA in feces. Studies have found that AA and lactic acid can be used by BA-producing bacteria to produce BA (Louis et al., 2004). At the same time, the increase in *Akkermansia* and *Escherichia/Shigella* did not cause an increase in acetate in feces, which may also be one of the reasons for the increase in BA. In this study, the increase in AA and CA may result from the combined effects of the gut microbiota, mainly the increase of *Clostridium XI* and *Clostridium sensu stricto*, which still needs further research.

Ezetimibe is a selective intestinal cholesterol absorption inhibitor that acts on the brush border of the small intestinal mucosa, specifically binds to the Niemann-Pick C1-like 1 transporter on the intestinal mucosa, and selectively inhibits the absorption of exogenous cholesterol (Law et al., 2003). In a pilot study, Akira Kurozumi et al. investigated the effects of postprandial lipid abnormalities induced by HFD loading on vascular endothelial function in T2DM and evaluated the effects of ezetimibe on endothelial function. This study found that ezetimibe can potentially inhibit the aggravation of vascular endothelial dysfunction by improving dyslipidemia after HFD loading (Kurozumi et al., 2016). Ezetimibe restored the postprandial dysregulation of lipids but did not affect glucose metabolism in a double-blind randomized crossover trial (Kikuchi et al., 2012). Consistently, in this study, TC and HDL-C levels were decreased by ezetimibe, but TG levels showed no significant difference in obese mice, which were different from the results of other studies (Pandor et al., 2009). However, after ezetimibe intervention, this study did not find a significant difference in body weight, visceral fat, insulin,

adiponectin, leptin, blood glucose, and OGTT. Robert Krysiak et al. showed that 14-day ezetimibe treatment induces relatively small changes in fat tissue hormonal function in patients with isolated hypercholesterolemia (Krysiak et al., 2014). In addition, one study showed that 14-day treatment with ezetimibe did not alter circulating adiponectin, resistin, or leptin levels in healthy men (Gouni-Berthold et al., 2008).

One study showed that the gut microbiota could shift the host's cholesterol absorption/synthesis balance (Le Roy et al., 2019). In this study, the  $\alpha$ -diversity and predominant bacteria were altered by ezetimibe, showing that the relative abundance of some low-abundance bacteria changed. Similar results were obtained with orlistat intervention, that is, *Desulfovibrio* decreased after ezetimibe intervention, and *Desulfovibrio* was negatively correlated with TG and HDL-C levels after ezetimibe intervention. Almada Caroline et al. found that inactivated probiotics caused a decrease in the abundance of *Bacteroides* (Almada et al., 2021). This study found a higher abundance of *Bacteroides*, which was negatively correlated with the expression levels of serum miR-122-5p that was found to be significantly enriched in glucose metabolism-related signaling pathways (Li et al., 2020). An experiment on obese rats induced by HFD and treated with diabetes drugs found that berberine can increase the *Bacteroides* content, a class of putative SCFA-producing bacteria (Zhang et al., 2015). However, there was no significant difference in SCFAs, in accordance with the findings of human research (Jin et al., 2021). Besides, this study did not find significant effects of ezetimibe on body weight and accumulation of visceral fat, blood glucose, insulin, leptin, and adiponectin. This is probably because ezetimibe only caused a few low-abundance bacterial changes and had little apparent effects on mouse glucose and lipid metabolism, but only affected the cholesterol metabolism pathway. A recent study found that an HFD promoted the flourishing of *Proteobacteria* (Chang et al., 2017). In addition, a group of patients with diabetic cardiovascular complications and a group of T2DM patients had a significant increase in the proportion of *Proteobacteria* (Larsen et al., 2010). In this study, ezetimibe decreased *Proteobacteria*, which was not significantly different from the NCD group. Another study found that intestinal epithelial cells (IECs) responded to infection by activating Srebp2 and the cholesterol biosynthetic pathway, resulting in higher fecal cholesterol levels and a bloom of *Proteobacteria* (Berger et al., 2017). This may be related to the high-cholesterol environment in the intestine. The negative feedback regulation of a large amount of cholesterol accumulation in the intestine inhibited IEC activation of cholesterol synthesis, inhibited *Proteobacteria* proliferation, and reduced the serum cholesterol content.

In conclusion, the 20-week HFD intervention caused a typical obesity phenotype, damaged gut microbiota, and decreased SCFA production. Orlistat and ezetimibe intervention could characteristically alleviate the weight gain, serum TC, HDL-C, and dyslipidemia induced by

HFD. These different anti-obesity effects might, at least partly, result from their different abilities to reduce the phylum *Firmicutes* and increase SCFA-producing bacteria, eventually leading to an increase in the gut BA content. The enhanced anti-obesity effects of orlistat might result from its stronger ability to alter gut microbiota and SCFAs, at least partly. However, some specific drug-related microorganisms potentially related to glucose and lipid metabolism need to be further studied.

## Limitation

The limitation of this work lies in the data analysis approach. The data analysis uses QIIME instead of QIIME2. No one is maintaining QIIME to ensure the validity of results.

## Data availability statement

The data presented in the study are deposited in the Sequenced Read Archive (SRA) repository, accession number (PRJNA816265).

## Ethics statement

The animal study was reviewed and approved by Experimental Animal Center, West China Second Hospital, Sichuan University.

## Author contributions

HT, FH, JJ, RC, and JW designed the study. JW and JJ performed the experiments, analyzed the data, and drafted the manuscript. RC, XS, ZM, YL, QZ, YR, and YX participated in partial experiments and data collection process. FH, RC, and JW

revised the manuscript. All authors reviewed the manuscript. All authors agreed to have two corresponding authors.

## Funding

This work was supported by the Basic and clinical research of endocrine and metabolic diseases, big data, translational medicine, and precision medicine (Grant Number: ZYGD18022).

## Acknowledgments

The authors would like to thank Chengdu Basebio Biotechnology Co., Ltd. for providing assistance on bioinformatics analysis and Enago (<http://www.enago.jp>) for the English language review. We also appreciate the support of the Public Health and Preventive Medicine Provincial Experiment Teaching Center at Sichuan University and the Food Safety Monitoring and Risk Assessment Key Laboratory of Sichuan Province.

## Conflict of interest

The authors declare that the research was conducted in the absence of any commercial or financial relationships that could be construed as a potential conflict of interest.

## Publisher's note

All claims expressed in this article are solely those of the authors and do not necessarily represent those of their affiliated organizations, or those of the publisher, the editors and the reviewers. Any product that may be evaluated in this article, or claim that may be made by its manufacturer, is not guaranteed or endorsed by the publisher.

## References

- Almada, C. N., Almada-Érix, C. N., Costa, W. K. A., Graça, J. S., Cabral, L., Noronha, M. F., et al. (2021). Wheat-durum pasta added of inactivated *Bifidobacterium animalis* decreases glucose and total cholesterol levels and modulates gut microbiota in healthy rats. *Int. J. Food. Sci. Nutr.* 72, 781–793. doi: 10.1080/09637486.2021.1877261
- Berger, C. N., Crepin, V. F., Roumeliotis, T. I., Wright, J. C., Carson, D., Pevsner-Fischer, M., et al. (2017). *Citrobacter rodentium* Subverts ATP Flux and Cholesterol Homeostasis in Intestinal Epithelial Cells In Vivo. *Cell Metab.* 26, 738–752.e736. doi: 10.1016/j.cmet.2017.09.003
- Bian, Y., Lei, J., Zhong, J., Wang, B., Wan, Y., Li, J., et al. (2022). Kaempferol reduces obesity, prevents intestinal inflammation, and modulates gut microbiota in high-fat diet mice. *J. Nutr. Biochem.* 99, 108840. doi: 10.1016/j.jnutbio.2021.108840
- Cani, P. D., and de Vos, W. M. (2017). Next-Generation Beneficial Microbes: The Case of *Akkermansia muciniphila*. *Front. Microbiol.* 8, 1765. doi: 10.3389/fmicb.2017.01765
- Chang, C. J., Lin, C. S., Lu, C. C., Martel, J., Ko, Y. F., Ojcius, D. M., et al. (2017). Corrigendum: *Ganoderma lucidum* reduces obesity in mice by modulating the composition of the gut microbiota. *Nat. Commun.* 8, 16130. doi: 10.1038/ncomms16130
- Cox, L. M., and Blaser, M. J. (2013). Pathways in microbe-induced obesity. *Cell Metab.* 17, 883–894. doi: 10.1016/j.cmet.2013.05.004
- de la Cuesta-Zuluaga, J., Mueller, N.T., Álvarez-Quintero, R., Velásquez-Mejía, E.P., Sierra, J.A., Corrales-Agudelo, V., et al. (2018). Higher Fecal Short-Chain Fatty Acid Levels Are Associated with Gut Microbiome Dysbiosis, Obesity,



Hypertension and Cardiometabolic Disease Risk Factors. *Nutrients* 11, 51. doi: 10.3390/nu11010051

Dubinski, P., Czarzasta, K., and Cudnoch-Jedrzejewska, A. (2021). The influence of gut microbiota on the cardiovascular system under conditions of obesity and chronic stress. *Curr. Hypertens. Rep.* 23, 31. doi: 10.1007/s11906-021-01144-7

Everard, A., Lazarevic, V., Gaia, N., Johansson, M., Ståhlman, M., Backhed, F., et al. (2014). Microbiome of prebiotic-treated mice reveals novel targets involved in host response during obesity. *Isme J.* 8, 2116–2130. doi: 10.1038/ismej.2014.45

Fan, Y., and Pedersen, O. (2021). Gut microbiota in human metabolic health and disease. *Nat. Rev. Microbiol.* 19, 55–71. doi: 10.1038/s41579-020-0433-9

Fei, N., and Zhao, L. (2013). An opportunistic pathogen isolated from the gut of an obese human causes obesity in germfree mice. *Isme J.* 7, 880–884. doi: 10.1038/ismej.2012.153

Fernandes, J., Su, W., Rahat-Rozenbloom, S., Wolever, T. M., and Comelli, E. M. (2014). Adiposity, gut microbiota and faecal short chain fatty acids are linked in adult humans. *Nutr. Diabetes* 4, e121. doi: 10.1038/nutd.2014.23

Galperin, M. Y., Brover, V., Tolstoy, I., and Yutin, N. (2016). Phylogenomic analysis of the family Peptostreptococcaceae (Clostridium cluster XI) and proposal for reclassification of Clostridium litorale (Fendrich et al. 1991) and Eubacterium acidaminophilum (Zindel et al. 1989) as Peptoclostridium litorale gen. nov. comb. nov. and Peptoclostridium acidaminophilum comb. nov. *Int. J. Syst. Evol. Microbiol.* 66, 5506–5513. doi: 10.1099/ijsem.0.001548

Garcia-Ribera, S., Amat-Bou, M., Climent, E., Llobet, M., Chenoll, E., Corripio, R., et al. (2020). Specific dietary components and gut microbiota composition are associated with obesity in children and adolescents with Prader-Willi Syndrome. *Nutrients* 12, 1063. doi: 10.3390/nu12041063

Gouni-Berthold, I., Berthold, H. K., Chamberland, J. P., Krone, W., and Mantzoros, C. S. (2008). Short-term treatment with ezetimibe, simvastatin or their combination does not alter circulating adiponectin, resistin or leptin levels in healthy men. *Clin. Endocrinol. (Oxf)* 68, 536–541. doi: 10.1111/j.1365-2265.2007.03080.x

Hoffman, D. J., Powell, T. L., Barrett, E. S., and Hardy, D. B. (2021). Developmental origins of metabolic diseases. *Physiol. Rev.* 101, 739–795. doi: 10.1152/physrev.00002.2020

Hussain, A., Mahawar, K., Xia, Z., Yang, W., and El-Hasani, S. (2020). Obesity and mortality of COVID-19. Meta-analysis. *Obes. Res. Clin. Pract.* 14, 295–300. doi: 10.1016/j.orcp.2020.07.002

Jin, J., Cheng, R., Ren, Y., Shen, X., Wang, J., Xue, Y., et al. (2021). Distinctive gut microbiota in patients with overweight and obesity with dyslipidemia and its responses to long-term orlistat and ezetimibe intervention: a randomized controlled open-label trial. *Front. Pharmacol.* 12, 732541. doi: 10.3389/fphar.2021.732541

Kang, X., Liang, H., Luo, Y., Li, Z., He, F., Han, X., et al. (2021). Anti-adipogenesis and metabolism-regulating effects of heat-inactivated Streptococcus thermophilus MN-ZLW-002. *Lett. Appl. Microbiol.* 72, 677–687. doi: 10.1111/lam.13398

Ke, J., An, Y., Cao, B., Lang, J., Wu, N., Zhao, D., et al. (2020). Orlistat-Induced Gut Microbiota Modification in Obese Mice. *Evid. Based Complement Altern. Med.* 2020, 9818349. doi: 10.1155/2020/9818349

Kikuchi, K., Nezu, U., Inazumi, K., Miyazaki, T., Ono, K., Orime, K., et al. (2012). Double-blind randomized clinical trial of the effects of ezetimibe on postprandial hyperlipidaemia and hyperglycaemia. *J. Atheroscler. Thromb.* 19, 1093–1101. doi: 10.5551/jat.12427

Klünemann, M., Andrejev, S., Blasche, S., Mateus, A., Phapale, P., Devendran, S., et al. (2021). Bioaccumulation of therapeutic drugs by human gut bacteria. *Nature* 597, 533–538. doi: 10.1038/s41586-021-03891-8

Koh, A., De Vadder, F., Kovatcheva-Datchary, P., and Backhed, F. (2016). From dietary fiber to host physiology: short-chain fatty acids as key bacterial metabolites. *Cell* 165, 1332–1345. doi: 10.1016/j.cell.2016.05.041

Kosoglou, T., Statkevich, P., Johnson-Levonas, A. O., Paolini, J. F., Bergman, A. J., Alton, K. B., et al. (2005). Ezetimibe: a review of its metabolism, pharmacokinetics and drug interactions. *Clin. Pharmacokinet* 44, 467–494. doi: 10.2165/00003088-200544050-00002

Krysiak, R., Zmuda, W., and Okopień, B. (2014). The effect of ezetimibe on adipose tissue hormones in patients with isolated hypercholesterolemia. *Pharmacol. Rep.* 66, 442–447. doi: 10.1016/j.pharep.2014.03.006

Kurozumi, A., Okada, Y., Mori, H., Kobayashi, T., Masuda, D., Yamashita, S., et al. (2016). Detrimental effects of high-fat diet loading on vascular endothelial function and therapeutic efficacy of ezetimibe and statins in patients with type 2 diabetes. *Endocr. J.* 63, 431–440. doi: 10.1507/endocrj.EJ15-0623

Larsen, N., Vogensen, F. K., van den Berg, F. W., Nielsen, D. S., Andreasen, A. S., Pedersen, B. K., et al. (2010). Gut microbiota in human adults

with type 2 diabetes differs from non-diabetic adults. *PLoS ONE* 5, e9085. doi: 10.1371/journal.pone.0009085

Law, M. R., Wald, N. J., and Rudnicka, A. R. (2003). Quantifying effect of statins on low density lipoprotein cholesterol, ischaemic heart disease, and stroke: systematic review and meta-analysis. *BMJ.* 326, 1423. doi: 10.1136/bmj.326.7404.1423

Lawson, P. A., and Rainey, F. A. (2016). Proposal to restrict the genus Clostridium Prazmowski to Clostridium butyricum and related species. *Int. J. Syst. Evol. Microbiol.* 66, 1009–1016. doi: 10.1099/ijsem.0.000824

Le Roy, T., Lécuyer, E., Chassaing, B., Rhimi, M., Lhomme, M., Boudebouze, S., et al. (2019). The intestinal microbiota regulates host cholesterol homeostasis. *BMC Biol.* 17, 94. doi: 10.1186/s12915-019-0715-8

Ley, R. E., Backhed, F., Turnbaugh, P., Lozupone, C. A., Knight, R. D., Gordon, J. I., et al. (2005). Obesity alters gut microbial ecology. *Proc. Natl. Acad. Sci. U.S.A.* 102, 11070–11075. doi: 10.1073/pnas.0504978102

Li, L., Li, C., Lv, M., Hu, Q., Guo, L., Xiong, D., et al. (2020). Correlation between alterations of gut microbiota and miR-122-5p expression in patients with type 2 diabetes mellitus. *Ann. Transl. Med.* 8, 1481. doi: 10.21037/atm-20-6717

Liang, H., Jiang, F., Cheng, R., Luo, Y., Wang, J., Luo, Z., et al. (2021). A high-fat diet and high-fat and high-cholesterol diet may affect glucose and lipid metabolism differentially through gut microbiota in mice. *Exp. Anim.* 70, 73–83. doi: 10.1538/expanim.20-0094

López-Moreno, A., Suárez, A., Avanzi, C., Monteoliva-Sánchez, M., and Aguilera, M. (2020). Probiotic strains and intervention total doses for modulating obesity-related microbiota dysbiosis: a systematic review and meta-analysis. *Nutrients* 12, 1921. doi: 10.3390/nu12071921

Louis, P., Duncan, S. H., McCrae, S. I., Millar, J., Jackson, M. S., Flint, H. J., et al. (2004). Restricted distribution of the butyrate kinase pathway among butyrate-producing bacteria from the human colon. *J. Bacteriol.* 186, 2099–2106. doi: 10.1128/JB.186.7.2099-2106.2004

Louis, P., and Flint, H. J. (2009). Diversity, metabolism and microbial ecology of butyrate-producing bacteria from the human large intestine. *FEMS Microbiol. Lett.* 294, 1–8. doi: 10.1111/j.1574-6968.2009.01514.x

Lv, Y., Qin, X., Jia, H., Chen, S., Sun, W., Wang, X., et al. (2019). The association between gut microbiota composition and BMI in Chinese male college students, as analysed by next-generation sequencing. *Br. J. Nutr.* 122, 986–995. doi: 10.1017/S0007114519001909

Lynch, S. V., and Pedersen, O. (2016). The Human Intestinal Microbiome in Health and Disease. *N. Engl. J. Med.* 375, 2369–2379. doi: 10.1056/NEJMra1600266

Magne, F., Gotteland, M., Gauthier, L., Zazueta, A., Pesoa, S., Navarrete, P., et al. (2020). The firmicutes/bacteroidetes ratio: a relevant marker of gut dysbiosis in obese patients? *Nutrients* 12, 1474. doi: 10.3390/nu12051474

Mayoral, L. P., Andrade, G. M., Mayoral, E. P., Huerta, T. H., Canseco, S. P., Rodal Canales, F. J., et al. (2020). Obesity subtypes, related biomarkers and heterogeneity. *Indian J. Med. Res.* 151, 11–21. doi: 10.4103/ijmr.IJMR\_1768\_17

Milano, W., De Biasio, V., Di Munzio, W., Foggia, G., and Capasso, A. (2020). Obesity: the new global epidemic pharmacological treatment, opportunities and limits for personalized therapy. *Endocr. Metab. Immune Disord. Drug Targets* 20, 1232–1243. doi: 10.2174/1871530320666200515112853

Murphy, R., Tsai, P., Jüllig, M., Liu, A., Plank, L., Booth, M., et al. (2017). Differential changes in gut microbiota after gastric bypass and sleeve gastrectomy bariatric surgery vary according to diabetes remission. *Obes. Surg* 27, 917–925. doi: 10.1007/s11695-016-2399-2

Pan, Y., Zheng, X., and Xiang, Y. (2021). Structure-function elucidation of a microbial consortium in degrading rice straw and producing acetic and butyric acids via metagenome combining 16S rDNA sequencing. *Bioresour. Technol.* 340, 125709. doi: 10.1016/j.biortech.2021.125709

Pandor, A., Ara, R. M., Tumor, I., Wilkinson, A. J., Paisley, S., Duenas, A., et al. (2009). Ezetimibe monotherapy for cholesterol lowering in 2,722 people: systematic review and meta-analysis of randomized controlled trials. *J. Intern. Med.* 265, 568–580. doi: 10.1111/j.1365-2796.2008.02062.x

Parker, B. J., Wearsch, P. A., Veloo, A. C. M., and Rodriguez-Palacios, A. (2020). The genus alistipes: gut bacteria with emerging implications to inflammation, cancer, and mental health. *Front. Immunol.* 11, 906. doi: 10.3389/fimmu.2020.00906

Patil, D. P., Dhotre, D. P., Chavan, S. G., Sultan, A., Jain, D. S., Lanjekar, V. B., et al. (2012). Molecular analysis of gut microbiota in obesity among Indian individuals. *J. BioSci.* 37, 647–657. doi: 10.1007/s12038-012-9244-0

Qin, J., Li, Y., Cai, Z., Li, S., Zhu, J., Zhang, F., et al. (2012). A metagenome-wide association study of gut microbiota in type 2 diabetes. *Nature* 490, 55–60. doi: 10.1038/nature11450

- Rahat-Rozenbloom, S., Fernandes, J., Gloor, G. B., and Wolever, T. M. (2014). Evidence for greater production of colonic short-chain fatty acids in overweight than lean humans. *Int. J. Obes. (Lond.)* 38, 1525–1531. doi: 10.1038/ijo.2014.46
- Rooks, M. G., Veiga, P., Wardwell-Scott, L. H., Tickle, T., Segata, N., Michaud, M., et al. (2014). Gut microbiome composition and function in experimental colitis during active disease and treatment-induced remission. *Isme J.* 8, 1403–1417. doi: 10.1038/ismej.2014.3
- Scheithauer, T. P. M., Rampanelli, E., Nieuwdorp, M., Vallance, B. A., Verchere, C. B., van Raalte, D. H., et al. (2020). Gut Microbiota as a Trigger for Metabolic Inflammation in Obesity and Type 2 Diabetes. *Front. Immunol.* 11, 571731. doi: 10.3389/fimmu.2020.571731
- Schwiertz, A., Taras, D., Schäfer, K., Beijer, S., Bos, N. A., Donus, C., et al. (2010). Microbiota and SCFA in lean and overweight healthy subjects. *Obesity (Silver Spring)* 18, 190–195. doi: 10.1038/oby.2009.167
- Sergeev, I. N., Aljutaily, T., Walton, G., and Huarte, E. (2020). Effects of synbiotic supplement on human gut microbiota, body composition and weight loss in obesity. *Nutrients* 12, 222. doi: 10.3390/nu12010222
- Shapiro, H., Suez, J., and Elinav, E. (2017). Personalized microbiome-based approaches to metabolic syndrome management and prevention. *J. Diabetes* 9, 226–236. doi: 10.1111/1753-0407.12501
- Singh, A. K., and Singh, R. (2020). Pharmacotherapy in obesity: a systematic review and meta-analysis of randomized controlled trials of anti-obesity drugs. *Expert Rev. Clin. Pharmacol.* 13, 53–64. doi: 10.1080/17512433.2020.1698291
- Son, J. W., and Kim, S. (2020). Comprehensive review of current and upcoming anti-obesity drugs. *Diabetes Metab. J.* 44, 802–818. doi: 10.4093/dmj.2020.0258
- Tak, Y. J., and Lee, S. Y. (2021). Long-term efficacy and safety of anti-obesity treatment: where do we stand? *Curr. Obes. Rep.* 10, 14–30. doi: 10.1007/s13679-020-00422-w
- Teixeira, T. F., Grześkowiak, Ł., Franceschini, S. C., Bressan, J., Ferreira, C. L., Peluzio, M. C., et al. (2013). Higher level of faecal SCFA in women correlates with metabolic syndrome risk factors. *Br. J. Nutr.* 109, 914–919. doi: 10.1017/S0007114512002723
- Torgerson, J. S., Hauptman, J., Boldrin, M. N., and Sjöström, L. (2004). XENical in the prevention of diabetes in obese subjects (XENDOS) study: a randomized study of orlistat as an adjunct to lifestyle changes for the prevention of type 2 diabetes in obese patients. *Diabetes Care* 27, 155–161. doi: 10.2337/diacare.27.1.155
- Turnbaugh, P. J., Hamady, M., Yatsunenko, T., Cantarel, B. L., Duncan, A., Ley, R. E., et al. (2009). A core gut microbiome in obese and lean twins. *Nature* 457, 480–484. doi: 10.1038/nature07540
- Turnbaugh, P. J., Ley, R. E., Mahowald, M. A., Magrini, V., Mardis, E. R., Gordon, J. I., et al. (2006). An obesity-associated gut microbiome with increased capacity for energy harvest. *Nature* 444, 1027–1031. doi: 10.1038/nature05414
- Voigt, R. M., Forsyth, C. B., Green, S. J., Mutlu, E., Engen, P., Vitaterna, M. H., et al. (2014). Circadian disorganization alters intestinal microbiota. *PLoS ONE* 9, e97500. doi: 10.1371/journal.pone.0097500
- Yamamura, R., Nakamura, K., Ukawa, S., Okada, E., Nakagawa, T., Imae, A., et al. (2021). Fecal short-chain fatty acids and obesity in a community-based Japanese population: the DOSANCO Health Study. *Obes. Res. Clin. Pract.* 15, 345–350. doi: 10.1016/j.orcp.2021.06.003
- Yu, E. W., Gao, L., Stastka, P., Cheney, M. C., Mahabamunuge, J., TorRes. Soto, M., et al. (2020). Fecal microbiota transplantation for the improvement of metabolism in obesity: The FMT-TRIM double-blind placebo-controlled pilot trial. *PLoS Med.* 17, e1003051. doi: 10.1371/journal.pmed.1003051
- Zhang, X., Zhao, Y., Xu, J., Xue, Z., Zhang, M., Pang, X., et al. (2015). Modulation of gut microbiota by berberine and metformin during the treatment of high-fat diet-induced obesity in rats. *Sci. Rep.* 5, 14405. doi: 10.1038/srep14405
- Zhou, Y., Tian, S., Qian, L., Jiang, S., Tang, Y., Han, T., et al. (2021). DHA-enriched phosphatidylserine ameliorates non-alcoholic fatty liver disease and intestinal dysbacteriosis in mice induced by a high-fat diet. *Food Funct.* 12, 4021–4033. doi: 10.1039/D0FO03471A
- Zimmermann, M., Zimmermann-Kogadeeva, M., Wegmann, R., and Goodman, A. L. (2019). Separating host and microbiome contributions to drug pharmacokinetics and toxicity. *Science* 363. doi: 10.1126/science.aat9931



## OPEN ACCESS

## EDITED BY

Gulnaz T. Javan,  
Alabama State University, United States

## REVIEWED BY

Courtnee Bell,  
Alabama State University, United States  
Jonathan J. Parrott,  
Arizona State University West Campus,  
United States

## \*CORRESPONDENCE

Yubin Luo  
luoyubin2016@163.com  
Yi Liu  
yi2006liu@163.com

†These authors have contributed  
equally to this work

## SPECIALTY SECTION

This article was submitted to  
Microbial Symbioses,  
a section of the journal  
Frontiers in Microbiology

RECEIVED 10 June 2022

ACCEPTED 12 August 2022

PUBLISHED 02 September 2022



## CITATION

Huang T, Pu Y, Wang X, Li Y, Yang H,  
Luo Y and Liu Y (2022) Metabolomic  
analysis in spondyloarthritis:  
A systematic review.  
*Front. Microbiol.* 13:965709.  
doi: 10.3389/fmicb.2022.965709

## COPYRIGHT

© 2022 Huang, Pu, Wang, Li, Yang, Luo  
and Liu. This is an open-access article  
distributed under the terms of the  
[Creative Commons Attribution License  
\(CC BY\)](https://creativecommons.org/licenses/by/4.0/). The use, distribution or  
reproduction in other forums is  
permitted, provided the original  
author(s) and the copyright owner(s)  
are credited and that the original  
publication in this journal is cited, in  
accordance with accepted academic  
practice. No use, distribution or  
reproduction is permitted which does  
not comply with these terms.

# Metabolomic analysis in spondyloarthritis: A systematic review

Tianwen Huang<sup>1,2,3†</sup>, Yaoyu Pu<sup>1,2,3†</sup>, Xiangpeng Wang<sup>1,2,3</sup>,  
Yanhong Li<sup>1,2,3</sup>, Hang Yang<sup>1,2,3</sup>, Yubin Luo <sup>1,2,3\*</sup> and  
Yi Liu <sup>1,2,3\*</sup>

<sup>1</sup>Department of Rheumatology and Immunology, West China Hospital, Sichuan University, Chengdu, China, <sup>2</sup>Rare Diseases Center, West China Hospital, Sichuan University, Chengdu, China, <sup>3</sup>Institute of Immunology and Inflammation, Frontiers Science Center for Disease Related Molecular Network, West China Hospital, Chengdu, China

Spondyloarthritis (SpA) is a group of rheumatic diseases that cause joint inflammation. Accumulating studies have focused on the metabolomic profiling of SpA in recent years. We conducted a systematic review to provide a collective summary of previous findings on metabolomic profiling associated with SpA. We systematically searched PubMed, Medline, Embase and Web of Science for studies on comparisons of the metabolomic analysis of SpA patients and non-SpA controls. The Newcastle–Ottawa Scale (NOS) was used to assess the quality of the included articles. From 482 records identified, 31 studies were included in the analysis. A number of metabolites were differentially distributed between SpA and non-SpA cases. SpA patients showed higher levels of glucose, succinic acid, malic acid and lactate in carbohydrate metabolism, higher glycerol levels and lower fatty acid (especially unsaturated fatty acid) levels in lipid metabolism, and lower levels of tryptophan and glutamine in amino acid metabolism than healthy controls. Both conventional and biological therapy of SpA can insufficiently reverse the aberrant metabolism state toward that of the controls. However, the differences in the results of metabolic profiling between patients with SpA and other inflammatory diseases as well as among patients with several subtypes of SpA are inconsistent across studies. Studies on metabolomics have provided insights into etiological factors and biomarkers for SpA. Supplementation with the metabolites that exhibit decreased levels, such as short-chain fatty acids (SCFAs), has good treatment prospects for modulating immunity. Further studies are needed to elucidate the role of disordered metabolic molecules in the pathogenesis of SpA.

## KEYWORDS

spondyloarthritis, ankylosing spondylitis, metabolomics, biomarkers, dysbiosis

## Introduction

Spondyloarthritis (SpA) is a group of several related but phenotypically distinct disorders, including ankylosing spondylitis (AS), psoriatic arthritis (PsA), inflammatory bowel disease-associated SpA (IBD-SpA), reactive arthritis (ReA), juvenile idiopathic arthritis (JIA), enthesitis-related arthritis (ERA), and undifferentiated SpA (uSpA) (Taurog et al., 2016). According to the location of the joint involved, SpA can also be classified as either axial (axSpA) or peripheral (pSpA). This rheumatic disease mainly affects the back, pelvis, neck and some larger joints and manifests as pain, stiffness and fatigue. During the past decades, progress has been made in exploring the pathogenesis of SpA, genetic risk associations, HLA-B27-mediated pathology and the contribution of the type 3 immune response (Ranganathan et al., 2017). However, much remains to be fully elucidated. Moreover, although abundant evidence has proven that gut dysbiosis is common in SpA, especially AS (Yin et al., 2020; Zhou C. et al., 2020; Chen et al., 2021), the mechanisms mediating the crosstalk between the intestinal lumen and the immune system are still not completely defined.

Developments in molecular biology, along with the emergence of various new-omics techniques, have provided powerful tools for the advancement of etiological studies on SpA. Metabolomics is the large-scale study of small molecules, commonly known as metabolites, which directly reflect the underlying biochemical activity and state of cells/tissues. By the use of high-throughput techniques, metabolomics can be used not only to identify promising novel biomarkers but also to provide insights into etiology, leading to the development of therapeutic targets (Johnson et al., 2016; Wishart, 2016). In recent years, an increasing number of studies have been conducted to investigate the broad network of metabolites in SpA using various human biological samples, including serum, plasma, tissue, urine and feces (Gao et al., 2008; Fischer et al., 2012; Jiang et al., 2013; Zeft et al., 2014; Chen et al., 2015; Shao et al., 2016; Stoll et al., 2016; Butbul et al., 2020; Vernocchi et al., 2020; Funk and Becker, 2021). However, some studies have inconsistent results or even the opposite results. This may be caused by different standards for collecting samples and different measurement and analysis methods. Further analysis is needed.

Here, we conducted a systematic review of studies on metabolomics analysis of patients with SpA, aiming to summarize previous findings on the differences in the metabolic profiles between SpA and non-SpA participants, the dynamic alteration of metabolites in SpA before and after treatment and the differences among SpA subtypes. Furthermore, we discuss possible mechanisms by which altered metabolites are involved in the pathogenesis of SpA.

## Methods

This systematic review was registered with the International Prospective Register of Systematic Reviews (PROSPERO) database (registration no. CRD42022314657).

### Search strategy

This study was conducted following the recommendations of the Preferred Reporting Items for Systematic Reviews and Meta-Analyses Guidelines (PRISMA) (Moher et al., 2009). Published studies were retrieved after a literature search including the following 4 electronic databases: PubMed, Medline (ovidsp), Embase (ovidsp) and Web of Science. The literature search was performed in January 2022 (date of last search: January 3rd, 2022). The search strategy is shown in **Supplementary Table 1**. To ensure literature saturation, the reference lists of included studies or relevant reviews identified through the search were reviewed manually by 2 independent reviewers.

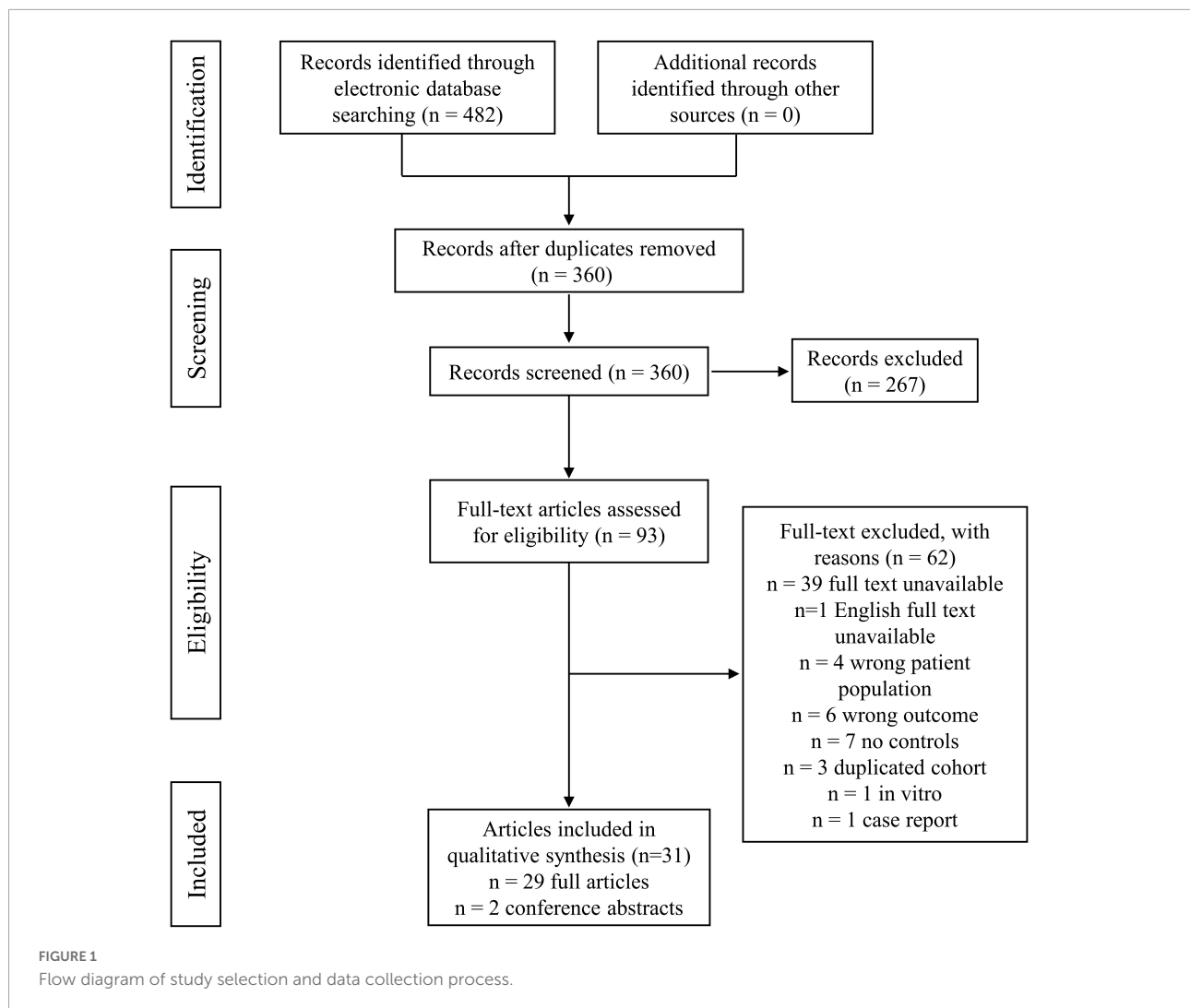
### Inclusion/exclusion criteria

The inclusion criteria were as follows: studies comparing the metabolomic profiling of human biological specimens from SpA patients to those of controls. We included SpA or any of the following subtypes: axSpA, pSpA, AS, PsA, IBD-SpA, JIA, ERA, ReA, and uSpA. No restrictions in terms of patient population age, disease stage or geographical location or publication dates of studies were applied. Whenever full-text articles were unavailable, abstracts were included if considered critically relevant. The exclusion criteria were as follows: (1) reviews, guidelines or editorials; (2) animal studies or *in vitro* studies; (3) studies using irrelevant omics techniques, such as transcriptomic and proteomics; and (4) studies in which cases only contained SpA patients without controls.

### Study selection and data collection process

Two reviewers independently screened the search results by title and abstract to determine which records were possibly eligible for inclusion in the systematic review. Subsequently, the full texts of all studies that potentially met the eligibility criteria were carefully assessed for final inclusion. Discrepancies in the final decision between reviewers were resolved by a reassessment performed by a third reviewer. The reasons for excluding studies were recorded. The data collected included the following: (1) publication information, including name of first author, year of publication and study geographic location; (2) patient





demographics and characteristics close to the time of specimen collection, including age, sex, Bath Ankylosing Spondylitis Disease Activity Index (BASDAI), Ankylosing Spondylitis Disease Activity Score (ASDAS), C-reactive protein (CRP), erythrocyte sedimentation rate (ESR), and disease duration; (3) type of specimen; (4) methods used for metabolite identification and analysis; and (5) differentially distributed metabolites across comparison groups and alterations in major metabolic pathways associated with SpA.

## Quality assessment

The quality of the included studies was evaluated using the Newcastle–Ottawa Scale (NOS) (Wells et al., 2013), which is one of the most commonly used tools for quality assessments of non-randomized studies in systematic reviews. This scale consists of three domains, including the selection of the study groups, the comparability of the groups and the

ascertainment of either the exposure or outcome of interest for case–control or cohort studies, respectively. Two well-trained authors applied NOS independently, and the discrepancies were resolved by discussion.

## Results

### Study selection and characteristics

The search results and the selection strategy are shown in Figure 1. Briefly, of the 482 records resulting from the initial electronic database search, 31 studies were finally included after rigorous screening according to the inclusion and exclusion criteria. The characteristics of the selected studies are summarized in Table 1. These studies included 1,176 SpA patients and 1,357 control participants. In the total 31 studies, 29 studies were original articles available as full text, while the other

TABLE 1 Characteristics of studies included in the systematic review.

Study	Region	Sample type	Analytical technique	SpA group							Control group		
				Subtype (No.)	Male/female	Age (yr)	Disease duration (yr)	CRP (mg/L)	ESR (mm/h)	BASDAI	Control (No.)	Male/ female	Age (yr)
SpA													
Berlinberg et al. (2021)	United States	Colon biopsies	LC-MS	axSpA (21) CD-axSpA (12)	axSpA 11/10 CD-axSpA 5/7	axSpA 44.9 ± 12.1 CD-axSpA 51.4 ± 11.1	axSpA 9.9 ± 9.8 CD-axSpA 11.9 ± 8.0	NR	NR	axSpA 4.8 ± 2.4 CD-axSpA 5.1 ± 2.2	HC (24) CD (27)	HC 12/12 CD 14/13	HC 45.2 ± 11.8 CD 35.1 ± 18.1
Gupta et al. (2021)	India	Serum	<sup>1</sup> H NMR	SpA (81)	71/10	31.0 (23.0, 39.5)	6.0 (3.0, 12.0)	31.7 (4.3, 68.0)	60.0 (30.5, 92.5)	4.6 (2.6, 5.8)	HC (87)	72/14	32.2 ± 6.0
AS													
Gao et al. (2008)	China	Plasma	LC-MS and GC-MS	AS (15)	15/0	20.5 (7.0, 50.0)	At least 6 months	NR	NR	NR	HC (24)	Match with SpA groups	Match with SpA groups
Fischer et al. (2012)	United Kingdom	Serum	LC-MS	AS (18)	17/1	39.9 ± 12.8	NR	32.7 ± 37.3	42.0 ± 24.5	6.8 ± 1.9	HC (9)	8/1	40.9 ± 11.4
Jiang et al. (2013)	China	Serum	GC-TOF MS and UPLC-QTOF MS	AS (27)	27/0	31.0 (18.0, 55.0)	NR	13.9 ± 23.9	34.7 ± 26.2	NR	RA (27) OA (27) Gout (33) HC (60)	RA 0/27 OA 0/27 Gout 33/0 HC 30/30	RA 53.0 (40.0, 68.0) OA 58.0 (39.0, 73.0) Gout 51.0 (30.0, 69.0) HC 34.0 (25.0, 74.0)
Chen et al. (2015)	China	Serum	GC-MS	AS (33)	22/11	30.9 ± 7.8	At least 6 months	NR	NR	NR	HC (33)	19/14	33.9 ± 8.5
Shao et al. (2016)	China	Feces	<sup>1</sup> H NMR	AS (40)	24/16	34.0 ± 9.6	NR	7.6 ± 5.2	12.1 ± 8.7	NR	HC (34) RA (35)	HC 19/15 RA 10/25	HC 31.6 ± 10.2 RA 39.8 ± 7.9
Wang et al. (2016)	China	Plasma, Urine, ligament tissue	<sup>1</sup> H NMR	AS 44	38/6	31.8 ± 10.9	6.8 ± 3.5	NR	NR	3.2 ± 1.8	HC (44)	38/6	33.8 ± 9.7

(Continued)

TABLE 1 (Continued)

Study	Region	Sample type	Analytical technique	SpA group							Control group		
				Subtype (No.)	Male/female Age (yr)		Disease duration (yr)	CRP (mg/L)	ESR (mm/h)	BASDAI	Control (No.)	Male/female	Age (yr)
He et al. (2019)	China	Feces	GC-MS	AS (49)	26/23	43.0 ± 9.6	NR	8.7 ± 5.2	13.6 ± 8.7	3.7 ± 2.1	HC (38)	20/18	43.1 ± 8.5
Zhou Y. et al. (2020)	China	Serum	UPLC-TQ-MS	AS (30)	20/10	34.0 (24.0, 46.0)	NR	19.9 ± 12.6	49.4 ± 23.1	NR	HC (30) RA (32)	HC 16/14 RA 14/18	HC 47.0 (21.0, 52.0) RA 44.0 (32.0, 60.0)
Bogunia-Kubik et al. (2021)	Poland	Serum	<sup>1</sup> H NMR	AS (29) PsA (23)	AS 22/7 PsA 14/9	AS 45.0 (26.0, 75.0) PsA 43.0 (29.0, 71.0)	AS 11.0 (1.0, 40.0) PsA 8.0 (2.0, 41.0)			AS 8.2 (5.7, 10.0) PsA 8.0 (6.0, 9.0)	RA (26)	5/21	55.0 (23.0, 74.0)
Eryavuz Onmaz et al. (2021)	Turkey	Serum	LC-MS	AS (85)	55/30	40.1 ± 9.4;	NR;	12.7 (3.0, 89.1);	20.7 (4.6, 103.5);	5.1 ± 1.1;	HC (50)	27/23	41.6 ± 6.8
lv et al. (2021)	China	Saliva	GC-MS	AS 37	24/13	33.9 ± 1.9	14.5 (3.0, 59.8) months	7.1 (1.8, 15.8)	16.4 ± 2.7	3.1 (2.1, 3.9)	HC (41)	27/14	33.3 ± 1.7
Onmaz et al. (2021)	Turkey	Serum	LC-MS	AS 60	38/22	42.1 ± 8.1	9.7 ± 7.8	5.7 (1.4, 50.7)	14.5 (2.0, 60.0)	4.9 ± 1.7	HC (60)	35/25	42.9 ± 8.5
Ou et al. (2021)	China	Serum	LC-MS	AS 32	29/3	28.6 ± 7.5	94.3 ± 48.8 months	21.1 (12.4, 44.0)	29.5 (12.5, 46.5)	6.9 ± 2.0	HC (40)	37/3	27.1 ± 5.6

(Continued)

TABLE 1 (Continued)

Study	Region	Sample type	Analytical technique	SpA group							Control group		
				Subtype (No.)	Male/female	Age (yr)	Disease duration (yr)	CRP (mg/L)	ESR (mm/h)	BASDAI	Control (No.)	Male/ female	Age (yr)
PsA													
Madsen et al. (2010)	Sweden	Plasma	LC-MS and GC-MS	PsA (20)	10/10	48.0 ± 12.0	15.0 ± 12.0	NR	NR	NR	RA (25)	9/16	51.1 ± 17.8
Kapoor et al. (2013)	United Kingdom	Urine	<sup>1</sup> H NMR	PsA (20)	10/10	NR	NR	NR	NR	NR	Baseline vs. 12 weeks after TNFi therapy		
Armstrong et al. (2014)	United States	Serum	GC-TOF MS	PsA (10)	5/5	15.0 ± 13.6	7.9 ± 6.8	NR	NR	NR	HC (10)	5/5	46.0 ± 15.0
Nanus et al. (2015)	United Kingdom	Urine	GC-MS	PsA (20)	10/10	48.0 ± 12.0	At least 6 months	14.2 ± 17.2	NR	NR	Baseline vs. 12 weeks after TNFi therapy		
Souto-Carneiro et al. (2020)	Germany	Serum	<sup>1</sup> H NMR	PsA (73)	44/29	56.2 (30.0, 78.0)	9.0 (0, 24)	6.7 ± 13.8	NR	NR	negRA (49)	10/39	64.2 (32.0, 83.0)
Rocha et al. (2021)	Spain	Synovium	MALDI-MSI	PsA 12	6/6	52.0 ± 13.0	NR	1.2 ± 1.8	NR	NR	OA (13)	2/11	73.0 ± 11.0
JIA													
Zeft et al. (2014)	United States	Exhaled breath	SIFT-MS	JIA (21)	NR	(5.0, 21.0)	NR	NR	NR	NR	HC (55)	NR	(5.0, 21.0)
Stoll et al. (2016)	United States	Feces	LC-MS	JIA/ERA (24)	12/12	14.0 (7.0, 17.0)	NR	NR	NR	NR	HC (19)	7/12	11.0 (7.0, 18.0)
Butbul et al. (2020)	Israel	Urine	GC-MS	JIA (11)	3/8	12.0 ± 6.2	6.3 ± 5.2	NR	NR	NR	HC (11)	Match with SpA groups	Match with SpA groups

(Continued)



TABLE 1 (Continued)

Study	Region	Sample type	Analytical technique	SpA group							Control group		
				Subtype (No.)	Male/female	Age (yr)	Disease duration (yr)	CRP (mg/L)	ESR (mm/h)	BASDAI	Control (No.)	Male/female	Age (yr)
Vernocchi et al. (2020)	Italy	Feces	GC-MS and <sup>1</sup> H NMR	JIA (60)	16/44	7.0 ± 4.1	<6 months	1.4 ± 1.6	24.6 ± 20.4	NR	HC (25)	11/14	9.8 ± 2.9
Funk and Becker (2021)	United States	Plasma	GC-TOF-MS; Q-TOF-MS	JIA (30)	9/21	9.5 (5.0, 15.0)	NR	1.5 (0.5, 3.2)	16.0	NR	Baseline vs. 3 months after MTX therapy		
Ahmed et al. (2019)	India	Serum, synovial fluid	<sup>1</sup> H NMR	ReA (19) uSpA (13)	ReA 12/7	26.0	NR	NR	NR	NR	HC (18)	17/1	29.0
Guleria et al. (2019)	India	Serum	<sup>1</sup> H NMR	ReA (52)	44/8	29.0 ± 10.9	NR	7.4 ± 7.8	77.8 ± 37.6	NR	HC (82) RA (29)	HC 57/25 RA 2/27	HC 36.4 ± 9.3 RA 40.1 ± 11.8
Li et al. (2019)	United Kingdom	Serum, synovial fluid	LC-MS	ReA (7)	7/0	25.0 ± 4.3	9.0 ± 4.4 weeks	12.1 ± 15.9	9.8 ± 11.7	NR	HC (23) RA (20)	HC 9/14 RA 6/14	HC 48.0 ± 15.1 RA 54.1 ± 17.1
<b>ReA</b>													
Muhammed et al. (2020)	India	Serum, synovial fluid	<sup>1</sup> H NMR	ReA/uSpA (30) ReA (19) uSpA (11)	24/6	27.9 ± 9.1	NR	NR	NR	NR	RA (25) OA (21)	RA 5/20 OA 5/16	RA 41.5 ± 12.6 OA 59.8 ± 8.2
Dubey et al. (2021)	India	Synovial fluid	<sup>1</sup> H NMR	ReA (58)	49/9	29.1 ± 10.9	NR	NR	NR	NR	RA (21) OA (20)	RA 4/27 OA 4/16	RA 45.8 ± 12.6 OA 59.5 ± 8.3

This systematic review included 31 studies, in which a total of 1,176 SpA patients and 1,357 control participants were included. Among these studies, 13 studies included AS patients, 7 studies included PsA patients, 5 studies included JIA patients, 5 studies included ReA patients, 2 studies included uSpA patients, 1 study included ERA patients, 1 study included IBD-SpA and 1 study enrolled cases with mixed subtypes of SpA without describing a specific subtype. Descriptive statistics are presented as [mean ± SD or median (range)].

LC-MS, liquid chromatography-mass spectrometry; <sup>1</sup>H NMR, proton nuclear magnetic resonance; GC-MS, gas chromatography-mass spectrometry; GC-TOF MS, gas chromatography time-of-flight mass spectrometry; UPLC-QTOF MS, ultra-high performance liquid chromatography-triple quadrupole mass spectrometry; UPLC-TQ-MS, ultra-performance liquid chromatography coupled with triple-quadrupole tandem mass spectrometry; MALDI-MSI, matrix-assisted laser desorption/ionization mass spectrometry imaging; SIFT-MS, selected ion flow tube mass spectrometry; Q-TOF-MS, quadrupole time-of-flight mass spectrometry; SpA, spondyloarthritis; axSpA, axial SpA; CD-axSpA, Crohn's-axSpA; AS, ankylosing spondylitis; PsA, psoriatic arthritis; JIA, juvenile idiopathic arthritis; ReA, reactive arthritis; uSpA, undifferentiated SpA; HC, healthy control; RA, rheumatoid arthritis; negRA, seronegative RA; OA, osteoarthritis; CD, Crohn's disease; yr, year; BASDAI, Bath Ankylosing Spondylitis Disease Activity Index; TNFi, TNF-alpha inhibitors; NR, not reported.

2 studies (Zeft et al., 2014; Butbul et al., 2020) were conference abstracts. 22 of 31 studies conducted metabolomics comparisons between SpA cases and healthy controls. 12 of 31 studies compared SpA cases with cases of other rheumatic diseases, such as rheumatoid arthritis (RA), osteoarthritis (OA) and gout. 7 studies analyzed the dynamic alterations in metabolic profiles in SpA patients before and after treatment (Gao et al., 2008; Kapoor et al., 2013; Nanus et al., 2015; Butbul et al., 2020; Bogunia-Kubik et al., 2021; Funk and Becker, 2021; Gupta et al., 2021; Ou et al., 2021). Regarding the metabolomic analysis in different subtypes of SpA, 13 studies included AS patients (Gao et al., 2008; Fischer et al., 2012; Jiang et al., 2013; Chen et al., 2015; Shao et al., 2016; Wang et al., 2016; He et al., 2019; Zhou Y. et al., 2020; Bogunia-Kubik et al., 2021; Eryavuz Onmaz et al., 2021; Lv et al., 2021; Onmaz et al., 2021; Ou et al., 2021). 7 studies included PsA patients (Madsen et al., 2010; Kapoor et al., 2013; Armstrong et al., 2014; Nanus et al., 2015; Souto-Carneiro et al., 2020; Bogunia-Kubik et al., 2021; Rocha et al., 2021). 5 studies included JIA patients (Zeft et al., 2014; Stoll et al., 2016; Butbul et al., 2020; Vernocchi et al., 2020; Funk and Becker, 2021). 5 studies included ReA patients (Ahmed et al., 2019; Guleria et al., 2019; Li et al., 2019; Muhammed et al., 2020; Dubey et al., 2021). 2 studies included uSpA patients (Ahmed et al., 2019; Muhammed et al., 2020), 1 study included ERA patients (Stoll et al., 2016), 1 study included IBD-SpA (Berlinberg et al., 2021). 1 study enrolled cases with mixed subtypes of SpA without describing a specific subtype (Gupta et al., 2021). Only 3 studies compared different metabolic profiles among different subtypes of SpA (Ahmed et al., 2019; Bogunia-Kubik et al., 2021; Gupta et al., 2021).

Biospecimens from different sources of tissues in SpA patients were applied for metabolic profiling and analysis. Nineteen studies assessed the metabolome by serum/plasma. Feces (Shao et al., 2016; Stoll et al., 2016; He et al., 2019; Vernocchi et al., 2020), urine (Kapoor et al., 2013; Nanus et al., 2015; Wang et al., 2016; Butbul et al., 2020), and synovial fluid (Ahmed et al., 2019; Li et al., 2019; Muhammed et al., 2020; Dubey et al., 2021) were commonly studied in these metabolomic researches. In addition, tissues such as ligament tissue (Wang et al., 2016), colon biopsies (Berlinberg et al., 2021), synovial membrane tissue (Rocha et al., 2021), saliva (Lv et al., 2021), and exhaled breath (Zeft et al., 2014) were also used for analysis in 1 study each. Depending on the characteristics of different tissues, metabolites were profiled by different platforms and methods. Most enrolled studies used proton nuclear magnetic resonance ( $^1\text{H}$  NMR), liquid chromatography–mass spectrometry (LC–MS), and gas chromatography–mass spectrometry (GC–MS). Zeft et al. (2014) used selected ion flow tube mass spectrometry (SIFT-MS) for testing exhaled breath. Rocha et al. (2021) used matrix-assisted laser desorption ionization-mass spectrometry imaging (MALDI-MSI) for testing synovial membrane samples.

The results of the methodologic quality assessment by the NOS tool are summarized in **Supplementary Table 2**. The included studies had relatively good methodological quality. The definition and selection method for SpA cases were illustrated adequately in most studies. Nevertheless, control participants were explained only in one-third of cases. 18 of 31 studies showed fully comparable data between SpA patients and controls regarding the comparability of essential factors, such as sex and age. Data from 7 studies showed less comparison. Different distributions of both sex and age were observed in 6 studies, which might contribute to the risk of bias. The rate of unidentified metabolites for any reason in both groups was similar in all studies.

## Differences in metabolic profiling between spondyloarthritis patients and healthy controls

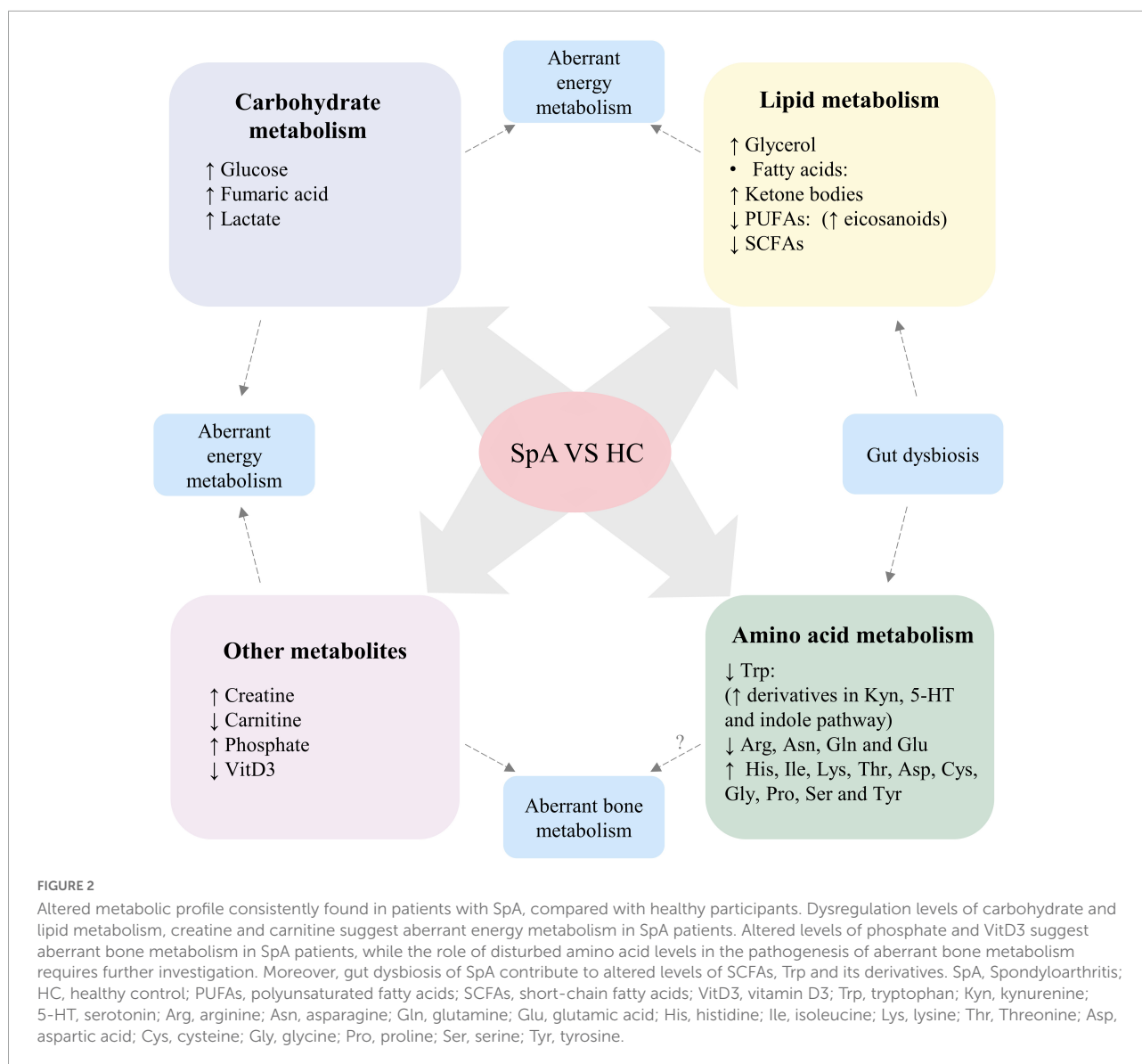
Compared with healthy controls, distinct alterations of metabolic profiles, including metabolites involved in carbohydrate metabolism, lipid metabolism and amino acid metabolism, were found in patients with SpA (**Figure 2**).

### Carbohydrate metabolism

Several studies consistently revealed that levels of metabolites involved in glycolysis and the tricarboxylic acid cycle (TCA cycle) were increased, such as glucose, glyceraldehyde, succinic acid, fumaric acid, and malic acid (Gao et al., 2008; Jiang et al., 2013; Shao et al., 2016; Ahmed et al., 2019; Guleria et al., 2019; Stahly et al., 2019; Lv et al., 2021; Onmaz et al., 2021). Two studies including patients with ReA showed decreased levels of pyruvate in serum (Ahmed et al., 2019; Guleria et al., 2019). Levels of lactate, an anaerobic oxidation product of glucose, were found to be elevated in the serum of SpA patients and positively correlated with disease activity (Gupta et al., 2021). In addition, upregulation of the levels of some products of carbohydrate metabolism, including mannose, glucuronic acid, gluconic acid, and propanedioic acid, were found in the serum and feces of SpA patients (Armstrong et al., 2014; Ahmed et al., 2019; He et al., 2019). Interestingly, Lewis et al. (2020) concluded that there was a positive correlation between pain and sugar intake in teens with active JIA, indicating the perturbation of carbohydrate metabolism in SpA.

### Lipid metabolism

Lipid dysregulation was a common finding in most metabolomic studies of SpA, but these results were not consistent across studies. Two studies both reported elevated levels of glycerol in the serum of AS patients (Gao et al., 2008; Wang et al., 2016). Triglyceride levels were found to be increased in serum by Onmaz et al. (2021). Another analysis conducted



by Wang et al. (2016) revealed downregulated levels in plasma and conversely upregulated levels in ligament tissue. One study conducted by Onmaz et al. (2021) showed elevated cholesterol levels in the serum of AS patients. He et al. (2019) showed lower levels of cholesterol in male AS patients than in healthy males by utilizing feces. Regarding lipoproteins, two studies independently indicated both decreased levels of low-density lipoprotein (LDL) and very low-density lipoprotein (VLDL) in serum (Guleria et al., 2019; Gupta et al., 2021). Onmaz et al. (2021) found upregulated levels of LDL and downregulated levels of high-density lipoprotein (HDL) in serum.

Fatty acids can be divided into saturated fatty acids and unsaturated fatty acids according to whether the hydrocarbon chain is saturated. Short-chain fatty acids (SCFAs) constitute an important part of saturated fatty acids because of their

indispensable function in regulating the normal physiological functions of the body. Commonly altered SCFAs found in metabolomic studies include acetate, propionate, and butyrate. Two studies found increased acetate levels in the serum of SpA patients (Guleria et al., 2019; Gupta et al., 2021), while three studies found decreased acetate, propionate and butyrate levels in urine and feces (Shao et al., 2016; Wang et al., 2016; He et al., 2019). Moreover, levels of unsaturated fatty acids, especially polyunsaturated fatty acids (PUFAs), were consistently found to be decreased both in serum and colon tissue in four studies (Chen et al., 2015; Guleria et al., 2019; Berlinberg et al., 2021; Gupta et al., 2021). Ketone bodies, including acetoacetate, acetone and  $\beta$ -hydroxybutyrate, are intermediate metabolites of fatty acids during decomposition and oxidation in the liver. The levels of  $\beta$ -hydroxybutyrate and acetoacetate were consistently

found to be increased in serum and saliva (Wang et al., 2016; Glaser et al., 2017; Ahmed et al., 2019; Guleria et al., 2019; Lv et al., 2021). However, the results of acetone were inconsistent in different studies. Studies including AS patients (Wang et al., 2016) and ReA patients (Ahmed et al., 2019) reported higher levels of acetone in patients compared with healthy control. Nevertheless, some other studies, including SpA patients (Gupta et al., 2021) and ReA patients (Guleria et al., 2019), reported lower levels of acetone than those in healthy controls.

Carnitine is an important molecule in lipid metabolism. Acetyl-L-carnitine, derived from carnitine, also plays an important role in fatty acid metabolism by facilitating the movement of acetyl-CoA into the matrices of mammalian mitochondria during the oxidation of fatty acids. Two studies including AS cases reported decreased levels of carnitine and acetyl-L-carnitine (Jiang et al., 2013; Zhou Y. et al., 2020), while one study found the converse results in JIA patients (Kiykim et al., 2015).

### Amino acid metabolism

Perturbation of amino acid metabolism is also common in SpA and was reported in nearly half of the enrolled studies. Overall, the levels of ten amino acids, including histidine, isoleucine, lysine, threonine, aspartic acid, cysteine, glycine, proline, serine, and tyrosine, were found to be higher than those in healthy controls, regardless of sample type. Conversely, the levels of five amino acids: tryptophan, arginine, asparagine, glutamine, and glutamic acid, were found to be decreased. Inconsistent findings across studies were reported for other amino acids (Shao et al., 2016; Wang et al., 2016; Glaser et al., 2017; Zhou Y. et al., 2020; Gupta et al., 2021). Downregulation of phenylalanine (Shao et al., 2016; Zhou Y. et al., 2020), valine (Shao et al., 2016; Wang et al., 2016) and alanine (Wang et al., 2016; Glaser et al., 2017) levels were reported in one-third of the studies, respectively. Downregulation of leucine (Shao et al., 2016; Wang et al., 2016) and methionine (Shao et al., 2016; Gupta et al., 2021) levels were reported in two-fifths of the studies, respectively, while the other studies reported upregulation in the levels of these amino acids (Wang et al., 2016; Guleria et al., 2019; Zhou Y. et al., 2020; Gupta et al., 2021).

Several studies also reported altered levels of the primary derivatives of amino acids in SpA patients (Shao et al., 2016; Wang et al., 2016; Husni et al., 2017; Ahmed et al., 2019; Guleria et al., 2019; Zhou Y. et al., 2020; Onmaz et al., 2021). Both Husni et al. (2017) and Onmaz et al. (2021) found elevated levels of asymmetric dimethylarginine (ADMA), symmetric dimethylarginine (SDMA) and methylated arginine. Additionally, the altered levels of arginine and its derivatives in SpA patients remained after biological or conventional therapy when compared with the levels observed in healthy controls. TNF inhibitor treatment can reverse the aberrant metabolic state and promote the development of a metabolic state that is more similar to that of the controls more efficiently than

that achieved with conventional therapy. Arginine, ornithine and citrulline are involved in the urea cycle. Consistent with the observed downregulation of arginine levels, several studies reported decreased levels of ornithine and citrulline in AS patients (Shao et al., 2016; Zhou Y. et al., 2020), whereas only one study including ReA patients found increased citrulline levels (Guleria et al., 2019), indicating the overall downregulation of the activity of the urea cycle in SpA. In addition, as a methyl group donor that functions in the normal metabolic cycle of methionine, betaine levels were found to be increased in two studies (Wang et al., 2016; Ahmed et al., 2019).

Creatine is an endogenous amino acid derivative synthesized from three amino acids: arginine, glycine and methionine. It is an important molecule for energy storage. Creatinine is the product of creatine during catabolism. Two studies consistently showed increased creatine levels as well as decreased creatinine levels in the serum of AS patients (Zhou Y. et al., 2020; Gupta et al., 2021). Similarly, another study detected decreased creatinine levels in the urine of AS patients (Wang et al., 2016). However, a higher level of creatinine was found in the serum of ReA patients (Guleria et al., 2019).

Despite the downregulation of tryptophan levels, the levels of its derivatives, which are involved in the kynurenine pathway, serotonin pathway and indole derivative pathway, were found to be elevated. Two independent studies observed upregulation of kynurenine levels in the serum of AS and JIA patients (Korte-Bouws et al., 2019; Eryavuz Onmaz et al., 2021). Eryavuz Onmaz et al. (2021) observed increased quinolinic acid levels and decreased levels of kynurenic acid and 3-hydroxykynurenine, which were more different in newly diagnosed AS groups than in therapy groups when compared with healthy controls. After examining colon biopsy tissues of axSpA patients, Berlinberg et al. (2021) showed elevated levels of indole-3-acetate (IAA), indole-3-acetaldehyde (I3Ald) and serotonin.

### Alterations in the metabolism of other molecules

Aberrant choline metabolism was observed in different subtypes of SpA, but the results are inconsistent across studies. Enrolling patients with AS, Gao et al. (2008) and Wang et al. (2016) found decreased choline levels in plasma and ligament tissue, respectively. Shao et al. (2016) found the opposite results in feces. Utilizing the serum of patients, Gupta et al. (2021) found increased choline levels in SpA. However, Guleria et al. (2019) came to the opposite conclusion in ReA.

Vitamin D3 (Vit D3) and related derivatives are essential for calcium and phosphate metabolism. The downregulations of Vit D3 and derivatives were observed in three studies (Fischer et al., 2012; Comak et al., 2013; Li et al., 2019). Additionally, one study found that the levels of Vit D3 were inversely proportional to disease activity in JIA patients (Comak et al., 2013). In addition, elevated levels of phosphate in serum were detected by Gao et al. (2008) and Armstrong et al. (2014). Taken



together, these results suggest an imbalance in bone metabolism in patients with SpA.

## Differences in metabolic profiling between spondyloarthritis patients and patients with other rheumatic diseases

The joint symptoms of SpA, especially PsA and ReA, can be similar to those observed in other rheumatic diseases, such as RA, OA, and gout, which have brought difficulties in clinical diagnosis and treatment. Hence, it is important to distinguish SpA from other types of arthritis by detecting specific biomarkers. Metabolomics studies conducted in SpA cases and non-SpA cases have found different metabolic profiles among different disease states, which could contribute to the identification of specific metabolites that exhibit alterations for the accurate diagnosis of SpA.

### Spondyloarthritis cases vs. rheumatoid arthritis cases

Overall, 10 of 12 studies conducted metabolomics comparisons between SpA and rheumatoid arthritis (RA) to identify potential biomarkers to distinguish these pathologies.

Rocha et al. (2018) found that sugar was decreased in PsA synovial tissues than in RA synovial tissues by MALDI-MSI. Conversely, elevated levels of glucose in serum were observed in ReA patients (Guleria et al., 2019). Regarding lactate, the product of anaerobic glycolysis, PsA patients showed higher levels than those observed in RA patients, while two studies showed opposite results in ReA patients (Guleria et al., 2019; Souto-Carneiro et al., 2020; Dubey et al., 2021).

Lipid profiles could be used to differentiate between PsA and RA to a large extent. Higher glycerol and cholesterol levels were found in both PsA and ReA patients than in RA patients (Madsen et al., 2010; Dubey et al., 2021). Additionally, ReA patients showed lower levels of LDL and VLDL in serum and synovial fluid (Guleria et al., 2019; Dubey et al., 2021). The level of acetate, however, was highly heterogeneous among different studies. Increases or decreases in acetate levels in PsA and ReA patients were reported (Guleria et al., 2019; Souto-Carneiro et al., 2020; Bogunia-Kubik et al., 2021; Dubey et al., 2021). Levels of PUFAs were consistently found to be increased in PsA patients (Madsen et al., 2010; Souto-Carneiro et al., 2020). In addition, lysophosphatidic acids, phospholipids and sphingolipids showed higher expression levels in PsA than in RA patients (Rocha et al., 2018). Altered levels of carnitine were also observed in PsA and ReA patients, but there were gaps in relevant data that need further assessment (Toth et al., 2019; Dubey et al., 2021).

The levels of most amino acids (alanine, arginine, asparagine, aspartic acid, glutamic acid, glycine, proline, serine, tyrosine, histidine, isoleucine, leucine, lysine, methionine,

threonine, tryptophan, and valine) were found to be higher in SpA patients than in RA patients, with the exception that lower levels of phenylalanine, cysteine and glutamine were observed in SpA patients (Madsen et al., 2010; Souto-Carneiro et al., 2020; Zhou Y. et al., 2020; Dubey et al., 2021). In addition, elevated levels of creatine were found in the serum of PsA patients, while the same trend for creatinine was found in ReA patients (Guleria et al., 2019; Souto-Carneiro et al., 2020).

Although there is no difference in total 25(OH)D3 values between ReA and RA patients, a lower level of phosphoric acid was reported in PsA patients, indicating more disturbed bone metabolism in SpA than RA patients (Madsen et al., 2010; Li et al., 2019).

### Spondyloarthritis vs. other inflammatory diseases

Lower levels of glucose, lactate and acetate and higher levels of glycerol, LDL, VLDL, and choline were found in the synovial fluid of ReA patients than in OA patients. In addition, elevated levels of amino acids, including histidine, isoleucine, phenylalanine, and glutamic acid, were found in the same study group, with the exception of reduced alanine levels (Dubey et al., 2021). Another study including PsA patients also found that the synovial membrane where inflammatory infiltrates were accompanied by elevated levels of plasmalogen and phosphatidic acids but reduced levels of phosphatidylcholines (Rocha et al., 2021).

Only one study compared the different metabolic profiles observed between AS and gout patients (Jiang et al., 2013). Succinic acid and malic acid levels were lower in the serum of AS patients. Additionally, levels of amino acids, including lysine, valine, alanine, cysteine, taurine, citrulline, and creatine, were found to be reduced (Jiang et al., 2013). Both axSpA and CD-axSpA patients showed elevated levels of IAA and I3Ald than those in Crohn's disease (CD) patients (Berlinberg et al., 2021). However, these results need further validation due to the lack of sufficient evidence.

### Dynamic alterations in the metabolic profile before and after treatment of spondyloarthritis

TNF-alpha inhibitors (TNFi) have been widely used for SpA treatment. Five of 7 enrolled studies reported dynamic alterations in metabolites after TNFi therapy in SpA (Kapoor et al., 2013; Nanus et al., 2015; Manasson et al., 2017; Butbul et al., 2020; Bogunia-Kubik et al., 2021), while the other two studies focused on the influence of conventional therapy (Funk and Becker, 2021; Gupta et al., 2021).

Kapoor et al. (2013) and Bogunia-Kubik et al. (2021) found decreased levels of isobutyrate and acetone in AS as well as decreased levels of acetate in PsA after TNFi therapy.

Elevated levels of amino acids, including histidine, leucine and phenylalanine, were also found in AS patients after therapy. Another study including PsA patients receiving TNFi therapy showed lower levels of glutamine than those observed at baseline. Additionally, the two studies both found elevated creatine and creatinine levels in SpA patients after treatment. Regarding the alteration of adrenal metabolites in SpA patients receiving TNFi therapy, Butbul et al. (2020) found that the levels of most urine adrenal metabolites in JIA patients raised to normal values as in the controls. Moreover, Nanus et al. (2015) found a decreased ratio of tetrahydrocortisol (THF + 5 $\alpha$ THF) to tetrahydrocortisone (THE) metabolites, a decreased ratio of urinary free cortisol to urinary free cortisone, and a decreased ratio of THF to 5 $\alpha$ THF in the urine of PsA patients after therapy. These results suggested that TNF- $\alpha$  is a significant regulator of adrenal metabolism, which is further involved in the pathology of SpA.

An IL-17 inhibitor (IL-17i) is another biological agent with similar efficacy to that of TNFi used for the treatment of SpA patients, especially PsA patients. Increased levels of acetate and hexanoate were observed in PsA patients in one study (Manasson et al., 2017). Additionally, acetate and hexanoate were positively correlated with Clostridiales taxa after IL-17i therapy rather than TNFi treatment. The results indicated that IL-17i might affect the metabolism of gut microbiota (Manasson et al., 2017).

Reduced levels of glucose and elevated levels of LDL, PUFAs, isoleucine, glutamic acid and glycine were found by Gupta et al. (2021) in the serum of SpA patients after conventional therapy, which partly corrected the aberrant metabolism observed in SpA patients. In addition, in the serum of JIA patients, MTX therapy reduced the level of omega-3 unsaturated fatty acids (docosahexanoic acid and linoleic acid), which are anti-inflammatory mediators (Funk and Becker, 2021).

Taken together, these data suggest that both conventional and biological therapy of SpA can reverse the aberrant metabolic state to one that is more similar to that of the controls, albeit in an insufficient way. Nevertheless, no studies have successfully identified specific metabolites that can be used to predict treatment response.

## Differences in metabolic profiling among spondyloarthritis subtypes

Although a similar pathogenesis is shared by different subtypes of SpA, the clinical features and prognosis could be different, which could be accompanied by alterations in metabolic profiling. Gupta et al. (2021) conducted differential analysis between peripheral and axial SpA and found higher levels of lactate and N-acetyl glycoproteins as well as lower levels of LDL, PUFAs, and choline in pSpA patients than in axSpA patients. Levels of amino acids, including glutamate, proline,

arginine, phenylalanine, leucine and isoleucine, were elevated in peripheral SpA, with the exception that alanine, glutamine, and histidine levels were reduced. Bogunia-Kubik et al. (2021) observed more decreased levels of creatine, lysine and acetate in the serum of PsA than in AS. These results collectively suggested distinct inflammatory states among different SpA subtypes. Inconsistently, Ahmed et al. (2019) failed to find a significant difference in the metabolic profile in both serum and synovial tissue between ReA and undifferentiated pSpA, indicating that these two subtypes could be combined into one in diagnosis with one treatment.

## Discussion

Metabolomic profiling has been increasingly applied for the comprehensive identification of the metabolic changes occurring in SpA. Here, we systematically reviewed 31 studies on the metabolomic profiling of SpA and summarized key findings on the dysregulation of major metabolic pathways (carbohydrate, lipid and amino acid metabolism) in SpA cases compared with those observed in healthy controls and/or non-SpA cases. The dynamic alteration of metabolomic profiling of SpA cases before and after treatment, as well as differences among different subtypes, were also reviewed. More detailed altered metabolic profiles between SpA cases and non-SpA cases are summarized in [Supplementary Table 3](#). To our knowledge, this is the first systematic review of metabolomic analysis in SpA.

## Metabolomics as a tool for precise diagnosis

By detecting different molecules involved in metabolism, metabolomics is widely applied as a tool for biomarker discovery. Here, based on the significantly altered metabolites that were identified, several studies have successfully established diagnostic models for differentiating patients with SpA from healthy participants or those with other inflammatory diseases with a high specificity and sensitivity (Madsen et al., 2010; Guleria et al., 2019; Souto-Carneiro et al., 2020; Ou et al., 2021). However, these results need to be further validated with larger study cohorts before they can be applied in the clinic. In addition, since researchers failed to identify specific biomarkers for predicting treatment response in SpA, more metabolomics analyses in longitudinal cohort studies are of great importance.

## Metabolomics as a tool for the exploration of pathogenesis

Moreover, because of the sensitivity of metabolomics, subtle alterations in biological pathways can be detected to provide

insight into the mechanisms of pathogenesis that underlie SpA. After comparisons with those of healthy controls, some altered metabolic patterns are similar between SpA patients and patients with other rheumatic diseases such as RA, such as increased levels of glucose and decreased levels of lipid and membrane metabolites, suggesting that these arthritides share the same mechanisms of immunoinflammatory dysregulation, while the specific metabolites found to be altered only in SpA suggest a novel pathogenesis mechanism.

### Elevated levels of anaerobic metabolism in spondyloarthritis patients

Elevated levels of glucose, succinic acid, malic acid, and lactate has been supported by abundant evidence, indicating the ineffective utilization of glucose and elevated anaerobic metabolism. The alteration of carbohydrate metabolism could lead to adenosine triphosphate (ATP) insufficiency. Partly caused by muscle breakdown from TNF- $\alpha$ -induced inflammation, an elevated level of creatine was also observed, which may play a major role in securing a continuous replenishment of the ATP pool and further lead to T-cell proliferation (Zhang et al., 2009).

### Elevated levels of lipolysis and ectopic fat deposition in spondyloarthritis

Decreased levels of fatty acids, especially unsaturated fatty acids, suggest their augmented utilization under inflammatory conditions. Fatty acids are metabolized by  $\beta$ -oxidation to meet the energy demand, which is proven by the elevated level of ketone bodies. Consistently, an *in vitro* study conducted by Xu et al. (2015) found upregulations in the levels of fatty acid  $\beta$ -oxidation-related proteins in the fibroblast-like ligament cells of AS patients. On the other hand, the demand of proinflammatory ( $\omega$ 6- PUFAs) and anti-inflammatory ( $\omega$ 3- PUFAs) mediators is increased to perpetuate the immunometabolic response. Arachidonic acid, a representative  $\omega$ 6-PUFA, is correlated with disease activity in SpA (Pompeia et al., 2003; Von Hegedus et al., 2017; Coras et al., 2019b, 2021). Conversely,  $\omega$ 3- PUFAs have been proposed to act as anti-inflammatory mediators and potentially affect innate and adaptive immune function, as well as the production of cytokines and reactive oxygen species (Gheita et al., 2012; Miles and Calder, 2012). The dysregulation of glycerol, triglyceride and lipoprotein can be attributed to their augmented utilization in repairing membranes of affected cells and organelles or their oxidative damage due to systemic inflammation (Castoldi et al., 2020). Interestingly, Wang et al. (2016) found that TG levels decreased in plasma but increased in ligament tissue, which may be a phenomenon associated with the deposition of ectopic fat. Since fat depositions at vertebral edges in spinal MRI were considered the most typical findings in SpA, aberrant lipid metabolism, ectopic fat deposition and further fat metaplasia may lead to new bone formation in the ligament

and entheses and are thus involved in the pathogenesis of SpA (Hermann et al., 2012; Maksymowych et al., 2014). In addition, choline can promote the transport and utilization of fat; thus, the dysregulation of choline observed in several studies may be related to ectopic fat deposition and alterations in lipid metabolites (Borges Haubert et al., 2015).

### Aberrant amino acid metabolism in spondyloarthritis patients

Aberrant amino acid metabolism is a common finding in metabolomics studies of SpA and may be associated with catabolic processes and tissue degradation for energy supplementation and protein synthesis. Proline, for example, is an important amino acid for protein synthesis, and its dysregulation may correlate with impairment of the citric acid cycle and inflammatory disease progression (Li et al., 2016).

Tryptophan is an essential amino acid and has an important role in the regulation of human immunity. Evidence has shown that in conditions characterized by immune system activation or inflammation, most circulating tryptophan is converted to kynurenine by indoleamine 2,3-dioxygenase 1 and 2 (IDO-1, IDO-2), thus activating the kynurenine pathway and leading to increased levels of proinflammatory cytokines and the dysregulation of kynurenine pathway metabolites (Kim and Jeon, 2018). Inflammatory conditions induce decreased levels of kynurenic acid, which has an antioxidant effect by performing its functions through G-protein-coupled receptor 35 (GPR35) and aryl hydrocarbon receptor (AhR) in peripheral tissues (Wang et al., 2021). Quinolinic acid performs its physiological functions by binding to N-methyl-D-aspartic acid (NMDA) receptors, which are expressed in osteoblasts and osteoclasts as well as in the central nervous system (Suva and Gaddy, 2016). Hence, increased quinolinic acid levels may be associated with altered bone metabolism in patients with SpA. In addition, alterations in tryptophan metabolism in SpA may influence T cells by affecting the plasticity of effector CD4 T cells by driving them away from regulatory and toward proinflammatory CD4 T-cell phenotypes (Hatton and Weaver, 2009; Mezrich et al., 2010).

Downregulation of glutamine levels may be attributed to its consumption and conversion to glutamate by inflammatory cells, such as activated macrophages (Covarrubias et al., 2015). Glutaminolysis is considered to be one of the main sources of energy for effector T cells and facilitates Th17 development (Kono et al., 2019). Previous research reported that glutaminolysis played a key role in the cell growth of fibroblast-like synoviocytes in RA (Takahashi et al., 2017), which may also be involved in SpA.

Due to the activation of protein arginine methyltransferases (PRMTs) by inflammation and oxidative stress, the levels of methylarginine derivatives (ADMA, SDMA, and L-NMMA) increased while the levels of arginine decreased. NO, which has antiatherogenic properties and inhibits platelet aggregation

and leukocyte adhesion, can be inhibited by ADMA and results in a higher risk of cardiovascular disease in SpA (Förstermann and Sessa, 2012; Zobel et al., 2017; Liu et al., 2018). Moreover, methylarginine derivatives have been shown to be related to the production of proinflammatory cytokines, such as TNF- $\alpha$  and IL-6 via the ROS/NF- $\kappa$ B-dependent pathway, thus contributing to the inflammatory process in turn (Schepers et al., 2011; Tripepi et al., 2011).

In addition, amino acids such as alanine, valine and threonine can activate the mammalian target of rapamycin (mTOR) pathway and induce aerobic glycolysis, innate immune activation and consequent cytokine production (Dutchak et al., 2018). T-cell activation in AS is also known to be mediated by the PI3K-AKT-mTOR pathway (Finlay et al., 2012; Perl, 2016).

### Gut dysbiosis and altered microbial metabolites in spondyloarthritis

The microbiome, the community of microorganisms that has coevolved with human hosts, plays a pivotal role in human health and disease. Gut dysbiosis in SpA is associated with altered microbial metabolites, which can serve as messengers for microbes to communicate with each other and engage in crosstalk with host cells, contributing to the dysregulation of the host innate immune system and the pathogenesis of SpA. SCFAs are mainly produced within the intestinal lumen by bacterial fermentation of undigested dietary carbohydrates. They are the most widely studied microbiota metabolites in autoimmune diseases (Scalise et al., 2021). By increasing intestinal wall permeability and decreasing the levels of regulatory T cells and the production of Foxp3 and IL-10, decreased levels of SCFAs appear to have a crucial role in aberrant immunoregulation (Hamer et al., 2008; Smith et al., 2013). In addition, Lucas et al. (2018) found that supplementation with SCFAs in mice could increase systemic bone density, reduce bone resorption, and reduce osteoclasts, suggesting that downregulation of SCFA levels may play an important role in the aberrant bone metabolism observed in SpA.

Tryptophan metabolism occurs principally in the intestine since IDO-1 is mainly located inside intestinal cells, while tryptophanase is exclusive to bacteria. The important effects of tryptophan and its derivatives have been discussed above. Here, combined with shotgun metagenomics, Berlinberg et al. (2021) found that the microbial community in axSpA patients exhibited lower levels of tryptophan synthesis and higher levels of tryptophan metabolism toward indoles than those observed in healthy controls and patients with CD. Indoles are absorbed across the intestinal epithelium of the host and signal through either AhR or the pregnane X receptor (PXR) to modulate host responses, including barrier and immune functions (Berlinberg et al., 2021). In addition, upregulation of AhR levels has been proven to be correlated with expansion of type 3 innate lymphoid cells (ILC3s), which

may link intestinal pathology to Th17 immunity in SpA (Blijdorp et al., 2019; Venken et al., 2019; Berlinberg et al., 2020).

Ethanol, which is the end-product of fermentation of different carbohydrates by gut microbiota, was found to be elevated in the feces of SpA patients. Shao et al. (2016), Vernocchi et al. (2020), and Bogunia-Kubik et al. (2021) demonstrated decreased ethanol levels after TNFi treatment, suggesting a correlation of gut dysbiosis and the perturbation of microbiota-derived metabolites with active inflammatory conditions in SpA. Similar results were also found for the contents of dehydrocholic acid and trimethylamine oxide (TMAO), which are both products of microbiota metabolism (Coras et al., 2019a; Funk and Becker, 2021).

In addition, by integrating 16S ribosomal DNA identification (16S rDNA) and metabolomics, Lorente et al. (2020) and Lv et al. (2021) found that salivary microbiota and metabolites of AS patients have more proinflammatory effects. Interestingly, the sequence of an HLA-B\*27:05 ligand was observed to be highly similar to the sequence of a protein from *Campylobacter*, the levels of which were found to be increased in AS saliva, partly explaining the pathogenesis of HLA-B27 in SpA.

### Other altered metabolites related to aberrant bone metabolism in spondyloarthritis

Increased activity of 11 $\beta$ -hydroxysteroid dehydrogenase 1 (11 $\beta$ -HSD1) in SpA patients after TNFi therapy was observed (Nanus et al., 2015). The results suggest that TNF- $\alpha$ , a regulator of glucocorticoid metabolism *in vivo*, could further contribute to the loss of bone mineral density in periarticular. Furthermore, recent study indicated that by activating 11 $\beta$ -HSD1, TNF- $\alpha$  could regulate dickkopf-1 protein (DKK-1), an inhibitor of the Wnt signaling pathway (Raza et al., 2010; Hardy et al., 2012).

In addition, disorders of bone metabolism are also reflected by the downregulation of VitD3 levels and the elevation of phosphate levels. Studies have revealed that the inflammatory condition of arthritis could influence vitamin D metabolism, which further dampens its role as a Th17-cell suppressor (Gracey et al., 2014; Harrison et al., 2020).

### Limitations

This systematic review has several limitations. First, the small cohort size in nearly half of the enrolled studies and bias between study groups due to different sex and age distributions may affect the credibility of the results. Second, the heterogeneity of results among studies may be attributed to differences in metabolite detection methods, sources of samples, and procedures of sample preprocessing and extraction. Lastly, the potential use of meta-analysis is limited since few quantitative data are available.



## Conclusion and prospects

In summary, metabolomics studies show distinct metabolic profiles between SpA and non-SpA participants, which creates a new road in finding diagnostic biomarkers for precise diagnosis and exploring pathogenesis.

Nevertheless, the diagnostic model established in several studies needs to be further validated in larger cohorts. Metabolomics studies in prospective follow-up SpA patients would also be advantageous in identifying metabolomics biomarkers for predicting the progression and treatment responses of SpA patients.

Modulating immunity and inflammation by the oral supplementation of metabolites with levels that are reduced in disease states, especially microbial-derived metabolites such as SCFAs, is considered a promising treatment for autoimmune diseases, including SpA (Rosser et al., 2020). Evidence that administration of butyrate and propionate in transgenic HLA-B27/β2m rats attenuates bowel inflammation has given future perspectives for its feasibility in SpA treatment (Asquith et al., 2017). These findings, however, need to be further confirmed by clinical trials.

Regarding the exploration of pathogenesis, integrating metabolomics with other technologies, such as transcriptomics, proteomics and metagenomics, may help to find potential key targets for treatment. In addition, more *in vitro* and *in vivo* studies are needed to determine the role of disordered metabolic molecules in the pathogenesis of SpA.

## Author contributions

TH, YP, and YBL contributed to the conception and design of the study. TH, XW, YHL, and HY contributed to data collection. TH, YP, and XW contributed to the interpretation of

the data. TH and YP drafted the article. YL critically revised the manuscript. All authors approved the manuscript.

## Funding

This study was supported by the National Natural Science Foundation of China (to YP, grant no. 82101616 and to YBL, grant no. 81973540), 1-3-5 Project for Disciplines of Excellence, West China Hospital, Sichuan University (to YL, grant nos. ZYGD18015 and ZYJC18003).

## Conflict of interest

The authors declare that the research was conducted in the absence of any commercial or financial relationships that could be construed as a potential conflict of interest.

## Publisher's note

All claims expressed in this article are solely those of the authors and do not necessarily represent those of their affiliated organizations, or those of the publisher, the editors and the reviewers. Any product that may be evaluated in this article, or claim that may be made by its manufacturer, is not guaranteed or endorsed by the publisher.

## Supplementary material

The Supplementary Material for this article can be found online at: <https://www.frontiersin.org/articles/10.3389/fmicb.2022.965709/full#supplementary-material>

## References

- Ahmed, S., Chowdhury, A., Chaurasia, S., Kumar, S., Singh, R., Misra, R., et al. (2019). Nuclear magnetic resonance-based metabolomics reveals similar metabolomics profiles in undifferentiated peripheral spondyloarthritis and reactive arthritis. *Int. J. Rheum. Dis.* 22, 725–733. doi: 10.1111/1756-185X.13490
- Armstrong, A. W., Wu, J., Azizi, B., Dhillon, J., Johnson, M. A., Grapov, D., et al. (2014). Metabolomics in psoriatic disease: Pilot study reveals metabolite differences in psoriasis and psoriatic arthritis. *F1000Research* 3:248. doi: 10.12688/f1000research.4709.1
- Asquith, M., Davin, S., Stauffer, P., Michell, C., Janowitz, C., Lin, P., et al. (2017). Intestinal metabolites are profoundly altered in the context of HLA-B27 expression and functionally modulate disease in a rat model of spondyloarthritis. *Arthritis Rheumatol.* 69, 1984–1995. doi: 10.1002/art.40183
- Berlinberg, A. J., Stahly, A., Kuhn, K. A., Gerich, M. E., Fennimore, B. P., Scott, F. I., et al. (2021). Multi 'omics analysis of intestinal tissue in ankylosing spondylitis identifies alterations in the tryptophan metabolism pathway. *Front. Immunol.* 12:587119. doi: 10.3389/fimmu.2021.587119
- Berlinberg, A., Lefferts, A., Regner, E., Stahly, A., and Kuhn, K. (2020). Metabolic regulation of type 3 innate lymphoid cells by intestinal bacteria-derived indoles in ankylosing spondylitis. *Arthritis Rheumatol.* 72(Suppl. 10), 3075–3076. doi: 10.1002/art.41538
- Blijdorp, I. C. J., Menegatti, S., van Mens, L. J. J., van de Sande, M. G. H., Chen, S., Hreggvidsdottir, H. S., et al. (2019). Expansion of interleukin-22- and granulocyte-macrophage colony-stimulating factor-expressing, but not interleukin-17A-expressing, group 3 innate lymphoid cells in the inflamed joints of patients with spondyloarthritis. *Arthritis Rheumatol.* 71, 392–402. doi: 10.1002/art.40736
- Bogunia-Kubik, K., Wojtowicz, W., Swierkot, J., Mielko, K. A., Qasem, B., Wielinska, J., et al. (2021). Disease differentiation and monitoring of anti-TNF treatment in rheumatoid arthritis and spondyloarthropathies. *Int. J. Mol. Sci.* 22:7389. doi: 10.3390/ijms22147389
- Borges Haubert, N. J., Marchini, J. S., Carvalho Cunha, S. F., Suen, V. M., Padovan, G. J., Jordao, A. A. J., et al. (2015). Choline and fructooligosaccharide:



Non-alcoholic fatty liver disease, cardiac fat deposition, and oxidative stress markers. *Nutr. Metab. Insights* 8, 1–6. doi: 10.4137/nmi.S24385

Butbul, Y., Keinan, A., Hartmann, M. F., Wudy, S. A., and Tiosano, D. (2020). The effect of anti-TNF on adrenal steroid metabolism in juvenile idiopathic arthritis: A steroid metabolomics approach. *Pediatr. Rheumatol.* 18(Suppl. 2):82. doi: 10.1186/s12969-020-00470-5

Castoldi, A., Monteiro, L. B., van Teijlingen Bakker, N., Sanin, D. E., Rana, N., Corrado, M., et al. (2020). Triacylglycerol synthesis enhances macrophage inflammatory function. *Nat. Commun.* 11:4107. doi: 10.1038/s41467-020-17881-3

Chen, R., Dong, D., Wang, Y., Liu, Q., Xie, W., Li, M., et al. (2015). Serum fatty acid profiles and potential biomarkers of ankylosing spondylitis determined by gas chromatography-mass spectrometry and multivariate statistical analysis. *Biomed. Chromatogr.* 29, 604–611. doi: 10.1002/bmc.3321

Chen, Z., Zheng, X., Wu, X., Wu, J., Li, X., Wei, Q., et al. (2021). Adalimumab therapy restores the gut microbiota in patients with ankylosing spondylitis. *Front. Immunol.* 12:700570. doi: 10.3389/fimmu.2021.700570

Comak, E., Koyun, M., Dogan, C. S., Uslu Gokceoglu, A., Akman, S., and Ozdem, S. (2013). Association between vitamin D deficiency and disease activity in juvenile idiopathic arthritis. *Ann. Rheum. Dis.* 71(Suppl. 3), 702. doi: 10.1136/annrheumdis-2012-eular.1135

Coras, R., Guma, M., Kavanaugh, A., Boyd, T., Huynh, D., Lagerborg, K. A., et al. (2019a). Choline metabolite, trimethylamine N-oxide (TMAO), is associated with inflammation in psoriatic arthritis. *Clin. Exp. Rheumatol.* 37, 481–484.

Coras, R., Kavanaugh, A., Boyd, T., Huynh, Q., Pedersen, B., Armando, A. M., et al. (2019b). Pro- and anti-inflammatory eicosanoids in psoriatic arthritis. *Metabolomics* 15:65. doi: 10.1007/s11306-019-1527-0

Coras, R., Kavanaugh, A., Kluzniak, A., Holt, D., Weilgosz, A., Aaron, A., et al. (2021). Differences in oxylipin profile in psoriasis versus psoriatic arthritis. *Arthritis Res. Ther.* 23:200.

Covarrubias, A. J., Aksoylar, H. I., and Horng, T. (2015). Control of macrophage metabolism and activation by mTOR and Akt signaling. *Semin. Immunol.* 27, 286–296. doi: 10.1016/j.smim.2015.08.001

Dubey, D., Kumar, S., Rawat, A., Guleria, A., Kumari, R., Ahmed, S., et al. (2021). NMR-based metabolomics revealed the underlying inflammatory pathology in reactive arthritis synovial joints. *J. Proteome Res.* 20, 5088–5102. doi: 10.1021/acs.jproteome.1c00620

Dutchak, P. A., Estill-Terpack, S. J., Plec, A. A., Zhao, X., Yang, C., Chen, J., et al. (2018). Loss of a negative regulator of mTORC1 induces aerobic glycolysis and altered fiber composition in skeletal muscle. *Cell Rep.* 23, 1907–1914. doi: 10.1016/j.celrep.2018.04.058

Eryavuz Onmaz, D., Sivrikaya, A., Abusoglu, S., Humeyra Yerlikaya, F., Unlu, A., Isik, K., et al. (2021). Altered kynurenine pathway metabolism in patients with ankylosing spondylitis. *Int. Immunopharmacol.* 99:108018. doi: 10.1016/j.intimp.2021.108018

Finlay, D. K., Rosenzweig, E., Sinclair, L. V., Feijoo-Carnero, C., Hukelmann, J. L., Rolf, J., et al. (2012). PDK1 regulation of mTOR and hypoxia-inducible factor 1 integrate metabolism and migration of CD8+ T cells. *J. Exp. Med.* 209, 2441–2453. doi: 10.1084/jem.20112607

Fischer, R., Trudgian, D. C., Wright, C., Kessler, B. M., Bowness, P., Thomas, G., et al. (2012). Discovery of candidate serum proteomic and metabolomic biomarkers in ankylosing spondylitis. *Mol. Cell. Proteomics* 11:M111.013904. doi: 10.1074/mcp.M111.013904

Förstermann, U., and Sessa, W. C. (2012). Nitric oxide synthases: Regulation and function. *Eur. Heart J.* 33, 837a–837d. doi: 10.1093/eurheartj/ehs304

Funk, R. S., and Becker, M. L. (2021). Metabolomic profiling identifies exogenous and microbiota-derived metabolites as markers of methotrexate efficacy in juvenile idiopathic arthritis. *Front. Pharmacol.* 12:768599. doi: 10.3389/fphar.2021.768599

Gao, P., Li, X., Kong, H., Yin, P., Lu, X., Xu, G., et al. (2008). Integrated GC-MS and LC-MS plasma metabolomics analysis of ankylosing spondylitis. *Analyst* 133, 1214–1220. doi: 10.1039/b807369d

Gheita, T., Kamel, S., Helmy, N., El-Laithy, N., and Monir, A. (2012). Omega-3 fatty acids in juvenile idiopathic arthritis: Effect on cytokines (IL-1 and TNF- $\alpha$ ), disease activity and response criteria. *Clin. Rheumatol.* 31, 363–366. doi: 10.1007/s10067-011-1848-5

Glaser, A. E. A., Midgley, A., Wright, H. L., Phelan, M. M., Peak, M., and Beresford, M. W. (2017). Differences of the metabolome of autoimmune diseases. *Pediatr. Rheumatol.* 15(Suppl. 2):85. doi: 10.1186/s12969-017-0185-x

Grace, E., Green, B., Yip, P., Ayearst, R., Anton, A., Lin, A., et al. (2014). The immunological basis of the sex-bias in ankylosing spondylitis: Th17 expansion is restricted to male patients and correlates with sex-related alteration in vitamin D metabolism. *Clin. Exp. Rheumatol.* 32:809.

Guleria, A., Kumar, D., Kumar, S., Chaurasia, S., Ahmed, S., Misra, R., et al. (2019). NMR-based serum metabolomics revealed distinctive metabolic patterns in reactive arthritis compared with rheumatoid arthritis. *J. Proteome Res.* 18, 130–146. doi: 10.1021/acs.jproteome.8b00439

Gupta, L., Aggarwal, A., Guleria, A., Rawat, A., and Kumar, D. (2021). NMR-based clinical metabolomics revealed distinctive serum metabolic profiles in patients with spondyloarthritis. *Magn. Reson. Chem.* 59, 85–98. doi: 10.1002/mrc.5083

Hamer, H. M., Jonkers, D., Venema, K., Vanhoutvin, S., Troost, F. J., and Brummer, R. J. (2008). Review article: The role of butyrate on colonic function. *Aliment Pharmacol. Ther.* 27, 104–119. doi: 10.1111/j.1365-2036.2007.03562.x

Hardy, R., Juarez, M., Naylor, A., Tu, J., Rabbitt, E. H., Filer, A., et al. (2012). Synovial DKK1 expression is regulated by local glucocorticoid metabolism in inflammatory arthritis. *Arthritis Res. Ther.* 14:R226. doi: 10.1186/ar4065

Harrison, S. R., Li, D., Jeffery, L. E., Raza, K., and Hewison, M. (2020). Vitamin D, autoimmune disease and rheumatoid arthritis. *Calcif Tissue Int.* 106, 58–75. doi: 10.1007/s00223-019-00577-2

Hatton, R. D., and Weaver, C. T. (2009). Duality in the Th17-Treg developmental decision. *F1000 Biol. Rep.* 1:5. doi: 10.3410/b1-5

He, Z., Wang, M., Li, H., and Wen, C. (2019). GC-MS-based fecal metabolomics reveals gender-attributed fecal signatures in ankylosing spondylitis. *Sci. Rep.* 9:3872. doi: 10.1038/s41598-019-40351-w

Hermann, K. G., Baraliakos, X., van der Heijde, D. M., Jurik, A. G., Landewé, R., Marzo-Ortega, H., et al. (2012). Descriptions of spinal MRI lesions and definition of a positive MRI of the spine in axial spondyloarthritis: A consensual approach by the ASAS/OMERACT MRI study group. *Ann. Rheum. Dis.* 71, 1278–1288. doi: 10.1136/ard.2011.150680

Husni, M. E., Rai, V., Rabanal, M. L., and Chandrasekharan, U. (2017). Increase in arginase activity and related arginine metabolites in patients with rheumatoid arthritis (RA) and psoriatic arthritis (PSA): Potential mechanisms for endothelial dysfunction. *Arthritis Rheumatol.* 69(Suppl. 10), 1583.

Jiang, M., Li, L., Niu, X., Liang, F., Wang, M., Zhan, J., et al. (2013). Serum metabolic signatures of four types of human arthritis. *J. Proteome Res.* 12, 3769–3779. doi: 10.1021/pr400415a

Johnson, C. H., Ivanisevic, J., and Siuzdak, G. (2016). Metabolomics: Beyond biomarkers and towards mechanisms. *Nat. Rev. Mol. Cell Biol.* 17, 451–459. doi: 10.1038/nrm.2016.25

Kapoor, S. R., Buckley, C. D., Raza, K., Filer, A., Fitzpatrick, M. A., Young, S. P., et al. (2013). Metabolic profiling predicts response to anti-tumor necrosis factor alpha therapy in patients with rheumatoid arthritis. *Arthritis Rheum.* 65, 1448–1456. doi: 10.1002/art.37921

Kim, Y. K., and Jeon, S. W. (2018). Neuroinflammation and the immune-kynurenine pathway in anxiety disorders. *Curr. Neuropharmacol.* 16, 574–582. doi: 10.2174/1570159x15666170913110426

Kiykim, E., Aktuglu-Zeybek, A. C., Zubarioglu, T., Cansever, M. S., Aydin, A., Barut, K., et al. (2015). Determination of free carnitine and acyl-carnitine status of patients with juvenile idiopathic arthritis. *Ann. Rheum. Dis.* 74(Suppl. 2):1235. doi: 10.1136/annrheumdis-2015-eular.4175

Kono, M., Yoshida, N., Maeda, K., Suárez-Fueyo, A., Kyttaris, V. C., and Tsokos, G. C. (2019). Glutaminase 1 inhibition reduces glycolysis and ameliorates lupus-like disease in MRL/lpr mice and experimental autoimmune encephalomyelitis. *Arthritis Rheumatol.* 71, 1869–1878. doi: 10.1002/art.41019

Korte-Bouws, G. A. H., Albers, E., Voskamp, M., Hendriksen, H., de Leeuw, L. R., Gunturkun, O., et al. (2019). Juvenile arthritis patients suffering from chronic inflammation have increased activity of both IDO and GTP-CH1 pathways but decreased BH4 efficacy: Implications for well-being, including fatigue, cognitive impairment, anxiety, and depression. *Pharmaceuticals* 12:9. doi: 10.3390/ph12010009

Lewis, K., Osier, N., Carter, P., Brooks, S., Nguyen, C., Carrasco, R., et al. (2020). Carbohydrate and sugar intake predict pain in teens with active jia disease but not in teens in remission or controls: A cross-sectional, case-control metabolomics pilot study. *Arthritis Rheumatol.* 72(Suppl. 1), 198–199. doi: 10.1002/art.41304

Li, D., Jenkinson, C., Jeffery, L. E., Harrison, S. R., Chun, R. F., Adams, J. S., et al. (2019). Serum and synovial fluid vitamin D metabolites and rheumatoid arthritis. *J. Steroid Biochem. Mol. Biol.* 187, 1–8. doi: 10.1016/j.jsbmb.2018.10.008

Li, Y., Xiao, W., Luo, W., Zeng, C., Deng, Z., Ren, W., et al. (2016). Alterations of amino acid metabolism in osteoarthritis: Its implications for nutrition and health. *Amino Acids* 48, 907–914. doi: 10.1007/s00726-015-2168-x

Liu, X., Xu, X., Shang, R., and Chen, Y. (2018). Asymmetric dimethylarginine (ADMA) as an important risk factor for the increased cardiovascular diseases and heart failure in chronic kidney disease. *Nitric Oxide* 78, 113–120. doi: 10.1016/j.niox.2018.06.004

- Lorente, E., Fontela, M. G., Barnea, E., Martín-Galiano, A. J., Mir, C., Galocha, B., et al. (2020). Modulation of natural HLA-B\*27:05 ligandome by ankylosing spondylitis-associated endoplasmic reticulum aminopeptidase 2 (ERAP2). *Mol. Cell Proteomics* 19, 994–1004. doi: 10.1074/mcp.RA120.002014
- Lucas, S., Omata, Y., Hofmann, J., Bottcher, M., Iljazovic, A., Sarter, K., et al. (2018). Short-chain fatty acids regulate systemic bone mass and protect from pathological bone loss. *Nat. Commun.* 9:55. doi: 10.1038/s41467-017-02490-4
- Lv, L., Jiang, H., Yan, R., Xu, D., Wang, K., Wang, Q., et al. (2021). The salivary microbiota, cytokines, and metabolome in patients with ankylosing spondylitis are altered and more proinflammatory than those in healthy controls. *mSystems* 6:e0117320. doi: 10.1128/mSystems.01173-20
- Madsen, R. K., Trygg, J., Lundstedt, T., Gabrielsson, J., Sennbro, C.-J., Alenius, G.-M., et al. (2010). Diagnostic properties of metabolic perturbations in rheumatoid arthritis. *Arthritis Res. Ther.* 13:R19. doi: 10.1186/ar3243
- Maksymowicz, W. P., Wichuk, S., Chiowchanwisawakit, P., Lambert, R. G., and Pedersen, S. J. (2014). Fat metaplasia and backfill are key intermediaries in the development of sacroiliac joint ankylosis in patients with ankylosing spondylitis. *Arthritis Rheumatol.* 66, 2958–2967. doi: 10.1002/art.38792
- Manasson, J., Solomon, G. E., Ubeda, C., Yang, L., Fanok, M., Scher, J. U., et al. (2017). The effect of biologic therapies on the gut microbial composition in psoriatic arthritis. *Arthritis Rheumatol.* 69(Suppl. 10), 637.
- Mezrich, J. D., Fechner, J. H., Zhang, X., Johnson, B. P., Burlingham, W. J., and Bradfield, C. A. (2010). An interaction between kynurenine and the aryl hydrocarbon receptor can generate regulatory T cells. *J. Immunol.* 185, 3190–3198. doi: 10.4049/jimmunol.0903670
- Miles, E. A., and Calder, P. C. (2012). Influence of marine n-3 polyunsaturated fatty acids on immune function and a systematic review of their effects on clinical outcomes in rheumatoid arthritis. *Br. J. Nutr.* 107(Suppl. 2), S171–S184. doi: 10.1017/S0007114512001560
- Moher, D., Liberati, A., Tetzlaff, J., and Altman, D. G. (2009). Preferred reporting items for systematic reviews and meta-analyses: The PRISMA statement. *J. Clin. Epidemiol.* 62, 1006–1012. doi: 10.1016/j.jclinepi.2009.06.005
- Muhammed, H., Kumar, S., Chaurasia, S., Majumder, S., Singh, R., Agarwal, V., et al. (2020). Metabolomics analysis revealed significantly higher synovial Phe/Tyr ratio in reactive arthritis and undifferentiated spondyloarthropathy. *Rheumatology* 59, 1587–1590. doi: 10.1093/rheumatology/kez493
- Nanus, D. E., Hughes, B., Stewart, P. M., Filer, A. D., Fisher, B. A., Taylor, P. C., et al. (2015). TNF $\alpha$  regulates cortisol metabolism in vivo in patients with inflammatory arthritis. *Ann. Rheum. Dis.* 74, 464–469. doi: 10.1136/annrheumdis-2013-203926
- Onmaz, D. E., Sivrikaya, A., Abusoglu, S., Yerlikaya, F. H., Unlu, A., Isik, K., et al. (2021). Determination of serum methylarginine levels by tandem mass spectrometric method in patients with ankylosing spondylitis. *Amino Acids* 53, 1329–1338. doi: 10.1007/s00726-021-03046-z
- Ou, J., Xiao, M., Huang, Y., Tu, L., Chen, Z., Cao, S., et al. (2021). Serum metabolomics signatures associated with ankylosing spondylitis and TNF inhibitor therapy. *Front. Immunol.* 12:630791. doi: 10.3389/fimmu.2021.630791
- Perl, A. (2016). Activation of mTOR (mechanistic target of rapamycin) in rheumatic diseases. *Nat. Rev. Rheumatol.* 12, 169–182. doi: 10.1038/nrrheum.2015.172
- Pompeia, C., Lima, T., and Curi, R. (2003). Arachidonic acid cytotoxicity: Can arachidonic acid be a physiological mediator of cell death? *Cell Biochem. Funct.* 21, 97–104. doi: 10.1002/cbf.1012
- Ranganathan, V., Gracey, E., Brown, M. A., Inman, R. D., and Haroon, N. (2017). Pathogenesis of ankylosing spondylitis - recent advances and future directions. *Nat. Rev. Rheumatol.* 13, 359–367. doi: 10.1038/nrrheum.2017.56
- Raza, K., Hardy, R., and Cooper, M. S. (2010). The 11 $\beta$ -hydroxysteroid dehydrogenase enzymes—arbiters of the effects of glucocorticoids in synovium and bone. *Rheumatology* 49, 2016–2023. doi: 10.1093/rheumatology/keq212
- Rocha, B., Cillero-Pastor, B., Paine, M. R. L., Heeren, R. M. A., Ruiz-Romero, C., Canete, J. D., et al. (2021). Identification of a distinct lipidomic profile in the osteoarthritic synovial membrane by mass spectrometry imaging. *Osteoarthritis Cartilage* 29, 750–761. doi: 10.1016/j.joca.2020.12.025
- Rocha, B., Ruiz-Romero, C., Blanco, F. J., Cillero-Pastor, B., Heeren, R. M., Cuervo, A., et al. (2018). Mass spectrometry imaging analysis of synovium differentiate patients with psoriatic and rheumatoid arthritis. *Ann. Rheum. Dis.* 77(Suppl. 2), 219–220. doi: 10.1136/annrheumdis-2018-eular.4466
- Rosser, E. C., Piper, C. J. M., Matei, D. E., Blair, P. A., Rendeiro, A. F., Orford, M., et al. (2020). Microbiota-derived metabolites suppress arthritis by amplifying aryl-hydrocarbon receptor activation in regulatory B cells. *Cell Metab* 31, 837–851.e10. doi: 10.1016/j.cmet.2020.03.003
- Scalise, G., Ciancio, A., Mauro, D., and Ciccio, F. (2021). Intestinal microbial metabolites in ankylosing spondylitis. *J. Clin. Med.* 10:3354. doi: 10.3390/jcm10153354
- Schepers, E., Barreto, D. V., Liabeuf, S., Glorieux, G., Eloit, S., Barreto, F. C., et al. (2011). Symmetric dimethylarginine as a proinflammatory agent in chronic kidney disease. *Clin. J. Am. Soc. Nephrol.* 6, 2374–2383. doi: 10.2215/cjn.01720211
- Shao, T.-J., He, Z.-X., Xie, Z.-J., Li, H.-C., Wang, M.-J., and Wen, C.-P. (2016). Characterization of ankylosing spondylitis and rheumatoid arthritis using 1H NMR-based metabolomics of human fecal extracts. *Metabolomics* 12:70. doi: 10.1007/s11306-016-1000-2
- Smith, P. M., Howitt, M. R., Panikov, N., Michaud, M., Gallini, C. A., Bohlooly, Y. M., et al. (2013). The microbial metabolites, short-chain fatty acids, regulate colonic Treg cell homeostasis. *Science* 341, 569–573. doi: 10.1126/science.1241165
- Souto-Carneiro, M., Toth, L., Behnisch, R., Urbach, K., Klika, K. D., Carvalho, R. A., et al. (2020). Differences in the serum metabolome and lipidome identify potential biomarkers for seronegative rheumatoid arthritis versus psoriatic arthritis. *Ann. Rheum. Dis.* 79, 499–506. doi: 10.1136/annrheumdis-2019-216374
- Stahly, A., Regner, E., Lefferts, A., Brown, B., D'Alessandro, A., and Kuhn, K. (2019). Metabolomics screening in axial spondyloarthritis: Identifying potential biomarkers. *Arthritis Rheumatol.* 71(Suppl. 10), 1078–1079. doi: 10.1002/art.41108
- Stoll, M. L., Cron, R. Q., Kumar, R., Lefkowitz, E. J., Morrow, C. D., and Barnes, S. (2016). Fecal metabolomics in pediatric spondyloarthritis implicate decreased metabolic diversity and altered tryptophan metabolism as pathogenic factors. *Genes Immun.* 17, 400–405. doi: 10.1038/gene.2016.38
- Suva, L. J., and Gaddy, D. (2016). Back to the future: Evaluation of the role of glutamate in bone cells. *Calcif Tissue Int.* 99, 112–113. doi: 10.1007/s00223-016-0135-5
- Takahashi, S., Saegusa, J., Sendo, S., Okano, T., Akashi, K., Irino, Y., et al. (2017). Glutaminase 1 plays a key role in the cell growth of fibroblast-like synoviocytes in rheumatoid arthritis. *Arthritis Res. Ther.* 19:76. doi: 10.1186/s13075-017-1283-3
- Taurog, J. D., Chhabra, A., and Colbert, R. A. (2016). Ankylosing spondylitis and axial spondyloarthritis. *N. Engl. J. Med.* 374, 2563–2574. doi: 10.1056/NEJMr1406182
- Toth, L., Urbach, K., Lorenz, H. M., Carvalho, R. A., Souto-Carneiro, M., and Klika, K. D. (2019). Comparative metabolomic and lipidomic analysis of serum samples from patients with seronegative rheumatoid arthritis and psoriatic arthritis. *Ann. Rheum. Dis.* 78(Suppl. 1):A78. doi: 10.1136/annrheumdis-2018-EWRR2019.157
- Tripepi, G., Mattace Raso, F., Sijbrands, E., Seck, M. S., Maas, R., Boger, R., et al. (2011). Inflammation and asymmetric dimethylarginine for predicting death and cardiovascular events in ESRD patients. *Clin. J. Am. Soc. Nephrol.* 6, 1714–1721. doi: 10.2215/cjn.11291210
- Venken, K., Jacques, P., Mortier, C., Labadia, M. E., Decruy, T., Coudensys, J., et al. (2019). ROR $\gamma$ t inhibition selectively targets IL-17 producing iNKT and  $\gamma\delta$ T cells enriched in Spondyloarthritis patients. *Nat. Commun.* 10:9. doi: 10.1038/s41467-018-07911-6
- Vernocchi, P., Marini, F., Capuani, G., Tomassini, A., Conta, G., Del Chierico, F., et al. (2020). Fused omics data models reveal gut microbiome signatures specific of inactive stage of juvenile idiopathic arthritis in pediatric patients. *Microorganisms* 8:1540. doi: 10.3390/microorganisms8101540
- Von Hegedus, J. H., Madari, Q. S. R., Muller, P. C. E. H., Kloppenburg, M., Toes, R. E. M., Huizinga, T. W. J., et al. (2017). Characterisation of lipid mediator profile and immune cells in synovial fluid of juvenile idiopathic arthritis. *Arthritis Rheumatol.* 69(Suppl. 10).
- Wang, D., Li, D., Zhang, Y., Chen, J., Zhang, Y., Liao, C., et al. (2021). Functional metabolomics reveal the role of AHR/GPR35 mediated kynurenic acid gradient sensing in chemotherapy-induced intestinal damage. *Acta Pharm. Sin. B* 11, 763–780. doi: 10.1016/j.apsb.2020.07.017
- Wang, W., Yang, G.-J., Zhang, J., Chen, C., Jia, Z.-Y., Li, J., et al. (2016). Plasma, urine and ligament tissue metabolite profiling reveals potential biomarkers of ankylosing spondylitis using NMR-based metabolic profiles. *Arthritis Res. Ther.* 18:244. doi: 10.1186/s13075-016-1139-2
- Wells, G., Shea, B., O'Connell, D., Peterson, J., Welch, V., Losos, M., et al. (2013). *The Newcastle-Ottawa Scale (NOS) for Assessing the Quality of Nonrandomised Studies in Meta-Analyses*. Ottawa, CA: Ottawa Hospital Research Institute.
- Wishart, D. S. (2016). Emerging applications of metabolomics in drug discovery and precision medicine. *Nat. Rev. Drug Discov.* 15, 473–484. doi: 10.1038/nrd.2016.32
- Xu, W. D., Yang, X. Y., Li, D. H., Zheng, K. D., Qiu, P. C., Zhang, W., et al. (2015). Up-regulation of fatty acid oxidation in the ligament as a contributing factor of ankylosing spondylitis: A comparative proteomic study. *J. Proteomics* 113, 57–72. doi: 10.1016/j.jprot.2014.09.014

- Yin, J., Sternes, P. R., Wang, M., Song, J., Morrison, M., Li, T., et al. (2020). Shotgun metagenomics reveals an enrichment of potentially cross-reactive bacterial epitopes in ankylosing spondylitis patients, as well as the effects of TNFi therapy upon microbiome composition. *Ann. Rheum. Dis.* 79, 132–140. doi: 10.1136/annrheumdis-2019-215763
- Zeft, A., Costanzo, D., Alkhouri, N., Patel, N., Grove, D., Spalding, S. J., et al. (2014). Metabolomic analysis of breath volatile organic compounds reveals unique breathprints in children with juvenile idiopathic arthritis. *Arthritis Rheumatol.* 66:S159. doi: 10.1002/art.38543
- Zhang, Y., Li, H., Wang, X., Gao, X., and Liu, X. (2009). Regulation of T cell development and activation by creatine kinase B. *PLoS One* 4:e5000. doi: 10.1371/journal.pone.0005000
- Zhou, C., Zhao, H., Xiao, X. Y., Chen, B. D., Guo, R. J., Wang, Q., et al. (2020). Metagenomic profiling of the pro-inflammatory gut microbiota in ankylosing spondylitis. *J. Autoimmun.* 107:102360. doi: 10.1016/j.jaut.2019.102360
- Zhou, Y., Zhang, X., Chen, R., Liu, Y., Liu, X., Gao, M., et al. (2020). Serum amino acid metabolic profiles of ankylosing spondylitis by targeted metabolomics analysis. *Clin. Rheumatol.* 39, 2325–2336. doi: 10.1007/s10067-020-04974-z
- Zobel, E. H., von Scholten, B. J., Reinhard, H., Persson, F., Teerlink, T., Hansen, T. W., et al. (2017). Symmetric and asymmetric dimethylarginine as risk markers of cardiovascular disease, all-cause mortality and deterioration in kidney function in persons with type 2 diabetes and microalbuminuria. *Cardiovasc. Diabetol.* 16:88. doi: 10.1186/s12933-017-0569-8



## OPEN ACCESS

## EDITED AND REVIEWED BY

M. Pilar Francino,  
Fundación para el Fomento de la  
Investigación Sanitaria y Biomédica de  
la Comunitat Valenciana  
(FISABIO), Spain

## \*CORRESPONDENCE

Yubin Luo  
✉ luoyubin2016@163.com  
Yi Liu  
✉ yi2006liu@163.com

†These authors have contributed  
equally to this work

## SPECIALTY SECTION

This article was submitted to  
Microbial Symbioses,  
a section of the journal  
Frontiers in Microbiology

RECEIVED 16 November 2022

ACCEPTED 30 November 2022

PUBLISHED 12 December 2022

## CITATION

Huang T, Pu Y, Wang X, Li Y, Yang H,  
Luo Y and Liu Y (2022) Corrigendum:  
Metabolomic analysis in  
spondyloarthritis: A systematic review.  
*Front. Microbiol.* 13:1100290.  
doi: 10.3389/fmicb.2022.1100290

## COPYRIGHT

© 2022 Huang, Pu, Wang, Li, Yang,  
Luo and Liu. This is an open-access  
article distributed under the terms of  
the [Creative Commons Attribution  
License \(CC BY\)](#). The use, distribution  
or reproduction in other forums is  
permitted, provided the original  
author(s) and the copyright owner(s)  
are credited and that the original  
publication in this journal is cited, in  
accordance with accepted academic  
practice. No use, distribution or  
reproduction is permitted which does  
not comply with these terms.

# Corrigendum: Metabolomic analysis in spondyloarthritis: A systematic review

Tianwen Huang<sup>1,2,3†</sup>, Yaoyu Pu<sup>1,2,3†</sup>, Xiangpeng Wang<sup>1,2,3</sup>,  
Yanhong Li<sup>1,2,3</sup>, Hang Yang<sup>1,2,3</sup>, Yubin Luo <sup>1,2,3\*</sup> and  
Yi Liu <sup>1,2,3\*</sup>

<sup>1</sup>Department of Rheumatology and Immunology, West China Hospital, Sichuan University, Chengdu, China, <sup>2</sup>Rare Diseases Center, West China Hospital, Sichuan University, Chengdu, China,

<sup>3</sup>Institute of Immunology and Inflammation, Frontiers Science Center for Disease Related Molecular Network, West China Hospital, Chengdu, China

## KEYWORDS

spondyloarthritis, ankylosing spondylitis, metabolomics, biomarkers, dysbiosis

## A corrigendum on

**Metabolomic analysis in spondyloarthritis: A systematic review**

by Huang, T., Pu, Y., Wang, X., Li, Y., Yang, H., Luo, Y., and Liu, Y. (2022). *Front. Microbiol.* 13:965709. doi: 10.3389/fmicb.2022.965709

In the published article, there was an error. We mistakenly described the trend of changes in the levels of some metabolites after treatment of SpA patients.

A correction has been made to **Results**, “*Dynamic alterations in the metabolic profile before and after treatment of spondyloarthritis*,” Paragraphs 2 and 4. These sentences previously stated:

“*Kapoor et al. (2013) and Bogunia-Kubik et al. (2021) found elevated levels of isobutyrate and acetone in AS as well as elevated levels of acetate in PsA after TNFi therapy. Decreased levels of amino acids, including histidine, leucine and phenylalanine, were also found in AS patients after therapy. Another study including PsA patients receiving TNFi therapy showed higher levels of glutamine than those observed at baseline. Additionally, the two studies both found decreased creatine and creatinine levels in SpA patients after treatment.*”

And

“*In addition, in the serum of JIA patients, MTX therapy increased the level of omega-3 unsaturated fatty acids (docosahexanoic acid and linoleic acid), which are anti-inflammatory mediators.*”

The corrected sentence appears below:

“*Kapoor et al. (2013) and Bogunia-Kubik et al. (2021) found decreased levels of isobutyrate and acetone in AS as well as decreased levels of acetate in PsA after TNFi therapy. Elevated levels of amino acids, including histidine, leucine and phenylalanine, were also found in AS patients after therapy. Another study including PsA patients receiving TNFi therapy showed lower levels of glutamine than those observed at baseline. Additionally, the two studies both found elevated creatine and creatinine levels in SpA patients after treatment.*”



And

“In addition, in the serum of JIA patients, MTX therapy reduced the level of omega-3 unsaturated fatty acids (docosahexanoic acid and linoleic acid), which are anti-inflammatory mediators.”

The authors apologize for this error and state that this does not change the scientific conclusions of the article in any way. The original article has been updated.

## Publisher's note

All claims expressed in this article are solely those of the authors and do not necessarily represent those of their affiliated organizations, or those of the publisher, the editors and the reviewers. Any product that may be evaluated in this article, or claim that may be made by its manufacturer, is not guaranteed or endorsed by the publisher.

## References

Bogunia-Kubik, K., Wojtowicz, W., Swierkot, J., Mielko, K. A., Qasem, B., Wielinska, J., et al. (2021). Disease differentiation and monitoring of anti-TNF treatment in rheumatoid arthritis and spondyloarthropathies. *Int. J. Mol. Sci.* 22:7389. doi: 10.3390/ijms22147389

Kapoor, S. R., Buckley, C. D., Raza, K., Filer, A., Fitzpatrick, M. A., Young, S. P., et al. (2013). Metabolic profiling predicts response to anti-tumor necrosis factor alpha therapy in patients with rheumatoid arthritis. *Arthritis Rheum.* 65, 1448–1456. doi: 10.1002/art.37921



## OPEN ACCESS

## EDITED BY

Ilias Lagkouravdos,  
Technical University of Munich,  
Germany

## REVIEWED BY

Muhammad Bilal Sadiq,  
Forman Christian College, Pakistan  
Rachele Invernizzi,  
Broad Institute, United States

## \*CORRESPONDENCE

Chunyu Tan  
annaquintessence@163.com  
Yi Liu  
yi2006liu@163.com

†These authors have contributed  
equally to this work

## SPECIALTY SECTION

This article was submitted to  
Microbial Symbioses,  
a section of the journal  
Frontiers in Microbiology

RECEIVED 14 May 2022

ACCEPTED 20 September 2022

PUBLISHED 06 October 2022

## CITATION

Wu Y, Li Y, Luo Y, Zhou Y, Wen J,  
Chen L, Liang X, Wu T, Tan C and Liu Y  
(2022) Gut microbiome  
and metabolites: The potential key  
roles in pulmonary fibrosis.  
*Front. Microbiol.* 13:943791.  
doi: 10.3389/fmicb.2022.943791

## COPYRIGHT

© 2022 Wu, Li, Luo, Zhou, Wen, Chen,  
Liang, Wu, Tan and Liu. This is an  
open-access article distributed under  
the terms of the [Creative Commons  
Attribution License \(CC BY\)](https://creativecommons.org/licenses/by/4.0/). The use,  
distribution or reproduction in other  
forums is permitted, provided the  
original author(s) and the copyright  
owner(s) are credited and that the  
original publication in this journal is  
cited, in accordance with accepted  
academic practice. No use, distribution  
or reproduction is permitted which  
does not comply with these terms.

# Gut microbiome and metabolites: The potential key roles in pulmonary fibrosis

Yinlan Wu<sup>1,2,3†</sup>, Yanhong Li<sup>1,2,3†</sup>, Yubin Luo<sup>1,2,3</sup>, Yu Zhou<sup>4</sup>,  
Ji Wen<sup>1,2,3</sup>, Lu Chen<sup>1,2,3</sup>, Xiuping Liang<sup>1,2,3</sup>, Tong Wu<sup>1,2,3</sup>,  
Chunyu Tan<sup>1,2,3\*</sup> and Yi Liu<sup>1,2,3\*</sup>

<sup>1</sup>Department of Rheumatology and Immunology, West China Hospital, Sichuan University, Chengdu, China, <sup>2</sup>Rare Diseases Center, West China Hospital, Sichuan University, Chengdu, China, <sup>3</sup>Institute of Immunology and Inflammation, Frontiers Science Center for Disease-Related Molecular Network, West China Hospital, Chengdu, China, <sup>4</sup>Department of Respiratory and Critical Care Medicine, Chengdu First People's Hospital, Chengdu, China

There are a wide variety of microbiomes in the human body, most of which exist in the gastrointestinal tract. Microbiomes and metabolites interact with the host to influence health. Rapid progress has been made in the study of its relationship with abenteric organs, especially lung diseases, and the concept the of "gut–lung axis" has emerged. In recent years, with the in-depth study of the "gut–lung axis," it has been found that changes of the gut microbiome and metabolites are related to fibrotic interstitial lung disease. Understanding their effects on pulmonary fibrosis is expected to provide new possibilities for the prevention, diagnosis and even treatment of pulmonary fibrosis. In this review, we focused on fibrotic interstitial lung disease, summarized the changes the gut microbiome and several metabolites of the gut microbiome in different types of pulmonary fibrosis, and discussed their contributions to the occurrence and development of pulmonary fibrosis.

## KEYWORDS

gut microbiome, metabolites, pulmonary fibrosis, gut–lung axis, short chain fatty acid, amino acid

## Introduction

Interstitial lung disease (ILD) is an umbrella term characterized by chronic lung inflammation and elevated levels of chronic inflammatory cells with varying degrees of pulmonary fibrosis (Raghu et al., 2018). Patients with ILD have a poor prognosis and poor response to treatment due to pulmonary fibrotic lesions (Kalchiem-Dekel et al., 2018). ILD can be caused by connective tissue disease, radiation damage, particle inhalation and other reasons, but cases have no clear etiology, which is called idiopathic pulmonary fibrosis (IPF) (Kolb and Vášáková, 2019). Although there are many studies

on pulmonary fibrosis, the exact mechanism of its pathogenesis and development is still not completely clear.

The human body contains a variety of microorganisms, including bacteria, fungi, viruses, archaea and protozoa (Lynch and Pedersen, 2016), most of which are found in the gastrointestinal tract (Marsland et al., 2015). The various microbial communities that colonize the gut of the host are called the gut microbiota (Kc et al., 2020). With in-depth, comprehensive analyses of the microbiome and metabolome, it has been gradually found that metabolites and antigens of the gut microbiome may regulate the host (Cruz et al., 2021). The intestinal microbiome could affect the occurrence, progression and prognosis of diseases in various ways through bidirectional flow between the lung and intestine via the blood and lymphatic systems, such as inflammation, metabolism and cell signal transduction of microbial metabolites (Marsland et al., 2015; Dickson et al., 2018; Chioma et al., 2021). Thus, the concept of the “gut–lung axis” was proposed and gradually applied to study the pathogenesis and progression of various pulmonary diseases. For example, it has been reported that the dysbiosis of the gut microbiome in systemic sclerosis patients with ILD is more obvious and appears in the early stage of pulmonary fibrosis (Andréasson et al., 2016); It has also been demonstrated that the intestinal metabolite arginine is involved in collagen deposition in IPF patients (Wang et al., 2021). With the development of omics technology and bioinformatics analysis, many studies related to the “gut–lung axis” have been published recently, but there is no summary article on pulmonary fibrosis at present. In this review, we will summarize the alterations of the gut microbiota by different types of pulmonary fibrosis, and the contribution of several of the most well-known intestinal metabolites in the process of pulmonary fibrosis.

## Pathophysiology of interstitial lung disease

Many studies have pointed out that epithelial cells, myofibroblasts and the immune system play a major role in the progression of ILD under the influence of genetic factors, epigenetic reprogramming and environmental factors (Milara et al., 2018; Kadota et al., 2020; Valenzi et al., 2021). (1) Proliferation, apoptosis, senescence and epithelial-mesenchymal transition (EMT) occur in lung epithelial cells due to chronic inflammation, peroxidation stimulation, or gene expression and modification changes, thus participating in pulmonary fibrosis (Smirnova et al., 2016; Xu et al., 2016; Jablonski et al., 2017). Moreover, epithelial cells can secrete transforming growth factor- $\beta$  (TGF- $\beta$ ), tumor necrosis factor (TNF), a variety of matrix metalloproteinases and chemokines to promote the expression of myofibroblasts, leading to the remodeling of the extracellular matrix (ECM) (King et al., 2011; Selman and Pardo, 2014). (2) In the process of pulmonary

fibrosis, a large number of immune cells accumulate and release inflammatory factors (Wynn and Vannella, 2016; Gao et al., 2019). There are two subtypes of macrophages, namely classically activated macrophages (M1) and alternatively activated of macrophages (M2). M1 macrophages produce proinflammatory cytokines, such as TNF $\alpha$ , interleukin-1 (IL-1) and IL-6, to maintain chronic inflammation (Mills, 2012). M2 macrophages secrete a variety of growth factors, including TGF- $\beta$  and fibroblast growth factor, which contribute to over-repair (Duru et al., 2016). Neutrophil aggregation may participate in amplified tissue remodeling in lung injury through the release of proinflammatory cytokines and the generation of reactive oxygen species (Mayadas et al., 2014). IL-17 secreted by helper T lymphocyte type 17 (Th17) cells promotes lung fibroblast proliferation, resulting in increased type I collagen synthesis and TGF- $\beta$  and IL-6 expression (Lei et al., 2016). In several clinical and animal studies, there have been controversial results regarding the effects of regulatory cells (Tregs) on lung fibrosis (Reilkoff et al., 2013; Kamio et al., 2018), possibly due to a shift from a protective to a destructive phenotype of Tregs during inflammation (Boveda-Ruiz et al., 2013; Birjandi et al., 2016). (3) Fibroblasts, pericytes and mesenchymal progenitors differentiate into myofibroblasts, leading to lung pathologic excess, and thereby promoting pulmonary fibrosis (Martinez et al., 2017). Myofibroblasts are involved in the accumulation of ECM components, including collagen, fibronectin, tenascin and proteoglycan (Klingberg et al., 2013). The ECM promotes fibroblast differentiation through genetic alterations, indicating a positive feedback loop between fibroblasts and abnormal ECM (Klingberg et al., 2013; Parker et al., 2014).

Although there are many studies on the pathogenesis of pulmonary fibrosis, there are still many unclear details. The emergence of a new view of the “gut–lung axis” provides a new idea for the study of pulmonary fibrosis pathogenesis agents.

## Microbiome alteration in pulmonary fibrosis

### Microbiome alteration in idiopathic pulmonary fibrosis

Idiopathic pulmonary fibrosis, is the most common form of pulmonary fibrosis. The earliest and most common research on the microorganisms in IPF patients relates to the change in the lung microbiome. Richter et al. (2009) found that compared with healthy people, the bacterial load in the lungs of IPF patients increased *Haemophilus*, *Streptococcus*, *Neisseria* and *Veronella* at the species level. Another experiment demonstrated that pulmonary bacteria may play a pathogenic role in acute exacerbations of IPF and that increased relative abundance of specific species (*Streptococcus* and *Staphylococcus*) at diagnosis may be a biomarker of rapid disease progression

(Han et al., 2014). Moreover, Invernizzi et al. (2021) found an increased number of *Actinomyces* and *Veillonella* in patients with IPF compared with other lung diseases, and a correlation with survival. Huang et al. (2017) analyzed specific microbial colonization of the respiratory tract and found that there was a reasonable mechanistic link between the bacterial community and fibroblast reactivity.

Because the feces of IPF patients can be affected by factors other than the disease itself, such as age, living habits, genetic background, and treatment regimens, it is difficult to study. To date, there are no relevant data on the gut microbiome of IPF patients, but a recent animal model study has been conducted. Gong et al. (2021) found that 412 microorganisms at the genus level and 26 metabolites changed synchronously in the two mouse models [bleomycin (BLM)-induced and silica-induced] with the same trend, and there were significant differences from the control group. The combination of seven microorganisms (*Alloprevotella*, *Dubosiella*, *Helicobacter*, *Olsenella*, *Parasutterella*, *Rikenella*, and *Rikenellaceae RC9 gut group*) and nine metabolites (trigonelline, betaine, cytosine, thymidine, ophocholine, taurocholate, adenine, deoxyadenosine, and deoxycytidine) selected was validated to distinguish pulmonary fibrosis from normal controls. Among these, *Dubosiella* was positively correlated with betaine, but negatively correlated with cytosine, adenine, deoxyadenosine, and deoxycytidine; *Rikenella* was positively correlated with cytosine, thymidine, ophocholine, adenine, deoxyadenosine, and deoxycytidine (Gong et al., 2021).

## Microbiota changes in pulmonary fibrosis associated with systemic sclerosis

Systemic sclerosis (SSc), is an immune-mediated rheumatic disease characterized by vascular lesions and fibrosis of the skin and internal organs, with a high incidence of severe pulmonary fibrosis (Denton and Khanna, 2017; Perelas et al., 2020). A previous study observed a decrease in the symbiotic gut microbiome (e.g., *Faecalibacterium* and *Clostridium*) in SSc patients and an increase in bacteria (e.g., *Fusobacterium* and  $\gamma$ -*Proteobacteria*). As the severity of the disease increased, *Bacteroides fragilis* gradually decreased, and *Fusobacteria* gradually increased. Interestingly, these SSc patients also had increased numbers of *Bifidobacterium* and *Lactobacillus* (Volkman et al., 2016). In a clinical study, SSc patients with pulmonary fibrosis had a more severe gut microbiota imbalance than those without pulmonary fibrosis, and presented in the early stage of fibrosis, suggesting that changes in gut microbiota in susceptible people may have the potential to predict the development of fibrosis (Andréasson et al., 2016). In SSc skin and lung fibrosis mouse models immunized with dendritic cells loaded with topoisomerase I peptide, Mehta et al. (2017) found that an increase in the ratio of *Bacteroidetes*/*Firmicutes*

by oral administration of streptomycin caused progression of pulmonary fibrosis. At present, the theory that the gut microbiome could ameliorate the pulmonary symptoms of SSc has been applied in clinical treatment trials. In a 16-week clinical trial of patients with SSc treated with fecal microbiota transplantation (FMT) using commercially available anaerobic cultivated human intestinal microbiota, lung function [based on the diffusing capacity of lung carbon monoxide (DLCO)] improved significantly, which also proved the effect of the gut microbiota on lung lesions in SSc patients (Fretheim et al., 2020).

## Silicosis-related gut microbiota changes

Silicosis is an occupation-related progressive pulmonary fibrosis resulting from prolonged inhalation of dust with high concentrations of free silica (Barnes et al., 2019). Zhou et al. (2019) found that *Firmicutes* and *Actinobacteria* in silicosis patients were reduced at the phylum level in stool samples compared with those of healthy subjects. At the genus level, the *Devosia*, *Clostridiales*, *Alloprevotella* and *Rikenellaceae\_RC9* levels decreased, and the *Lachnospiraceae* and *Lachnoclostridium* levels increased. They also predicted that these bacteria were mainly involved in biological processes such as energy metabolism and transport, membrane structure and function, and gene expression (Zhou et al., 2019). The mechanism of microbiota in pulmonary fibrosis needs to be further verified. Similarly, changes in the microbiota were also found in animal models. Gong et al. (2021) found that at least 412 kinds of intestinal microbes at the genus level compared and 26 kinds of metabolites changed. Seven microorganisms and nine metabolites were associated with pulmonary fibrosis. Among them, the metabolite trigonelline was significantly increased (Gong et al., 2021), which has antioxidant, anti-inflammatory and cell-protective effects (Khalili et al., 2018).

## Radiation-induced lung fibrosis gut microbiome changes

Radiotherapy is an important treatment for cancer, but its therapeutic side effects cannot be ignored. For example, 10% to 30% of patients with lung or breast cancer who receive radiation therapy will develop radiation-induced pneumonitis, and they are likely to develop radiation-induced lung fibrosis (Fleckenstein et al., 2007; Chao et al., 2017). In mice with local chest irradiation, Chen et al. (2021) found that *Akkermansia*, *Desulfovibrio* and *Parasutterella* increased and *Rikenella* decreased at the genus level and that *Distasonis*, *Goldsteinii*, and *Rodentium* decreased at the species level. These changes were ameliorated after FMT (Chen et al., 2021).



All the above evidences indicate that the microbiota is altered in pulmonary fibrosis (**Table 1**). Although no specific mechanism of action of individual microbiota has been investigated, a growing body of literature has found that microbiota metabolites play an important role in pulmonary fibrosis, which will be discussed in detail next.

## Metabolites of the gut microbiome

In recent years, a number of studies have shown that intestinal microbial metabolites, including amino acids, short-chain fatty acids (SCFAs), bile acids, and valproic acid, are involved in the process of pulmonary fibrosis through ECM accumulation, energy metabolism, epigenetics, immune regulation and other pathways (**Chen et al., 2017; Bai et al., 2019; Fang et al., 2020**). We will discuss these in more detail next (**Table 2**).

### Amino acids

Amino acids, which can be obtained through the metabolic breakdown of proteins by the gut microbiome, are essential for cell survival, maintenance of normal function and proliferation (**Chung et al., 2015; Ren et al., 2017; Cummings et al., 2018**). IPF patients showed changes in amino acid metabolism, characterized by higher levels of proline, 4-hydroxyproline, alanine, valine, leucine, isoleucine, and lysine detected in lung tissue and exhaled breath (**Gaugg et al., 2019**). Many of these amino acids may function as signal transduction and regulatory molecules in diverse biological processes under various conditions, including gene expression, oxidative defense, and immune responses (**Figure 1; Hatazawa et al., 2018; Glatzová et al., 2021; Jian et al., 2021**).

### Glutamate

Glutamate is a free amino acid found in protein (**Tomé, 2018**). There is a glutamate–glutamine cycle between glutamate and glutamine. That is, the carbon skeleton of glutamate is used for *de novo* synthesis of glutamine (**Chen et al., 2018**), while glutamine is converted to glutamate by glutaminase and then converted to the tricarboxylic acid cycle (TCA) metabolite  $\alpha$ -ketoglutarate ( $\alpha$ -KG) (**Bai et al., 2019**). **Bernard et al. (2018)** found that TGF- $\beta$  stimulated the decomposition of glutamine by fibroblasts, resulting in an increase in  $\alpha$ -KG and glutamate and a decrease in glutamine levels. When extracellular glutamine was lost, TGF- $\beta$ -induced myofibroblast differentiation was prevented. Even after the removal of extracellular glutamine after fibroblast differentiation, the expression of the profibrotic markers fibronectin and hypoxia-inducible factor-1 $\alpha$  was decreased, and TGF- $\beta$ -induced metabolic reorganization was reversed (**Bernard et al., 2018**).

Similarly, **Hamanaka et al. (2019)** explained that TGF- $\beta$ -induced lung fibroblasts produced collagen, which requires glutamine and its conversion to glutamate through glutaminase. Furthermore, they confirmed that glutamate was converted to proline and glycine by the glutamate-consuming enzymes phosphoserine aminotransferase 1 and aldehyde dehydrogenase 18A1/D1-pyrroline-5-carboxylate synthetase (**Hamanaka et al., 2019**). In the lung tissues of human IPF patients, **Bai et al. (2019)** found that the deposition of glutamine decomposition products promoted anti-apoptosis of fibroblasts through epigenetic regulation of XIAP and survivin, members of the inhibitor of apoptosis protein family. All these studies suggested that the glutamate–glutamine cycle was a key component of fibroblast metabolic reprogramming.

### Arginine

Arginine can be metabolized through two pathways, namely, the enzymes nitric oxide synthase (NOS) and arginase (**Niese et al., 2010**). The former product includes nitric oxide (NO), which can participate in the regulation of respiratory inflammation and airway tension and can affect the immune stress of the respiratory tract (**Fu et al., 2020**). The latter produces ornithine and proline via arginase and ornithine aminotransferase (**Wu et al., 2021**). It has been suggested that inhibition of arginase could reduce collagen deposition and improve BLM-induced pulmonary fibrosis (**Roque and Romero, 2021**). **Niese et al. (2010)** found that proline, which can be metabolized by arginine, is usually a rate-limiting substrate in collagen synthesis and is crucial for collagen precipitation in pulmonary fibrosis.

**Li et al. (2021)** found loss of arginine succinate synthase 1 (ASS1), a rate-limiting enzyme responsible for the biosynthesis of the endogenous semi-essential amino acid, arginine during the urea cycle, in fibroblasts from patients with IPF. They demonstrated that ASS1 gene deletion promoted the invasive and fibrotic potential of lung fibroblasts. Further studies suggested that exogenous arginine deprivation attenuates fibroblast proliferation, migration, and invasion, thereby protecting mice from BLM-induced pulmonary fibrosis (**Li et al., 2021**). Therefore, we speculate that ASS1 deficiency in fibroblasts during IPF development may represent a compensatory feedback regulatory mechanism to control endogenous arginine homeostasis.

Arginine also indirectly affects pulmonary fibrosis through immune cells. **Gao et al. (2019)** observed that combined treatment with arginine and norvaline significantly inhibited the increase in Tregs,  $\gamma\delta$ T cells and Tregs/Th17 in BLM mice and ameliorated the decrease in Th17 cells, which inhibited the progression of pulmonary fibrosis. During the inflammation period, a small amount of the arginine metabolite NO is produced by metabolism in response to calcium-independent inducible nitric oxide synthase (iNOS) activated by Th1 cytokines for immune regulation and remodeling (**Bronte and Zanovello, 2005**). NO also dilates blood vessels and suppresses

TABLE 1 Intestinal microflora detection experiment of pulmonary fibrosis.

The type of pulmonary fibrosis	Detection object	Compare object	The changes of gut microbiome	Results	Conclusion	References
Idiopathic pulmonary fibrosis	Bleomycin mouse models	Normal mouse	<i>Alloprevotella</i> , <i>Helicobacter</i> , <i>Rikenella</i> , <i>Rikenellaceae</i> RC9 ↓ <i>Dubosiella</i> , <i>Olsenella</i> , <i>Parasutterella</i> ↑	The microflora of 412 genera were significantly different from that of the control group with 26 metabolites.	A link between the gut microbiome and pulmonary fibrosis was found in a mouse model and demonstrated that they could distinguish pulmonary fibrosis from normal controls.	Gong et al., 2021
Pulmonary fibers associated with SSc	SSc patients with pulmonary fibrosis	Health people	<i>Faecalibacterium</i> , <i>Clostridium</i> , <i>Bacteroides fragilis</i> ↓ <i>Fusobacterium</i> , <i>Bifidobacterium</i> , <i>Lactobacillus</i> , $\gamma$ - <i>Proteobacteria</i> ↑	Dysbiosis occurred in 75% of patients, and was more severe in SSc patients with pulmonary fibrosis	It suggests that abnormal gut microbiome may contribute to the development of systemic inflammation and fibrosis in SSc.	Andréasson et al., 2016
	TOPOIA DCs induced SSc mice by oral streptomycin in early life	TOPOIA DCs induced SSc mice fed without streptomycin	The ratio of <i>Bacteroidetes/Firmicutes</i> ↑	Exacerbation of pulmonary fibrosis and dysregulation of pulmonary T cell response	Changes in the gut microbiome caused by streptomycin can exacerbate fibrosis in lung areas of SSc.	Mehta et al., 2017
	SSc patients with intestinal symptoms after fecal microbiome transplantation	SSc patients with intestinal symptoms before fecal microbiota transplantation	–	Lung function was effectively improved	Regulating gut microbiome of SSc patients can effectively improve lung function.	Fretheim et al., 2020
Silicosis	Silica mouse models	Normal mouse	<i>Alloprevotella</i> , <i>Helicobacter</i> , <i>Rikenella</i> , <i>Rikenellaceae</i> RC9 ↓ <i>Dubosiella</i> , <i>Olsenella</i> , <i>Parasutterella</i> ↑	The microflora of 412 genera were significantly different from that of the control group with 26 metabolites.	A link between the gut microbiome and pulmonary fibrosis was found in a mouse model and demonstrated that they could distinguish pulmonary fibrosis from normal controls.	Gong et al., 2021
	Silicosis patients	Health people	<i>Firmicutes</i> , <i>Actinobacteria</i> <i>Devosia</i> , <i>Clostridiales</i> , <i>Alloprevotella</i> and <i>Rikenellaceae</i> RC9 ↓ <i>Lachnospiraceae</i> , <i>Lachnoclostridium</i> ↑	The microbiome in the gut of silicosis patients changes.	It shows the relationship between silica-induced progressive pulmonary fibrosis and changes in intestinal microbial diversity in humans	Zhou et al., 2019

SSc, systemic sclerosis; TOPOIA DCs, topoisomerase I peptide-loaded dendritic cells.

inflammation when produced in large amounts catalyzed by calcium-dependent cNOS. The arginine metabolite NO plays a bidirectional regulatory role in pulmonary fibrosis (Maarsingh et al., 2008). Arginine could induce an increase in glutathione (GSH) and inhibit the release of proinflammatory cytokines such as TNF- $\alpha$ , IL-1 $\beta$ , and interleukin-6 by macrophages (Wang et al., 2015). Arginine inhibited the activation of the NF- $\kappa$ B light chain enhancer regulating the activity of matrix metalloproteinase-2 (MMP-2) and MMP-9 (Hnia et al., 2008).

In general, arginine may contribute to the formation of pulmonary fibrosis by acting as a substrate for collagen deposition in pulmonary fibrosis or regulating immune

disorders. However, other studies have found that NO metabolized by arginine has a bidirectional regulatory effect in pulmonary fibrosis. The mechanism of arginine's role in pulmonary fibrosis has not been fully confirmed, and the bidirectional regulatory effect of arginine has not been fully explained, which will be investigated in future studies.

### Tryptophan

Tryptophan is metabolized by indoleamine 2,3-dioxygenase-1 (IDO) to produce kynurenine derivatives in inflammatory tissues (Sittig et al., 2021). Reducing tryptophan

TABLE 2 Effects of gut microbiome metabolites in pulmonary fibrosis.

Metabolites	Variation trend	Effector	Effector mechanism	References
Glutamate	Increase	Collagen production	Glutamic–glutamine cycle involves in collagen production of myofibroblasts	Bernard et al., 2018; Hamanaka et al., 2019
Arginine	Increase	Fibroblasts apoptosis	Glutamine promotes anti-apoptosis of IPF fibroblasts through epigenetic regulation of apoptosis suppressor proteins	Bai et al., 2019
		Airway tension	NO produced by arginine metabolism is involved in regulating airway tension and affecting respiratory immune stress	Fu et al., 2020
		Collagen deposition	Proline from arginine metabolism is the rate-limiting substrate in collagen synthesis and is essential for collagen precipitation in pulmonary fibrosis	Niese et al., 2010; Roque and Romero, 2021
		Fibroblasts activation	Arginine depletion attenuates the proliferation, migration and invasion of fibroblasts, thereby slowing down pulmonary fibrosis	Li et al., 2021
		Immune imbalance	Arginine combined with norvaline can correct the imbalance of immune cells in BLM mice	Gao et al., 2019
		Macrophage activation	Arginine induces the increase of GSH and inhibits the release of various proinflammatory cytokines from the macrophage	Hnia et al., 2008
Tryptophan	Decrease	Collagen degradation	Arginine inhibits the activation of NF- $\kappa$ B to reduce MMP-2 and MMP-9 activities	Wang et al., 2015
		T cell immune response	Metabolic derivatives of tryptophan produced by IDO reduce T cell inflammation	Lou et al., 2019
		T cell differentiation	Tryptophan and its metabolites regulate the transcription of multiple genes to affect T cell differentiation	Rothhammer and Quintana, 2019; Takei et al., 2020
Butyrate	-	Collagen generated	The metabolite 5-MTP reduces myofibroblasts aggregation, differentiation and collagen precipitation	Fang et al., 2020
		Gene expression	Butyrate inhibits Thy-1 gene expression and pulmonary fibrosis by inhibiting HDAC activation	Zhu et al., 2016
		Fibroblasts activation	Butyrate inhibits histone 3 acetylation to affect fibroblasts activation and exert antifibrotic effect	Park et al., 2021
Bile acid	Increase	TGF- $\beta$ 1 production	The combination of valproic acid and butyric acid reduces the amount of NF- $\kappa$ B entering the nucleus and the production of TGF- $\beta$ 1, thereby alleviating pulmonary fibrosis	Chen et al., 2006; Sakai and Tager, 2013
		Collagen generated	Bile acid stimulates fibrotic mediators to activate TGF- $\beta$ 1/SMAD3 signaling pathway and bile acid receptor FXR or induce the activation of alveolar epithelial cells and lung fibroblasts	Chen et al., 2016, 2017
PSA	Increase	Inflammatory response	PSA through TLR2 induces Foxp3 <sup>+</sup> Treg to produce IL-10 and TGF- $\beta$ 2	Round and Mazmanian, 2010
Valproic	Decrease	Epithelial-to-mesenchymal transition	Valproic affects histone H3K27 acetylation to inhibit epithelial-mesenchymal transition	Noguchi et al., 2015

IPF, idiopathic pulmonary fibrosis; NO, nitric oxide; BLM, bleomycin; GSH, glutathione; NF- $\kappa$ B, B-cell nuclear factor  $\kappa$ ; MMP, matrix metalloproteinase; IDO, indoleamine 2,3-dioxygenase-1; AhR, aryl hydrocarbon receptor; 5-MTP, 5-methoxytryptophan; HDAC, histone deacetylase; TGF- $\beta$ , transforming growth factor- $\beta$ ; PSA, polysaccharide A; TLR2, Toll-like receptor 2; Treg, regulatory T cell; IL-10, interleukin-10.

levels induced Treg polarization directly (Yue et al., 2015) or, through its IDO derivative, reduced T-cell inflammation (Lou et al., 2019). In the gut, various tryptophan metabolites affect immune homeostasis by interacting with aryl hydrocarbon receptor (AhR), which is expressed in immune cells and regulates the transcription of multiple genes (Rothhammer and Quintana, 2019). In a BLM-induced mouse model, Takei et al. (2020) found that Tregs were increased and proinflammatory T-cell subsets were inhibited by stimulation of AhR, and pulmonary fibrosis was reduced compared with the control group. Other tryptophan metabolites also

regulate lung inflammation and fibroblasts. Fibroblasts metabolize tryptophan to release 5-methoxytryptophan (5-MTP), which inhibits macrophage activation, and blocks the release of proinflammatory cytokines and chemokines, and the expression of COX2 in macrophages (Wang et al., 2016). Fang et al. (2020) reported that 5-MTP reduced BLM-induced collagen deposition, myofibroblast accumulation, and alveolar structure destruction in mouse models. *In vitro* experiments, confirmed that 5-MTP inhibited the differentiation of fibroblasts into myofibroblasts and slowed the progression of pulmonary fibrosis by disrupting the

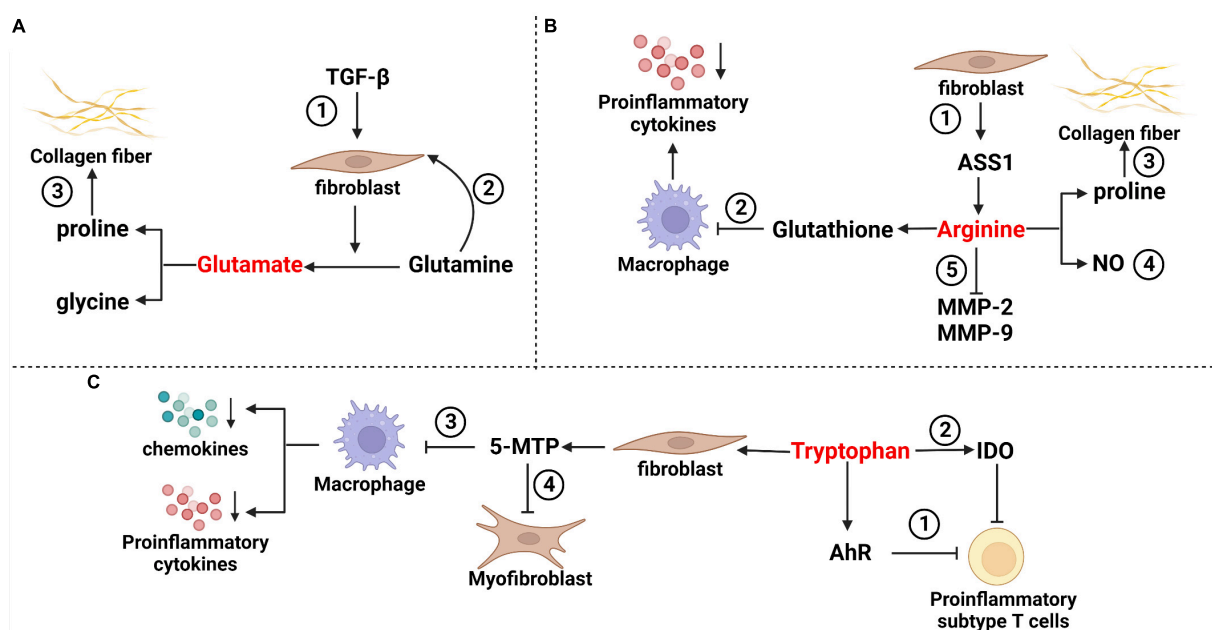


FIGURE 1

Mechanisms of partial amino acids in pulmonary fibrosis. **(A)** Glutamate in pulmonary fibrosis ① TGF- $\beta$  stimulated fibroblasts, and increased the decomposition of glutamine and glutamate levels. ② Glutamine promoted anti-apoptosis of fibroblasts through epigenetic regulation of XIAP and survivin. ③ Glutamate metabolite proline is a rate-limiting substrate for collagen formation in pulmonary fibrosis. **(B)** Arginine in pulmonary fibrosis ① Arginine has a variety of sources, including fibroblasts that can synthesize arginine via the ASS1 pathway often used in research experiments. ② Arginine can induce an increase in glutathione and inhibit the release of proinflammatory cytokines such as TNF- $\alpha$ , IL-1 $\beta$  and IL-6 from macrophages. ③ Arginine metabolite proline is a rate-limiting substrate for collagen formation in pulmonary fibrosis. ④ The NO isoforms of arginine metabolites include iNOS and cNOS, which have bidirectional effects on airway inflammation. ⑤ Arginine inhibits the activation of NF- $\kappa$ B light chain enhancer and reduces the activities of matrix metalloproteinase-2 (MMP-2) and MMP-9 in fibrosis. **(C)** Tryptophan in pulmonary fibrosis ① Tryptophan acts with aryl hydrocarbon receptors to inhibit proinflammatory subsets of T cells. ② Tryptophan metabolites produced by IDO can indirectly reduce T-cell inflammation. ③ Tryptophan is metabolized to 5-MTP in fibroblasts, which can inhibit macrophage activation and block the release of proinflammatory cytokines and chemokines. ④ 5-MTP inhibits myofibroblast formation by interfering with the TGF- $\beta$ /SMAD3 and PI3K/Akt pathways.

TGF- $\beta$ /Smad3 and PI3K/Akt pathways (Fang et al., 2020). Niacin, a tryptophan gut microbiota metabolite, can induce the differentiation of Treg cells and IL-10-producing T cells and can promote the anti-inflammatory properties of colonic macrophages and dendritic cells (Singh et al., 2014). Tryptophan adjusts pulmonary fibrosis progression through its various derivatives of systemic immune regulation and its influence on pulmonary fibrosis.

## Short-chain fatty acids

Short-chain fatty acids are metabolized by the microbiota in the cecum and colon based on dietary fibrosis and proteins and peptides (Macfarlane and Macfarlane, 2012). Different gut microbes produce different types and proportions of SCFAs (Yang and Rose, 2014; Mirkovič et al., 2015). SCFAs can enter the systemic circulation and directly affect the function and metabolism of abenteric organs and tissues, such as the lungs, liver and skeletal muscle tissue (Boets et al., 2017). According to the literature,

pulmonary SCFA levels are 370 times higher on average than those in blood (Segal et al., 2017). Ghorbani et al. (2015) found that high concentrations of SCFAs reduced alveolar epithelial cell line (A549) proliferation. SCFAs (mainly propionic acid and butyric acid) can completely restore respiratory epithelial barrier dysfunction caused by allergens or IL-4/IL-13 by improving the expression of tight junction proteins or inhibiting the MAPK pathway (Richards et al., 2020).

Zhu's team, in a mouse model of pulmonary fibrosis induced by lipopolysaccharide (LPS), demonstrated that butyrate pretreatment could inhibit ThY-1 gene expression and pulmonary fibrosis by inhibiting histone deacetylase (HDAC) activation and histone H4 deacetylation (Zhu et al., 2016). Park et al. (2021) observed that sodium butyrate treatment attenuated BLM-induced skin and lung fibrosis in a BLM-induced mouse model. They found that sodium butyrate modulates macrophage differentiation in mesenteric lymph nodes and bronchoalveolar lavage cells of model mice, and inhibits TGF- $\beta$  reactive proinflammatory expression by increasing histone 3 acetylation, thereby showing indirect

and direct antifibrotic effects on fibroblasts (Park et al., 2021). It has been reported that the combined action of valproic acid and butyric acid can reduce the amount of nuclear factor kappa B (NF- $\kappa$ B) entering the nucleus and the production of TGF- $\beta$ 1 by inhibiting threonine kinase (Akt)/protein kinase B gene expression, thereby alleviating pulmonary fibrosis (Chen et al., 2006; Sakai and Tager, 2013). At present, there are few studies on SCFAs, and the role of different types of SCFAs in different types of pulmonary fibrosis needs to be further explored in the future.

## Other metabolites

At present, with the development of metabolomics, an increasing number of relationships between microbial metabolites and pulmonary fibrosis have been discovered. For example, Chen et al. (2016) reported that bile acids induced the activation of alveolar epithelial cells and pulmonary fibroblasts *in vitro*. Repeated inhalation of bile acid has been shown to cause pulmonary fibrosis in a mouse model, showing significant pathological changes in pulmonary fibrosis, enhanced expression of type I collagen, and an increased number of myofibroblasts. It was further observed that the main mechanism of its action was to stimulate fibrosis mediators and activate the TGF- $\beta$ 1/Smad3 signaling pathway and bile acid receptor FXR to promote fibrosis (Chen et al., 2017). Polysaccharide A (PSA) produced by the human symbiont *Bacteroides fragilis* can induce Foxp3<sup>+</sup> Tregs to produce IL-10 and TGF- $\beta$ 2 through Toll-like receptor 2 (TLR2) expression, thereby regulating inflammation and alleviating the progression of pulmonary fibrosis. PSA can also induce the transformation of Foxp3<sup>+</sup> Tregs into Foxp3<sup>+</sup> Tregs expressing IL-10, which may be one of the mechanisms of PSA's anti-inflammatory properties (Round and Mazmanian, 2010). In addition, Noguchi et al. (2015) found *in vitro* that valproic acid can partially inhibit TGF- $\beta$ -induced epithelial-to-mesenchymal transition by improving histone H3K27 acetylation reduction, thus directly alleviating pulmonary fibrosis.

## Conclusion

The gut microbiome of patients/models with pulmonary fibrosis changed compared to healthy controls, although the changes in the microbiome of different types of pulmonary fibrosis were not consistent. The gut microbiome could participate in the process of pulmonary fibrosis through metabolites. For example, amino acid metabolism regulates fibroblasts to affect migration, transformation and collagen deposition. Amino acid metabolism can also regulate macrophage and T-cell activity to participate in

proinflammatory or profibrotic processes. Butyrate increases histone acetylation by inhibiting HDAC activation, thereby inhibiting TGF- $\beta$  and fibroblast expression. Bile acids activate the TGF- $\beta$ 1/Smad3 signaling pathway to induce the activation of alveolar epithelial cells and lung fibroblasts. At present, there are few studies on the single species/genus microbiome, and its specific mechanism in pulmonary fibrosis is not clear. In the future, in addition to the phenomenon of the changes in the gut microbiome and metabolites in pulmonary fibrosis, more research should be performed on their specific participation mechanisms. At present, the results of the gut microbiome and metabolites have been reported for clinical application. In the future, a deeper understanding of the association of the gut microbiome and metabolites with pulmonary fibrosis could provide a basis for finding diagnostic, therapeutic and prognostic targets.

## Author contributions

YIW and YhL wrote the review. CyT and YL contributed to the theme and structure of the review. YZ, JW, LC, XpL, and TW contributed to the literature search and summary. CyT, YL, and YbL made important modifications to important intellectual content. All authors read and approved the final manuscript.

## Funding

This work was supported by the National Natural Science Foundation of China (82001728 and 81973540), 1-3-5 project for Outstanding interdisciplinary project of West China Hospital, Sichuan University (ZYGD18015, ZYJC18003, and ZYJC18024), Sichuan Science and Technology Program (20YYJC3358), from zero to one Innovative Research Program of Sichuan University (2022SCUH0020).

## Conflict of interest

The authors declare that the research was conducted in the absence of any commercial or financial relationships that could be construed as a potential conflict of interest.

## Publisher's note

All claims expressed in this article are solely those of the authors and do not necessarily represent those of their affiliated organizations, or those of the publisher, the editors and the reviewers. Any product that may be evaluated in this article, or claim that may be made by its manufacturer, is not guaranteed or endorsed by the publisher.



## References

- Andréasson, K., Alrawi, Z., Persson, A., Jönsson, G., and Marsal, J. (2016). Intestinal dysbiosis is common in systemic sclerosis and associated with gastrointestinal and extraintestinal features of disease. *Arthritis Res. Ther.* 18:278. doi: 10.1186/s13075-016-1182-z
- Bai, L., Bernard, K., Tang, X., Hu, M., Horowitz, J. C., Thannickal, V. J., et al. (2019). Glutaminolysis epigenetically regulates antiapoptotic gene expression in idiopathic pulmonary fibrosis fibroblasts. *Am. J. Respir. Cell Mol. Biol.* 60, 49–57. doi: 10.1165/rcmb.2018-0180OC
- Barnes, H., Goh, N. S. L., Leong, T. L., and Hoy, R. (2019). Silica-associated lung disease: an old-world exposure in modern industries. *Respirology* 24, 1165–1175. doi: 10.1111/resp.13695
- Bernard, K., Logsdon, N. J., Benavides, G. A., Sanders, Y., Zhang, J., Darley-Usmar, V. M., et al. (2018). Glutaminolysis is required for transforming growth factor- $\beta$ 1-induced myofibroblast differentiation and activation. *J. Biol. Chem.* 293, 1218–1228. doi: 10.1074/jbc.RA117.000444
- Birjandi, S. Z., Palchevskiy, V., Xue, Y. Y., Nunez, S., Kern, R., Weigt, S. S., et al. (2016). CD4(+)CD25(hi)Foxp3(+) cells exacerbate bleomycin-induced pulmonary fibrosis. *Am. J. Pathol.* 186, 2008–2020. doi: 10.1016/j.ajpath.2016.03.020
- Boets, E., Gomand, S. V., Deroover, L., Preston, T., Vermeulen, K., De Preter, V., et al. (2017). Systemic availability and metabolism of colonic-derived short-chain fatty acids in healthy subjects: a stable isotope study. *J. Physiol.* 595, 541–555. doi: 10.1111/jp.272613
- Boveda-Ruiz, D., D'Alessandro-Gabazza, C. N., Toda, M., Takagi, T., Naito, M., Matsushima, Y., et al. (2013). Differential role of regulatory T cells in early and late stages of pulmonary fibrosis. *Immunobiology* 218, 245–254. doi: 10.1016/j.imbio.2012.05.020
- Bronte, V., and Zanovello, P. (2005). Regulation of immune responses by L-arginine metabolism. *Nat. Rev. Immunol.* 5, 641–654. doi: 10.1038/nri1668
- Chao, P. J., Lee, H. F., Lan, J. H., Guo, S. S., Ting, H. M., Huang, Y. J., et al. (2017). Propensity-score-matched evaluation of the incidence of radiation pneumonitis and secondary cancer risk for breast cancer patients treated with IMRT/VMAT. *Sci. Rep.* 7:13771. doi: 10.1038/s41598-017-14145-x
- Chen, B., Cai, H. R., Xue, S., You, W. J., Liu, B., and Jiang, H. D. (2016). Bile acids induce activation of alveolar epithelial cells and lung fibroblasts through farnesoid X receptor-dependent and independent pathways. *Respirology* 21, 1075–1080. doi: 10.1111/resp.12815
- Chen, B., You, W. J., Liu, X. Q., Xue, S., Qin, H., and Jiang, H. D. (2017). Chronic microaspiration of bile acids induces lung fibrosis through multiple mechanisms in rats. *Clin. Sci.* 131, 951–963. doi: 10.1042/cs20160926
- Chen, J., Ghazawi, F. M., Bakkar, W., and Li, Q. (2006). Valproic acid and butyrate induce apoptosis in human cancer cells through inhibition of gene expression of Akt/protein kinase B. *Mol. Cancer* 5:71. doi: 10.1186/1476-4598-5-71
- Chen, Q., Kirk, K., Shurubor, Y. I., Zhao, D., Arreguin, A. J., Shahi, I., et al. (2018). Rewiring of glutamine metabolism is a bioenergetic adaptation of human cells with mitochondrial DNA mutations. *Cell Metab.* 27, 1007.e5–1025.e5. doi: 10.1016/j.cmet.2018.03.002
- Chen, Z. Y., Xiao, H. W., Dong, J. L., Li, Y., Wang, B., Fan, S. J., et al. (2021). Gut microbiota-derived PGF2 $\alpha$  fights against radiation-induced lung toxicity through the MAPK/NF- $\kappa$ B pathway. *Antioxidants* 11:65. doi: 10.3390/antiox11010065
- Chioma, O. S., Hesse, L. E., Chapman, A., and Drake, W. P. (2021). Role of the microbiome in interstitial lung diseases. *Front. Med.* 8:595522. doi: 10.3389/fmed.2021.595522
- Chung, J., Bauer, D. E., Ghamari, A., Nizzi, C. P., Deck, K. M., Kingsley, P. D., et al. (2015). The mTORC1/4E-BP pathway coordinates hemoglobin production with L-leucine availability. *Sci. Signal.* 8:ra34. doi: 10.1126/scisignal.aaa5903
- Cruz, C. S., Ricci, M. F., and Vieira, A. T. (2021). Gut microbiota modulation as a potential target for the treatment of lung infections. *Front. Pharmacol.* 12:724033. doi: 10.3389/fphar.2021.724033
- Cummings, N. E., Williams, E. M., Kasza, I., Konon, E. N., Schaid, M. D., Schmidt, B. A., et al. (2018). Restoration of metabolic health by decreased consumption of branched-chain amino acids. *J. Physiol.* 596, 623–645. doi: 10.1113/jp275075
- Denton, C. P., and Khanna, D. (2017). Systemic sclerosis. *Lancet* 390, 1685–1699. doi: 10.1016/s0140-6736(17)30933-9
- Dickson, R. P., Erb-Downward, J. R., Falkowski, N. R., Hunter, E. M., Ashley, S. L., and Huffnagle, G. B. (2018). The lung microbiota of healthy mice are highly variable, cluster by environment, and reflect variation in baseline lung innate immunity. *Am. J. Respir. Crit. Care Med.* 198, 497–508. doi: 10.1164/rccm.201711-2180OC
- Duru, N., Wolfson, B., and Zhou, Q. (2016). Mechanisms of the alternative activation of macrophages and non-coding RNAs in the development of radiation-induced lung fibrosis. *World J. Biol. Chem.* 7, 231–239. doi: 10.4331/wjbc.v7.i4.231
- Fang, L., Chen, H., Kong, R., and Que, J. (2020). Endogenous tryptophan metabolite 5-Methoxytryptophan inhibits pulmonary fibrosis by downregulating the TGF- $\beta$ /SMAD3 and PI3K/AKT signaling pathway. *Life Sci.* 260:118399. doi: 10.1016/j.lfs.2020.118399
- Fleckenstein, K., Gauter-Fleckenstein, B., Jackson, I. L., Rabbani, Z., Anscher, M., and Vujaskovic, Z. (2007). Using biological markers to predict risk of radiation injury. *Semin. Radiat. Oncol.* 17, 89–98. doi: 10.1016/j.semradonc.2006.11.004
- Fretheim, H., Chung, B. K., Didriksen, H., Bækkevold, E. S., Midtvedt, Ø., Brunborg, C., et al. (2020). Fecal microbiota transplantation in systemic sclerosis: a double-blind, placebo-controlled randomized pilot trial. *PLoS One* 15:e0232739. doi: 10.1371/journal.pone.0232739
- Fu, A., Alvarez-Perez, J. C., Avizonis, D., Kin, T., Ficarro, S. B., Choi, D. W., et al. (2020). Glucose-dependent partitioning of arginine to the urea cycle protects  $\beta$ -cells from inflammation. *Nat. Metab.* 2, 432–446. doi: 10.1038/s42255-020-0199-4
- Gao, L., Zhang, J. H., Chen, X. X., Ren, H. L., Feng, X. L., Wang, J. L., et al. (2019). Combination of L-Arginine and L-Norvaline protects against pulmonary fibrosis progression induced by bleomycin in mice. *Biomed. Pharmacother.* 113:108768. doi: 10.1016/j.biopha.2019.108768
- Gaugg, M. T., Engler, A., Bregy, L., Nussbaumer-Ochsner, Y., Eiffert, L., Bruderer, T., et al. (2019). Molecular breath analysis supports altered amino acid metabolism in idiopathic pulmonary fibrosis. *Respirology* 24, 437–444. doi: 10.1111/resp.13465
- Ghorbani, P., Santhakumar, P., Hu, Q., Djiaideu, P., Wolever, T. M., Palaniyar, N., et al. (2015). Short-chain fatty acids affect cystic fibrosis airway inflammation and bacterial growth. *Eur. Respir. J.* 46, 1033–1045. doi: 10.1183/09031936.00143614
- Glatzová, D., Mavila, H., Saija, M. C., Chum, T., Cwiklik, L., Brdička, T., et al. (2021). The role of prolines and glycine in the transmembrane domain of LAT. *FEBS J.* 288, 4039–4052. doi: 10.1111/febs.15713
- Gong, G. C., Song, S. R., and Su, J. (2021). Pulmonary fibrosis alters gut microbiota and associated metabolites in mice: an integrated 16S and metabolomics analysis. *Life Sci.* 264:118616. doi: 10.1016/j.lfs.2020.118616
- Hamanaka, R. B., O'Leary, E. M., Witt, L. J., Tian, Y., Gökalp, G. A., Meliton, A. Y., et al. (2019). Glutamine metabolism is required for collagen protein synthesis in lung fibroblasts. *Am. J. Respir. Cell Mol. Biol.* 61, 597–606. doi: 10.1165/rcmb.2019-0008OC
- Han, M. K., Zhou, Y., Murray, S., Tayob, N., Noth, I., Lama, V. N., et al. (2014). Lung microbiome and disease progression in idiopathic pulmonary fibrosis: an analysis of the COMET study. *Lancet Respir. Med.* 2, 548–556. doi: 10.1016/s2213-2600(14)70069-4
- Hatazawa, Y., Qian, K., Gong, D. W., and Kamei, Y. (2018). PGC-1 $\alpha$  regulates alanine metabolism in muscle cells. *PLoS One* 13:e0190904. doi: 10.1371/journal.pone.0190904
- Hnia, K., Gayraud, J., Hugon, G., Ramonatxo, M., De La Porte, S., Matecki, S., et al. (2008). L-arginine decreases inflammation and modulates the nuclear factor-kappaB/matrix metalloproteinase cascade in mdx muscle fibrosis. *Am. J. Pathol.* 172, 1509–1519. doi: 10.2353/ajpath.2008.071009
- Huang, Y., Ma, S. F., Espindola, M. S., Vij, R., Oldham, J. M., Huffnagle, G. B., et al. (2017). Microbes are associated with host innate immune response in idiopathic pulmonary fibrosis. *Am. J. Respir. Crit. Care Med.* 196, 208–219. doi: 10.1164/rccm.201607-1525OC
- Invernizzi, R., Wu, B. G., Barnett, J., Ghai, P., Kingston, S., Hewitt, R. J., et al. (2021). The respiratory microbiome in chronic hypersensitivity pneumonitis is distinct from that of idiopathic pulmonary fibrosis. *Am. J. Respir. Crit. Care Med.* 203, 339–347. doi: 10.1164/rccm.202002-0460OC
- Jablonski, R. P., Kim, S. J., Cheres, P., Williams, D. B., Morales-Nebreda, L., Cheng, Y., et al. (2017). SIRT3 deficiency promotes lung fibrosis by augmenting alveolar epithelial cell mitochondrial DNA damage and apoptosis. *FASEB J.* 31, 2520–2532. doi: 10.1096/fj.201601077R
- Jian, H., Miao, S., Liu, Y., Wang, X., Xu, Q., Zhou, W., et al. (2021). Dietary valine ameliorated gut health and accelerated the development of nonalcoholic fatty liver disease of laying hens. *Oxid. Med. Cell Longev.* 2021:4704771. doi: 10.1155/2021/4704771

- Kadota, T., Yoshioka, Y., Fujita, Y., Araya, J., Minagawa, S., Hara, H., et al. (2020). Extracellular vesicles from fibroblasts induce epithelial-cell senescence in pulmonary fibrosis. *Am. J. Respir. Cell Mol. Biol.* 63, 623–636. doi: 10.1165/rcmb.2020-0002OC
- Kalchiem-Dekel, O., Galvin, J. R., Burke, A. P., Atamas, S. P., and Todd, N. W. (2018). Interstitial lung disease and pulmonary fibrosis: a practical approach for general medicine physicians with focus on the medical history. *J. Clin. Med.* 7:476. doi: 10.3390/jcm7120476
- Kamio, K., Azuma, A., Matsuda, K., Usuki, J., Inomata, M., Morinaga, A., et al. (2018). Resolution of bleomycin-induced murine pulmonary fibrosis via a splenic lymphocyte subpopulation. *Respir. Res.* 19:71. doi: 10.1186/s12931-018-0783-2
- Kc, D., Sumner, R., and Lippmann, S. (2020). Gut microbiota and health. *Postgrad. Med.* 132:274. doi: 10.1080/00325481.2019.1662711
- Khalili, M., Alavi, M., Esmacil-Jamaat, E., Baluchnejadmojarad, T., and Roghani, M. (2018). Trigonelline mitigates lipopolysaccharide-induced learning and memory impairment in the rat due to its anti-oxidative and anti-inflammatory effect. *Int. Immunopharmacol.* 61, 355–362. doi: 10.1016/j.intimp.2018.06.019
- King, T. E. Jr., Pardo, A., and Selman, M. (2011). Idiopathic pulmonary fibrosis. *Lancet* 378, 1949–1961. doi: 10.1016/s0140-6736(11)60052-4
- Klingsberg, F., Hinz, B., and White, E. S. (2013). The myofibroblast matrix: implications for tissue repair and fibrosis. *J. Pathol.* 229, 298–309. doi: 10.1002/path.4104
- Kolb, M., and Vašáková, M. (2019). The natural history of progressive fibrosing interstitial lung diseases. *Respir. Res.* 20:57. doi: 10.1186/s12931-019-1022-1
- Lei, L., Zhao, C., Qin, F., He, Z. Y., Wang, X., and Zhong, X. N. (2016). Th17 cells and IL-17 promote the skin and lung inflammation and fibrosis process in a bleomycin-induced murine model of systemic sclerosis. *Clin. Exp. Rheumatol.* 100, 14–22.
- Li, J. M., Yang, D. C., Oldham, J., Linderholm, A., Zhang, J., Liu, J., et al. (2021). Therapeutic targeting of argininosuccinate synthase 1 (ASS1)-deficient pulmonary fibrosis. *Mol. Ther.* 29, 1487–1500. doi: 10.1016/j.yjmt.2021.01.028
- Lou, Q., Liu, R., Yang, X., Li, W., Huang, L., Wei, L., et al. (2019). miR-448 targets IDO1 and regulates CD8(+) T cell response in human colon cancer. *J. Immunother. Cancer* 7:210. doi: 10.1186/s40425-019-0691-0
- Lynch, S. V., and Pedersen, O. (2016). The human intestinal microbiome in health and disease. *N. Engl. J. Med.* 375, 2369–2379. doi: 10.1056/NEJMr1600266
- Maarsingh, H., Zaagsma, J., and Meurs, H. (2008). Arginine homeostasis in allergic asthma. *Eur. J. Pharmacol.* 585, 375–384. doi: 10.1016/j.ejphar.2008.02.096
- Macfarlane, G. T., and Macfarlane, S. (2012). Bacteria, colonic fermentation, and gastrointestinal health. *J. AOAC Int.* 95, 50–60. doi: 10.5740/jaoacint.sge\_macfarlane
- Marsland, B. J., Trompette, A., and Gollwitzer, E. S. (2015). The gut-lung axis in respiratory disease. *Ann. Am. Thorac. Soc.* 12(Suppl. 2), S150–S156. doi: 10.1513/AnnalsATS.201503-133AW
- Martinez, F. J., Collard, H. R., Pardo, A., Raghu, G., Richeldi, L., Selman, M., et al. (2017). Idiopathic pulmonary fibrosis. *Nat. Rev. Dis. Primers* 3:17074. doi: 10.1038/nrdp.2017.74
- Mayadas, T. N., Cullere, X., and Lowell, C. A. (2014). The multifaceted functions of neutrophils. *Annu. Rev. Pathol.* 9, 181–218. doi: 10.1146/annurev-pathol-020712-164023
- Mehta, H., Goulet, P. O., Mashiko, S., Desjardins, J., Pérez, G., Koenig, M., et al. (2017). Early-life antibiotic exposure causes intestinal dysbiosis and exacerbates skin and lung pathology in experimental systemic sclerosis. *J. Invest. Dermatol.* 137, 2316–2325. doi: 10.1016/j.jid.2017.06.019
- Milara, J., Hernandez, G., Ballester, B., Morell, A., Roger, I., Montero, P., et al. (2018). The JAK2 pathway is activated in idiopathic pulmonary fibrosis. *Respir. Res.* 19:24. doi: 10.1186/s12931-018-0728-9
- Mills, C. D. (2012). M1 and M2 macrophages: oracles of health and disease. *Crit. Rev. Immunol.* 32, 463–488. doi: 10.1615/critrevimmunol.v32.i6.10
- Mirkoviae, B., Murray, M. A., Lavelle, G. M., Molloy, K., Azim, A. A., Gunaratnam, C., et al. (2015). The role of short-chain fatty acids, produced by anaerobic bacteria, in the cystic fibrosis airway. *Am. J. Respir. Crit. Care Med.* 192, 1314–1324. doi: 10.1164/rccm.201505-0943OC
- Niese, K. A., Chiamonte, M. G., Ellies, L. G., Rothenberg, M. E., and Zimmermann, N. (2010). The cationic amino acid transporter 2 is induced in inflammatory lung models and regulates lung fibrosis. *Respir. Res.* 11:87. doi: 10.1186/1465-9921-11-87
- Noguchi, S., Eitoku, M., Moriya, S., Kondo, S., Kiyosawa, H., Watanabe, T., et al. (2015). Regulation of gene expression by sodium valproate in epithelial-to-mesenchymal transition. *Lung* 193, 691–700.
- Park, H. J., Jeong, O. Y., Chun, S. H., Cheon, Y. H., Kim, M., Kim, S., et al. (2021). Butyrate improves skin/lung fibrosis and intestinal dysbiosis in bleomycin-induced mouse models. *Int. J. Mol. Sci.* 22:2765. doi: 10.3390/ijms22052765
- Parker, M. W., Rossi, D., Peterson, M., Smith, K., Sikström, K., White, E. S., et al. (2014). Fibrotic extracellular matrix activates a profibrotic positive feedback loop. *J. Clin. Invest.* 124, 1622–1635. doi: 10.1172/jci71386
- Perelas, A., Silver, R. M., Arrossi, A. V., and Highland, K. B. (2020). Systemic sclerosis-associated interstitial lung disease. *Lancet Respir. Med.* 8, 304–320. doi: 10.1016/s2213-2600(19)30480-1
- Raghu, G., Remy-Jardin, M., Myers, J. L., Richeldi, L., Ryerson, C. J., Lederer, D. J., et al. (2018). Diagnosis of idiopathic pulmonary fibrosis. an official ATS/ERS/JRS/ALAT clinical practice guideline. *Am. J. Respir. Crit. Care Med.* 198, e4–e68. doi: 10.1164/rccm.201807-1255ST
- Reilkoff, R. A., Peng, H., Murray, L. A., Peng, X., Russell, T., Montgomery, R., et al. (2013). Semaphorin 7a+ regulatory T cells are associated with progressive idiopathic pulmonary fibrosis and are implicated in transforming growth factor- $\beta$ 1-induced pulmonary fibrosis. *Am. J. Respir. Crit. Care Med.* 187, 180–188. doi: 10.1164/rccm.201206-1109OC
- Ren, W., Liu, G., Yin, J., Tan, B., Wu, G., Bazer, F. W., et al. (2017). Amino acid transporters in T-cell activation and differentiation. *Cell Death Dis.* 8:e2655. doi: 10.1038/cddis.2016.222
- Richards, L. B., Li, M., Folkerts, G., Henricks, P. A. J., Garssen, J., and van Esch, B. (2020). Butyrate and propionate restore the cytokine and house dust mite compromised barrier function of human bronchial airway epithelial cells. *Int. J. Mol. Sci.* 22:65. doi: 10.3390/ijms22010065
- Richter, A. G., Stockley, R. A., Harper, L., and Thickett, D. R. (2009). Pulmonary infection in Wegener granulomatosis and idiopathic pulmonary fibrosis. *Thorax* 64, 692–697. doi: 10.1136/thx.2008.110445
- Roque, W., and Romero, F. (2021). Cellular metabolomics of pulmonary fibrosis, from amino acids to lipids. *Am. J. Physiol. Cell Physiol.* 320, C689–C695. doi: 10.1152/ajpcell.00586.2020
- Rothhammer, V., and Quintana, F. J. (2019). The aryl hydrocarbon receptor: an environmental sensor integrating immune responses in health and disease. *Nat. Rev. Immunol.* 19, 184–197. doi: 10.1038/s41577-019-0125-8
- Round, J. L., and Mazmanian, S. K. (2010). Inducible Foxp3+ regulatory T-cell development by a commensal bacterium of the intestinal microbiota. *Proc. Natl. Acad. Sci. U.S.A.* 107, 12204–12209. doi: 10.1073/pnas.0909122107
- Sakai, N., and Tager, A. M. (2013). Fibrosis of two: epithelial cell-fibroblast interactions in pulmonary fibrosis. *Biochim. Biophys. Acta* 1832, 911–921. doi: 10.1016/j.bbdis.2013.03.001
- Segal, L. N., Clemente, J. C., Li, Y., Ruan, C., Cao, J., Danckers, M., et al. (2017). Anaerobic bacterial fermentation products increase tuberculosis risk in antiretroviral-drug-treated HIV patients. *Cell Host Microbe* 21, 530.e4–537.e4. doi: 10.1016/j.chom.2017.03.003
- Selman, M., and Pardo, A. (2014). Revealing the pathogenic and aging-related mechanisms of the enigmatic idiopathic pulmonary fibrosis. an integral model. *Am. J. Respir. Crit. Care Med.* 189, 1161–1172. doi: 10.1164/rccm.201312-2221PP
- Singh, N., Gurav, A., Sivaprakasam, S., Brady, E., Padia, R., Shi, H., et al. (2014). Activation of Gpr109a, receptor for niacin and the commensal metabolite butyrate, suppresses colonic inflammation and carcinogenesis. *Immunity* 40, 128–139. doi: 10.1016/j.immuni.2013.12.007
- Sittig, S. P., van Beek, J. J. P., Flórez-Grau, G., Weiden, J., Buschow, S. I., van der Net, M. C., et al. (2021). Human type 1 and type 2 conventional dendritic cells express indoleamine 2,3-dioxygenase 1 with functional effects on T cell priming. *Eur. J. Immunol.* 51, 1494–1504. doi: 10.1002/eji.202048580
- Smirnova, N. F., Schamberger, A. C., Nayakanti, S., Hatz, R., Behr, J., and Eickelberg, O. (2016). Detection and quantification of epithelial progenitor cell populations in human healthy and IPF lungs. *Respir. Res.* 17:83. doi: 10.1186/s12931-016-0404-x
- Takei, H., Yasuoka, H., Yoshimoto, K., and Takeuchi, T. (2020). Aryl hydrocarbon receptor signals attenuate lung fibrosis in the bleomycin-induced mouse model for pulmonary fibrosis through increase of regulatory T cells. *Arthritis Res. Ther.* 22:20. doi: 10.1186/s13075-020-2112-7
- Tomé, D. (2018). The roles of dietary glutamate in the intestine. *Ann. Nutr. Metab.* 73(Suppl. 5), 15–20. doi: 10.1159/000494777
- Valenzi, E., Tabib, T., Papazoglou, A., Sembrat, J., Trejo Bittar, H. E., Rojas, M., et al. (2021). Disparate interferon signaling and shared aberrant basaloid cells in single-cell profiling of idiopathic pulmonary fibrosis and systemic sclerosis-associated interstitial lung disease. *Front. Immunol.* 12:595811. doi: 10.3389/fimmu.2021.595811

- Volkman, E. R., Chang, Y. L., Barroso, N., Furst, D. E., Clements, P. J., Gorn, A. H., et al. (2016). Association of systemic sclerosis with a unique colonic microbial consortium. *Arthritis Rheumatol.* 68, 1483–1492. doi: 10.1002/art.39572
- Wang, B., Feng, L., Jiang, W. D., Wu, P., Kuang, S. Y., Jiang, J., et al. (2015). Copper-induced tight junction mRNA expression changes, apoptosis and antioxidant responses via NF- $\kappa$ B, TOR and Nrf2 signaling molecules in the gills of fish: preventive role of arginine. *Aquat. Toxicol.* 158, 125–137.
- Wang, Y., Zhao, J., Zhang, H., and Wang, C. Y. (2021). Arginine is a key player in fibroblasts during the course of IPF development. *Mol. Ther.* 29, 1361–1363. doi: 10.1016/j.ymthe.2021.02.023
- Wang, Y. F., Hsu, Y. J., Wu, H. F., Lee, G. L., Yang, Y. S., Wu, J. Y., et al. (2016). Endothelium-derived 5-methoxytryptophan is a circulating anti-inflammatory molecule that blocks systemic inflammation. *Circ. Res.* 119, 222–236. doi: 10.1161/circresaha.116.308559
- Wu, G., Meininger, C. J., McNeal, C. J., Bazer, F. W., and Rhoads, J. M. (2021). Role of L-arginine in nitric oxide synthesis and health in humans. *Adv. Exp. Med. Biol.* 1332, 167–187. doi: 10.1007/978-3-030-74180-8\_10
- Wynn, T. A., and Vannella, K. M. (2016). Macrophages in tissue repair, regeneration, and fibrosis. *Immunity* 44, 450–462.
- Xu, Y., Mizuno, T., Sridharan, A., Du, Y., Guo, M., Tang, J., et al. (2016). Single-cell RNA sequencing identifies diverse roles of epithelial cells in idiopathic pulmonary fibrosis. *JCI Insight* 1:e90558. doi: 10.1172/jci.insight.90558
- Yang, J., and Rose, D. J. (2014). Long-term dietary pattern of fecal donor correlates with butyrate production and markers of protein fermentation during in vitro fecal fermentation. *Nutr. Res.* 34, 749–759. doi: 10.1016/j.nutres.2014.08.006
- Yue, Y., Huang, W., Liang, J., Guo, J., Ji, J., Yao, Y., et al. (2015). IL4I1 is a novel regulator of M2 macrophage polarization that can inhibit T cell activation via L-tryptophan and arginine depletion and IL-10 production. *PLoS One* 10:e0142979. doi: 10.1371/journal.pone.0142979
- Zhou, Y., Chen, L., Sun, G., Li, Y., and Huang, R. (2019). Alterations in the gut microbiota of patients with silica-induced pulmonary fibrosis. *J. Occup. Med. Toxicol.* 14:5. doi: 10.1186/s12995-019-0225-1
- Zhu, P., Xing, S., Xu, Q., Xie, T., Gao, Y., and He, Z. (2016). [Effect and mechanism of inhibition of lipopolysaccharide-induced pulmonary fibrosis by butyric acid]. *Zhonghua Wei Zhong Bing Ji Jiu Yi Xue* 28, 8–14. doi: 10.3760/cma.j.issn.2095-4352.2016.01.003



## OPEN ACCESS

## EDITED BY

Cong-Qiu Chu,  
Oregon Health and Science University,  
United States

## REVIEWED BY

Shulan Su,  
Nanjing University of Chinese  
Medicine, China  
Zhu Chen,  
University of Science and Technology  
of China, China

## \*CORRESPONDENCE

Yi Zhao  
zhao.y1977@163.com  
Shilin Li  
lishilineagle@163.com  
Fanxin Zeng  
zengfx@pku.edu.cn

†These authors have contributed  
equally to this work

## SPECIALTY SECTION

This article was submitted to  
Microbial Symbioses,  
a section of the journal  
Frontiers in Microbiology

RECEIVED 29 April 2022

ACCEPTED 19 August 2022

PUBLISHED 18 October 2022

## CITATION

Zhu J, Wang T, Lin Y, Xiong M, Chen J,  
Jian C, Zhang J, Xie H, Zeng F,  
Huang Q, Su J, Zhao Y, Li S and Zeng F  
(2022) The change of plasma  
metabolic profile and gut microbiome  
dysbiosis in patients with rheumatoid  
arthritis.  
*Front. Microbiol.* 13:931431.  
doi: 10.3389/fmicb.2022.931431

## COPYRIGHT

© 2022 Zhu, Wang, Lin, Xiong, Chen,  
Jian, Zhang, Xie, Zeng, Huang, Su,  
Zhao, Li and Zeng. This is an  
open-access article distributed under  
the terms of the [Creative Commons  
Attribution License \(CC BY\)](https://creativecommons.org/licenses/by/4.0/). The use,  
distribution or reproduction in other  
forums is permitted, provided the  
original author(s) and the copyright  
owner(s) are credited and that the  
original publication in this journal is  
cited, in accordance with accepted  
academic practice. No use, distribution  
or reproduction is permitted which  
does not comply with these terms.

# The change of plasma metabolic profile and gut microbiome dysbiosis in patients with rheumatoid arthritis

Jing Zhu<sup>1,2†</sup>, Tingting Wang<sup>3†</sup>, Yifei Lin<sup>4†</sup>, Minghao Xiong<sup>3</sup>,  
Jianghua Chen<sup>5</sup>, Congcong Jian<sup>6</sup>, Jie Zhang<sup>3</sup>,  
Huanhuan Xie<sup>3</sup>, Fanwei Zeng<sup>7</sup>, Qian Huang<sup>8</sup>, Jiang Su<sup>2</sup>,  
Yi Zhao<sup>1,9\*</sup>, Shilin Li<sup>3\*</sup> and Fanxin Zeng<sup>3\*</sup>

<sup>1</sup>Department of Rheumatology and Immunology, West China Hospital, Sichuan University, Chengdu, China, <sup>2</sup>Department of Rheumatology and Immunology, Sichuan Provincial People's Hospital, University of Electronic Science and Technology of China, Chengdu, China, <sup>3</sup>Department of Clinical Research Center, Dazhou Central Hospital, Dazhou, China, <sup>4</sup>Precision Medicine Center, West China Hospital, Sichuan University, Chengdu, China, <sup>5</sup>North Sichuan Medical College, Nanchong, China, <sup>6</sup>School of Basic Medical Sciences, Chengdu University of Traditional Chinese Medicine, Chengdu, China, <sup>7</sup>Sichuan Province Orthopaedic Hospital, Chengdu, China, <sup>8</sup>Dazhou Vocational and Technical College, Dazhou, China, <sup>9</sup>Frontiers Science Center for Disease-Related Molecular Network, West China Hospital, Clinical Institute of Inflammation and Immunology, Sichuan University, Chengdu, China

**Objective:** Rheumatoid arthritis (RA) is a chronic inflammatory joint disease, which is associated with progressive disability, systemic complications, and early death. But its etiology and pathogenesis are not fully understood. We aimed to investigate the alterations in plasma metabolite profiles, gut bacteria, and fungi and their role of them in the pathogenesis of RA.

**Methods:** Metabolomics profiling of plasma from 363 participants including RA ( $n = 244$ ), systemic lupus erythematosus (SLE,  $n = 50$ ), and healthy control (HC,  $n = 69$ ) were performed using the ultra-high performance liquid chromatography-quadrupole time-of-flight mass spectrometry. The differentially expressed metabolites were selected among groups and used to explore important metabolic pathways. Gut microbial diversity analysis was performed by 16S rRNA sequencing and ITS sequencing (RA = 195, HC = 269), and the specific microbial floras were identified afterward. The diagnosis models were established based on significant differential metabolites and microbial floras, respectively.

**Results:** There were 63 differential metabolites discovered between RA and HC groups, mainly significantly enriched in the arginine and proline metabolism, glycine, serine, and threonine metabolism, and glycerophospholipid metabolism between RA and HC groups. The core differential metabolites included L-arginine, creatine, D-proline, ornithine, choline, betaine, L-threonine, LysoPC (18:0), phosphorylcholine, and glycerophosphocholine. The L-arginine and phosphorylcholine were increased in the RA group. The AUC of the predictive model was 0.992,



based on the combination of the 10 differential metabolites. Compared with the SLE group, 23 metabolites increased and 61 metabolites decreased in the RA group. However, no significant metabolic pathways were enriched between RA and SLE groups. On the genus level, a total of 117 differential bacteria genera and 531 differential fungal genera were identified between RA and HC groups. The results indicated that three bacteria genera (*Eubacterium\_hallii\_group*, *Escherichia-Shigella*, *Streptococcus*) and two fungal genera (*Candida* and *Debaryomyces*) significantly increased in RA patients. The AUC was 0.80 based on a combination of six differential bacterial genera and the AUC was 0.812 based on a combination of seven differential fungal genera. Functional predictive analysis displayed that differential bacterial and differential fungus both were associated with KEGG pathways involving superpathway of L-serine and glycine biosynthesis I, arginine, ornithine, and proline interconversion.

**Conclusion:** The plasma metabolism profile and gut microbe profile changed markedly in RA. The glycine, serine, and threonine metabolism and arginine and proline metabolism played an important role in RA.

#### KEYWORDS

rheumatoid arthritis, metabolomics, gut bacterial, gut fungus, metabolic pathway

## Introduction

Rheumatoid arthritis (RA) is a systemic autoimmune disease characterized by inflammation, especially persistent synovitis, and progressive joint damage with dominant extra-articular features (Smolen et al., 2016). It affects up to 1% of the general population worldwide, regardless of age group (Smolen et al., 2018). Although strict control and targeted therapy may retard the progress of RA, it still cannot be cured completely (Smolen et al., 2020).

With the rapid development of high-throughput technologies, including mass spectrometry (MS) and nuclear magnetic resonance spectroscopy (NMRS) (Kang et al., 2015), metabolomics was initiated recently to have exceptional advantages on some novel metabolic pathways and related metabolites (Zhang et al., 2018). Since metabolites are a specific manifestation of the metabolic process, they are indicative of a certain disease state (Horgan and Kenny, 2011). A number of previous studies have claimed the potential value of metabolites for RA (Chimenti et al., 2013; Kapoor et al., 2013; Priori et al., 2015; Cuppen et al., 2016). For example, arachidonic acid metabolism, sphingolipid metabolism, and arginine and proline metabolism were found essential in the therapeutic response of RA, due to achieving sustained drug-free remission (Hu et al., 2011; Teitsma et al., 2018; Wang et al., 2021). RA and systemic lupus erythematosus (SLE) are common autoimmune diseases. In fact, these two autoimmune diseases share several clinical manifestations, serological profiles, and

immunological characteristics. However, differences in the plasma metabolic profile between RA and SLE groups are rarely reported.

Due to biological coevolution, flora metabolism has also been found to affect human health through “functional acquisition.” Numerous pathological changes are found accompanied (Grover and Kashyap, 2014; Foster et al., 2016; Tang et al., 2020). Since the significant role of intestinal flora in RA was first identified in 1968 (Olhagen and Mansson, 1968), it was further considered to be involved in potential treatment. For instance, the diversity of gut microbiota is found to decrease in RA patients (Smolen et al., 2018), while the rare taxa, that is, *Actinobacteria* increased (Chen et al., 2016). The *prevotella copri* was more common in new-RA patients than in established RA or no-RA patients (Scher et al., 2013). Thus, the gut microbiota is also suggested to be potential markers of the development of RA.

However, most studies only focused on the correlation of the RA with either a certain specific metabolite or microbial flora (Song et al., 2020; Mun et al., 2021). Very few of them can combination both plasma and fecal metabolomics to comprehensively explore their correlation with RA, not to mention constructing a predictive model to predict the development of RA. Therefore, we aimed to investigate changes in plasma metabolite profiles, gut bacteria, and fungi, and to explore their role in the pathogenesis of RA.



## Materials and methods

### Study patients

The flow chart of this study is shown in [Figure 1](#). The RA patients were diagnosed according to the American College of Rheumatology 2010 classification ([Kay and Upchurch, 2012](#)), hospitalized in the Department of Rheumatology and Immunology in Dazhou Central Hospital from November 2017 to July 2020. The RA group exclusion criteria are as follows: (1) Age < 18 years old; (2) Combination other immune metabolic diseases and complications, such as diabetes, osteoarthritis, metabolic syndrome, and infection; (3) Used probiotics and antibiotics in the last 2 weeks; (4) Tumor patients; (5) Organ failure and organ transplant patients; and (6) Pregnant women. The collected data included patients' age, gender, 28-joint tender joint count (TJC28), 28-joint swelling joint count (SJC28), C-reactive protein (CRP), erythrocyte sedimentation rate (ESR), and so on.

The healthy control (HC) group included 338 participants, who underwent health examination in Dazhou Central Hospital from May 2020 to July 2020. The disease control group included 50 SLE patients hospitalized in Dazhou Central Hospital from September 2018 to August 2020. All SLE patients were diagnosed according to the American College of Rheumatology (ACR'97) and/or Systemic Lupus International Collaborating Clinic (SLICC'12) classification criteria ([Hochberg, 1997](#); [Petri et al., 2012](#)). The plasma samples from 363 participants (244 RA, 69 HC, 50 SLE) were analyzed by non-targeted metabolomics.

The stool samples from 464 participants (195 RA and 269 HC) were used to identify the microbial biomarkers and construct the predictive model.

This study was approved by the Ethics Committee of Dazhou Central Hospital. The subjects have signed informed consent.

### Plasma sample collection

Four milliliters of fasting venous blood were drawn and placed in an anticoagulant vacuum blood collection tube (BD Vacutainer®). After the blood was collected, the samples were placed in a refrigerator at 4°C to stand still for processing within 2 h after collection. First, each tube of blood was centrifuged at 3,500 rpm, 4°C for 10 min, and the supernatant was separated into two EP tubes, and then centrifuged again at 12,000 rpm, 4°C for 10 min. Finally, the supernatant plasma was transferred

into two new EP tubes and stored in the refrigerator at -80°C.

### Untargeted metabolomics analysis by UNPLC/Q-TOF-MS

The method detail of UNPLC/Q-TOF-MS was shown in [Supplementary Method File](#). The hierarchical cluster was performed to display the relationship and difference between metabolites. The multidimensional statistical analysis, including principal component analysis (PCA), partial least-squares discriminant analysis (PLS-DA), and orthogonal partial least-squares discriminant analysis (OPLS-DA), were also performed to help cluster the metabolites. Besides, a permutation test was performed for the validation of the model. Metabolic pathways [impact < 0.2,  $-\log_{10}(p)$  value > 1.3] and greater metabolic abundance were identified by KEGG database.

### Fecal sample collection

The fresh stool was collected and delivered immediately at low temperatures, then divided into individual parts of 200 mg and stored at -80°C until extraction.

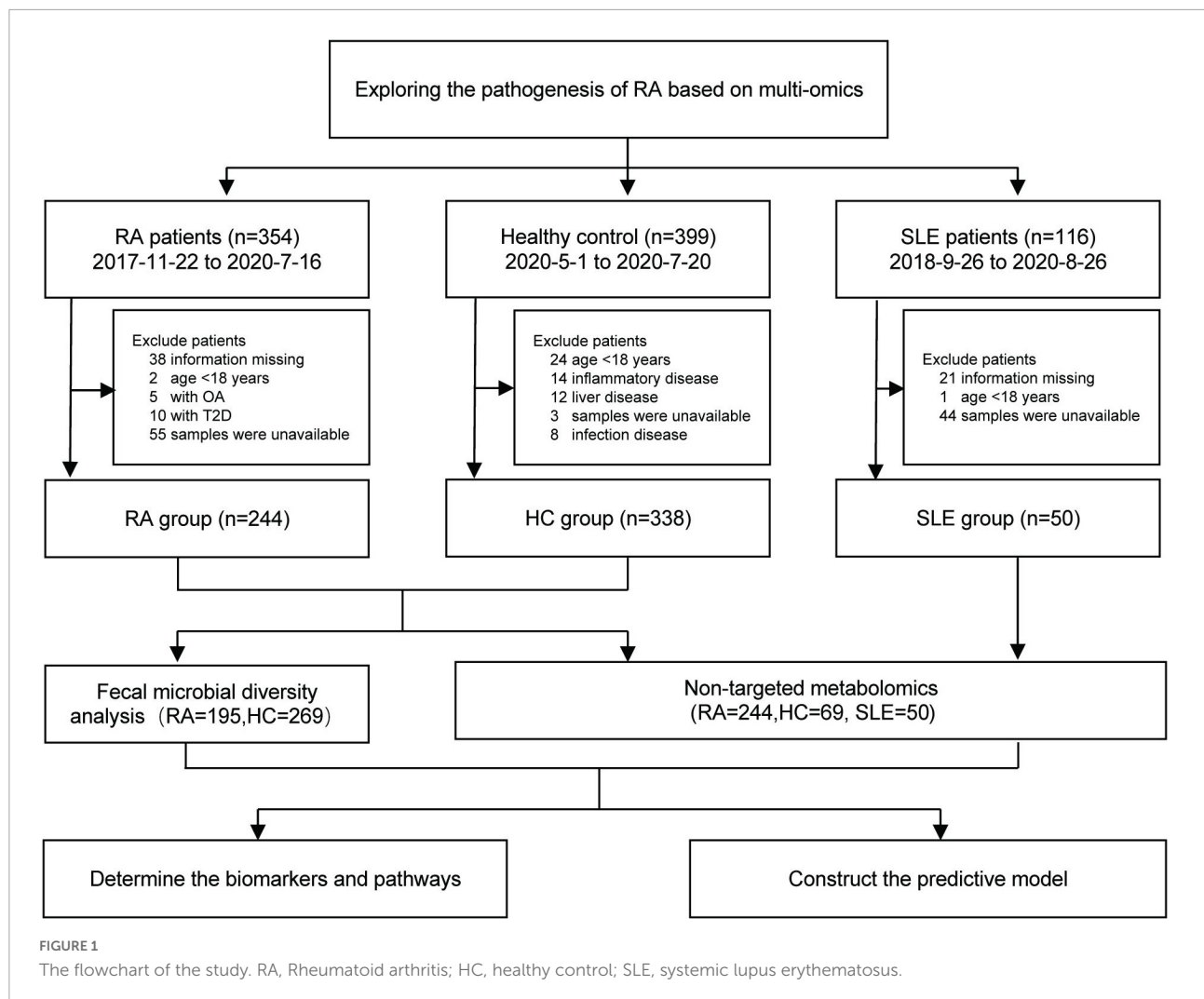
### Fecal sample DNA extraction and Illumina MiSeq sequencing

According to the manufacturer's protocol, total DNA was extracted from fecal samples. Bacterial 16S rRNA gene fragments (V3-V4) were amplified from the extracted DNA using the primers 338F ACTCCTACGGGAGGCAGCAG and 806R GGACTACHVGGGTWTCTAAT, and fungal internally transcribed spacer (ITS) gene fragments were amplified from the extracted DNA using the primers ITS1F CTTGGTCATTTAGAGGAAGTAA and ITS2R GCTGCGTTCTTCATCGATGC.

The following PCR Amplicons were subjected to paired-end sequencing on an Illumina MiSeq sequencing platform using a PE250 kit.

### Amplification sequence processing and analysis

Taxonomic assignment of ASVs was performed using the Naive Bayes consensus taxonomy classifier implemented in Qiime2 and the SILVA 16S rRNA and ITS database. ASV analysis, Community diversity analysis, Genus and Species difference analysis, model predictive



analysis, and PICRUST2 (Phylogenetic Investigation of Communities by Reconstruction of Unobserved States 2) function prediction analysis were performed based on the 16S rRNA bacterial and ITS Fungal sequencing data.

The method of microbial diversity analysis is detailed in [Supplementary Method File](#).

## Statistical analysis

The One-Way ANOVA and *t*-test were performed using SPSS Statistics (V.24.0.0.0) (SPSS Inc., Chicago, United States). The bar graph was performed using GraphPad Prism (v6.0) (GraphPad Software, Inc., CA, United States). And the Principal Co-ordinates Analysis, PCA, Phylogenetic Investigation of Communities by Reconstruction of Unobserved States, Receiver Operating

Characteristic (ROC) curve, OPLS-DA, and Correlation heat map analysis were performed using R software (Version 3.4.4).

## Results

### Baseline characteristics of healthy control, systemic lupus erythematosus, and rheumatoid arthritis participants

The baseline characteristics of the three groups are presented in [Table 1](#). The RA group included 244 patients (age,  $57.8 \pm 12.7$  years; 72.5% women), with average DAS28(3)  $5.5 \pm 1.5$ . The HC group included 338 cases (age,  $49.3 \pm 7.7$  years; 18.6% women). The disease control SLE group included 50 cases (age,  $46.2 \pm 9.4$  years; 98.0% women). There are significant differences in the other clinical indicators of

TABLE 1 The characteristics of the patients with RA or SLE and healthy controls.

Parameters	HC( <i>n</i> = 338)	RA( <i>n</i> = 244)	SLE( <i>n</i> = 50)	<i>P</i>
Age (y)	49.3 ± 7.7	57.8 ± 12.7	46.2 ± 9.4	<0.0001
Sex, F, No. (%)	63 (18.6)	177 (72.5)	49 (98)	<0.0001
RF (U/ML)	–	300.9 ± 312.3	26.0 ± 91.0	<0.0001
DAS28(3)	–	5.5 ± 1.5	–	–
CRP (mg/L)	–	43.2 ± 40.0	4.8 ± 5.8	<0.0001
ESR (mm/h)	–	68.7 ± 30.2	25.5 ± 17.1	<0.0001
TJC28	–	9.9 ± 8.8	–	–
SJC28	–	8.0 ± 8.0	–	–
WBC (10 <sup>9</sup> /L)	5.3 ± 1.3	7.2 ± 2.9	5.8 ± 2.6	<0.0001
NEUT (10 <sup>9</sup> /L)	3.2 ± 1.0	5.2 ± 2.6	2.7 ± 2.0	<0.0001
LY (10 <sup>9</sup> /L)	1.6 ± 0.4	1.3 ± 0.6	31.0 ± 32.9	<0.0001

The *p*-value < 0.05 means a significant difference between groups. RA, Rheumatoid arthritis; HC, healthy control; RF, rheumatoid factor; DAS28, Disease Activity Score 28; CRP, C-reactive protein; ESR, Erythrocyte Sedimentation Rate; TJC28, Tender 28-joint count; SJC28, Swollen 28-joint count; WBC, white blood cell; NEUT, Neutrophil; LY, lymphocyte.

the three groups, such as white blood cells, neutrophils, and lymphocytes (all *p* < 0.0001).

## Plasma metabolomics profiles of healthy control, systemic lupus erythematosus, and rheumatoid arthritis participants

Based on an untargeted metabolomics analysis by UNPLC/Q-TOF-MS, we detected 486 peaks in positive and negative ion modes. After excluding 62 metabolites by the natural isotopic peaks, the rest 424 metabolites were finally included for analysis. The PCA results of metabolites indicated that HC group could be distinguished markedly from RA and SLE groups, whereas SLE and RA groups showed less obvious separation (Supplementary Figures 1A,B). Results of the permutation test were shown in Supplementary Figures 1C,D. A total of 63 differential metabolites were identified between RA and HC groups, 21 of which increased and 42 of which decrease in the RA group compared with the HC group (Supplementary Figures 1E,F).

After KEGG pathway analysis, there were three metabolic pathways that most significantly changed between RA and HC groups, arginine and proline metabolism, glycine, serine and threonine metabolism, and glycerophospholipid metabolism (Figure 2A). Among them, a total of 10 differential metabolites were discovered, including L-arginine, creatine, D-proline, ornithine, choline, betaine, L-threonine, 1-stearoyl-2-hydroxy-sn-glycero-3-phosphocholine [LysoPC(18:0)], phosphorylcholine, and glycerophosphocholine (Figure 2B and Supplementary Table 1). The L-arginine and phosphorylcholine were increased in the RA group (all *p* < 0.01). The correlation heatmap indicated that the patient's disease activity [DAS28(3)] was negatively correlated with

glycerophosphocholine, and inflammation indicators (IL-6, CRP) were negatively correlated with D-proline, L-arginine, L-threonine, LysoPC (18:0), and glycerophosphocholine (Figure 2C). The result of the ROC analysis indicated that the predictive model showed a high discriminatory power to predict the RA status and the area under the curve (AUC) was 0.992 based on a combination of the 10 differential metabolites (Figure 2D).

Compared with the disease control, the RA and SLE groups were distinguished significantly in the OPLS-DA analysis (Figures 3A,B). A total of 84 differential metabolites were identified by the differentiated analysis (Figure 3C). Compared with the SLE group, the difference analysis result displayed 23 metabolites increased in RA patients, such as deoxycholic acid, d-galacturonic acid, and L-aspartate. The other 61 metabolites were lower in the RA group, including L-glutamine, L-threonine, and L-alanine. However, all the fold changes of differential metabolites were 0.9–1.2, and no significant metabolic pathway was enriched in the KEGG pathway analysis based on all differential metabolites between RA and SLE groups (Figure 3D).

## Gut microbiota changes of rheumatoid arthritis participants

Fecal samples were obtained from 464 human participants, including 195 RA cases and another 269 HC volunteers. Bacterial 16S rRNA and fungal ITS amplification provided a series of ASVs to analyze the difference between the two groups.

### 16S rRNA bacterial community analysis

The clear boundary described the significant difference between RA and HC groups and proved that the number of sequencing samples was sufficient. On the species level, a total of 596 bacterial species were identified between the two groups,

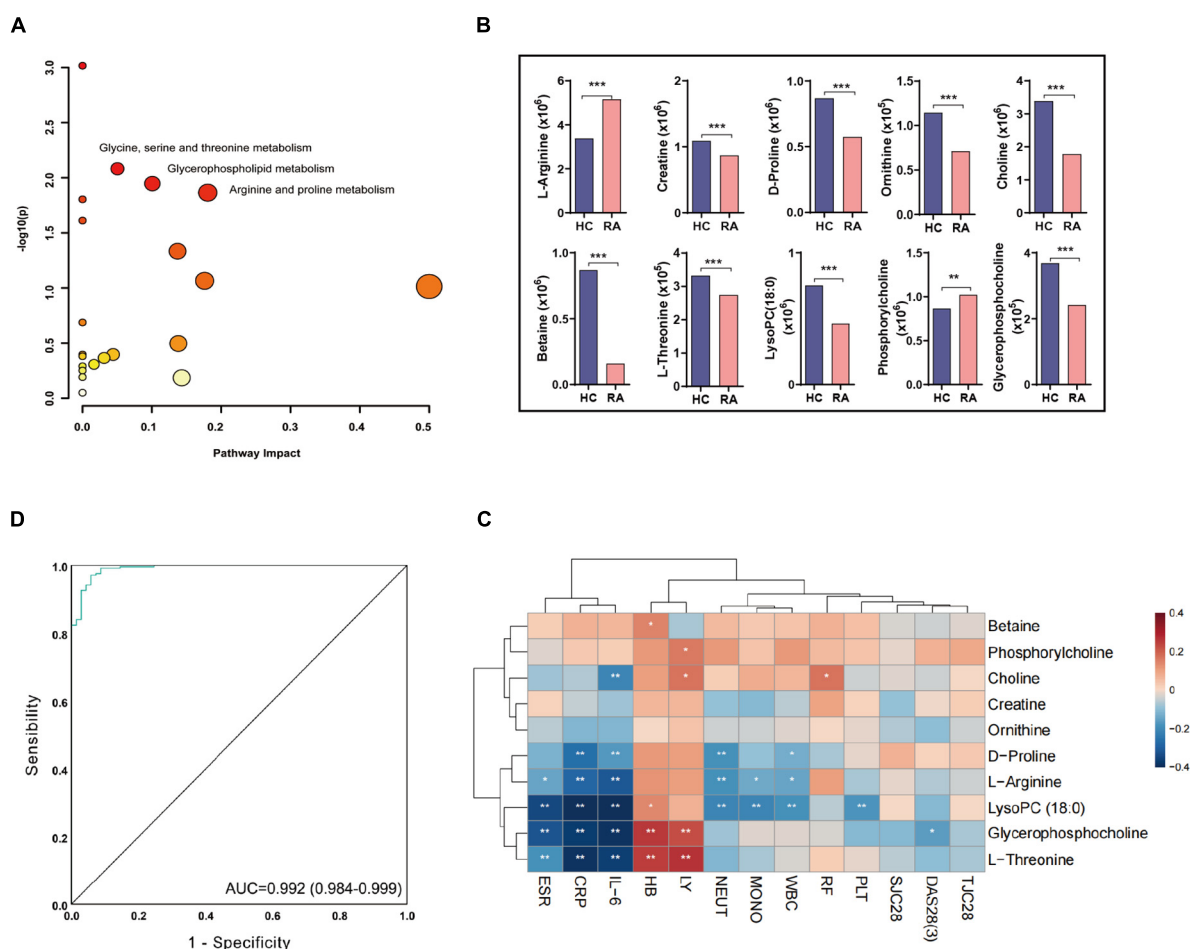


FIGURE 2

The biomarkers and pathway in RA based on plasma metabolomics. (A) The three significant pathways are based on 10 differential metabolites between RA and HCs (Pathway impact < 0.2,  $-\log_{10}(p)$  value > 1.5 and greater metabolic abundance). (B) The metabolite content differences between RA and HC. \* $P < 0.05$ , \*\* $P < 0.01$ , \*\*\* $P \leq 0.001$ . (C) The correlation heatmap between metabolites and clinical information. (D) The ROC curve of the combination of 10 differential metabolites for classifying RA patients from HC. RA, rheumatoid arthritis; HC, healthy control; DAS28, disease activity score-28; TJC28, tender joint count 28; SJC28, joint swelling count 28; ESR, erythrocyte sedimentation rate; CRP, C-reactive protein; RF, rheumatoid factor; WBC, white blood cell count; LY, lymphocyte count; NEUT, neutrophil count; MONO, monocyte count; HB, hemoglobin; PLT, platelet count; ROC, receiver operating characteristic.

including 219 unique bacterial species in the RA group and 147 unique bacterial species in HC (Supplementary Figure 2A). The beta of principal coordinates analysis (PCoA) suggested that there were significant differences in the horizontal community distribution of bacterial species between the two groups (Supplementary Figure 2B). By Wilcoxon rank-sum test, 169 differential bacterial species were identified, and the top 10 bacterial communities based on mean proportions were shown in Supplementary Figure 2C ( $p < 0.05$ ). However, most names of differential specie names could not be identified.

On the genus level, there were 293 common bacterial genera between the two groups, 68 unique genera in the RA group and 41 unique genera in the HC group (Figure 4A). The PCoA analysis displayed that there were differences in the distribution of bacterial communities between the two

groups (Figure 4B). The dominant bacteria genus in RA group includes *Blautia* (11.0%), *Faecalibacterium* (7.1%), *Escherichia-Shigella* (9.6%), *Bifidobacterium* (6.1%), *Subdoligranulum* (5.4%); the dominant bacteria genera in the HC group were *Blautia* (10.8%), *Faecalibacterium* (10.4%), *Bifidobacterium* (6.9%), *Bacteroides* (6.7%), and *Megamonas* (7.4%) (Figure 4C). A total of 117 differential bacteria genera were identified between groups by Wilcoxon rank-sum test, and the top 10 bacterial communities base on mean proportions were shown in Figure 4D ( $p < 0.05$ ). Furthermore, the results of linear discriminant analysis effect size (LEfSe) identified that six key differential bacteria genera were screened again between groups (LDA score > 4.0 and  $p < 0.05$ ), including *Eubacterium\_hallii\_group*, *Escherichia-Shigella*, *Megamonas*, *Bacteroides*, *Faecalibacterium*, and *Streptococcus* (Figure 4E).

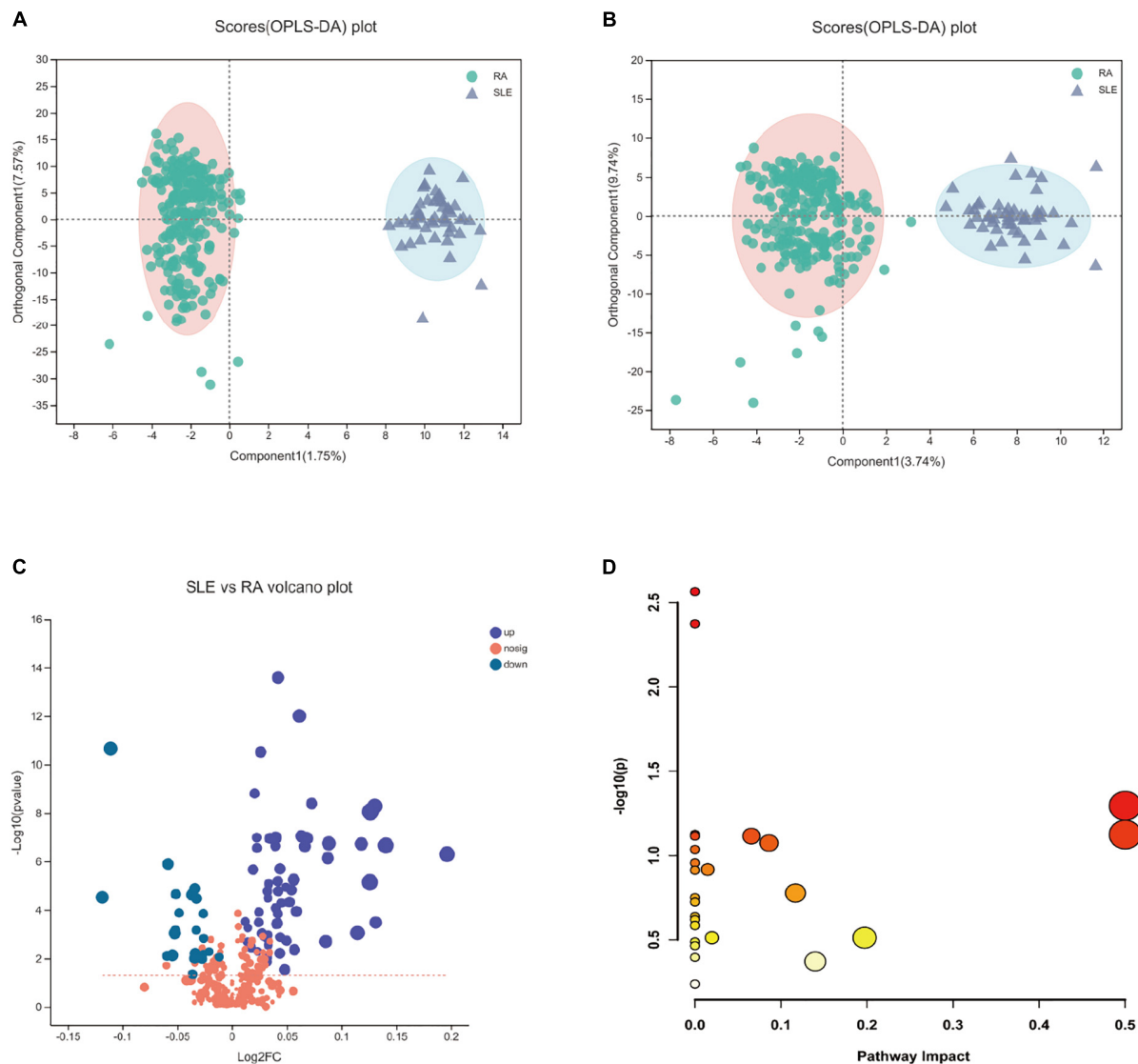


FIGURE 3

The orthogonal partial least-squares discriminant analysis (OPLS-DA) and KEGG pathway analysis in RA patients compared to SLE patients. (A,B) The OPLS-DA plots between RA and SLE, cation, and anion, respectively. (C) The volcano plot of RA vs. SLE. (D) The KEGG pathway analysis results based on the significant metabolites between RA and SLE. RA, rheumatoid arthritis; SLE, systemic lupus erythematosus.

Among them, *Eubacterium\_hallii\_group*, *Escherichia-Shigella*, and *Streptococcus* increased in RA patients. Hence, the six most important differential bacterial genera were selected for predictive model analysis, and the AUC was 0.80 of the ROC curves (Figure 4F).

### Fungal internally transcribed spacer analysis

On the fungal species level, there were 686 common fungal species between the two groups, 980 unique fungal species in the RA group, and 311 unique fungal species in HC group (Supplementary Figure 3A). The PCoA analysis on the species level showed that there were significant differences in the horizontal community distribution between the two groups

(Supplementary Figure 3B). Using Wilcoxon rank-sum test, a total of 160 differential fungal species were identified; the top 15 fungus communities based on mean proportions are shown in Supplementary Figure 3C ( $p < 0.05$ ).

On the fungal genus level, the PCoA plot of beta diversity analysis showed that there were significant differences in the distribution of fungal communities between the two groups (Figure 5A). There were 411 common fungal genera between the two groups, 401 of which were specific fungal genera in the RA group, and 117 specific fungal genera in the HC group (Figure 5B). A total of 531 differential fungal genera were identified between RA and HC groups. Community bar diagram analysis showed that there were also significant differences in



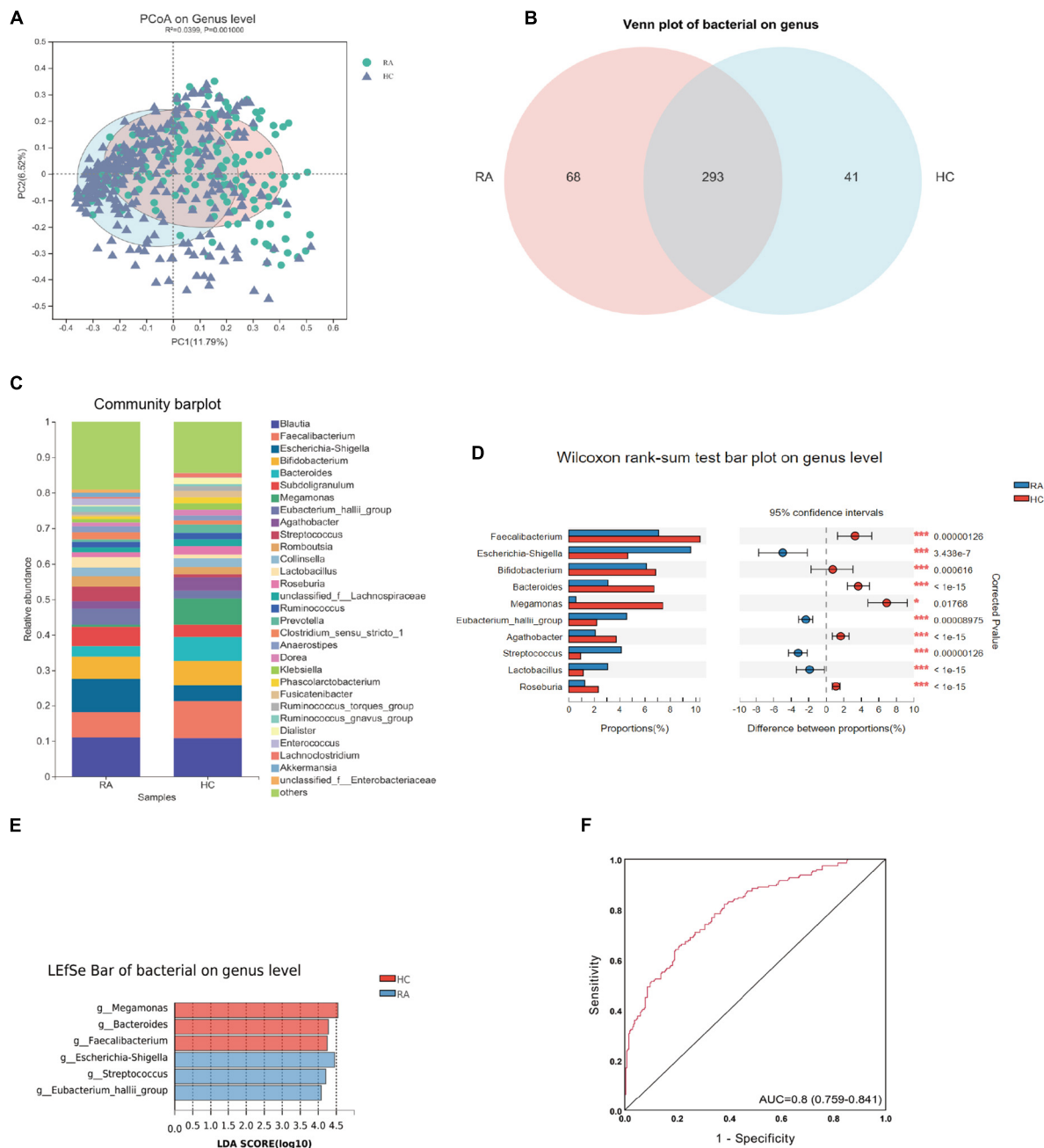


FIGURE 4

The differential bacterial flora and predicted enzymes based on 16s rRNA (genus level) between RA and HC groups. (A) The Venn plot between RA and HC groups. (B) The PCoA analysis between RA and HC. (C) The Bar graph of bacterial flora composition in RA and HC. (D) The top 10 significant bacteria between RA and HC. (E) The LDA bar of bacterial flora in RA and HC. (F) The ROC curve of the combination of six differential bacteria for classifying RA patients from HC. RA, rheumatoid arthritis; HC, healthy control; ROC, receiver operating characteristic.

the fungal composition, relative abundance, and proportion between the two groups. The dominant fungal genera in the RA group were *Candida* (41.0%), *Aspergillus* (9.3%), *Debaryomyces* (3.7%), and *Penicillium* (3.4%); and the dominant fungus genera in the HC group were *Candida* (16.3%), *Aspergillus* (11.4%), *Penicillium* (5.9%), and *Cryptococcus\_f\_Tremellaceae*

(4.4%) (Figure 5C). Using Wilcoxon rank-sum test, the top 10 fungal communities based on mean proportions are shown in Figure 5D. Specifically, *Cryptococcus*, *Apiotrichum*, *Cladosporium*, *Rhodotorula*, and *Monascus* were significantly more abundant in the HC group; and *Candida*, *Debaryomyces*, *Wallemia*, *Kazachstania*, and *Xeromycesis* were significantly

more enriched in the RA group ( $p < 0.05$ ). The LEfSe analysis result discovered that there were seven important different fungal genera between groups (LDA score  $> 4.0$ ) including *Cryptococcus*, *Penicillium*, *Aspergillus*, *Cladosporium*, *Monascus*, *Candida*, and *Debaryomyces* (Figure 5E). Specifically, the *Candida* and *Debaryomyces* both increased in RA patients. The result of the ROC analysis suggested that the AUC of the prediction model was 0.812 based on a combination of the above seven differential fungal genera (Figure 5F).

## Functional predictive analysis

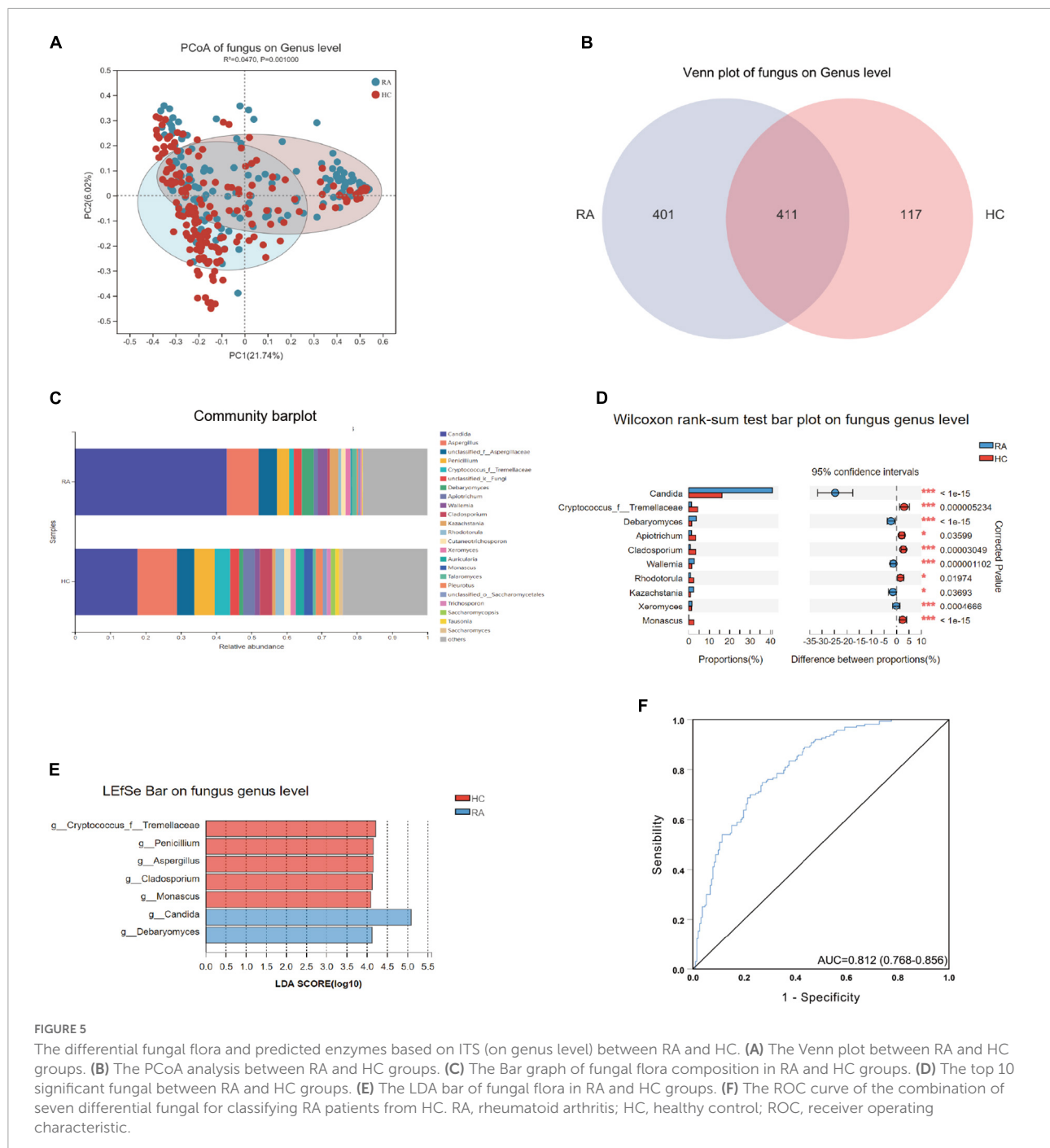
We predicted changes in modules and pathways using PICRUSt2 and calculated the mean proportion of important enzymes in modules and pathways between the RA and HC groups using the STAMP software. PICRUSt2 analysis of the bacteria suggested that these changes in the relative ASV abundance might be associated with the regulation of pathways involving superpathway of L-serine and glycine biosynthesis I, arginine, ornithine, and proline interconversion (Supplementary Figure 4). The most important enzymes associated with the above pathways were predicted, namely choline dehydrogenase, D-amino-acid oxidase, glycine amidinotransferase, betaine-aldehyde dehydrogenase, ornithine aminotransferase, and lysophospholipase (Figure 6A). The functional predictive analysis of fungus also displayed that host metabolic pathways were regulated by fungi including superpathway of L-threonine biosynthesis, urea cycle, L-proline biosynthesis II (from arginine), superpathway of L-serine and glycine biosynthesis I (Supplementary Figure 5), and predictive enzymes including choline dehydrogenase, lysophospholipase, ornithine aminotransferase, choline-phosphate cytidylyltransferase, arginase, phospholipase A (2), and glycine amidinotransferase (Figure 6B). The metabolic network diagram revealed that the three KEGG pathways were enriched based on the 10 key differential metabolites between RA and HC groups (Figure 6C). The three metabolic pathways were interconnected by creatine and choline. Finally, the correlations between metabolites, bacteria, and fungi were analyzed. The results showed that changes in amino acid metabolism were associated with changes in gut microbes in RA patients. D-Proline concentration in plasma was significantly positively correlated with the abundance of *Agathobacter*, *Roseburia*, and *Cladosporium*, and negatively correlated with *Candida*. Among bacteria, we found that *Escherichia-Shigella* abundance was positively correlated with plasma Creatine concentration, while *Bacteroides* genus was negatively correlated with plasma Creatine concentration. The plasma L-Arginine concentration is increased in RA patients and is positively correlated with *Rhodotorula* of fungi in the stool (Figure 6D).

## Discussion

As RA is a chronic autoimmune disease, its etiology has not been fully understood yet. Genetic and environmental factors are important risk factors for disease incidence and development. In this study, we mainly focused on the metabolic disorder during RA disease progression using multi-omics approaches. We sought to apply plasma metabolomics profiling and gut microbial community profile to identify potential biomarkers for predicting RA-patient. The metabolomics analysis highlighted three main metabolic pathways: the glycine, serine, and threonine metabolism, glycerophospholipid metabolism, and arginine and proline metabolism. The AUC of the multivariate prediction models based on a combination of the 10 differential metabolites was 0.992. Additionally, the 16S rRNA sequencing results showed that the intestinal bacterial diversity and bacterial structure changed significantly in RA patients compared with the HC group. The AUC of the ROC curve was 0.80 to predict the RA, based on six core differential bacterial genera (LDA  $> 4$ ). Further, the fungal diversity in RA patient group increased significantly more than in HC, and the AUC of the prediction model was 0.812 based on a combination of seven core differential fungal genera. Functional predictive analysis suggested that the superpathway of L-serine and glycine biosynthesis I, and arginine, ornithine, and proline interconversion might be regulated by bacterial and fungus. These results revealed that arginine and proline metabolism and glycine, serine, and threonine metabolism could play an important role in the disease incidence and development of RA.

The plasma metabolic changes, caused by the chronic inflammation, usually served as biomarkers for diagnosis (Chimenti et al., 2015). Our study showed that plasma levels of many kinds of amino acids (AAs) were reduced in RA patients, including L-tryptophan, L-alanine, L-threonine, and L-leucine, compared to healthy controls. These findings were similar to another study (Wang et al., 2018), which suggested that tryptophan (Trp) and glycine were decreased in patients with RA. These metabolites have been associated with immune system activation. For instance, serum alanine level was associated with synovial B-lymphocyte stimulator expression, while the serum levels of threonine and leucine were associated with synovial expression of IL-1 $\beta$  and IL-8 (Narasimhan et al., 2018). Trp, as one of the rarest essential AAs, might degrade to affect immunity through kynurenines and regulate T cells (Murray, 2016).

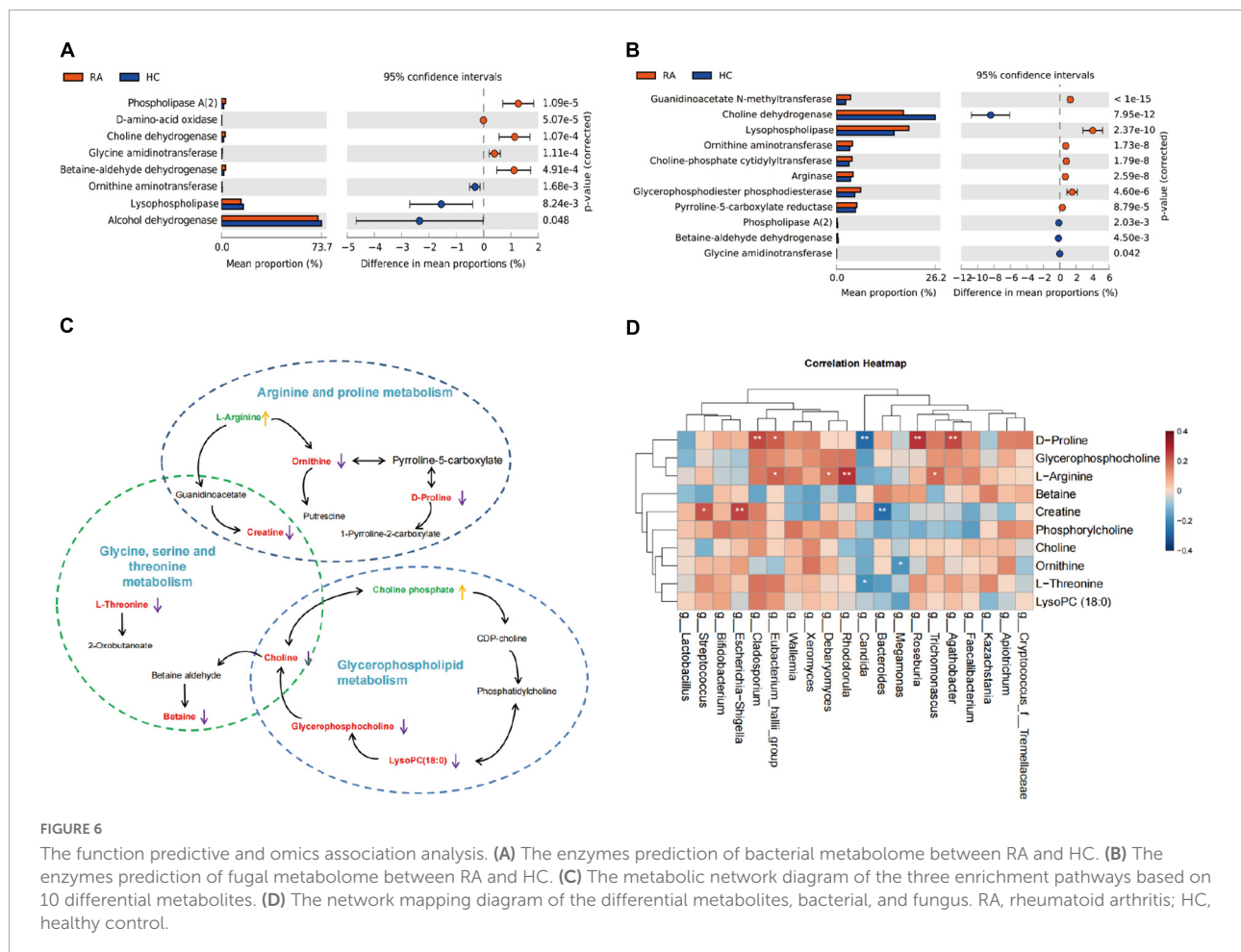
A large body of evidence indicated that arginine metabolism played an important role in the occurrence and development of RA disease (Radhakutty et al., 2017; Brunner et al., 2020). In our study, the plasma level of arginine was higher in RA patients than in HC by non-target metabolomics, which was also validated in target metabolomics analysis. This result is consistent with the previous study that displayed patients with RA had higher plasma concentrations of



arginine (Radhakutty et al., 2017; Brunner et al., 2020). Brunner and his colleagues reported RANKL that cellular programming required extracellular arginine (Brunner et al., 2020). This evidence indicated that it could improve outcomes in murine arthritis models by systemic arginine restriction, and preosteoclast metabolic quiescence would be induced by arginine removal. It may be a possibility for the effective intervention of RA by arginine restriction. These studies suggested that the core AAs exhibited potential application

value in the diagnosis, disease progression, and therapy of RA.

Choline, as a bridge of glycerophospholipid metabolism and glycine, serine, and threonine metabolism, was decreased in the blood of the RA group in our study. This is consistent with Rekha Narasimhan et al.'s study (Narasimhan et al., 2018). Choline C-11 PET scanning was transferred to joints in inflammatory arthritis (Roivainen et al., 2003) and increased in fibrocyte-like synoviocytes (Beckmann et al., 2015). Evidence



of a previous research revealed that Choline was presented in synovial fibroblasts and associated with TNF- $\alpha$  production and migration (Guma et al., 2015). In our study, choline, L-threonine, and D-proline levels were inversely correlated with the RA disease activity defined by DAS28(3). This indicated that these plasma metabolites may be strongly linked to RA disease progression and serve as potential predictive markers.

RA and SLE are both typical chronic inflammatory autoimmune diseases, and with complicated pathogenesis. It is difficult to identify and clarify accurate etiology for them. Many previous studies have reported that abnormal metabolic activities are critical in SLE pathogenesis. For example, glycolysis and mitochondrial oxidative metabolism both were raised in SLE patients and the SLE mouse model (Yin et al., 2015). Another paper revealed that citrate and pyruvate were decreased in both SLE and RA patients compared with healthy controls, and the serum level of formate was markedly decreased in SLE patients (Ouyang et al., 2011). In our study, we compared the RA and SLE and found that the RA metabolic profile was different from the SLE group. However, there was no significant change in metabolic pathways between RA and SLE groups. Additionally,

the fold change value of all differential metabolites was small (0.9-1.2), which may support a hypothesis that the changes in the plasma metabolic are similar for RA and SLE patients.

In recent years, numerous studies proved that there were alterations in intestinal microbiota composition, especially in autoimmune diseases (Wu and Wu, 2012; Luckey et al., 2013; Taneja, 2014), including RA. Previous studies showed that gut microbiome dysbiosis could induce the production of proinflammatory cytokines, interleukin-17, and increased levels of Th17 cells (Luckey et al., 2013). The role of gut microbiota in the pathogenesis of arthritis was demonstrated in experimental murine models (Chen et al., 2016; Liu et al., 2016; Wang et al., 2020a). For instance, *L. bifidus* could induce joint swelling in germ-free mice (Abdollahi-Roodsaz et al., 2008). In our study, we identified 68 genera unique in the RA group and 41 unique genera in the HC group, and 117 differential bacterial genera were further identified. On the genus level, the *Lactobacillus*, *Eubacterium\_hallii*, *Escherichia-Shigella*, and *Streptococcus* were more abundant in RA patients. Our results were similar to a previous study that reported that some *Lactobacillus* species might cause arthritis (Simelyte et al., 2003). *Eubacterium\_hallii*,

as one of the major butyrate producers (Louis et al., 2010), may play anti-rheumatic and anti-inflammatory effects by butyrate, which was proved that it inhibited arthritis and suppressed the expression of inflammatory cytokines in the CIA mice model (Hui et al., 2019). However, the change tendency of *Eubacterium\_hallii* in our study was increased in patients with RA. Moreover, the abundance of *Bacteroides* was higher in healthy controls. This was consistent with a recent previous study that reported the decrement of a redox reaction-related gene of the genus *Bacteroides* in RA (Kishikawa et al., 2020).

Notably, in this study, we systematically analyzed the profile of fecal fungal biodiversity and community structure between RA and HCs. At the genus level, there were 401 specific fungal genera in the RA group, which were significantly more than the HC group. The LDA effect size analysis indicated that the seven discovered different fungal genera as a combination of biomarkers to diagnose RA included *Cryptococcus*, *Penicillium*, *Aspergillus*, *Cladosporium*, *Monascus*, *Candida*, and *Debaryomyces*. Especially, the *Candida* and *Debaryomyces* were more enriched in RA patients, which could be a potential biomarker for the prediction of early RA. Bishu et al. (2014), reported that there was clearly a trend toward increased susceptibility to *C. albicans* colonization in RA, and the risk of mucosal candidiasis in RA patients may increase by using biologic drugs selectively targeting the IL-23/IL-17 axis. Furthermore, Jain et al. (2021) discovered that yeast *Debaryomyces hansenii* were more likely to localize and be abundant within incompletely healed intestinal wounds of mice and inflamed tissue results from Crohn's disease patients. Another study also confirmed that *Debaryomyces hansenii* could control the proliferation of opportunistic bacteria in the mucosa of intestinal microbiota disorder mice (Zeng et al., 2019). Although our results analyzed the fungal profile and changing trend in RA patients, the relationship of fungi with RA disease and the biological functions of fungi are still unclear and needs further exploration.

A recent study has reported that aberrant gut microbiota alters the host metabolome and impacts renal failure in humans, and gut microbiota is an important determinant of the host fecal and serum metabolic landscape (Wang et al., 2020b). A previous study has suggested that the serum metabolome can be impacted by dysbiosis of the human gut microbiota, and *Prevotella copri* and *Bacteroides vulgatus* are identified as the main species driving the association between biosynthesis of branched-chain AAs and insulin resistance (Pedersen et al., 2016). In our study, we analyzed the fecal bacterial community and fungal community structure and species diversity of RA patients and healthy controls and performed a functional predictive analysis of the identified differential communities. The results showed that plasma amino acid metabolism was associated with changes in gut microbes in RA patients. Especially, the arginine and proline metabolism pathways

were significantly affected by microbiota changes. The expression of the metabolite L-Arginine was increased in RA patients and positively correlated with *Rhodotorula* in fungi. D-Proline levels were significantly positively correlated with abundances of *Agathobacter*, *Roseburia*, and *Cladosporium*, and negatively correlated with *Candida*. *Escherichia-Shigella* abundance was positively correlated with plasma Creatine levels, while *Bacteroides* genus was negatively correlated with Creatine. Our results are consistent with those of a previous study that found that *Megamonas* was decreased in RA patients, which participates in the metabolism of carbohydrate fermentation into SCFAs (Feng et al., 2019). The functional predictive analysis results suggested that differential genera affect the host metabolic pathway of L-threonine biosynthesis, L-serine and glycine biosynthesis I, and "arginine, ornithine, and proline interconversion" through a variety of enzymes, such as choline dehydrogenase, D-amino-acid oxidase, glycine amidinotransferase, ornithine aminotransferase, lysophospholipase, choline-phosphate cytidyltransferase, arginase, and phospholipase A (2), which from the functional prediction is based on a differential microbial genus. Interestingly, the functional prediction results showed a higher abundance of choline dehydrogenase, glycine amidinotransferase, phospholipase A (2), lower abundance of ornithine aminotransferase, and lysophospholipase, in bacteria of the RA group compared with HC group, however, the abundance of these enzymes was the exact opposite in fungi of RA patients.

There were several limitations. First, the critical role of metabolites biomarkers and microbial biomarkers need to be validated further. Second, though the glycine, serine, and threonine metabolism could help us draw a positive conclusion that they could be considered as a bridge between plasma and microbial metabolomes, the pathological mechanism from genotype to phenotype is not clear. Third, the untargeted metabolomics and microbiome were not using the same batch of personnel in the healthy control group, and a cautious interpretation of our result was needed when applying our model to other populations.

## Conclusion

In conclusion, we provided a list of metabolites, bacteria, and fungus, whose abundance changed in RA as potential biomarkers and built plasma metabolic/microbe-markers-based models for potentially clinical diagnosis of RA. The function prediction analysis of plasma metabolomics, intestinal bacteria, and intestinal fungi displayed that RA disease was related to changes in arginine and proline metabolism and glycine, serine, and threonine metabolism. Gut microbiome analysis combined with plasma metabolomics can shed new light on the pathogenesis of RA.



## Data availability statement

The data presented in the study are deposited in the NGDC database, accession number PRJCA011639.

## Ethics statement

The study was reviewed and approved by the Medical Ethics Committees of Dazhou Central Hospital.

## Author contributions

FZ, SL, and JZ contributed conception and design of the study. All authors were involved in organizing the database, performing the statistical analysis, drafting the article, and revising it critically for important intellectual content, agreed to be accountable for all aspects of the work and approved the final version to be published.

## Funding

This study was supported by the Innovative Scientific Research Project of Medical Youth in Sichuan Province (Q20073), the Medical Research Project of Sichuan Province (S20001), the Dazhou-Sichuan University Intelligent Medical Laboratory in Dazhou (2020CDDZ-02), the Key Projects Fund of Science and Technology Department of Sichuan Province (2021YFS0165, 22DZYF1942, 22ZDYF1766, 22ZDYF1948, and

22MZGC0090), and the Scientific Research Fund of Sichuan Health and Health Committee (21PJ085).

## Acknowledgments

We thank Prof. Xiuqin Zhang (Peking University) for constructive comments on the manuscript.

## Conflict of interest

The authors declare that the research was conducted in the absence of any commercial or financial relationships that could be construed as a potential conflict of interest.

## Publisher's note

All claims expressed in this article are solely those of the authors and do not necessarily represent those of their affiliated organizations, or those of the publisher, the editors and the reviewers. Any product that may be evaluated in this article, or claim that may be made by its manufacturer, is not guaranteed or endorsed by the publisher.

## Supplementary material

The Supplementary Material for this article can be found online at: <https://www.frontiersin.org/articles/10.3389/fmicb.2022.931431/full#supplementary-material>

## References

- Abdollahi-Roodsaz, S., Joosten, L. A., Koenders, M. I., Devesa, I., Roelofs, M. F., Radstake, T. R., et al. (2008). Stimulation of TLR2 and TLR4 differentially skews the balance of T cells in a mouse model of arthritis. *J. Clin. Invest.* 118, 205–216. doi: 10.1172/JCI32639
- Beckmann, J., Schubert, J., Morhenn, H. G., Grau, V., Schnettler, R., and Lips, K. S. (2015). Expression of choline and acetylcholine transporters in synovial tissue and cartilage of patients with rheumatoid arthritis and osteoarthritis. *Cell Tissue Res.* 359, 465–477. doi: 10.1007/s00441-014-2036-0
- Bishu, S., Su, E. W., Wilkerson, E. R., Reckley, K. A., Jones, D. M., McGeachy, M. J., et al. (2014). Rheumatoid arthritis patients exhibit impaired *Candida albicans*-specific Th17 responses. *Arthritis. Res. Ther.* 16:R50. doi: 10.1186/ar4480
- Brunner, J. S., Vulliam, L., Hofmann, M., Kieler, M., Lercher, A., Vogel, A., et al. (2020). Environmental arginine controls multinuclear giant cell metabolism and formation. *Nat. Commun.* 11:431. doi: 10.1038/s41467-020-14285-1
- Chen, J., Wright, K., Davis, J. M., Jeraldo, P., Marietta, E. V., Murray, J., et al. (2016). An expansion of rare lineage intestinal microbes characterizes rheumatoid arthritis. *Genome Med.* 8:43. doi: 10.1186/s13073-016-0299-7
- Chimenti, M. S., Triggianese, P., Conigliaro, P., Candi, E., Melino, G., and Perricone, R. (2015). The interplay between inflammation and metabolism in rheumatoid arthritis. *Cell Death Dis.* 6:e1887. doi: 10.1038/cddis.2015.246
- Chimenti, M. S., Tucci, P., Candi, E., Perricone, R., Melino, G., and Willis, A. E. (2013). Metabolic profiling of human CD4+ cells following treatment with methotrexate and anti-TNF-alpha infliximab. *Cell Cycle* 12, 3025–3036. doi: 10.4161/cc.26067
- Cuppen, B. V., Fu, J., van Wietmarschen, H. A., Harms, A. C., Koval, S., Marijnissen, A. C., et al. (2016). Exploring the inflammatory metabolomic profile to predict response to TNF-alpha Inhibitors in rheumatoid arthritis. *PLoS One* 11:e0163087. doi: 10.1371/journal.pone.0163087
- Feng, J., Zhao, F., Sun, J., Lin, B., Zhao, L., Liu, Y., et al. (2019). Alterations in the gut microbiota and metabolite profiles of thyroid carcinoma patients. *Int. J. Cancer* 144, 2728–2745. doi: 10.1002/ijc.32007
- Foster, J. A., Lyte, M., Meyer, E., and Cryan, J. F. (2016). Gut microbiota and brain function: An evolving field in neuroscience. *Int. J. Neuropsychopharmacol.* 19:yv114. doi: 10.1093/ijnp/pyv114
- Grover, M., and Kashyap, P. C. (2014). Germ-free mice as a model to study effect of gut microbiota on host physiology. *Neurogastroenterol. Motil.* 26, 745–748. doi: 10.1111/nmo.12366
- Guma, M., Sanchez-Lopez, E., Lodi, A., Garcia-Carbonell, R., Tiziani, S., Karin, M., et al. (2015). Choline kinase inhibition in rheumatoid arthritis. *Ann. Rheum. Dis.* 74, 1399–1407. doi: 10.1136/annrheumdis-2014-205696

- Hochberg, M. C. (1997). Updating the American College of rheumatology revised criteria for the classification of systemic lupus erythematosus. *Arthritis Rheum.* 40:1725. doi: 10.1002/art.1780400928
- Horgan, R., and Kenny, L. (2011). Omic technologies: Genomics, transcriptomics, proteomics and metabolomics. *Obstet. Gynaecol.* 13, 189–195.
- Hu, P. F., Chen, Y., Cai, P. F., Jiang, L. F., and Wu, L. D. (2011). Sphingosine-1-phosphate: A potential therapeutic target for rheumatoid arthritis. *Mol. Biol. Rep.* 38, 4225–4230. doi: 10.1007/s11033-010-0545-9
- Hui, W., Yu, D., Cao, Z., and Zhao, X. (2019). Butyrate inhibit collagen-induced arthritis via Treg/IL-10/Th17 axis. *Int. Immunopharmacol.* 68, 226–233. doi: 10.1016/j.intimp.2019.01.018
- Jain, U., Ver Heul, A. M., Xiong, S., Gregory, M. H., Demers, E. G., Kern, J. T., et al. (2021). Debaromyces is enriched in Crohn's disease intestinal tissue and impairs healing in mice. *Science* 371, 1154–1159. doi: 10.1126/science.abd0919
- Kang, J., Zhu, L., Lu, J., and Zhang, X. (2015). Application of metabolomics in autoimmune diseases: Insight into biomarkers and pathology. *J. Neuroimmunol.* 279, 25–32. doi: 10.1016/j.jneuroim.2015.01.001
- Kapoor, S. R., Filer, A., Fitzpatrick, M. A., Fisher, B. A., Taylor, P. C., Buckley, C. D., et al. (2013). Metabolic profiling predicts response to anti-tumor necrosis factor alpha therapy in patients with rheumatoid arthritis. *Arthritis Rheum.* 65, 1448–1456. doi: 10.1002/art.37921
- Kay, J., and Upchurch, K. S. (2012). ACR/EULAR 2010 rheumatoid arthritis classification criteria. *Rheumatology (Oxford)* 51 Suppl 6, vi5–vi9. doi: 10.1093/rheumatology/kes279
- Kishikawa, T., Maeda, Y., Nii, T., Motooka, D., Matsumoto, Y., Matsushita, M., et al. (2020). Metagenome-wide association study of gut microbiome revealed novel aetiology of rheumatoid arthritis in the Japanese population. *Ann. Rheum. Dis.* 79, 103–111. doi: 10.1136/annrheumdis-2019-215743
- Liu, X., Zeng, B., Zhang, J., Li, W., Mou, F., Wang, H., et al. (2016). Role of the gut microbiome in modulating arthritis progression in mice. *Sci. Rep.* 6:30594. doi: 10.1038/srep30594
- Louis, P., Young, P., Holtrop, G., and Flint, H. J. (2010). Diversity of human colonic butyrate-producing bacteria revealed by analysis of the butyryl-CoA:acetate CoA-transferase gene. *Environ. Microbiol.* 12, 304–314. doi: 10.1111/j.1462-2920.2009.02066.x
- Luckey, D., Gomez, A., Murray, J., White, B., and Taneja, V. (2013). Bugs & us: The role of the gut in autoimmunity. *Indian J Med Res* 138, 732–743.
- Mun, S., Lee, J., Park, M., Shin, J., Lim, M. K., and Kang, H. G. (2021). Serum biomarker panel for the diagnosis of rheumatoid arthritis. *Arthritis Res. Ther.* 23:31. doi: 10.1186/s13075-020-02405-7
- Murray, P. J. (2016). Amino acid auxotrophy as a system of immunological control nodes. *Nat. Immunol.* 17, 132–139. doi: 10.1038/ni.3323
- Narasimhan, R., Coras, R., Rosenthal, S. B., Sweeney, S. R., Lodi, A., Tiziani, S., et al. (2018). Serum metabolomic profiling predicts synovial gene expression in rheumatoid arthritis. *Arthritis Res. Ther.* 20:164. doi: 10.1186/s13075-018-1655-3
- Olhagen, B., and Mansson, I. (1968). Intestinal Clostridium perfringens in rheumatoid arthritis and other collagen diseases. *Acta Med. Scand.* 184, 395–402. doi: 10.1111/j.0954-6820.1968.tb02478.x
- Ouyang, X., Dai, Y., Wen, J. L., and Wang, L. X. (2011). (1)H NMR-based metabolomic study of metabolic profiling for systemic lupus erythematosus. *Lupus* 20, 1411–1420. doi: 10.1177/0961203311418707
- Pedersen, H. K., Gudmundsdottir, V., Nielsen, H. B., Hyötyläinen, T., Nielsen, T., Jensen, B. A., et al. (2016). Human gut microbes impact host serum metabolome and insulin sensitivity. *Nature* 535, 376–381. doi: 10.1038/nature18646
- Petri, M., Orbai, A. M., Alarcon, G. S., Gordon, C., Merrill, J. T., Fortin, P. R., et al. (2012). Derivation and validation of the Systemic Lupus International Collaborating Clinics classification criteria for systemic lupus erythematosus. *Arthritis Rheum.* 64, 2677–2686. doi: 10.1002/art.34473
- Priori, R., Casadei, L., Valerio, M., Scrivo, R., Valesini, G., and Manetti, C. (2015). (1)H-NMR-Based metabolomic study for identifying serum profiles associated with the response to etanercept in patients with rheumatoid arthritis. *PLoS One* 10:e0138537. doi: 10.1371/journal.pone.0138537
- Radhakutty, A., Mangelsdorf, B. L., Drake, S. M., Rowland, A., Smith, M. D., Mangoni, A. A., et al. (2017). Opposing effects of rheumatoid arthritis and low dose prednisolone on arginine metabolomics. *Atherosclerosis* 266, 190–195. doi: 10.1016/j.atherosclerosis.2017.10.004
- Röivainen, A., Parkkola, R., Yli-Kerttula, T., Lehtikainen, P., Viljanen, T., Mottonen, T., et al. (2003). Use of positron emission tomography with methyl-11C-choline and 2-18F-fluoro-2-deoxy-D-glucose in comparison with magnetic resonance imaging for the assessment of inflammatory proliferation of synovium. *Arthritis Rheum.* 48, 3077–3084. doi: 10.1002/art.11282
- Scher, J. U., Szczesnak, A., Longman, R. S., Segata, N., Ubeda, C., Bielski, C., et al. (2013). Expansion of intestinal Prevotella copri correlates with enhanced susceptibility to arthritis. *Elife* 2:e01202. doi: 10.7554/eLife.01202
- Simelyte, E., Rimpiläinen, M., Zhang, X., and Toivanen, P. (2003). Role of peptidoglycan subtypes in the pathogenesis of bacterial cell wall arthritis. *Ann. Rheum. Dis.* 62, 976–982. doi: 10.1136/ard.62.10.976
- Smolen, J. S., Aletaha, D., and McInnes, I. B. (2016). Rheumatoid arthritis. *Lancet* 388, 2023–2038. doi: 10.1016/S0140-6736(16)30173-8
- Smolen, J. S., Aletaha, D., Barton, A., Burmester, G. R., Emery, P., Firestein, G. S., et al. (2018). Rheumatoid arthritis. *Nat. Rev. Dis. Primers* 4:18001. doi: 10.1038/nrdp.2018.1
- Smolen, J. S., Landewe, R. B. M., Bijlsma, J. W. J., Burmester, G. R., Dougados, M., Kerschbaumer, A., et al. (2020). EULAR recommendations for the management of rheumatoid arthritis with synthetic and biological disease-modifying antirheumatic drugs: 2019 update. *Ann. Rheum. Dis.* 79, 685–699. doi: 10.1136/annrheumdis-2019-216655
- Song, L., Yin, Q., Kang, M., Ma, N., Li, X., Yang, Z., et al. (2020). Untargeted metabolomics reveals novel serum biomarker of renal damage in rheumatoid arthritis. *J. Pharm. Biomed. Anal.* 180, 113068. doi: 10.1016/j.jpba.2019.113068
- Taneja, V. (2014). Arthritis susceptibility and the gut microbiome. *FEBS Lett.* 588, 4244–4249. doi: 10.1016/j.febslet.2014.05.034
- Tang, Y., Liu, S., Shu, H., Yanagisawa, L., and Tao, F. (2020). gut microbiota dysbiosis enhances migraine-like pain via TNFalpha upregulation. *Mol. Neurobiol.* 57, 461–468. doi: 10.1007/s12035-019-01721-7
- Teitsma, X. M., Yang, W., Jacobs, J. W. G., Petho-Schramm, A., Borm, M. E. A., Harms, A. C., et al. (2018). Baseline metabolic profiles of early rheumatoid arthritis patients achieving sustained drug-free remission after initiating treat-to-target tocilizumab, methotrexate, or the combination: Insights from systems biology. *Arthritis Res. Ther.* 20:230. doi: 10.1186/s13075-018-1729-2
- Wang, B., He, Y., Tang, J., Ou, Q., and Lin, J. (2020a). Alteration of the gut microbiota in tumor necrosis factor-alpha antagonist-treated collagen-induced arthritis mice. *Int. J. Rheum. Dis.* 23, 472–479. doi: 10.1111/1756-185X.13802
- Wang, B., Wu, L., Chen, J., Dong, L., Chen, C., Wen, Z., et al. (2021). Metabolism pathways of arachidonic acids: Mechanisms and potential therapeutic targets. *Signal Transduct. Target Ther.* 6:94. doi: 10.1038/s41392-020-00443-w
- Wang, M., Huang, J., Fan, H., He, D., Zhao, S., Shu, Y., et al. (2018). treatment of rheumatoid arthritis using combination of methotrexate and tripterygium glycosides tablets-A quantitative plasma pharmacokinetic and pseudotargeted metabolomic approach. *Front. Pharmacol.* 9:1051. doi: 10.3389/fphar.2018.01051
- Wang, X., Yang, S., Li, S., Zhao, L., Hao, Y., Qin, J., et al. (2020b). Aberrant gut microbiota alters host metabolome and impacts renal failure in humans and rodents. *Gut* 69, 2131–2142. doi: 10.1136/gutjnl-2019-319766
- Wu, H. J., and Wu, E. (2012). The role of gut microbiota in immune homeostasis and autoimmunity. *Gut Microbes* 3, 4–14. doi: 10.4161/gmic.19320
- Yin, Y., Choi, S. C., Xu, Z., Perry, D. J., Seay, H., Croker, B. P., et al. (2015). Normalization of CD4+ T cell metabolism reverses lupus. *Sci. Transl. Med.* 7:274ra218. doi: 10.1126/scitranslmed.aaa0835
- Zeng, A., Peng, M., Liu, H., Guo, Z., Xu, J., Wang, S., et al. (2019). Effects of Debaromyces hansenii treatment on intestinal mucosa microecology in mice with antibiotic-associated diarrhea. *PLoS One* 14:e0224730. doi: 10.1371/journal.pone.0224730
- Zhang, X., Li, J., Xie, B., Wu, B., Lei, S., Yao, Y., et al. (2018). Comparative Metabolomics Analysis of Cervicitis in Human Patients and a Phenol Mucilage-Induced Rat Model Using Liquid Chromatography Tandem Mass Spectrometry. *Front. Pharmacol.* 9:282. doi: 10.3389/fphar.2018.00282

# Frontiers in Microbiology

Explores the habitable world and the potential of microbial life

The largest and most cited microbiology journal which advances our understanding of the role microbes play in addressing global challenges such as healthcare, food security, and climate change.

## Discover the latest Research Topics

[See more →](#)

### Frontiers

Avenue du Tribunal-Fédéral 34  
1005 Lausanne, Switzerland  
[frontiersin.org](https://frontiersin.org)

### Contact us

+41 (0)21 510 17 00  
[frontiersin.org/about/contact](https://frontiersin.org/about/contact)

